Charles University

Faculty of Science

Study programme: Organic chemistry

Branch of study: Organic chemistry

Miroslav Kuba

Novel fluorescent nucleotides for metabolic labelling and for the construction of DNA probes

Nové fluorescenční nukleotidy pro metabolické značení a konstrukci DNA sond

Dissertation

Supervisor: prof. Ing. Michal Hocek, Ph.D., DSc.

Prague, 2022

This dissertation was worked out at the Institute of Organic Chemistry and Biochemistry, Academy of Sciences of the Czech Republic, Prague, from September 2016 to June 2022.

Declaration

I hereby declare that I have worked out my dissertation by myself and that all the literature sources used are listed in the literature list. Neither this work, nor its significant part was used to obtain other academic title.

Prague, 23.06.2022 Miroslav Kuba

Acknowledgement

First and foremost, I would like to thank my supervisor Prof. Michal Hocek for an interesting project, guidance, trust and support. I am thankful to Dr. Radek Pohl for his help with measuring and interpreting complex NMR spectra, and Ing. Kateřina Nováková for the measurement of MALDI-TOF spectra. I would like to thank Dr. Pedro Güixens-Gallardo for introducing me to fluorescence, to Dr. Tomáš Kraus for his valuable advices, suggestions, scientific discussions and for performing cell-based experiments with my compounds. My thanks also belong to Ivana Ivancová for her patience and encouragement through the bad days and company in the good ones. I am grateful to my family, who supported me during my studies.

My Ph.D. work was a part of a multidisciplinary project performed by Prof. Hocek's research group at the Institute of Organic Chemistry and Biochemistry AS CR. I executed all the synthesis and biophysical experiments described in the thesis. Dr. Radek Pohl analysed the measurements and interpreted complex NMR spectra. Ing. Kateřina Nováková measured the MALDI-TOF mass spectra of prepared oligonucleotides, and the mass spectra of all of the synthesised compounds were measured by the mass spectrometry team at IOCB Prague. Dr. Jan Hodek and Dr. Jan Weber provided RNA and cDNA of SARS-CoV-2 virus (IOCB, virology department). Cell-based experiments were performed and processed by Dr. Tomáš Kraus at IOCB Prague, super-resolution microscopy was performed at BIOCEV (IMCF). The parts of the thesis, which were performed by collaborating researchers, are distinctly denoted in the thesis.

This work was supported by the Academy of Sciences of the Czech Republic (the *Praemium Academiae*), the Czech Science Fundation (17-14791S and P206/12/G151), the European Regional Development Fund OP RDE (No. CZ.02.1.01/0.0/0.0/16_019/ 0000729), and by Gilead Sciences, Inc. (Foster City, CA, USA).

Abstract

The aim of the thesis was to synthesize new nucleosides, nucleotides and the corresponding DNA probes bearing various fluorescent labels, which can be used for bioanalytical applications.

In the first part of the thesis, 2'-deoxycytidine and the corresponding nucleoside triphosphate bearing tryptophan-based imidazolinone fluorophore were synthesized by Sonogashira cross-coupling reaction. The fluorophore showed sensitivity to pH and viscosity. Nucleotide was used for the construction of modified oligonucleotides (ON) and DNA by primer extension (PEX) or polymerase chain reaction (PCR). Labelled ON probe was used for sensing interaction with single-strand binding protein, which resulted in increased fluorescence intensity of modified ON.

Next, thymidine and thymidine triphosphate labelled by bezylidene-tetrahydroxanthylium fluorophore were synthesized by copper-catalyzed azide-alkyne cycloaddition (CuAAC). Fluorescence of the fluorophore is dependent on the polarity and viscosity of the environment. Incorporation of the modified nucleotide into DNA, by PEX or PCR, led to dramatic increase of the fluorescence presumably due to the interactions of the fluorophore in the major groove. Unfortunately, the modified nucleotide was not suitable for in cellulo imaging due to its cytotoxicity. The modified dsDNA was used as fluorescent probe for sensing interactions with small molecules and proteins by change of fluorescence. Finally, the nucleotide was applied in real-time PCR as a new approach to directly visualize the DNA synthesis. Benzylidene-tetrahydroxanthylium fluorophore was also attached to 2'-deoxycytidine via triethylene glycol linker to address issues with cell experiments, however, the incorporation into DNA in live cells was not successful.

Additionally, thiazole orange (TO) modified 2'-deoxycytidine and the corresponding triphosphate were synthesized by CuAAC. TO is known to bind nucleic acids and change fluorescence intensity and lifetime depending on viscosity. The nucleotide was incorporated into DNA probes by PEX and PCR and their

photophysical properties were evaluated. TO-modified nucleotide was successfully transported into live cells and incorporated into genomic DNA, what allowed real-time imaging of DNA synthesis in live cells using fluorescence lifetime imaging.

Further, 2'-deoxycytidine and its triphosphate bearing near-infrared BODIPY fluorophore tethered via propargylether or triethylene glycol linker were synthesized. New nucleosides showed dependence of fluorescence lifetime on the viscosity of environment. Corresponding nucleoside triphosphates were used as substrates for enzymatic synthesis of DNA. Modified DNA probes were used for sensing interactions with proteins by changing fluorescence lifetime. Nucleotide bearing BODIPY via triethylene glycol linker was also incorporated into DNA in live cells.

Finally, 2'-deoxycytidine triphosphate bearing silicon rhodamine fluorophore was prepared by strain-promoted azide-alkyne cycloaddition reaction. Photophysical properties, as well as enzymatic incorporation into DNA, were studied. New nucleotide was transported into cells and incorporated into genomic DNA, what allowed super-resolution imaging of DNA.

Abstrakt

Cílem této dizertační práce byla syntéza nových nukleosidů, nukleotidů a příslušných DNA sond nesoucích různé fluorescenční značky pro bioanalytické aplikace.

V první části práce byl pomocí Sonogashiry cross-kapling reakce syntetizován 2'-deoxycytidin a jeho trifosfát nesoucí imidazolinový fluorofor na bázi tryptofanu. Daný fluorofor vykazoval citlivost na pH a viskozitu. Nukleotid byl použit pro konstrukci modifikovaných oligonukleotidů (ON) a DNA prodlužováním primeru (PEX) nebo polymerázovou řetězovou reakcí (PCR). Značená ON sonda byla použita pro snímání interakce se single-strand vazebným proteinem, což vedlo ke zvýšení intenzity fluorescence modifikovaného ON.

Dále byl připraven thymidin a thymidin-5'-*O*-trifosfát, nesoucí benzyliden-tetrahydroxanthyliový fluorofor, pomocí mědí katalyzované azid-alkynové cykloadice (CuAAC). Fluorescence fluoroforu je závislá na polaritě a viskozitě prostředí. Inkorporace modifikovaného nukleotidu do DNA pomocí PEX nebo PCR vedlo k dramatickému zvýšení fluorescence, pravděpodobně díky interakcím fluoroforu ve velkém žlábku. Bohužel, modifikovaný nukleotid nebyl vhodný pro vizualizace v buňkách kvůli své cytotoxicitě. Modifikovaná dsDNA byla použita jako fluorescenční sonda pro snímání interakcí s malými molekulami a proteiny změnou fluorescence. Nakonec byl nukleotid aplikován v real-time PCR, jako nový způsob přímé vizualizace syntézy DNA. Benzyliden-tetrahydroxanthyliový fluorofor byl také připojen k 2'-deoxycytidinu přes triethylenglykolový linker, aby se vyřešili problémy s buněčnými experimenty, nicméně začlenění do DNA v živých buňkách nebylo úspěšné.

Následně, 2'-deoxycytidin a jeho trifosfát modifikovaný thiazol orange (TO) byly také syntetizovány pomocí CuAAC. Je známo, že TO váže nukleové kyseliny a mění intenzitu fluorescence a lifetime v závislosti na viskozitě. Nukleotid byl inkorporován do DNA sond pomocí PEX a PCR a byly hodnoceny jejich fotofyzikální

vlastnosti. TO-modifikovaný nukleotid byl úspěšně transportován do živých buněk a začleněn do genomové DNA, což umožnilo zobrazení syntézy DNA v živých buňkách v reálném čase pomocí fluorescenčního zobrazování.

Dále byl připraven 2'-deoxycytidin a jeho trifosfát nesoucí near-infrared BODIPY fluorofor navázaný přes propargylether nebo triethylenglykolový linker. Nové nukleosidy prokázaly závislost doby života fluorescence na viskozitě prostředí. Odpovídající nukleosidtrifosfáty byly použity jako substráty pro enzymovou syntézu DNA. Modifikované DNA sondy byly použity pro monitorování interakcí s proteiny změnou doby života fluorescence. Nukleotid nesoucí BODIPY vázaný přes triethylenglykolový linker byl také enzymově zabudován do DNA v živých buňkách.

Nakonec byl připraven i 2'-deoxycytidintrifosfát nesoucí křemíkový rhodamin fluorofor pomocí strain-promoted azid-alkyn cykloadiční reakce. Byly studovány fotofyzikální vlastnosti a také enzymatická inkorporace do DNA. Nový nukleotid byl transportován do buněk, inkorporován do genomové DNA a umožnil zobrazení DNA s vysokým rozlišením.

List of abbreviations

ACN	acetonitrile
BODIPY	4,4-difluoro-4-bora-3a,4a-diaza-s-indacene
BSA	bovine serum albumin
CCVJ	9-(2-carboxy-2-cyanovinyl)julolidine
CFP	cyan fluorescent protein
COSY	correlation spectroscopy
Ct	threshold cycle
CuAAC	copper-catalyzed azide-alkyne cycloaddition
Da	Dalton
DAF	dimethyl aniline furaldehyde
DAPI	4',6-diamidino-2-phenylindole
DCM	dichloromethane
DCVJ	9-(2-carboxy-2-cyanovinyl)julolidine
DIPEA	N,N-diisopropyl(ethyl)amine
DMF	dimethylformamide
DMSO	dimethyl sulfoxid
DNA	deoxyribonucleic acid
dNTP	2'-deoxynucleoside-5'-*O*-triphosphate
ds	double-stranded
EDTA	ethylenediaminetetraacetic acid
equiv.	equivalent

ESI	electrospray ionization
FAM	6-carboxyfluorescein
FLIM	fluorescence lifetime imaging
FPs	fluorescent proteins
FRET	Förster resonance energy transfer
GFP	green fluorescent protein
GQ	G-quadruplex
HMBC	heteronuclear multiple bond correlation
HPLC	high performance liquid chromatography
HRMS	high resolution mass spectrometry
HSQC	heteronuclear single quantum coherence spectroscopy
iEDDA	inverse electron-demand Diels Alder
MALDI-TOF	matrix-assister laser desorption/ionization-time of flight
max.	maximum
MG	methyl green
min	minutes
n.d.	not determined
NIR	near infrared
NMR	nuclear magnetic resonance
nt	nucleotide
NTC	no template control
NTP	nucleoside-5'-*O*-triphosphate
ON	oligonucleotide

PAGE	polyacrylamide gel electrophoresis
PBS	phosphate-buffered saline
PCR	polymerase chain reaction
PEX	primer extension
pm	parts per milion
RdRP	RNA-dependent RNA polymerase
RNA	ribonucleic acid
rpm	rounds per minute
r.t.	room temperature
rt	real-time
RT	reverse transcription
SNI	single nucleotide incorporation
SNTT	synthetic nucleoside triphosphate transporter
SPAAC	strain-promoted azide-alkyne cycloaddition
ss	single-stranded
SSB	single-strand binding protein
STED	stimulated emission depletion
TAMRA	5-carboxytetramethylrhodamine
TBTA	tris[(1-benzyl-1*H*-1,2,3-triazol-4-yl)methyl]amine
TCA	trichloroacetic acid
TEAB	triethylammonium bicarbonate
TFA	trifluoroacetic acid
THF	tetrahydrofuran

THPTA	tris((1-hydroxy-propyl-1H-1,2,3-triazol-4-yl)methyl)amine
TCSPC	time-correlated single photon counting
TLC	thin-layer chromatography
TO	thiazole orange
U2OS	human bone osteosarcoma cells
UV	ultraviolet

Table of Contents

1 INTRODUCTION

1.1 Discovery and structural characteristics of DNA

Deoxyribonucleic acid (DNA) is a biomacromolecule with the role of carrying the genetic information. The DNA was first discovered and isolated in 1869 by Friedrich Miescher, who was studying chemical composition of leukocytes. Miescher distinguished isolated product from the proteins based on different properties, resistance to protease digestion and presence of large amounts of phosphorus.[1,2] However, the correct structure of the DNA was established in 1953 by James Watson and Francis Crick.[3]

DNA is polyanionic biopolymer which is composed from nucleotide constituents. Nucleotides consist of deoxyribose sugar moiety with phosphate group at 5' position and nucleobase (adenine, cytosine, guanine or thymine) attached to the anomeric position of the sugar moiety. The nucleotides are connected to each other by phosphordiester bond between sugar moiety of one nucleotide and phosphate group of the other. This linear linkage of nucleotides represents primary structure of the nucleic acids. The secondary structure of DNA represents the shape of the nucleic acids and is influenced by interactions between nucleobases. In double helix DNA, the strands are held together due to the interactions of complementary nuclebases through hydrogen bonding. The nucleobases pair according to the Watson-Crick base-pairing rule (Figure 1), cytosin (**C**) pairs with guanine (**G**) and adenine (**A**) pairs with thymine (**T**). Base-stacking between adjacent nuclebases also contributes to the stability of DNA.[4–7]

DNA duplexes exist in three major helical forms, A-DNA, B-DNA and Z-DNA (Figure 2)[8] depending on humidity and the amount of salts.[9] A-DNA and B-DNA are right-handed double helixes, while Z-DNA helix twists in a left-hand direction. B-DNA, which is the most occurring DNA structure in nature, contains wide major groove and narrow minor groove, which serve as binding sites for interactions of the DNA with proteins.[10] A-DNA, shorter and more compact structure, mostly occurs

under dehydrated or low water content conditions.[11] The Z-DNA helix is unstable structure and its formation can be promoted by alternating purine-pyrimidine sequences (such as GCGC).[12]

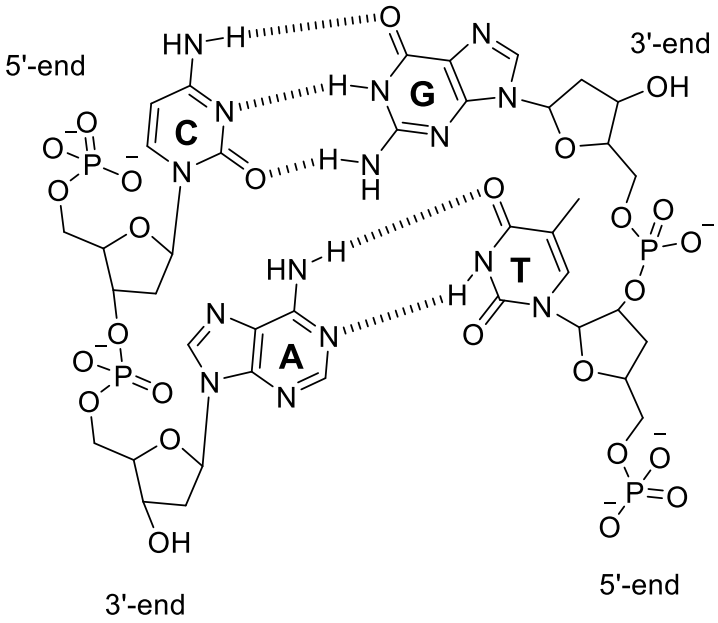

Figure 1 Watson-Crick base pairing of nuclebases through hydrogen bonds.

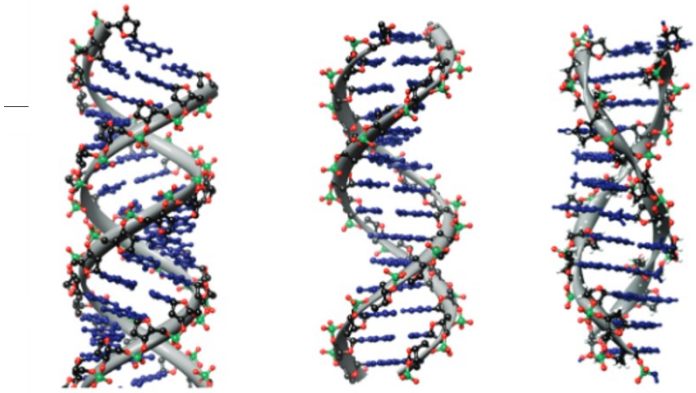

Figure 2 DNA structures A-DNA, B-DNA and Z-DNA from left to right. (Figure was taken from reference[8])

1.2 Methods of DNA synthesis

1.2.1 Solid-phase oligonucleotide synthesis

Chemical synthesis of oligonucleotides (ONs) is a rapid and inexpensive technique that provides short DNA sequeneces.[13] The synthesis can be performed by various approaches such as H-phosphonate[14,15], phosphite triester[16], phosphodiester[17] or phosphotriester[18,19] method. The most commonly used technique is phosphoramidite synthesis (Scheme 1). Full automation of this process was achieved in the late 1980s.[20]

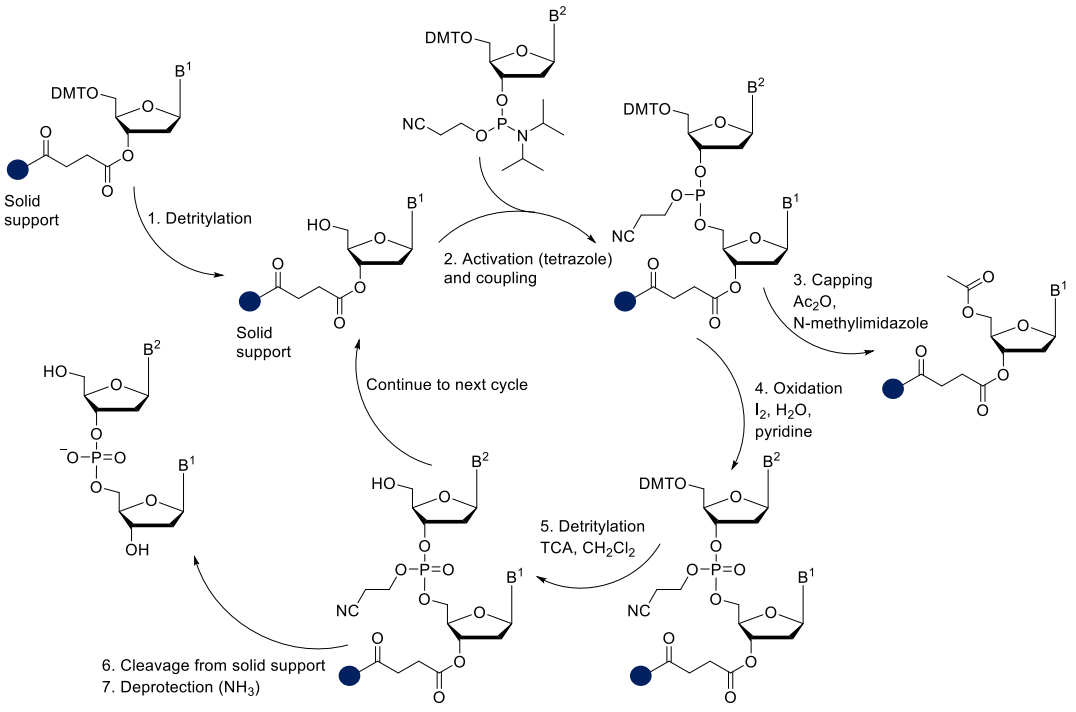

Scheme 1 Phosphoramidite synthesis of oligonucleotides.

Chemical synthesis of ONs proceeds from 3'- to 5'-end. The first step of the synthesis is detritylation under acidic conditions. Subsequently coupling reaction with nucleoside 3'-phosphoramidite takes place and leads to formation of phosphite triester. Following coupling, capping of unreacted 5'-OH groups takes place in presence of acetic anhydride and N-methylimidazole. Next, oxidation of phosphite triester by iodine in mixture of water/pyridine takes place and phosphate triester is

formed. Final step is detritylation followed by repetition of cycles to achieve oligonucleotides with length and sequence of interest. At the end, ONs are cleaved from solid support, deprotected and then purified by HPLC or desalted using spin-columns.

This method is advantageous for preparation of short ONs in high amounts, however it is difficult to prepare oligonucleotides that are longer than 100 nt. Another problem might also arise if the goal is to synthesize functionalized ON, in which case compatibility of functional groups with reaction conditions must be taken into consideration.

1.2.2 Enzymatic synthesis of DNA

The enzymatic synthesis of DNA is very useful alternative to chemical synthesis,[21] especially if it is desired to prepare longer ONs (>100 nt) or introduce modification that is not compatible with solid-phase synthesis. Unlike the chemical synthesis, enzymatic synthesis proceeds in the 5' to 3' direction. The most common enzymatic methods to prepare DNA are primer extension (PEX; Scheme 2) and polymerase chain reaction (PCR; Scheme 3, 4).

PEX is used to prepare short DNA with modification in single strand. The reaction is promoted by a DNA polymerase in suitable buffer and in presence of 2'-deoxynucleoside triphosphates (dNTPs; natural, modified or mixture), primer and template. The primer is usually radioactively (^{32}P) or fluorescently labelled at 5'-end to allow detection of products on gel.

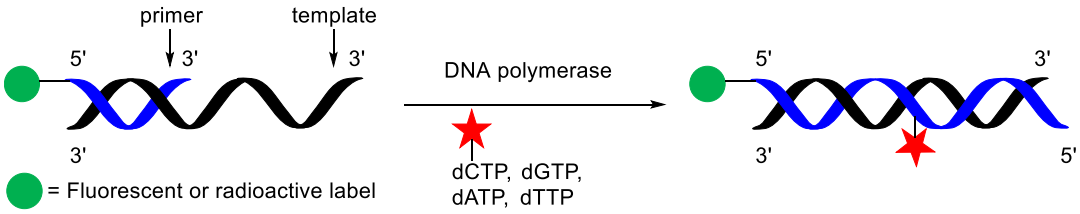

Scheme 2 Enzymatic synthesis of DNA by primer extension.

Polymerase chain reaction is used for amplification of longer DNA sequences and allows detection of very low amounts of DNA. This method was developed in the 1980s.[22]

This process is based on repetition of thermal cycles. First step of each cycle is denaturation of template (usually around 95°C). Subsequent annealing of primers is dependent on their sequence and length and is generally carried out at 45-55°C. At the end the primer is extended usually at 75°C.

PCR is very useful in combination with fluorescence detection because it can monitor amplification of target DNA during PCR (in real time).[23] This technique is called real-time PCR and is frequently used for detection of small quantities of DNA in diagnostic applications. One of the most commonly used methods for detection of PCR amplicons in real-time utilizes non-emissive fluorescent dyes that emit light once intercalated into DNA (Scheme 3).[24–26] The most commonly used intercalator is SYBR Green I dye (Figure 3).[27,28] However, DNA-binding dyes bind to all DNA present in PCR and therefore false positive results can be produced if, for example, primer dimers are formed. This problem can be overcome using specific hybridization probes, such as TaqMan probes.[29,30]

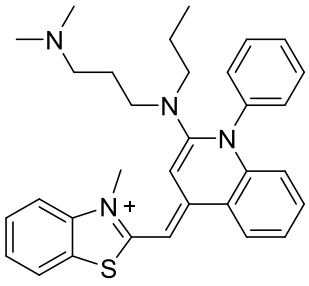

Figure 3 Structure of SYBR Green I.

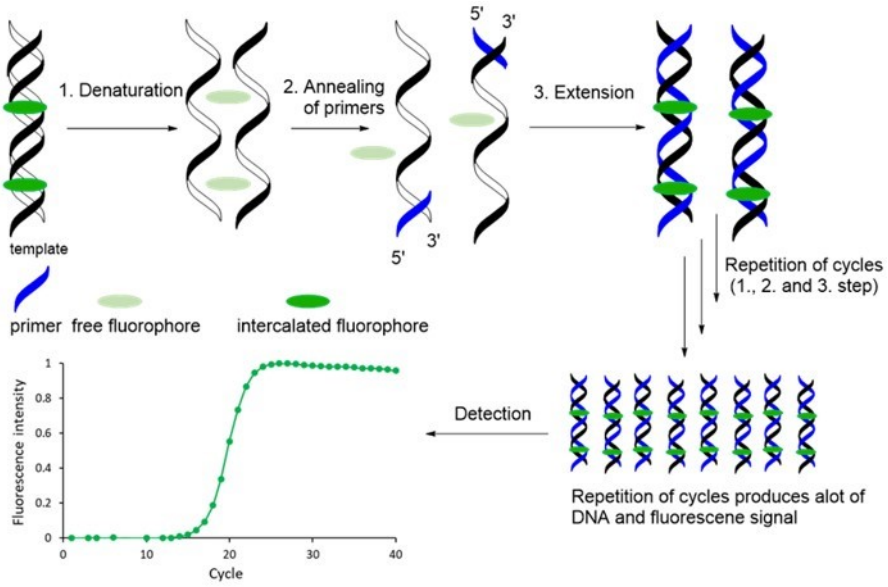

Scheme 3 Real-time polymerase chain reaction using intercalating dye.

TaqMan probes are oligonucleotides that are labelled by a fluorophore at the 5'-end and by a quencher at the 3'-end. The probe is non-fluorescent due to the quenching of the fluorophore by quencher via Förster resonance energy transfer (FRET).[31] Quenching occurs due to the close proximity of quencher and fluorescent dye in oligonucleotide. These probes are designed to anneal to the specific sequence of amplicons. During the PCR amplification, the probes are hydrolyzed by polymerase (usually Taq polymerase) due to the 5'-3' exonuclease activity of the enzyme. Cleavage of the probe separates the fluorophore from the quencher and results in the fluorescence signal (Scheme 4).[32]

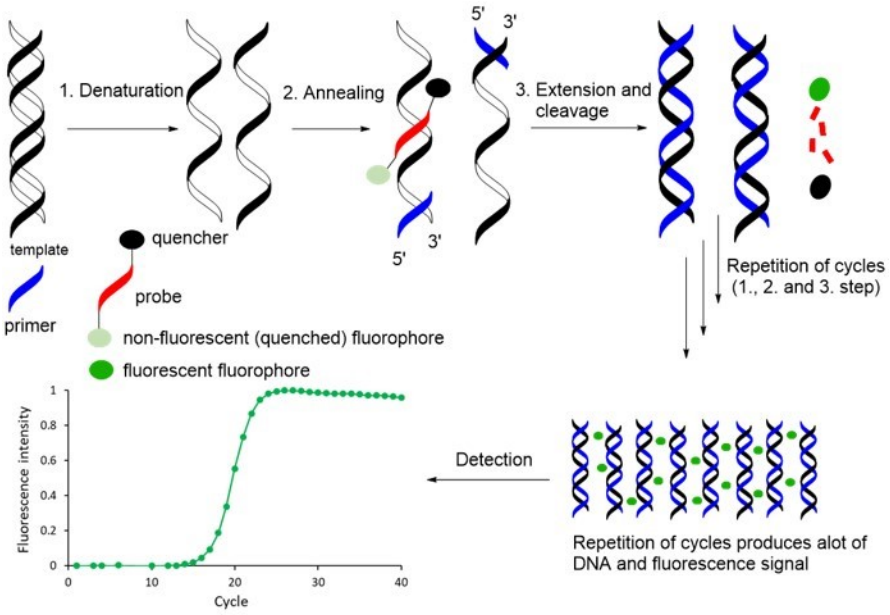

Scheme 4 Real-time PCR using TaqMan probe.

1.3 Post-synthetic functionalization of DNA

In some cases, the modified nucleotides are not accepted as substrates by DNA polymerases and at the same time the modification is not suitable for chemical synthesis of the DNA. To overcome these limitations, the post-synthetic introduction of modification to the DNA can be very useful. In this approach, the DNA (prepared by chemical or enzymatic synthesis) bears small reactive groups which chemoselectively react with the desired modification.

For example, single-stranded DNA with an azido group reacted with fluorescein derivative **1** through Staudinger ligation (Scheme 5 A). Fluorescein modified oligonucleotide was then utilized as a primer in a Sanger dideoxy sequencing reaction.[33] Panattoni et al.[34] described enzymatic and chemical synthesis of ONs containing alkyne linkers of various length and polarity. These alkyne-linked ONs were used for copper-catalyzed azide-alkyne cycloaddition (CuAAC) with 5-carboxyltetramethylrhodamine azide **2** (Scheme 5 B). The kinetic study revealed that the reaction with hydrophilic propargyl-diethylene glycol-linked ON reacted the fastest and it was approximately twice faster than the DNA bearing octadiynyl modification.

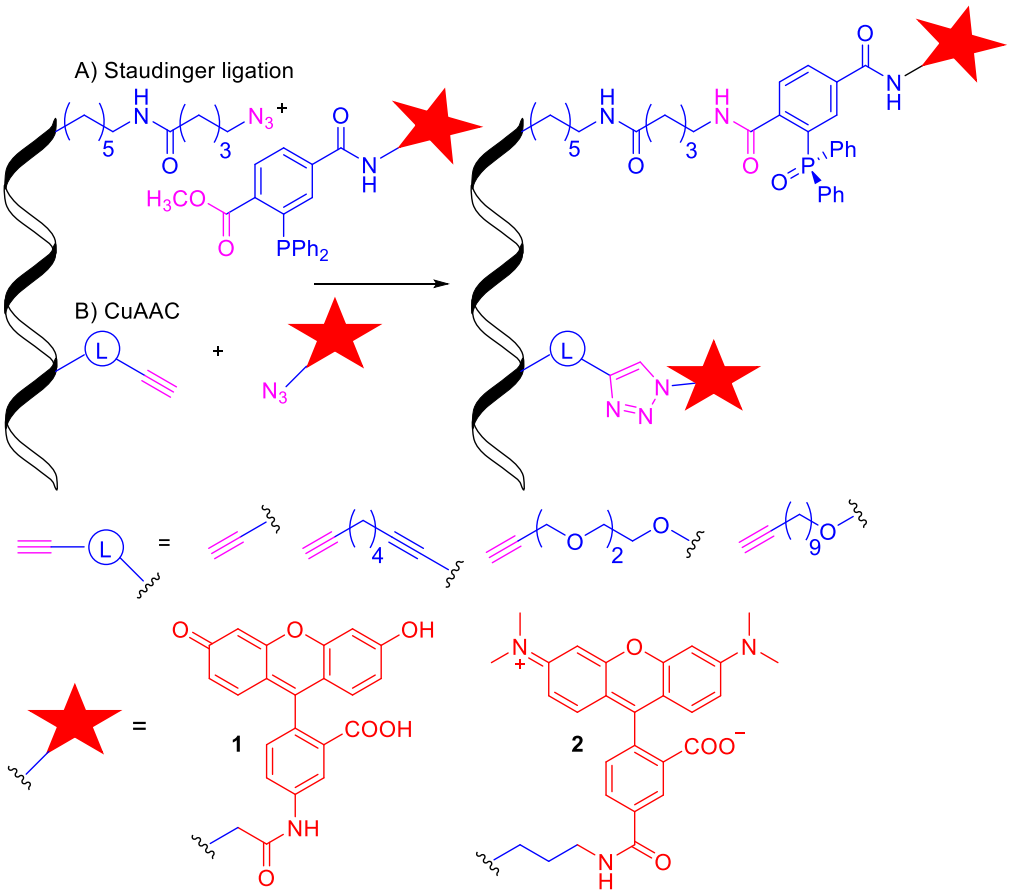

Scheme 5 Post-synthetic modification of oligonucleotides using Staudinger ligation or CuAAC.

Group of Tom Brown[35] reported enzymatic synthesis of DNA bearing azido or *trans*-cyclooctene moiety using primer extension, PCR amplification or reverse-transcription. The DNA product bearing azido group was labelled by Cy3-bicyclo[6.1.0]non-4-yne derivative **3** utilizing the strain-promoted azide-alkyne cycloaddition (SPAAC; Scheme 6 A). The DNA bearing *trans*-cyclooctene underwent the inverse electron-demand Diels-Alder (iEDDA; Scheme 6 B) reaction with 6-methyl-tetrazine-sulfo-Cy3 **4**.

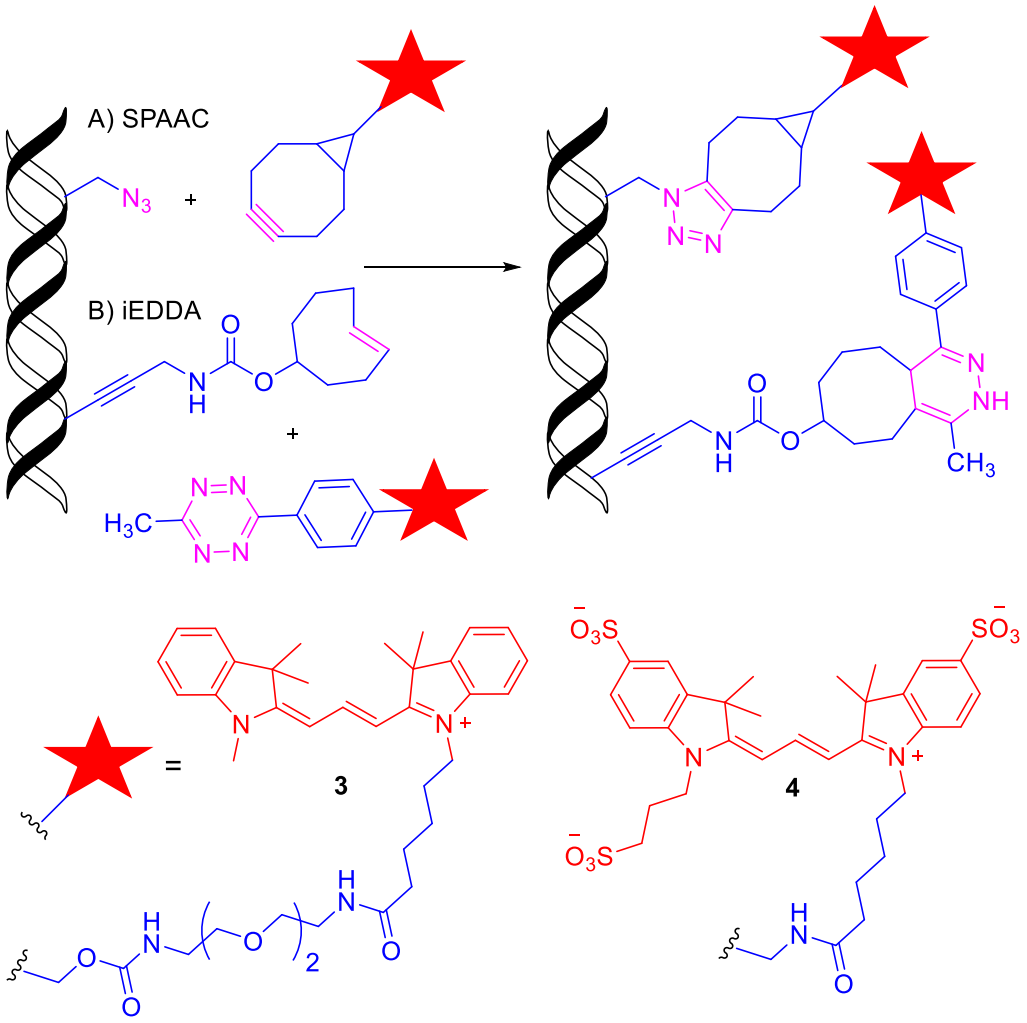

Scheme 6 Post-synthetic modification of DNA using SPAAC and iEDDA.

1.4 Synthesis of base-modified nucleosides and nucleotides

Base-modified 2'-deoxynucleoside triphosphates are usually modified in the positions 5 of pyrimidine[36] and 7 of 7-deazapurine[37] derivatives due to the tolerance of DNA polymerase. The most common method for functionalization of dNTPs involves metal-catalyzed reaction with halogenated nucleosides followed by Yoshikawa phosphorylation (Scheme 7, Path A). Alternatively, copper-catalyzed or strain-promoted azide-alkyne cycloaddition reaction can be utilized to prepare modified nucleosides and nucleotides (chapter 1.4.3 and chapter 1.4.4). In some cases, the functional groups are incompatible with acidic conditions of phosphorylation. In such case, the alternative approach consisting of phosphorylation and subsequent attachment of modification can be used (Scheme 7, Path B).

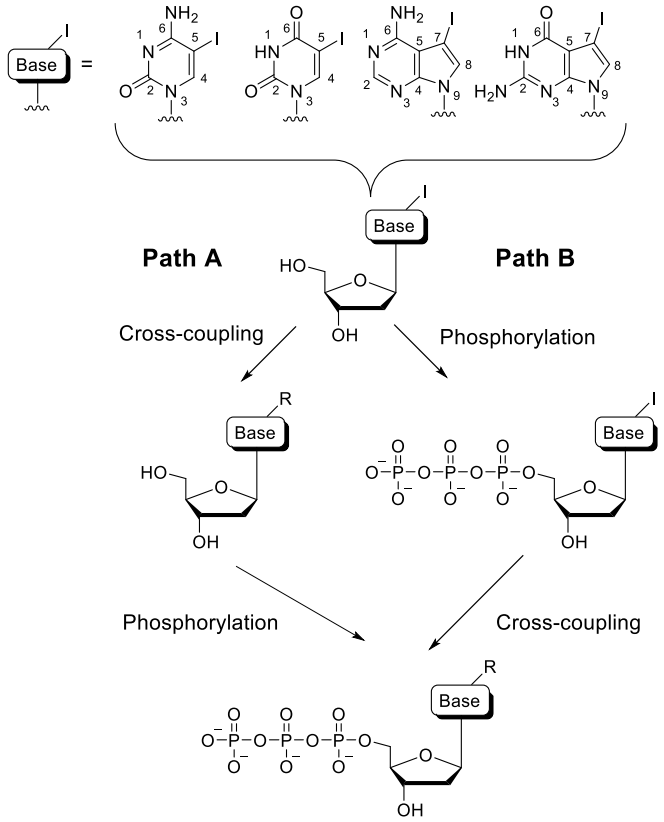

Scheme 7 General synthetic pathway for modified nucleos(t)ides employing cross-coupling and phosphorylation reaction.

1.4.1 Yoshikawa phosphorylation

The most commonly used method for phosphorylation of nucleosides (Scheme 8) was developed by Yoshikawa.[38] The phosphorylation starts by reaction of $POCl_3$ with 2'-deoxynucleoside **5**, which leads to phosphorodichlorate nucleoside **6**. Subsequently, compound **6** undergoes cyclization reaction with pyrophosphate. Final hydrolysis of cyclic triphosphate **7** yields desired product **8**.

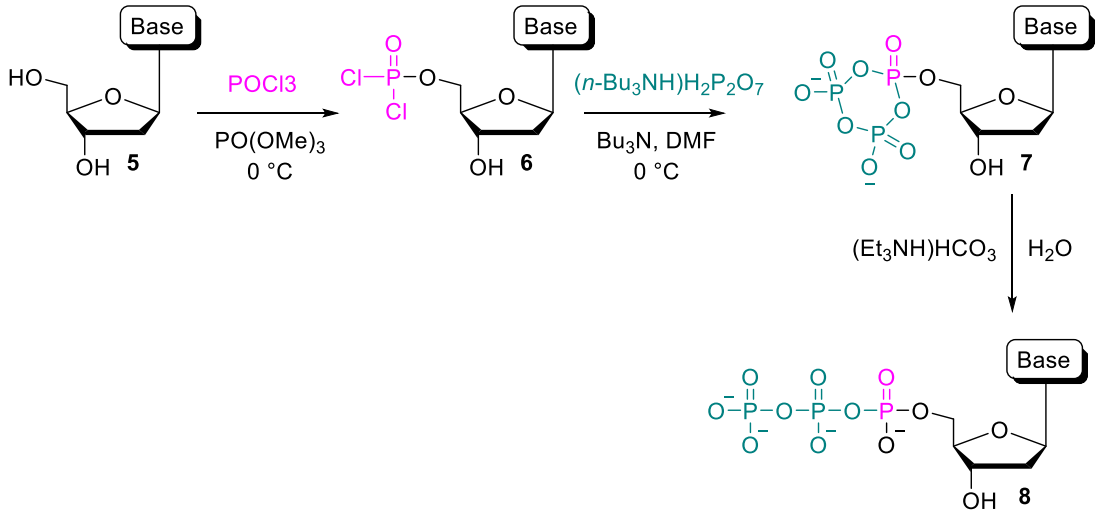

Scheme 8 Yoshikawa's phosphorylation of nucleosides.

1.4.2 Sonogashira cross-coupling reactions

The Sonogashira reaction is useful for the formation of carbon-carbon bond using terminal alkynes and vinyl or aryl halides in presence of palladium catalyst and copper co-catalyst.[39] The mechanism of cross-coupling reaction consists of two catalytic cycles (Scheme 9).[40] In the beginning of the catalytic cycle it is required to generate 14-electron palladium complex $Pd(0)L_2$, which is generally done *in situ* by reduction of palladium(II) complexes by solvents and electron donating ligands (amines, phosphanes). In the first step, the palladium(0) complex undergoes oxidative addition in presence of R^1-X (R^1 = vinyl, aryl, hetaryl; X = I, Br, Cl, OTf). Subsequently, transmetallation with the copper acetylide takes place and

$R^1Pd(-C{\equiv}CR^2)L_2$ complex is formed. Finally, *trans-cis* isomerization and reductive elimination step affords the final product as well as regenerates the catalyst.

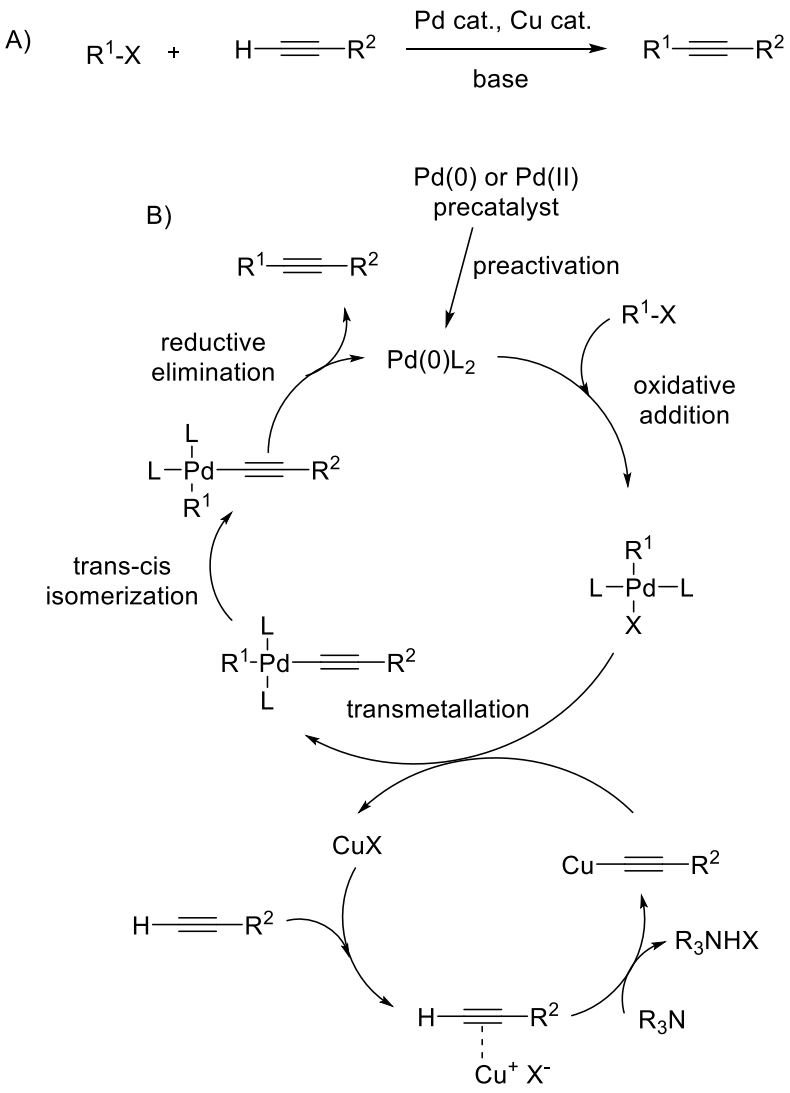

Scheme 9 A) General reaction scheme and B) mechanism of Sonogashira cross-coupling reaction.

This reaction found broad application including modification of nucleosides by fluorescent labels. For example, Sonogashira coupling of 7-iodo-7-deaza-2'-deoxyadenosine **9** with 4-(dimethylamino)phthalimide derivative **10** or 5-iodo-2'-deoxycytidine **12** with fluorene-linked acetylene **13** resulted in fluorescently labelled

nucleosides **11**[41] and **14**[42] (Scheme 10 A, B) which, after phosphorylation, were used for the construction of DNA probes for studying interactions with proteins. Morpholine naphthalimide deoxyuridine nucleoside **17** was prepared by coupling of 5-iodo-2'-deoxyuridne **15** with alkyne **16** (Scheme 10 C). Corresponding nucleoside triphosphate was utilized for the detection of miRNA through rolling circle amplification.[43]

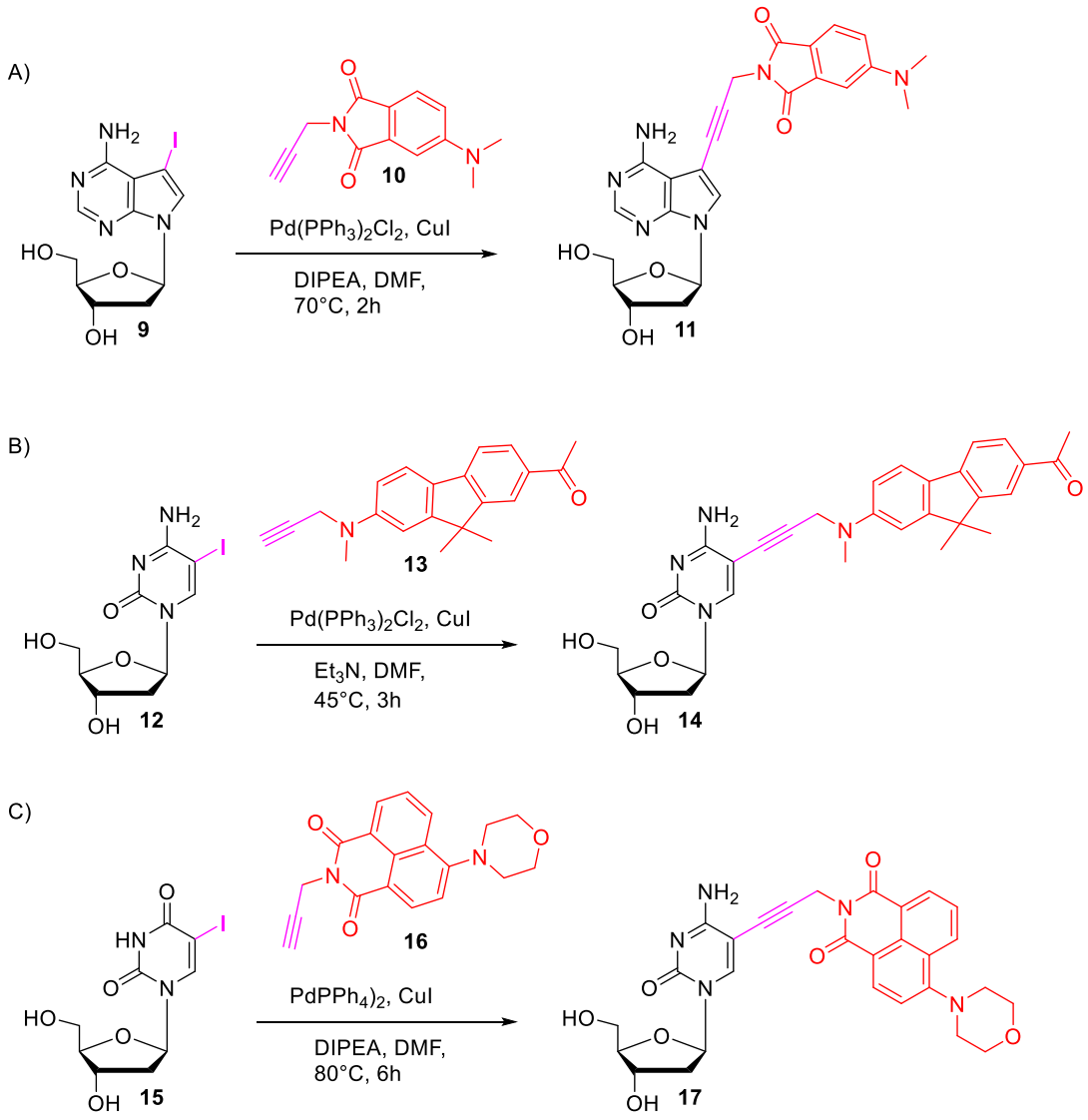

Scheme 10 Synthesis of selected fluorescent nucleosides utilizing Sonogashira coupling.

1.4.3 Copper-catalysed azide-alkyne cycloaddition reactions

The copper-catalyzed click reaction is 1,3-dipolar cycloaddition between an azide and terminal alkyne leading to formation of 1,5-disubstituted 1,2,3-triazoles. The reaction is catalyzed by Cu(I) catalyst which can be used directly or generated *in situ* from Cu(II) salts in presence of reducing agents (such as sodium-L-ascorbate).

CuAAC was studied and introduced by Meldal[44] and Sharpless[45]. There were various reaction mechanism proposals, however a recently suggested pathway (Scheme 11) by Fokin et al.[46] was confirmed by new research.[47] In the first step, Cu(I) coordinates the alkyne and forms π complex which makes the hydrogen of terminal alkyne more acidic. Subsequent deprotonation leads to Cu-acetylide bearing additional π-bound copper. The acetylide coordinates the azide forming a six-membered metallacycle, which afterwards contracts to triazol-copper derivative that finally undergoes protolysis to form the desired triazol product.

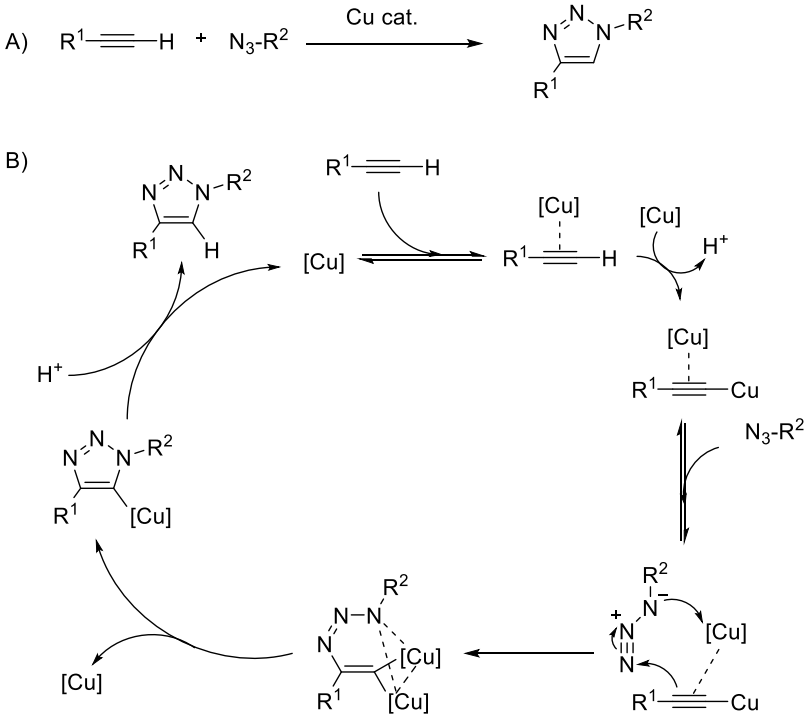

Scheme 11 A) General reaction scheme and B) mechanism of copper-catalyzed azide-alkyne cycloaddition.

The click reaction has been extensively used for modification of nucleic acids.[48,49] Noticeably, CuAAC was achieved even in live cell using 5-ethynyl-2'-deoxyuridine[50] for labelling of genomic DNA. Later, Luedtke group prepared new ethynyl modified nucleosides to study metabolic incorporation into genomic DNA and subsequent CuAAC with fluorescent dyes.[51–53] Recently, they designed new phosphotriester derivative of 5-azidomethyl-2'-deoxyuridine which showed enhanced incorporation into the DNA of cells and even animals.[54] CuAAC was also found to be useful for attaching fluorescent dyes on nucleosides and nucleotides. For example, coumarin-modified pyrimidine nucleoside[55] **20** was synthesized by click reaction of alkyne-modified coumarin **19** and methylazido-modified uridine **18** (Scheme 12 A) or TAMRA-, Sulfo-Cy3-, BODIPY-modified purine nucleotides[56] **22-24** were prepared by click reaction of ethynyl-modified nucleotide **21** with azido derivative of corresponding fluorophore (Scheme 12 B).

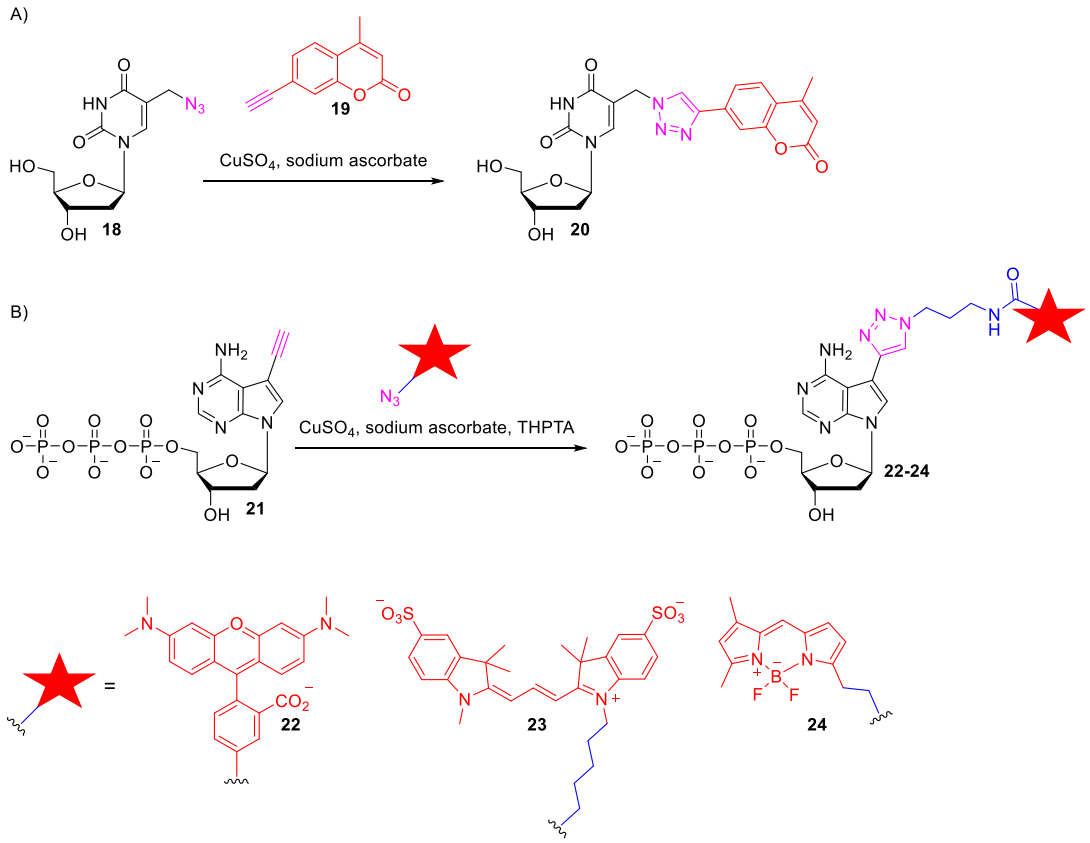

Scheme 12 Synthesis of selected fluorescent nucleos(t)ides utilizing CuAAC.

1.4.4 Strain-promoted azide-alkyne cycloaddition reactions

The strain-promoted 1,3-dipolar cycloaddition of an azide and cyclooctyne derivatives was developed by Bertozzi.[57] Unlike in copper-catalyzed click reaction, SPAAC proceeds in absence of copper and utilizes strained cycloalkynes instead. This copper-free alternative found broad application for labelling of biomolecules[35,58–60] and also cells[61–63]. SPAAC using nucleosides was also explored and described. For instance, the reactions of 8-azido-2'-deoxyadenosine **25** with dibenzocyclooctyne **26** and cyclooctyne **28** led to the formation of click adducts **27** and **29** respectively (Scheme 13).[64]

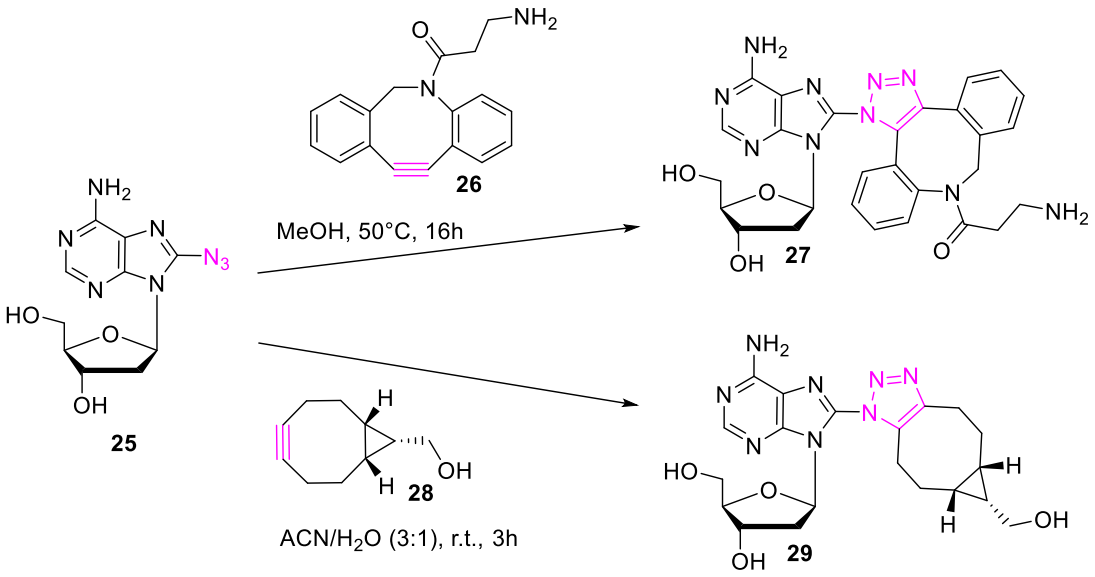

Scheme 13 Synthesis of modified nucleosides utilizing SPAAC.

1.5 Fluorescent dyes

Fluorophores are frequently used for labelling and detection of biomolecules such as amino acids, proteins or antibodies.[65] Among the other labelling methods, such as radioactive labelling,[66] isotope marking,[67] electrochemical[68] or calorimetric[69] sensors, the fluorescent labelling is preferable due to the non-destructive nature and high sensitivity of the technique.[65] Derivatization of synthetic fluorophores produced an array of various fluorophores with broad range of different properties and applications.

Biomolecules are commonly labelled by fluorescein (Figure 4 A) and cyanine dyes (Figure 4 B). Fluorescein is polycyclic dye with absorption maximum at 490 nm and emission at 512 nm in water. An advantage of the dye is the possibility to use 488 nm argon laser which makes it ideal for microscopy.[70] On the other hand, derivatives of fluorescein are prone to photobleaching[71] and are sensitive to pH[72] which makes analysis difficult.

Cyanine dyes possess two heteroaromatic rings (indole, quinoline, benzothiazole etc.) connected by a polymethine chain. The classification and properties of cyanines are dependent on the number of methine groups and the nature of aromatic ring. The most commonly used are Cy3 (λ_{Abs} = 548 nm, λ_{Em} = 563 nm, φ = 0.10), Cy5 (λ_{Abs} = 646 nm, λ_{Em} = 662 nm, φ = 0.28) and Cy7 (λ_{Abs} = 750 nm, λ_{Em} = 773 nm, φ = 0.30). The drawbacks of cyanine dyes include short fluorescence lifetimes, low fluorescence quantum yields and tendency to undergo aggregation in aqueous solution.[73–75]

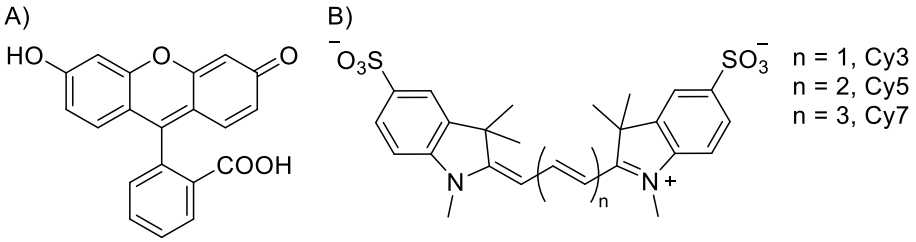

Figure 4 Structure of A) fluorescein and B) cyanine dyes.

Some fluorescent dyes are sensitive to local environment and respond to changes of viscosity or polarity by changing fluorescence properties. This type of probes has been utilized for characterization of cellular structures.[76,77]

Fluorescent molecular rotors are probes generally useful for sensing local viscosity.[78,79] These dyes are usually weakly fluorescent and/or have short fluorescence lifetime due to the intramolecular rotation which causes non-radiative relaxation. One of the most known representatives of fluorescence intensity based probes are 9-(dicyanovinyl)julolidine (DCVJ) and 9-(2-carboxy-2-cyanovinyl)julolidine (CCVJ). These dyes are weakly fluorescent due to the rotation around the julolidine-vinyl bond, however, if the rotation is blocked in highly viscous environment the fluorescence intensity increases (Figure 5).[78–81]

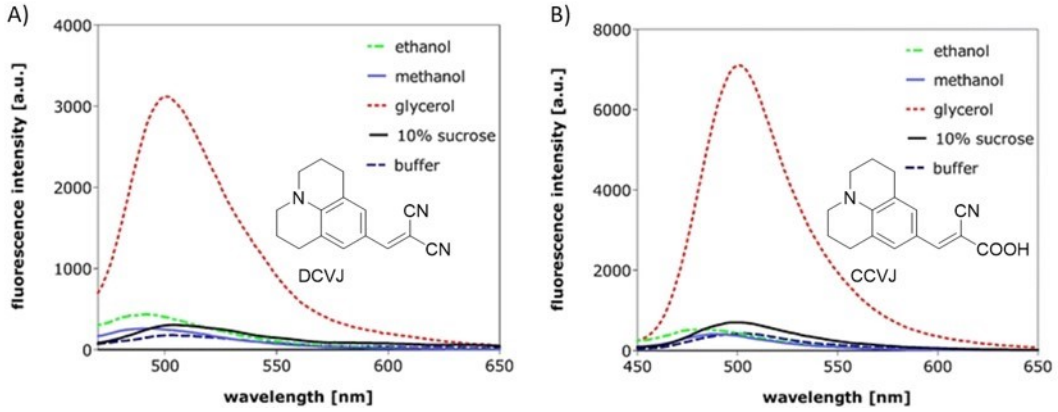

Figure 5 Fluorescence response of A) DCVJ and B) CCVJ in solvents of different viscosity and polarity.[81]

Fluorescence lifetime is another parameter which is useful for probing local environment, particularly because of the independence on the concentration of the fluorophore.[82–84] Probes based on meso-substituted boron dipyrromethene (BODIPY) display excellent sensitivity of fluorescence intensity and lifetime to viscosity. This sensitivity stems from the free intramolecular rotation between phenyl ring and boron dipyrromethene system, which can be restricted in more viscous environment and results in increased quantum yield and/or fluorescence lifetime. These properties

made some rotational BODIPY dyes (Figure 6) very useful for fluorescence lifetime imaging (FLIM) and probing viscosity in biological systems.[85–87]

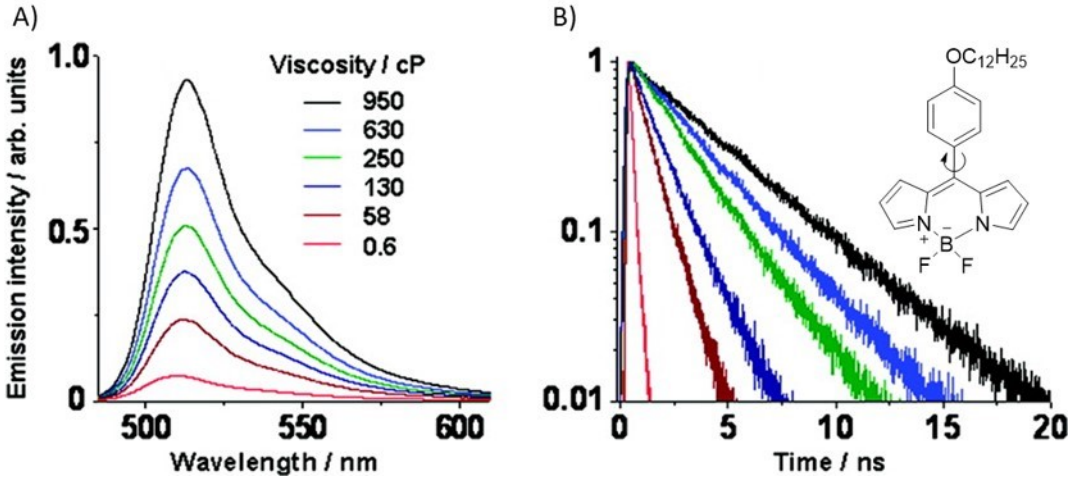

Figure 6 A) Fluorescence spectra and B) decay of BODIPY dye at different viscosity.[86]

Solvatochromic (polarity-sensitive) dyes are based on push-pull systems, in which electron-donating group (push; eg. tertiary amine) and electron-withdrawing group (pull; nitrile, carbonyl or sulfonyl) are connected to a polarizable π-system. Upon excitation the dyes increase dipole moment, the subsequent relaxation of the excited fluorophore is influenced by dipole-dipole interactions with the environment, which influences various photophysical properties of the fluorophores such as emission maxima, fluorescence lifetime and fluorescence quantum yield.[88]

One of the most known solvatochromic dyes is Prodan (Figure 7 A), however this dye absorbs in the UV region and that led to development of new derivatives with extended conjugation such as fluorene analogue (FR0, Figure 7 A) which absorbs at 400 nm. Emission of FR0 range from 434 nm in toluene to 570 nm in methanol.[88,89]

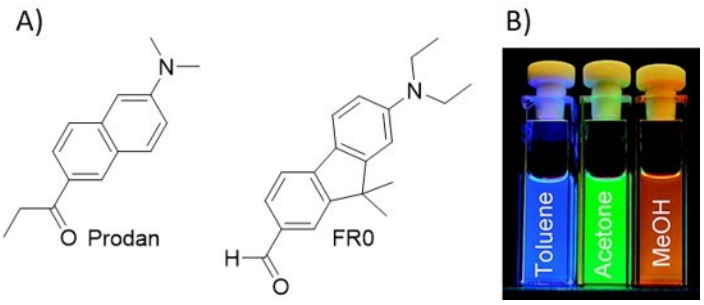

Figure 7 A) Structure of Prodan and FR0. B) Emission of FR0 in different solvents.[88]

Some solvatochromic dyes, for example Nile Red (Figure 8 A), exhibit dramatic increase of fluorescence in hydrophobic environment. This feature has been exploited for detection of lipids and hydrophobic domains.[90,91] Another example of such dye is dimethyl aniline furaldehyde (DAF, Figure 8 A). This dye shows strong fluorogenic response from water (buffer) to oil (2000-fold increase of fluorescence intensity, Figure 8 B) and was employed for imaging and studying of lipid droplets.[92]

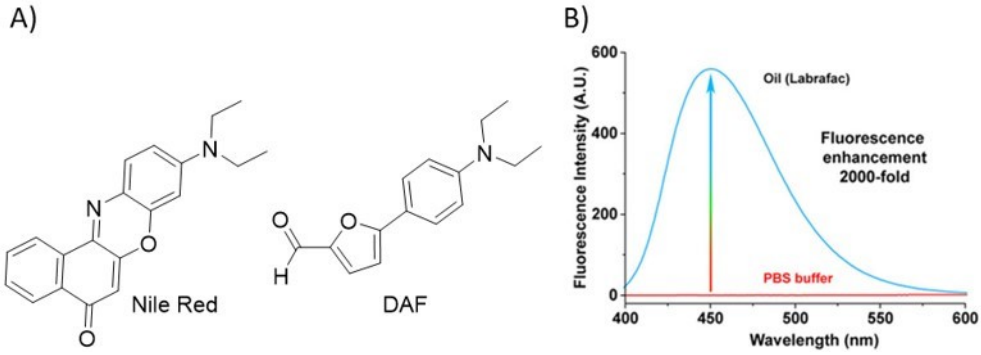

Figure 8 A) Structure of Nile Red and DAF. B) Fluorescence response of DAF in hydrophobic environment.[92]

1.6 Fluorescent nucleosides and nucleotides as tools for studying DNA

1.6.1 Application of DNA probes prepared by chemical synthesis

As it was mentioned in chapter 1.2.1, chemical synthesis of DNA is based on nucleoside phosphoramidites and produces short DNA sequences.

Usage of modified nucleoside phosphoramidites, for example fluorene modified 2'-deoxyuridine (**dU^{FL}**), allows synthesis of modified oligonucleotide probes. Some fluorene-labelled ONs show decrease of fluorescence intensity upon hybridization with not fully complementary ON strand (mismatched base opposit to **dU^{FL}**; dC, dG or dT) but exhibit increase of fluorescence selectively in case of fully matched target (dA opposite to **dU^{FL}**) and therefore can be applied for single nucleotide polymorphism (Figure 9 A).[93]

Another, conceptually different, probe for detection of DNA hybridization was prepared by introducing pyrene derivative (**dU^{Pyr}**) into DNA. Pyrene-modified ssDNA probe showed dual fluorescence at 440 nm and 540 nm and upon hybridization with complementary strand the fluorescence intensity at emission maxima changed, which results in the shift of emission color (Figure 9 B).[94]

Human telomeric DNA probes prepared by incorporation of 5-benzofuran-modified 2'-deoxyuridine (**dU^{BF}**) were used for sensing different DNA G-quadruplex (GQ) structures by change in fluorescence intensity (Figure 9 C). Moreover, these probes allowed detection of small GQ binding molecules.[95]

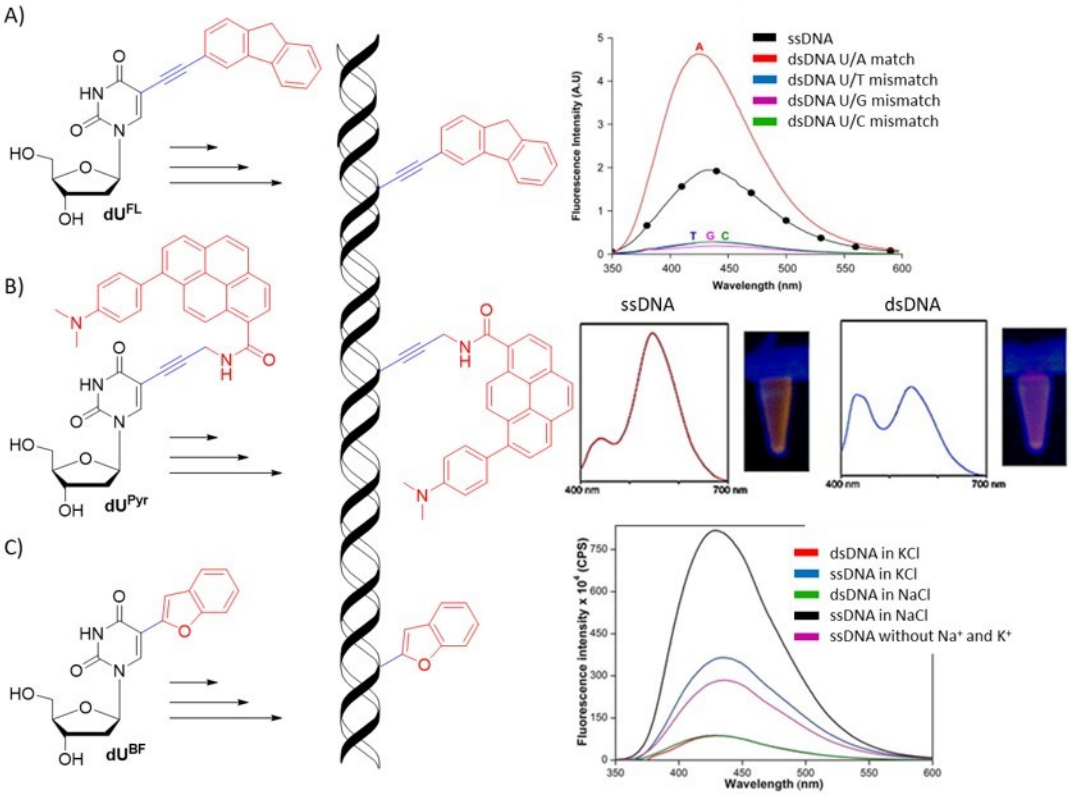

Figure 9 Chemical synthesis of DNA probes using modified nucleoside A) **dU^{FL}**, inset shows response of ssDNA probe in presence of matched or mismatched target,[93] B) **dU^{Pyr}**, inset shows response of ssDNA upon hybridization with complementary strand,[94] C) **dU^{BF}**, inset shows fluorescence response to different GQ structures.[95]

1.6.2 Application of DNA probes prepared by enzymatic synthesis

Synthesis of DNA using DNA polymerases and modified nucleotides enables preparation of various probes for studying DNA. For example, 2'-deoxycytidine 5'-triphosphate bearing dimethylaminobenzylidene fluorophore (**dC^{VDP}TP**) was used to construct intensity-based DNA probe for studying DNA-protein interactions. The probe exhibited 4-fold increase of fluorescence intensity upon binding of single-strand binding protein (SSB; Figure 10 A).[96]

Incorporation of BODIPY-modified nucleotide (**dC^{BDP}TP**) allowed synthesis of fluorescence lifetime DNA probes which were used for sensing interactions with p53 protein and lipids by changes of fluorescence lifetime (0.5-2.2 ns; Figure 10 B).[97]

Acetophenyl-thienyl-aniline modified nucleotide (**dC^{ATA}TP**) was utilized for preparation of solvatochromic DNA probes. These probes showed weak red emission but upon interaction with proteins or lipids a significant shift of emission color (to yellow or green) and an increase of fluorescence was observed (Figure 10 C).[98]

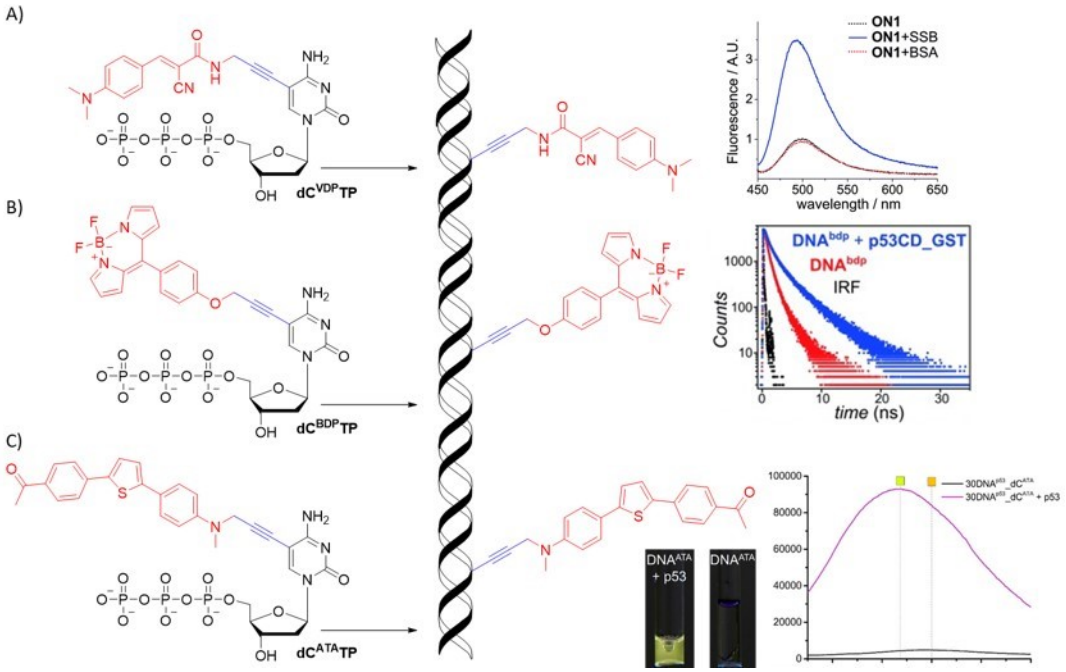

Figure 10 Enzymatic synthesis of DNA using modified nucleotide A) **dC^{VDP}TP**, inset shows fluorescence increase of modified ON upon binding with protein,[96] B) **dC^{BDP}TP**, inset shows fluorescence lifetime increase of modified ON upon binding with protein,[97] C) **dC^{ATA}TP**, inset shows change of emission color and intensity of modified ON upon binding with protein.[98]

1.6.3 Transport of fluorescent nucleosides and nucleotides into cells

Fluorescent labelling and imaging of genomic DNA are important tools for gaining better understanding of cellular processes.[99–101] Cellular DNA is most commonly stained using DNA groove binders[102] or intercalators[103]. However, these approaches are unable to monitor dynamic cellular events such as cell cycle and replication.[104] One possibility to overcome this problem is to use nucleoside bearing a small functional group which undergoes phosphorylation by cellular kinases and then gets incorporated into DNA. Subsequent chemical reaction of modified genomic DNA with fluorescent dye allows localization of DNA (Figure 11 A).[50,52,54,105,106] On the other hand, the common drawback of this method is low efficiency of phosphorylation of modified nucleosides by kinases.[107] Another option is to use nucleoside triphosphates (NTPs), however, various delivery methods had to be developed due to the impermeability of anionic NTPs through the cell membrane. One of the older methods represent microinjection.[108–111] For example, microinjection of **dU^{Cy3}TP** into living human cells enabled detection of chromosome areas in the nuclei (Figure 11 B).[112] Recently, Zawada et al. developed a new method based on synthetic nucleoside triphosphate transporter (SNTT). The transporter consists of cyclodextrin that forms non-covalent inclusion complex with triphosphate moiety of NTP and cell-penetrating peptide capable of crossing the cell membrane. It is hypothesized that upon penetrating to the cell, the transported NTP would be displaced from SNTT complex by cellular NTPs and thus available for DNA synthesis. Described mechanism is illustrated in Figure 11 D. Simplicity and efficiency of this approach makes it very promising for metabolic labelling of DNA.[113] For instance, SNTT in combination with hexamethyl phenyl-BODIPY-dCTP (**dC^{mBDP}TP**) was utilized for staining of chromatin and monitoring of mitosis in living cells (Figure 11 C).[114]

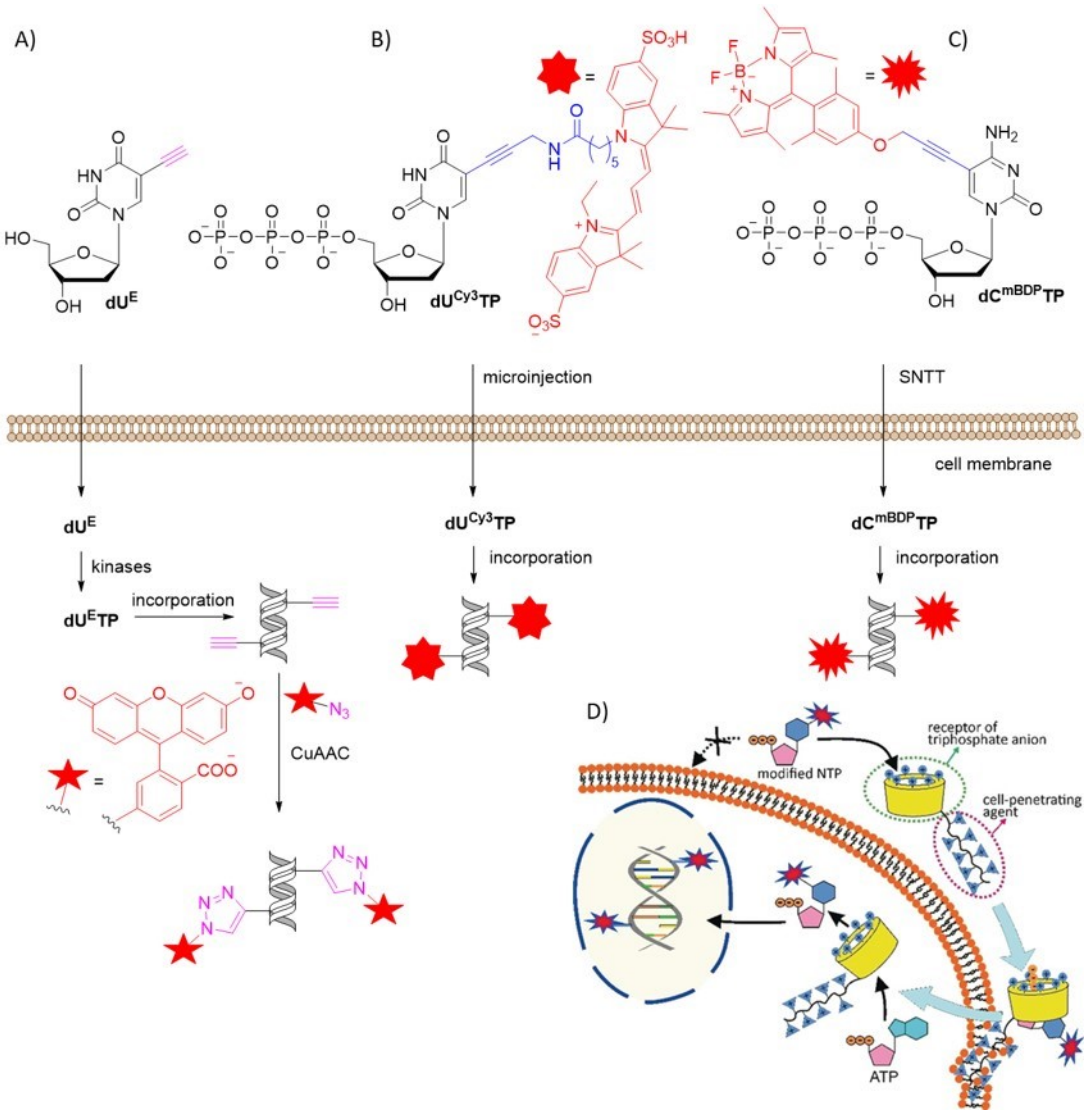

Figure 11 A), B), C) Methods for labelling of genomic DNA using modified nucleos(t)ides. D) Proposed mechanism for SNTT method.[113]

2 SPECIFIC AIMS OF THE WORK

1. Design and synthesis of modified nucleoside, nucleotide and DNA probes bearing tryptophan-based imidazolinone fluorophore to study DNA-protein interactions.

2. Design and synthesis of modified nucleoside, nucleotide and DNA probes bearing benzylidene-tetrahydroxanthylium fluorophore for bioanalytical applications.

3. Design and synthesis of thiazole orange modified nucleotide as fluorescent probe for visualization of DNA synthesis in cells.

4. Design and synthesis of modified nucleosides, nucleotides and DNA probes bearing near-infrared BODIPY fluorophore to study DNA-protein interactions.

5. Design and synthesis of silicon rhodamine modified nucleotide for super-resolution imaging of DNA in cells.

2.1 Rationale of the specific aims

Fluorescent labelling of DNA using fluorescent nucleosides and nucleotides is very important for biochemical[43,115–117] and cell-based[56,112–114,118,119] assays. It is highly desired to develop new fluorescent nucleotides with various characteristics, such as different color of emission, high fluorescence brightness and insensitivity to environment or, on the contrary, environment-sensitive dNTPs that change photophysical properties depending on the microenvironment.

Tryptophan-based imidazolinone fluorophore naturally occurs in cyan fluorescent protein. This fluorophore is fluorescent in native protein, however, free molecule prepared by chemical synthesis or upon denaturation of protein shows very low fluorescence.[120–125] Therefore, this fluorophore has potential for studying interactions of DNA with DNA binding proteins, which could enhance fluorescence by restricting rotation of the fluorophore.

Fluorophores that emit in the near infrared (NIR) region of spectrum are of high interest especially for bioimaging applications due to the deep tissue penetration and minimal interference with autofluorescence of biomolecules.[126,127] Therefore, we opted to use benzylidene-tetrahydroxanthylium[128] NIR dye as new modification for nucleotides and DNA. This fluorophore shows structural characteristics of molecular rotors and also solvatochromic dyes due to the possible rotation between aromatic rings and presence of push-pull-push system. Thus, this fluorophore may exert interesting photophysical behavior and could be promising for studying interactions of DNA with other biomolecules and for imaging applications.

Thiazole orange is well known for its ability to bind nucleic acids and change fluorescence intensity and lifetime depending on the microenvironment.[129–131] We anticipated that nucleotide bearing thiazole orange would change fluorescence intensity and/or lifetime upon incorporation into DNA. The nucleotide with such feature would be immensely unique as it could potentially allow real-time imaging of DNA synthesis in live cells.

BODIPY dyes were previously reported as labels for nucleoside triphosphates and DNA, however, the dyes used showed green emission and the environment-sensitives ones were not suitable for cell experiments.[97,114,132] Therefore, we decided to use rotational NIR BODIPY[133] dye that could be useful for sensing *in vitro* interactions of DNA with proteins by change of fluorescence lifetime and also for sensing changes in cellular environment.

Silicon rhodamine is NIR fluorophore that shows high fluorescence brightness, photostability and compatibility with stimulated emission depletion (STED) microscopy. Silicon rhodamine shows decreased background signal of non-specific hydrophobic interactions due to the propensity to form non-fluorescent spirolactone in nonpolar environment.[134–136] Thus, we planned to use silicon rhodamine modified nucleotide as new tool for super-resolution imaging.

3 RESULTS AND DISCUSSION

3.1 2'-Deoxycytidine and its triphosphate modified by tryptophan-based imidazolinone fluorophore. Synthesis, photophysical properties, enzymatic incorporation into DNA and applications

3.1.1 Introduction

Fluorescent proteins (FPs) represent an important tool for imaging of cellular structures and processes by fluorescence microscopy. Photophysical properties of FPs depend on structure and state of the fluorophore. For example, isomerism, ionization and interaction of fluorophore with biomolecules can have significant effect on spectral properties.[137] One of the most commonly used representative of FPs is green fluorescent protein (GFP).[138] This fluorescent protein contains 4-hydroxybenzylidene imidazolinone fluorophore (Figure 12 A), which is weakly fluorescent as free molecule prepared by chemical synthesis or upon denaturation of protein. The low fluorescence of the free fluorophore is caused by the free rotation between phenol and imidazoline moiety which leads to non-emissive pathway.[139–141] The fluorescence can be induced by blocking the bond rotation, for example by interactions with RNA[142] or proteins[143]. Various fluorescent tags with different photophysical properties were prepared by replacement of tyrosine residue in GFP by other amino acid residues, such as phenylalanine (Figure 12 B), histidine (Figure 12 C) or tryptophan (Figure 12 D).[120]

Inspired by tryptophan-based fluorophore from cyan fluorescent protein (Figure 12 D),[121–123] which is widely used for FRET studies,[124,125] we decided to use the fluorophore as new modification for DNA. Utilizing Sonogashira cross-coupling reaction we prepared 2'-deoxycytidine and its triphosphate bearing tryptophan-based imidazolinone fluorophore and studied their photophysical properties. The modified triphosphate was tested as substrate for enzymatic incorporation into DNA and the modified DNA probe was used for sensing of DNA-protein interactions.

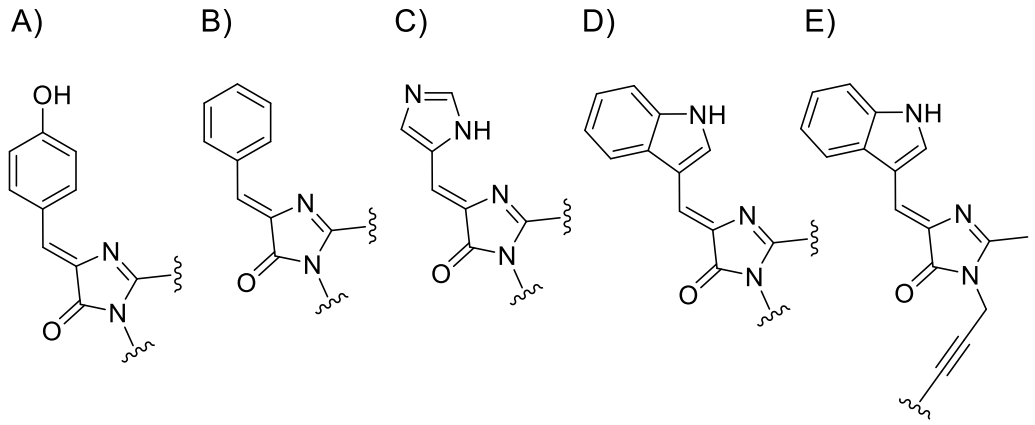

Figure 12 Structure of the chromophore in A) green, B) Sirius, C) blue and D) cyan fluorescent protein. E) Design of our new modification.

3.1.2 Synthesis

The synthesis of modified nucleoside and nucleotide was achieved by the Sonogashira cross-coupling reaction of 5-iodo-2'-deoxycytidine (**dC^{I}**) or the triphosphate (**dC^{I}TP**) with alkyne of the corresponding fluorophore **34** (Scheme 14). The synthesis of alkyne-linked fluorophore **34** was done in analogy to the synthesis of related derivatives.[144,145]

First, utilizing Vilsmeier-Haack formylation, the indole **30** was converted to indole-3-carbaldehyde **31** which subsequently underwent condensation with N-acetyl glycine in acetic anhydride and afforded oxazolone **32** as previously described.[146,147] Acrylamide **33** was then prepared in 60% yield by reaction of oxazolone **32** with propargylamine in DMF. Subsequent dehydration in pyridine led to formation of corresponding propargyl-imidazolinone **34** in 67% yield. The propargyl-linked chromophore **34** was then coupled with a nucleoside utilizing Sonogashira coupling with **dC^{I}**, forming **dC^{Trp}** in 67% yield. The triphosphate **dC^{Trp}TP** was prepared in similar manner using **dC^{I}TP**. Iodinated triphosphate **dC^{I}TP** was prepared following the literature.[148] According to the previous work,[137] the fluorophore can form

inseparable Z/E-isomers. We observed that according to the NMR spectra of compound **34** and nucleoside **dC^{Trp}** the Z-isomer was the major one and the E-isomer was the minor isomer (12-20%). It is noteworthy that the ratios of isomers in solution changed under daylight – seemingly due to the photoisomerization. The NMR spectra of nucleotide **dC^{Trp}TP** showed no isomerization (pure Z-isomer).

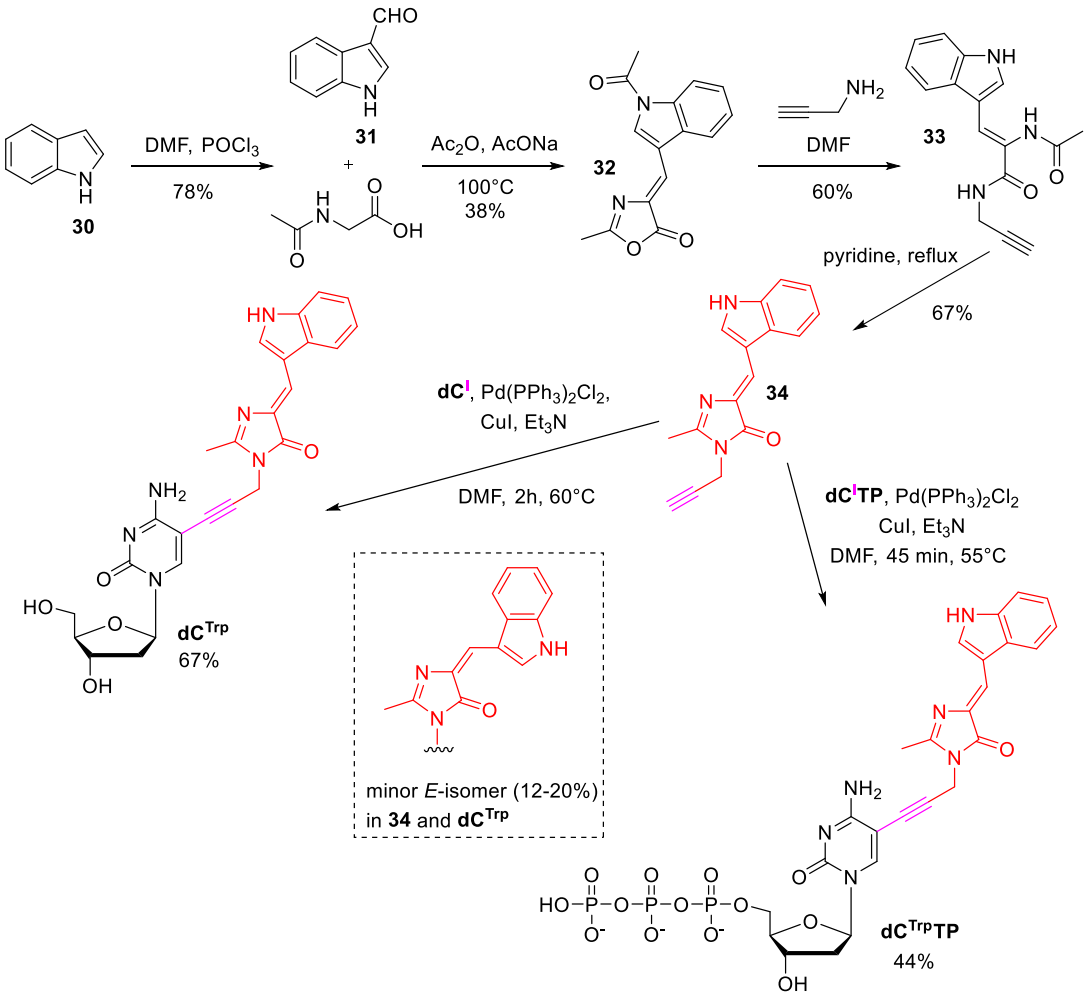

Scheme 14 Synthesis of **dC^{Trp}** and **dC^{Trp}TP**.

3.1.3 Photophysical properties

First, we studied solvatochromic properties of **dC^{Trp}** by measuring the absorption and emission spectra in solvents of different polarity. The results showed moderate solvatochromic effect with absorption maxima between 393-416 nm and emission maxima at 454-470 nm (Figure 13 A, Table 1). Absorption and emission spectra of **dC^{Trp}** were sensitive to pH (Figure 13 C, D). Due to the deprotonation of the indole ring, we observed a transition in absorption spectra at pH 11.5 and two maxima appeared at 453 nm and 473 nm. At pH 12.8, the emission maximum shifted from 469 nm to 498 nm and the fluorescence intensity increased ca. 3-fold.

The modified nucleoside **dC^{Trp}** showed very low quantum yields (0.02-0.04%) in low viscosity solvents (Table 1). On the other hand, significant increase of fluorescence was observed in viscous glycerol (Figure 13 B). These results indicated that the fluorophore could be useful for sensing changes of viscosity and pH in vicinity of DNA.

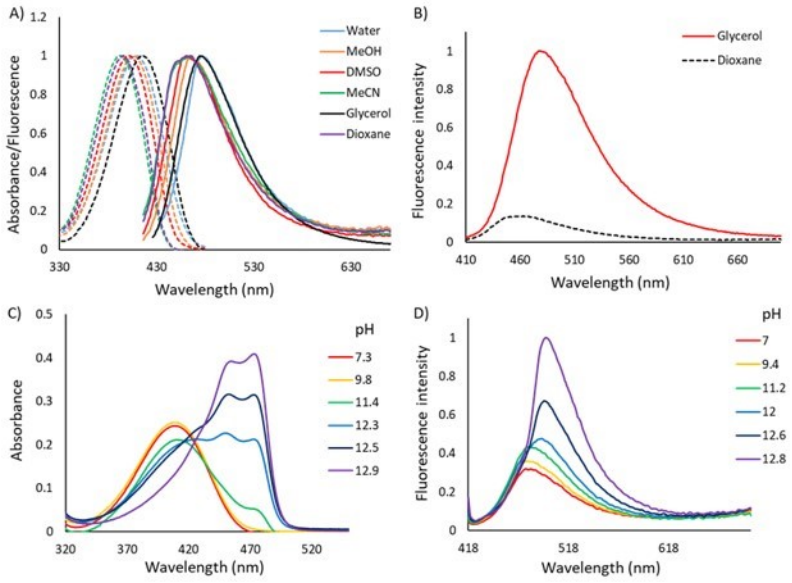

Figure 13 A) Normalized absorption (dashed lines) and fluorescence (solid lines; excitation wavelength was equivalent to the corresponding absorption maxima) spectra of **dC^{Trp}** in solvents of different polarity, B) comparison of fluorescence intensity

(excitation wavelength was 395 nm) of modified nucleoside in low viscosity solvent (dioxane) and viscous glycerol, C) absorption and D) fluorescence spectra (excitation wavelength was 408 nm) of **dC^{Trp}** at different pH in phosphate buffer.

Table 1 Photophysical properties of **dC^{Trp}** in different solvents.

Solvent	**λ_{abs}[a] (nm)**	**ε[b] ($M^{-1}cm^{-1}$)**	**λ_{em}[c] (nm)**	**Φ[d] (%)**
Acetonitrile	393	26645	465	0.027
Dioxane	395	25955	464	0.041
MeOH	406	29361	466	0.029
DMSO	402	25917	460	0.03
Water	408	25696	476	0.032
Glycerol	416	24361	474	0.42

[a] Position of the absorption maximum, [b] molar extinction coefficients, [c] position of the emission maximum, [d] fluorescence quantum yield measured using quinine sulfate in 0.5 M H_2SO_4 (Φ = 0.55 at 25°C) as reference.

3.1.4 Enzymatic synthesis of modified DNA

The modified nucleotide **dC^{Trp}TP** was first tested as a substrate for enzymatic synthesis of DNA by PEX using KOD XL polymerase (Figure 14 A). We studied incorporation using templates encoding for incorporation of one, two or four modified nucleotides (Temp1^{PEX}, Temp3^{PEX}, Temp2^{PEX}, Table 16). In all cases the polyacrylamide gel electrophoresis (PAGE) analysis showed that the primer extension using modified nucleotide gave full length products (Figure 14), which were additionally confirmed by MALDI-TOF analysis (Table 2). In all cases, 30 min reaction time at 60°C was enough to observe full length products.

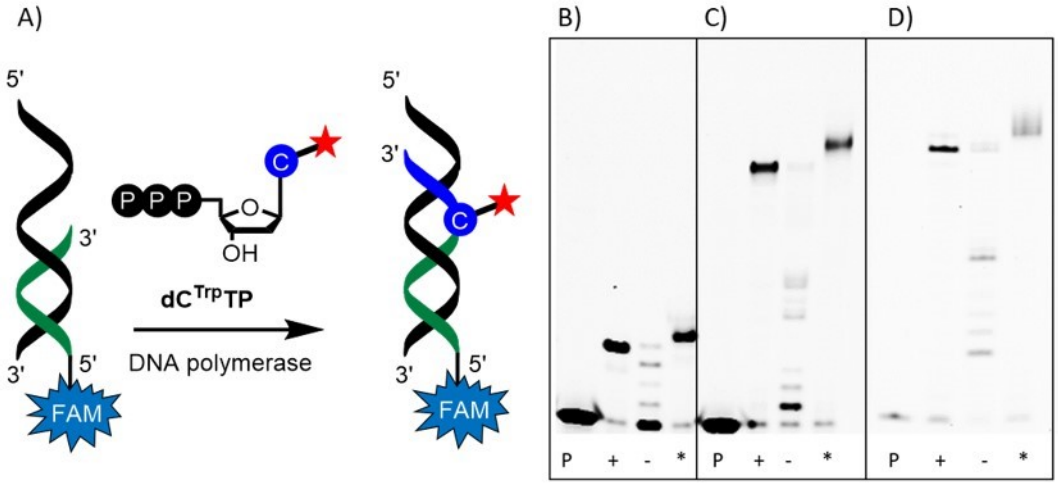

Figure 14 A) Scheme representing PEX with modified nucleotide for gel visualization. PAGE analysis of PEX using **dC^{Trp}TP**, KOD XL DNA polymerase and B) Temp1^{PEX}, C) Temp2^{PEX} or D) Temp3^{PEX} templates encoding for 1, 4 or 2 modifications, respectively. P: primer (Prim1^{PEX}-FAM). Positive control (+): PEX with all four natural dNTPs. Negative control (-): PEX with dATP, dGTP and dTTP in absence of dCTP. PEX with modified dNTP (*): PEX with **dC^{Trp}TP**, dATP, dGTP and dTTP.

Table 2 Table of oligonucleotides prepared in this study.

Oligonucleotide	Sequence (5′→3′). **C***: modified nucleotide.	$M_{calculated}$ (Da)	M_{found} (Da)
ON19_1C^{Trp}	CATGGGCGGCATGGG**C***GGG	6212.2	6212.5
ON31_4C^{Trp}	CATGGGCGGCATGGGA**C***TGAG**C***T**C***ATG**C***TAG	10662.5	10661.3
ON30_2C^{Trp}	TCAAGAGACATGCCTAGA**C***ATGT**C***TATTAT	9711.7	9711.7

Then we measured absorption and fluorescence spectra of the PEX product bearing 4 modifications **DNA31_4C^{Trp}**. Graphs in Figure 15 show that when the PEX was done in absence of KOD XL there was no fluorophore present in DNA, whereas in presence of the polymerase the purified DNA showed absorption and fluorescent properties corresponding to the chromophore.

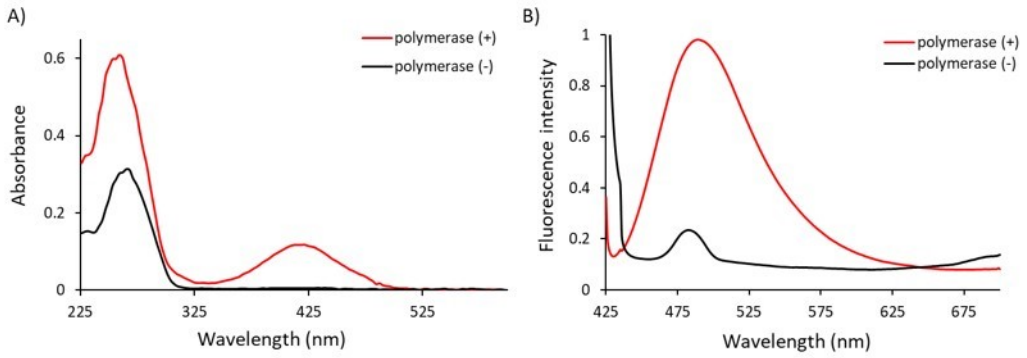

Figure 15 A) UV-vis absorption spectra (λ_{abs} = 416 nm) and B) fluorescence spectra (λ_{ex} = 416 nm, λ_{em} = 489 nm) of DNA obtained after incubation of the PEX reaction mixtures containing Prim1^{PEX}, Temp2^{PEX}, dATP, dGTP, dTTP, **dC^{Trp}TP** either with (red line) or without (black line) KOD XL DNA polymerase.

For testing PCR amplification, we used 98-mer (Temp1^{PCR}) and 235-mer (Temp2^{PCR}) DNA template. The amplification was done with different proportions of **dC^{Trp}TP** and dCTP in presence of natural triphosphates (dATP, dTTP and dGTP). The PCR using 98-mer template was efficient even if the dCTP was completely replaced by **dC^{Trp}TP**, on the other hand the amplification with 235-mer template was

less efficient and the sufficient amplification was observed at the percentage of 40% **dC^{Trp}TP** in regard to dCTP. In all cases, the mobility of modified DNA was slower than the natural DNA (positive control), which can be seen by visible shift on the agarose gels (Figure 16).

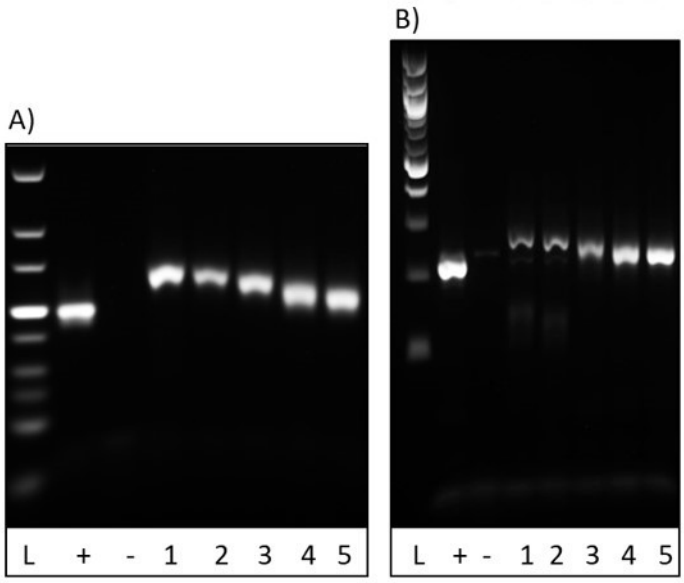

Figure 16 Agarose gel electrophoresis analysis of PCR amplification of 98-mer A) and 235-mer B) template with KOD XL polymerase and **dC^{Trp}TP**. L: DNA ladder. Positive control (+): all natural dNTPs are present. Negative control (-): absence of natural dCTP. PCR with modified dNTP (lane 1-5): dGTP, dTTP, dATP and a mixture of dCTP and **dC^{Trp}TP** (the content of **dC^{Trp}TP** decreases from 100% (lane 1) to 20% (lane 5)) is present.

3.1.5 Interaction of modified DNA with proteins

To test the potential of **dC^{Trp}** nucleotide for sensing interactions with proteins, we prepared single-stranded oligonucleotide bearing 1 modification (**ON19_1C^{Trp}**). This ON was prepared by primer extension and subsequent magnetoseparation[149]. With the ON probe **ON19_1C^{Trp}** in our hands, we studied its interaction with single-

strand binding protein from E. coli (SSB),[150,151] in similar manner as in previous works.[96,143] Upon addition of SSB (0.5 equivalents) to ON probe we observed ca. 2-fold increase in fluorescence intensity of the probe (Figure 17). The ratio of ON and SSB was 2:1 in accordance to the previous reports[151] stating that it is necessary to have at least 56-mer ON in order to wrap around the SSB tetramer. In order to prove that the increase of fluorescence was due to the interaction of DNA with protein, we performed negative control experiment with DNA non-binding protein bovine serum albumin (BSA), which resulted in no change of fluorescence intensity. This control experiment clearly shows that the increase in **ON19_1C^{Trp}** fluorescence is due to the interaction with SSB, which most likely increases viscosity in proximity of the modification.

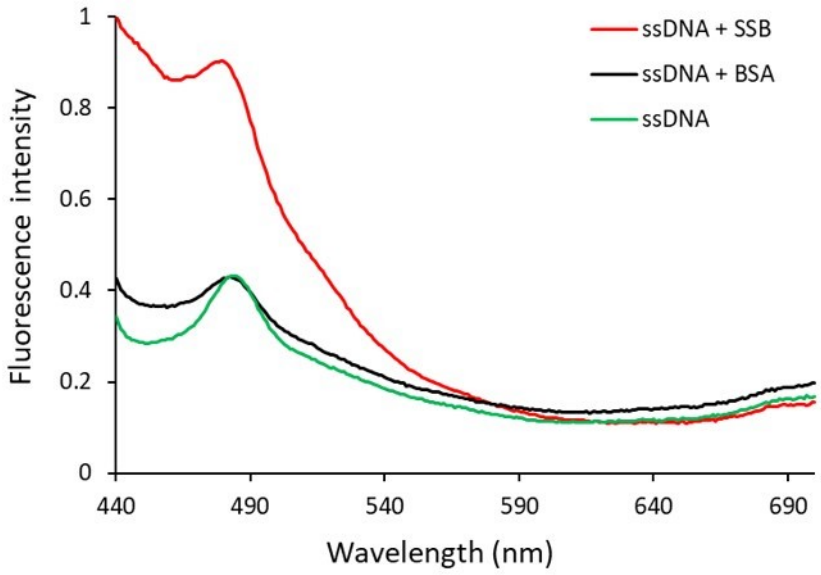

Figure 17 Emission spectra of **ON19_1C^{Trp}** in absence and in presence of SSB protein or BSA.

3.2 Thymidine and its triphosphate modified by benzylidene-tetrahydroxanthylium fluorophore. Synthesis, photophysical properties, enzymatic incorporation into DNA and applications

3.2.1 Introduction

Fluorescent dyes emitting in the near infrared (NIR) region of spectrum are widely used in biosensing and bioimaging applications. Main advantages of NIR dyes include deep tissue penetration and minimal interference with autofluorescence of biomolecules. These fluorophores emit at 650-900 nm and the most used representatives are cyanine dyes.[126,127] However, the drawback of common NIR dyes is problematic solubility in aqueous solutions, tendency to form aggregates and small Stokes shifts (<30 nm).[152] In contrast, fluorescent dyes based on benzylidene-tetrahydroxanthylium systems show large Stokes shifts (≈80 nm), solubility in aqueous solutions and emission in the NIR region (≈740 nm).[128]

Inspired by tetrahydroxanthylium-based fluorophores (Figure 18 A), we designed new alkyne derivative of the dye (Figure 18 B), attached it to the nucleoside and nucleotide using CuAAC reaction and subsequently studied their photophysical properties. The modified nucleotide was enzymatically incorporated into DNA and the modified DNA was used as probe to study DNA hybridization and interactions with other (bio)molecules. Use of modified nucleotide was also tested for real-time PCR and for cell-based experiments.

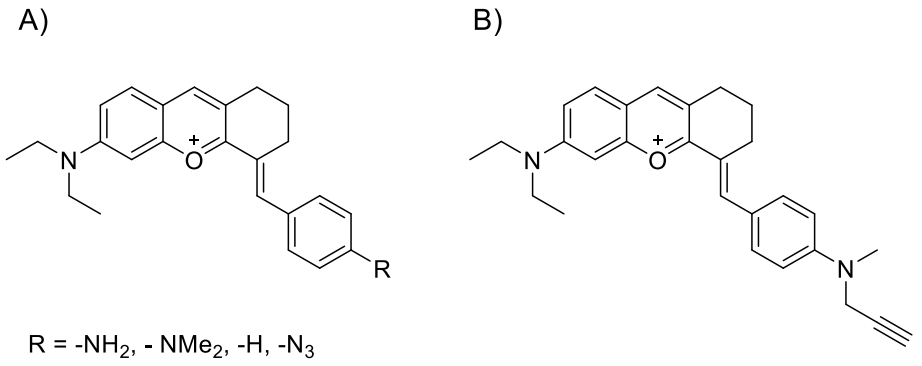

Figure 18 Structure of A) reported benzylidene-tetrahydroxanthylium dyes and B) our new fluorescent label based on benzylidene-tetrahydroxanthylium skelet.

3.2.2 Synthesis

The synthesis of fluorescent nucleoside and nucleotide was accomplished by CuAAC reaction of azido modified thymidine (**dT^{N3}**) or the triphosphate (**dT^{N3}TP**) with alkyne **43** (Scheme 17).

Azido modified thymidine **dT^{N3}** and its triphosphate **dT^{N3}TP** were prepared according to the literature.[35,61] First step of the synthesis is protection of thymidine **35** using tert-butyldiphenylsilyl chloride. Protected thymidine **35** then undergoes radical bromination followed by substitution using sodium azide. Finally, deprotection of protected azido thymidine **37** yields **dT^{N3}** which is subsequently phosphorylated to triphosphate **dT^{N3}TP**.

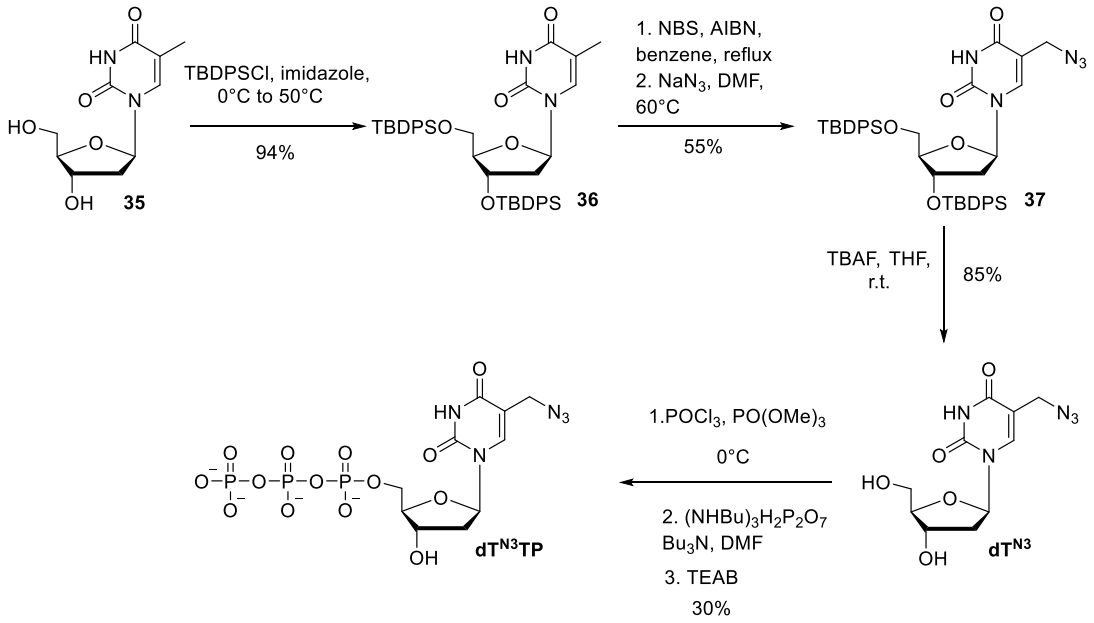

Scheme 15 Synthesis of **dT^{N3}** and **dT^{N3}TP**.

6-(Diethylamino)-1,2,3,4-tetrahydroxanthylium **39** was prepared by reaction of 4-(diethylamino)salicylaldehyde **38** with cyclohexanone in sulfuric acid as previously described.[128] The benzaldehyde **42** was prepared by propargylation of N-methylaniline **40** and subsequent formylation reaction of aniline **41**.[153]

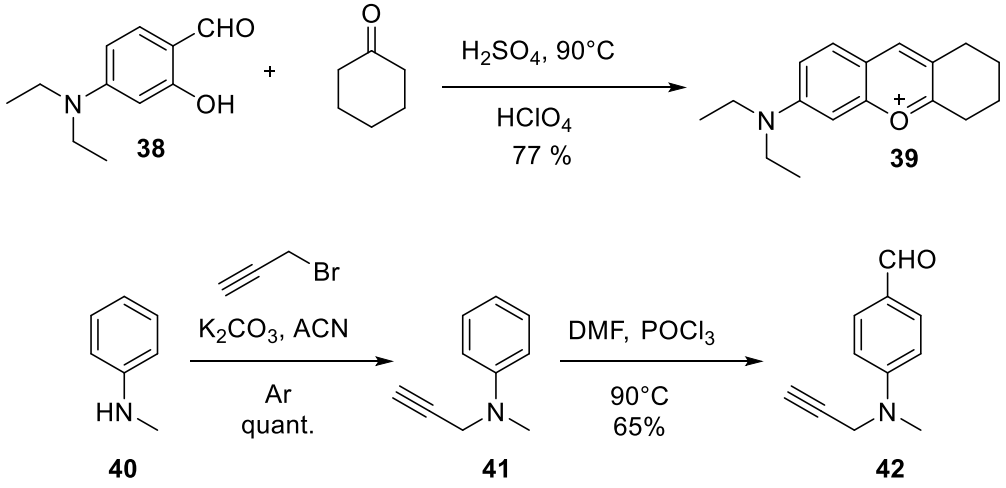

Scheme 16 Synthesis of tetrahydroxanthylium **39** and benzaldehyde **42**.

The alkyne **43** was prepared by condensation of tetrahydroxanthylium **39** with benzaldehyde **42** in acetic acid, similarly as the synthesis of related fluorophores.[128] Utilizing CuAAC reaction of alkyne **43** with **dT^{N3}** and **dT^{N3}TP**, the modified nucleoside **dT^{NNIR}** and nucleotide **dT^{NNIR}TP** were obtained in 55% and 25% yield respectively.

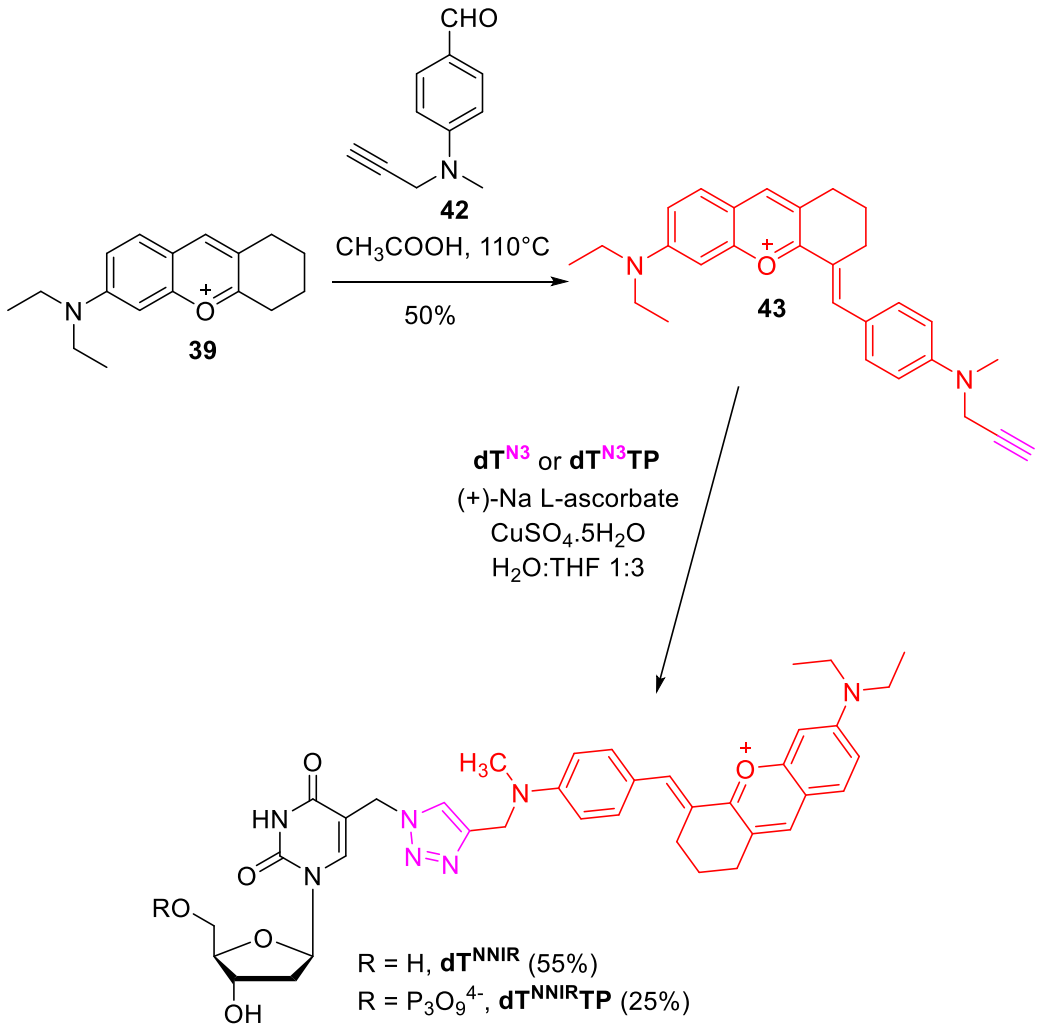

Scheme 17 Synthesis of **dT^{NNIR}** and **dT^{NNIR}TP**.

3.2.3 Photophysical properties

UV-vis absorption and fluorescence spectra of nucleoside **dT^{NNIR}** were measured in different solvents in order to evaluate solvatochromic properties. Absorption maxima were significantly dependent on solvent polarity (λ_{abs} = 622-694 nm), in the most polar solvent (water) the absorption maximum was at 622 nm and in dioxane at 694 nm. Emission maxima showed moderate sensitivity towards polarity (λ_{em} = 749-760 nm) and the modified nucleoside showed overall lage Stokes shifts ($\Delta\lambda$ = 60-127 nm). On the other hand, the intensity of fluorescence was strongly dependent on polarity and we observed ca. 14-fold increase of fluorescence quantum yield in dioxane (Φ = 4.55%) in comparison with quantum yield in water (Φ = 0.33%). Photophysical properties and summarized in Table 3.

The fluorogenic response was illustrated by measuring fluorescence of nucleoside in dioxane/water mixtures of different proportions. Figure 19 C shows that gradual increase of fluorescence was observed when the polarity of solvent mixture decreased. **NNIR** modification shows similar structural characteristics of common solvatochromic dyes due to the presence of push-pull-push system, therefore the relaxation of the excited fluorophore might be influenced by dipole-dipole interactions with the environment and lead to increased fluorescence intensity. To study the sensitivity of **dT^{NNIR}** to viscosity, we measured the fluorescence of the nucleoside in viscous solvent (glycerol) and compared it with the fluorescence in water. As expected, the fluorophore attached to the nucleoside behaved as molecular rotor and we observed 24.8-fold higher quantum yield in glycerol (Φ = 8.2%) than the quantum yield in water (Φ = 0.33%). Moreover, the response of **dT^{NNIR}** to the viscosity was demonstrated by measuring the solution of modified nucleoside in glycerol at different temperatures (viscosity), which showed gradual increase of fluorescence intensity due to the inhibited rotation of the fluorophore (Figure 19 B, Table 4). This behavior of the fluorophore is very interesting and could be useful for sensing environmental changes in proximity of DNA.

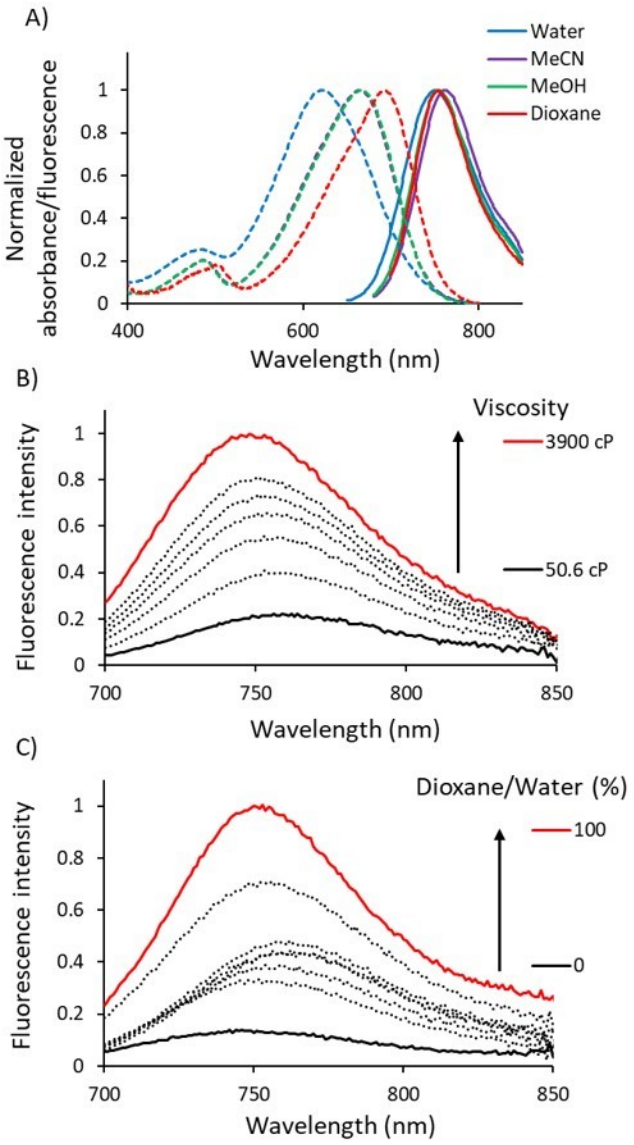

Figure 19 A) Normalized absorption (dashed lines) and fluorescence (solid lines) spectra of **dT^{NNIR}** in solvents of different polarity. B) Fluorescence spectra of **dT^{NNIR}** (λ_{ex} = 690 nm) in glycerol at different temperature (viscosity). C) Emission of **dT^{NNIR}** (λ_{ex} = 613 nm) in various dioxane/water ratios.

Table 3 Photophysical properties of modified nucleoside, nucleotide and DNA.

Sample	Solvent	λ_{abs}[a] (nm)	ε[b] (M^{-1} cm^{-1})	λ_{em}[c] (nm)	$\Delta\lambda$[d] (nm)	Φ[e] (%)
dT^{NNIR}	Water	622	20826	749	127	0.33
	MeCN	664	30703	760	96	0.28
	MeOH	666	35116	754	88	0.56
	1,4-Dioxane	694	16160	754	60	4.55
$dT^{NNIR}TP$	Water	623	11746	745	122	0.37
DNA19_1T^{NNIR}	Phosphate buffer	690	n.d.	745	55	6.84

[a] Position of the absorption maximum, [b] molar extinction coefficients, [c] position of the emission maximum, [d] Stokes shift, [e] fluorescence quantum yield measured using indocyanine green in DMSO (Φ = 0.13 at 25 °C) as reference, n.d. = not determined.

Table 4 Fluorescence quantum yields of modified **dT^{NNIR}** at different viscosity (solution of nucleoside in glycerol was measured at different temperatures).

Temperature (°C)	Viscosity (cP)	Φ[e] (%)
10	3900	11.0
20	1410	9.0
25	945	8.2
30	612	7.4
40	284	6.2
50	142	4.6
70	50.6	2.5

3.2.4 Enzymatic synthesis of modified DNA

The enzymatic incorporation of modified nucleotide **dT^{NNIR}TP** was examined in primer extension (Figure 20 A) and polymerase chain reaction experiments using KOD XL DNA polymerase. At first we tested incorporation of one fluorescent modification into DNA by PEX with short 19-mer template (Temp5^{PEX}) encoding for incorporation of one modification. PAGE analysis showed that **dT^{NNIR}TP** was accepted as substrate by enzyme and full length product was observed (Figure 20 B). The incorporation was somewhat slower and extended reaction time (60 min at 60°C) was required. Identity of product was also confirmed by MALDI-TOF analysis (Table 5). However, PEX with 31-mer template (Temp2^{PEX}) encoding for incorporation of 4 modifications failed and we did not observe full length product (Figure 20 C).

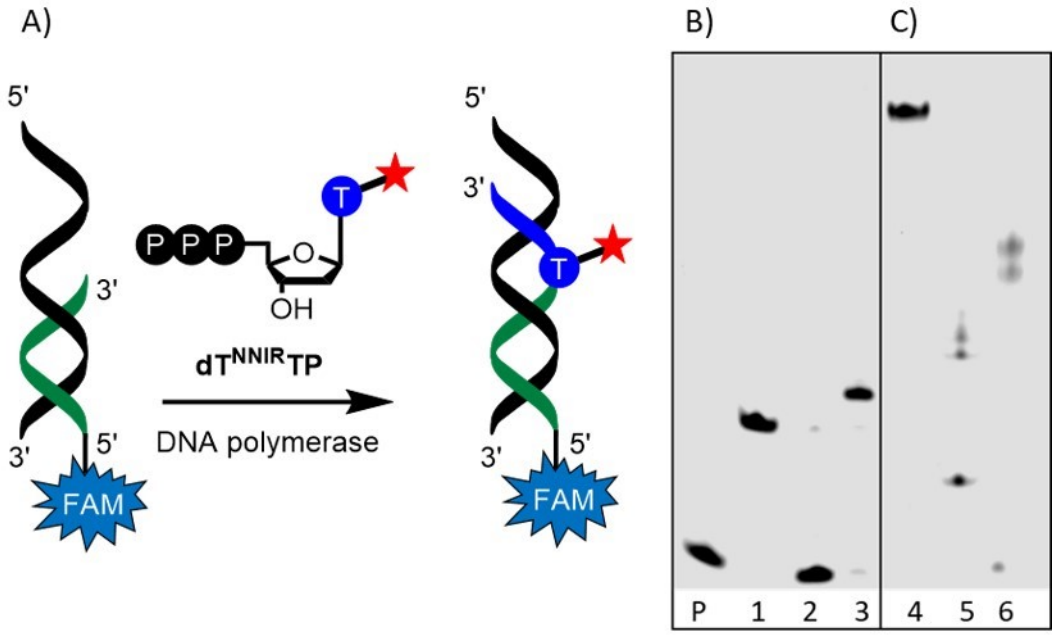

Figure 20 A) Scheme representing PEX with modified nucleotide for gel visualization. PAGE analysis of PEX using **dT^{NNIR}TP**, KOD XL DNA polymerase B) Temp5^{PEX}, C) Temp2^{PEX}. Primer (P), positive control (lane 1, 4; PEX with all natural dNTPs), negative control (lane 2, 5; PEX in absence of dTTP). PEX with **dT^{NNIR}TP** (lane 3, 6).

Alternatively, longer DNA was prepared by single-nucleotide incorporation (SNI), followed by extension of primer with natural dNTPs (Figure 21). Use of biotinylated template (Temp6^{PEX}-bio) allowed separation of ssDNA by magneto-separation.

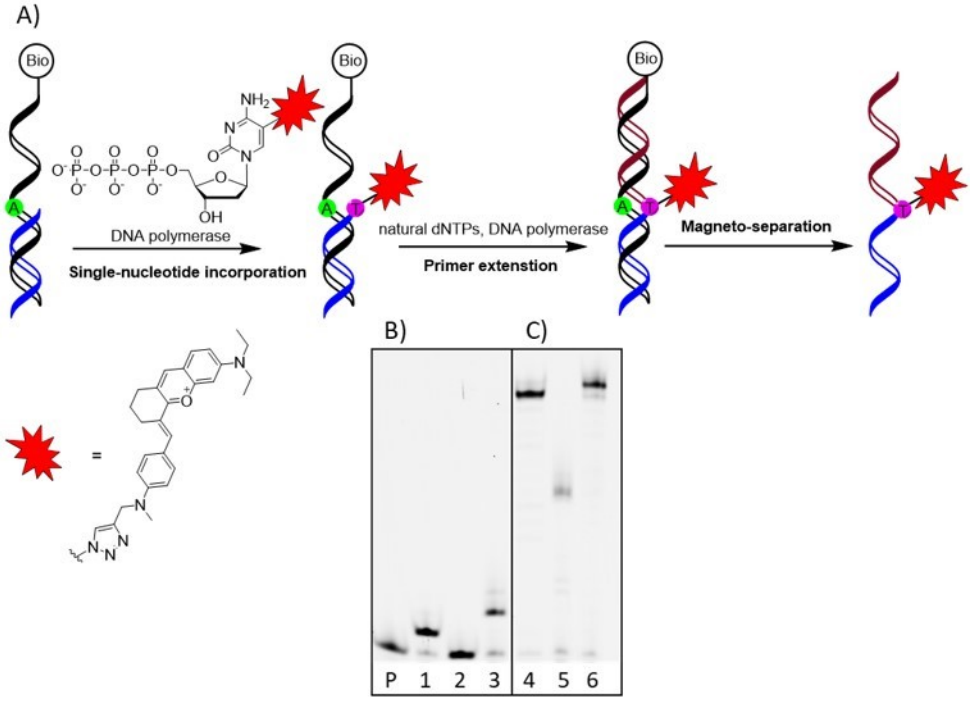

Figure 21 A) Illustration of SNI-PEX method with **dT^{NNIR}TP**. Page analysis of products of polymerase synthesis of oligonucleotides bearing a single modification by SNI-PEX. Primer (P); lane 1: positive control for SNI (only natural dTTP present); lane 2: negative control for SNI (no dNTPs present); lane 3: SNI with modified nucleotide (only **dT^{NNIR}TP** is present); lane 4: positive control for PEX (all natural dNTPs present); lane 5: negative control for PEX (absence of natural dTTP); lane 6: PEX with primer extended by **dT^{NNIR}TP** (all natural dNTPs present).

Table 5 Table of oligonucleotides prepared in this study.

Oligonucleotide	Sequence (5′→3′). T*: modified nucleotide.	$M_{calculated}$ (Da)	M_{found} (Da)
ON16_1T^{NNIR}	5′-CATGGGCGGCATGGG**T***-3′	5430.6	5431.7
ON19_1T^{NNIR}	5′-CATGGGCGGCATGGG**T***GGG-3′	6418.2	6419.6
ON19_1T^{N3}	5′-CATGGGCGGCATGGG**T***GGG-3′	6006.9	6007.9
ON31_1T^{NNIR}	5′-CATGGGCGGCATGGG**T***CTGAGCTCATGCTAG-3′	10060.6	10060.6
ON31_4T^{N3}	5′-CATGGGCGGCATGGGAC**T***GAGC**T***CA**T***GC**T***AG-3′	9781.4	9782.0

Fluorescently labelled DNA was also prepared by CuAAC reaction of alkyne **43** with azido-modified DNA. Oligonucleotides containing 1 (**ON19_1T^{N3}**) or 4 (**ON31_4T^{N3}**) azido groups were prepared by PEX with **dT^{N3}TP** (Figure 22 shows PAGE) and subsequent magneto-separation. CuAAC reaction was analyzed by PAGE, showing successful reaction (Figure 23 B, C).

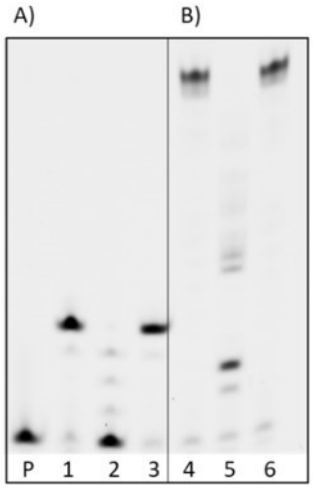

Figure 22 PAGE analysis of PEX using **dT^{N3}TP**, KOD XL DNA polymerase A) Temp5^{PEX} B) Temp2^{PEX}-TINA. Primer (P), positive control (lane 1, 4; PEX with all natural dNTPs), negative control (lane 2, 5; PEX in absence of dTTP). PEX with **dT^{N3}TP** (lane 3, 6).

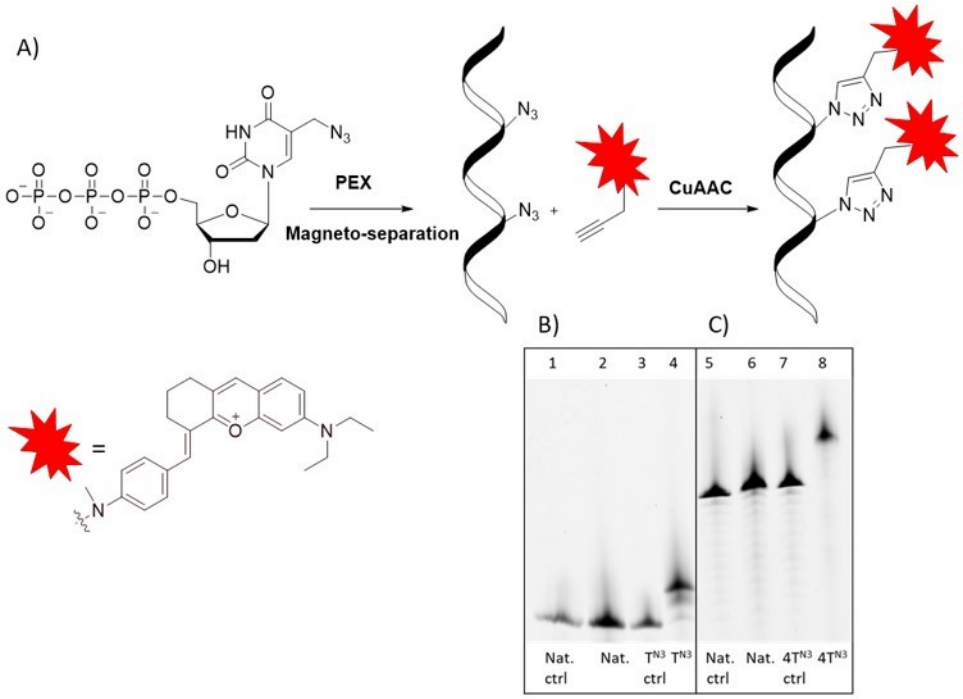

Figure 23 A) Illustration of CuAAC reaction of alkyne **43** with azido-modified DNA. Page analysis of CuAAC reaction performed using B) **ON19_1T^{N3}** or B) **ON31_4T^{N3}** with alkyne **43**. Lane 1, Nat. ctrl: natural ssDNA (ON19_1T) control before click reaction. Lane 2, Nat.: natural ssDNA (ON19_1T) treated in the conditions of click reaction. Lane 3, T^{N3} ctrl: **ON19_1T^{N3}**. Lane 4, T^{N3}: click reaction with **ON19_1T^{N3}**. Lane 5, Nat. ctrl: natural ssDNA (ON31_4T) control before click reaction. Lane 6, Nat.: natural ssDNA (ON31_4T) treated in the conditions of click reaction. Lane 7, 4T^{N3} ctrl: **ON31_4T^{N3}**. Lane 8, 4T^{N3}: click reaction with **ON31_4T^{N3}**.

Polymerase chain reaction was tested using different ratio of modified nucleotide **dT^{NNIR}TP** or **dT^{N3}TP** and natural dTTP (in presence of the natural dCTP, dATP and dGTP). In case of **dT^{NNIR}TP**, the PCR was problematic and a good amplification was observed when using only 10% or 5% of **dT^{NNIR}TP**, in experiment with 20% of **dT^{NNIR}TP** we observed formation of shorter product. Identity of modified DNA was proved by measuring fluorescence spectra of isolated PCR products (Figure 25). PCR amplification with **dT^{N3}TP** was efficient even in the absence of

natural dTTP, which was not surprising as the azido modification is very small and therefore tolerated by DNA polymerase. Agarose gels of PCR are shown in Figure 24.

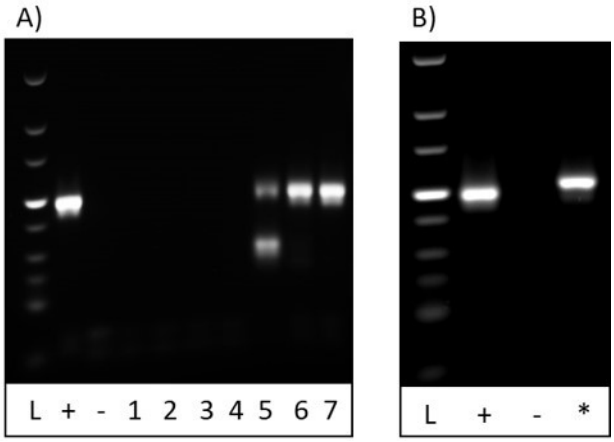

Figure 24 Agarose gel electrophoresis analysis of PCR amplification of 98-mer template (Temp1^{PCR}) with KOD XL polymerase and A) **dT^{NNIR}TP** or B) **dT^{N3}TP**. L: DNA ladder. Positive control (+): all natural dNTPs are present. Negative control (-): absence of natural dTTP. PCR with modified dNTP (*): **dT^{N3}TP**, dATP, dGTP and dCTP is present. PCR with modified dNTP (lane 1-7): dGTP, dCTP, dATP and a mixture of dTTP and **dT^{NNIR}TP** (the content of modified nucleotide decreases from 100% (lane 1) to 5% (lane 7)) is present.

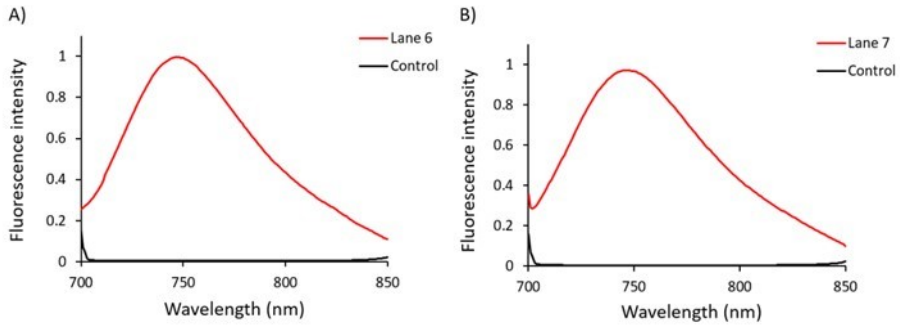

Figure 25 Fluorescence spectra of isolated PCR products and control experiments (PCR mixtures in absence of enzyme). Product of PCR with A) 10% or B) 5% **dT^{NNIR}TP** in mixture with natural dTTP. Lane 6 – product loaded on gel in Figure 23 A, Lane 7 – product loaded on gel in Figure 24 A).

3.2.5 Photophysical properties of modified DNA

At first we performed the same experiment as in previous chapter (chapter 3.1.4, Figure 15) using **dT^{NNIR}TP**. This experiment shows absorption and fluorescence spectra of purified DNA after PEX with **dT^{NNIR}TP** and in presence or absence of KOD XL DNA polymerase (Figure 26). The result of this experiment excludes non-specific binding of free **dT^{NNIR}TP** to DNA, as no absorption and fluorescence signal of fluorophore was detected in control experiments without enzyme.

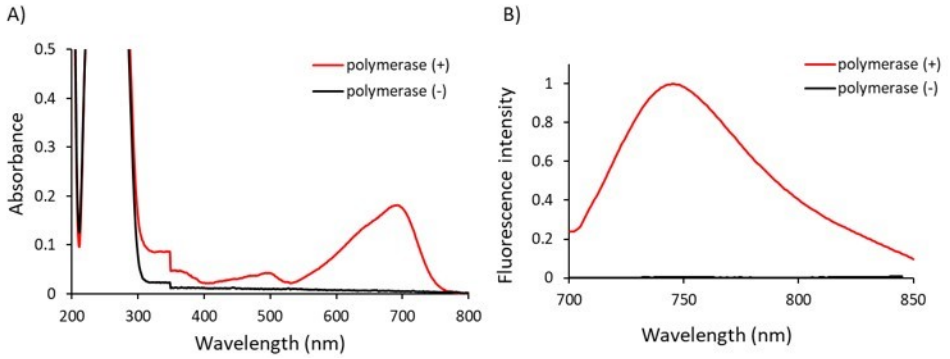

Figure 26 A) UV-vis absorption spectra (λ_{abs} = 690 nm) and B) fluorescence spectra (λ_{ex} = 690 nm, λ_{em} = 745 nm) of DNA obtained after incubation of PEX reaction mixtures containing **dT^{NNIR}TP**. Red lines represent experiments with and black lines without KOD XL DNA polymerase. The reaction mixtures were incubated at 60°C for 1 hour, then the reactions were stopped by cooling on ice. DNA from solutions were purified using QIAquick Nucleotide Removal Kit (QIAGEN).

Properties of modified DNA were then compared with modified nucleotide (Figure 27). We observed that the modified DNA **DNA19_1T^{NNIR}** exerted significantly red-shifted absorption to 690 nm (67 nm shift) in regard to nucleotide **dT^{NNIR}TP** (λ_{abs} = 623 nm). The emission maximum was not altered and the intensity of fluorescence was 59-fold higher (excited at 690 nm) in comparison with **dT^{NNIR}TP**. Due to the shift of the absorption maximum, the modified DNA could be excited at 720 nm and the enhancement of fluorescence intensity was 348-fold. The shift in

absorption resembles to absorption spectra of nucleoside **dT^{NNIR}** in dioxane (Figure 19 A, Table 3) and indicates increased hydrophobicity in the vicinity of the fluorophore. The observed fluorescence increase is presumably caused by less polar environment and also by restriction of intramolecular rotation of the fluorophore in environtment of DNA. These observations are in good correlation with polarity and viscosity sensitivity experiments of **dT^{NNIR}** in chapter 3.2.3.

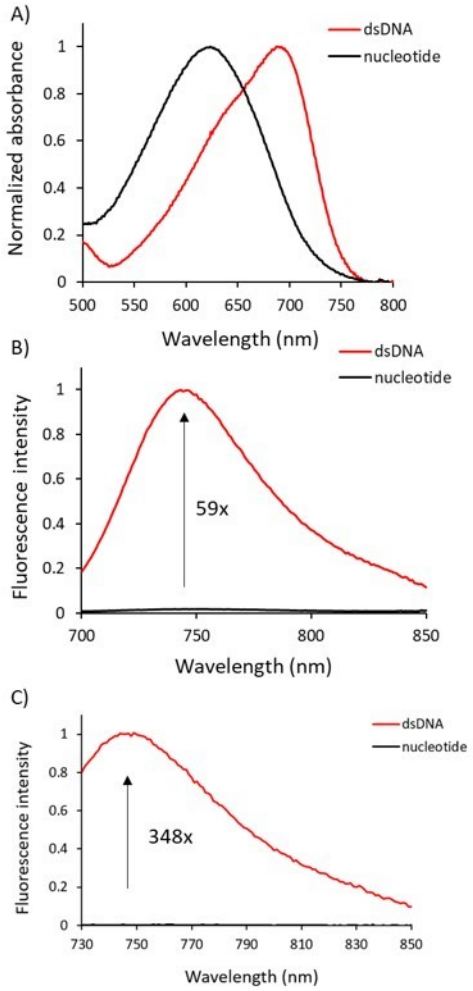

Figure 27 A) UV-vis absorption spectra of modified DNA (λ_{abs} = 690 nm) compared to **dT^{NNIR}TP** (λ_{abs} = 623 nm). B) Fluorescence spectra of modified dsDNA compared to **dT^{NNIR}TP** (λ_{ex} = 690 nm). D) Fluorescence spectra of modified dsDNA compared to **dT^{NNIR}TP** (λ_{ex} = 720 nm).

3.2.6 Mode of interaction of NNIR modification with DNA

According to the results in chapter 3.2.5, it is apparent that the **NNIR** modification is not completely exposed out of the DNA and it is most likely interacting with the DNA. Previously, it has been shown that small molecules can interact with DNA[154–156] and the factors that can influence the binding include hydrophobicity and presence of cationic charge.[157] The most common binding modes are minor or major groove binding and intercalation.[158] To determine the binding mode of the fluorophore with DNA, we performed displacement assay[159] with thiazole orange (TO; intercalator),[160] 4',6-diamidino-2-phenylindole (DAPI; minor groove binder)[161] or methyl green (MG; major groove binder).[162] Solution of modified DNA **DNA19_1T^{NNIR}** in phosphate buffer was titrated with the dyes mentioned above. Gradual increase of TO and DAPI concentration had small influence on fluorescence intensity of modified DNA. In case of MG, we observed gradual decrease of fluorescence intensity, probably due to the displacement of the fluorophore from its binding site by MG (Figure 29).

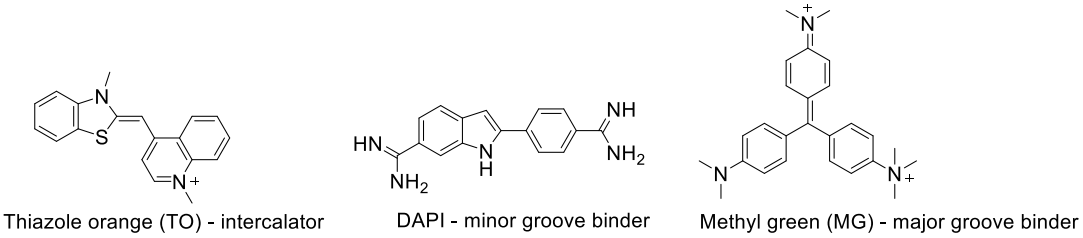

Figure 28 Structure of dyes used for determination of binding mode between DNA and fluorophore.

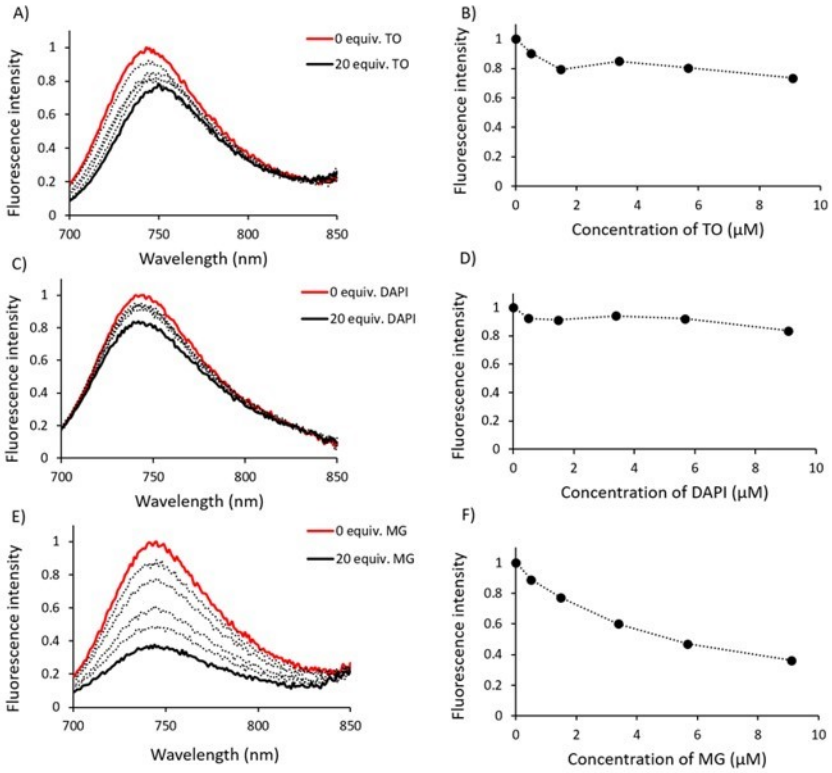

Figure 29 Fluorescence spectra of **DNA19_1T^{NNIR}** with increasing concentration of A) TO, C) DAPI or E) MG and fluorescence intensity plotted against concentration of B) TO, D) DAPI or F) MG. Samples were excited at 690 nm in phosphate buffer (4.5 mM, pH 7.4) at 25°C.

Furthermore, we determined UV melting temperature of **DNA19_1T^{NNIR}** (T_m = 79.5°C) and compared it with natural DNA **DNA19_1T** (T_m = 79.6°C). The result showed that the modification had negligible effect on stability of double-stranded DNA and also supports the hypothesis of groove binding, since it is known that intercalators stabilize duplex by increasing melting temperature.[163,164] Possible effect of intermolecular interaction of one modified DNA with other DNA was excluded by simple dilution experiment, which showed linear decrease of fluorescence upon dilution of DNA (Figure 31). These results suggest that **NNIR** modification interacts with DNA predominantly by major groove binding.

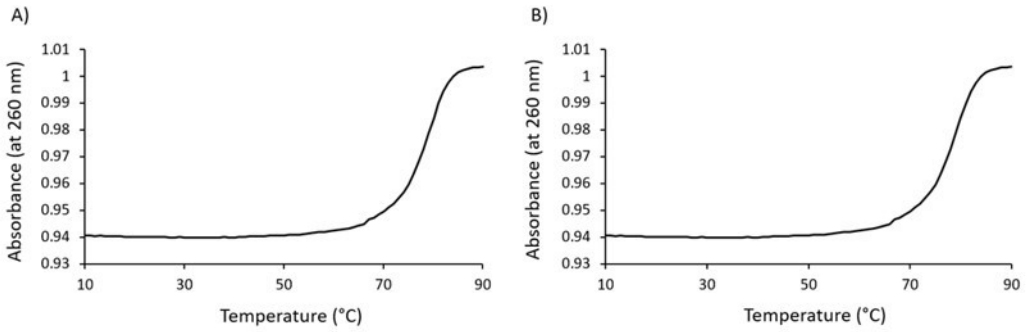

Figure 30 UV melting curves of A) DNA19_1T (T_m = 79.6°C) and B) **DNA19_1T^{NNIR}** (T_m = 79.5°C).

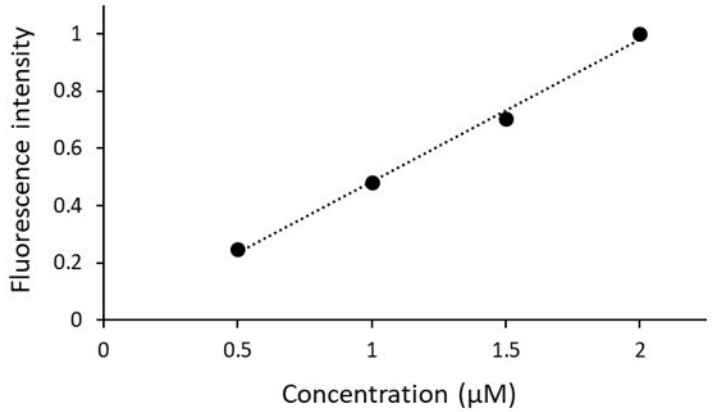

Figure 31 Concentration of **DNA19_1T^{NNIR}** plotted against fluorescence intensity (at 743 nm). Samples were excited at 690 nm in phosphate buffer at 25°C.

3.2.7 Hybridization and digestion studies of modified DNA

To investigate whether the **NNIR** modification can distinguish between ssDNA and dsDNA, we performed hybridization experiment (Figure 32). DNA used in this experiment was prepared using 5'-phosphorylated (5'-P) template. 5'-P DNA strand can be digested by lambda exonuclease[165] and this allows preparation of single-stranded DNA. We measured fluorescence intensity of ssDNA **ON19_1T^{NNIR}**, then upon its

hybridization with 5'-P complementary strand and subsequently after treatment with lambda exonuclease. The results revealed that upon hybridization of ssDNA **ON19_1T^{NNIR}** with complementary strand the fluorescence intensity decreased approximately 2-fold and after subsequent reaction with lambda exonuclease the fluorescence intensity again increased (Figure 33 A). Moreover, it was possible to monitor digestion in real time and the kinetics revealed that the reaction performed at 37°C is finished within 60 minutes (Figure 33 B). Therefore, the fluorophore could be useful for sensing DNA hybridizations.

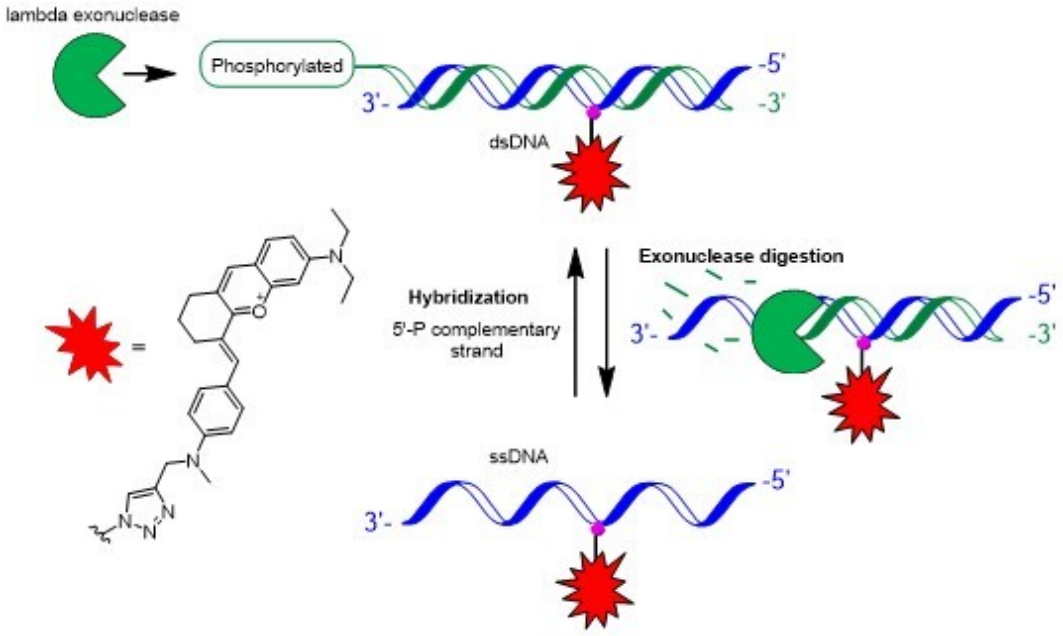

Figure 32 Illustration of digestion and hybridization experiment.

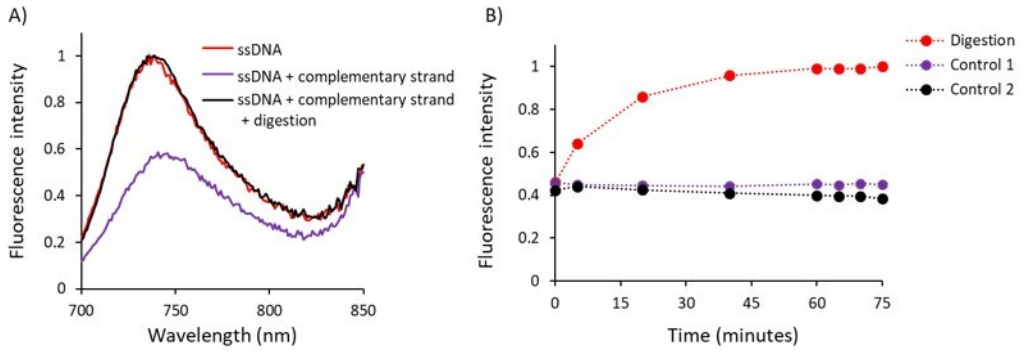

Figure 33 A) Hybridization and λ exonuclease digestion. Purple line represents **ON19_1T^{NNIR}** (ssDNA), red line shows fluorescence upon annealing with complementary strand (ssDNA + complementary strand), black line shows response after subsequent digestion of 5'-P strand (ssDNA + complementary strand + digestion). B) Kinetics of digestion in real time. Red line (Digestion) represents digestion reaction mixture with and purple line (Control 1) without lambda exonuclease, Control 2 (black line) contains reaction mixture with **DNA19_1T^{NNIR}** without 5'-P label. Samples were excited at 690 nm at 37°C.

3.2.8 Sensing interactions of DNA with small molecules and biomolecules

At first we examined interaction of **DNA19_1T^{NNIR}** with spermine (Figure 34). In presence of spermine, the fluorescence of modified DNA decreased ca. 2.2-fold. This change of fluorescence was observed in presence of high amounts of spermine (32 equivalents) and it is logical as this polyamine is minor groove binder.[166]

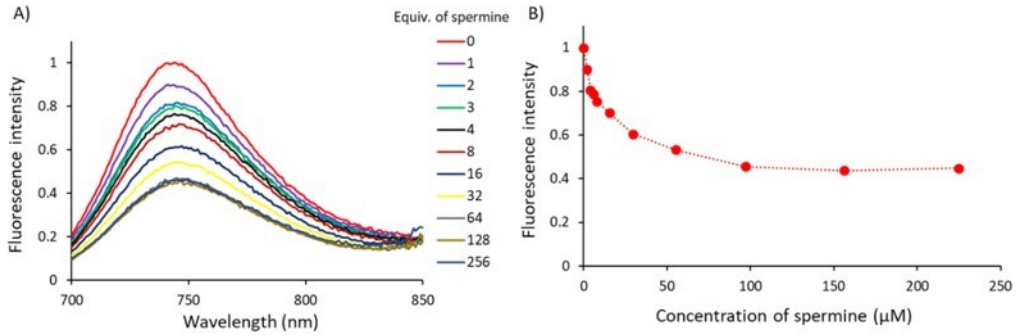

Figure 34 A) Fluorescence spectra of **DNA19_1T^{NNIR}** after addition of 0-256 equiv. of spermine. B) Fluorescence intensity plotted against concentration of spermine. Samples were excited at 690 nm in phosphate buffer at 25°C.

Then we studied interaction of DNA with H2A histone protein (Figure 35). **DNA19_1T^{NNIR}** was titrated by 1-4 equivalents of histone or BSA. The results revealed significant 5-fold decrease of fluorescence intensity upon titration of DNA by histone with a stoichiometry of interaction 1:2, further titration had negligible influence on fluorescence intensity. Experiment with non-DNA binding protein BSA showed negligible change in fluorescence intensity.

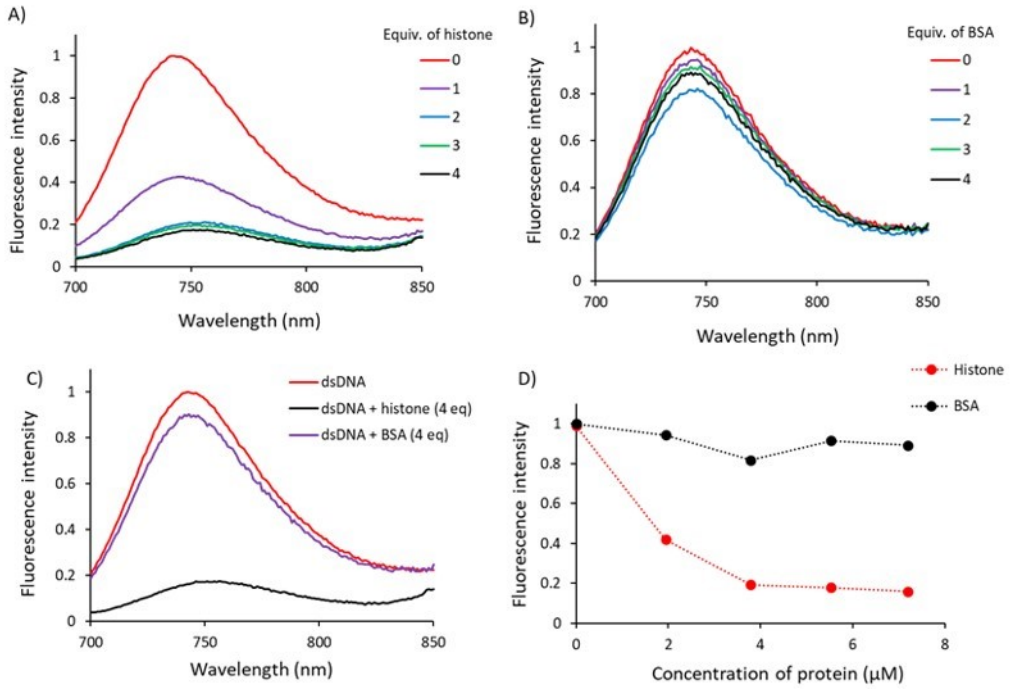

Figure 35 Fluorescence spectra of **DNA19_1T^{NNIR}** after A) addition of 0-4 equiv. of histone and B) addition of 0-4 equiv. of BSA. C) Comparison of fluorescence of **DNA19_1T^{NNIR}** without protein (red line), with 4 equiv. of histone (black line) and with 4 equiv. of BSA (purple line). D) Fluorescence intensity plotted against concentration of the protein (histone or BSA). Samples were excited at 690 nm in phosphate buffer at 25°C.

Next, we treated **DNA19_1T^{NNIR}**-histone complex with proteinase K and we expected that in the presence of enzyme the histone could be hydrolyzed and separated from DNA, which could lead to recovery of the fluorescence. The results in Figure 36 confirmed our expectations, and we observed that the fluorescence restored after digestion of the histone by proteinase K. Therefore, this probe could be also useful for monitoring activity of some enzymes. When the complex of DNA-histone was treated with 1 equiv. of 98-mer dsDNA, we also observed recovery of the fluorescence (Figure 36). We assume, that the decrease in fluorescence intensity of the modified DNA is due to the crowding out of the fluorophore from its binding site in DNA once it interacts with histone. The longer 98-mer dsDNA is more anionic than 19-mer

modified DNA and presumably acts as competitor and releases modified DNA from the complex with protein.

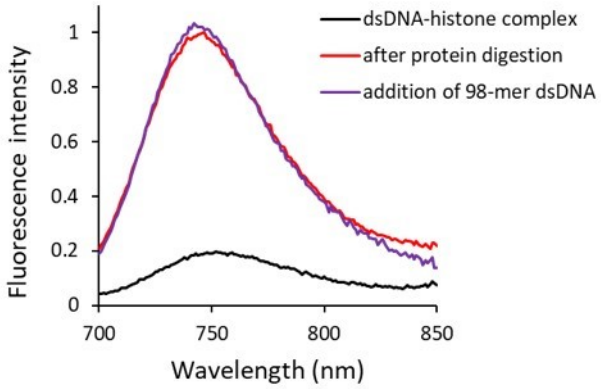

Figure 36 Fluorescence spectra of complex of **DNA19_1T^{NNIR}** with histone (black line) and after digestion of protein with proteinase K (red line) or after addition of 98-mer dsDNA (1 equiv.; purple line). Samples were excited at 690 nm in phosphate buffer at 25°C.

The modified DNA was then titrated by protamine (mixture of nuclear proteins)[167]. Figure 37 A, B shows that with increasing concentration of protamine the fluorescence of dsDNA was almost completely diminished (31-fold decrease). This effect can be also ascribed to displacement of fluorophore from DNA binding site. It is known, that protamine has strong affinity to heparin[168] and therefore we tested interaction of **DNA19_1T^{NNIR}**-protamine complex with heparin. Titration of DNA-protamine complex by heparin revealed that heparin behaved as strong competitor and we observed gradual increase of fluorescence (Figure 37 C, D). From these results we can conclude that the modified DNA probe can be used for sensing interactions with other biomolecules and could be potentially useful for sensing other biologically relevant molecules.

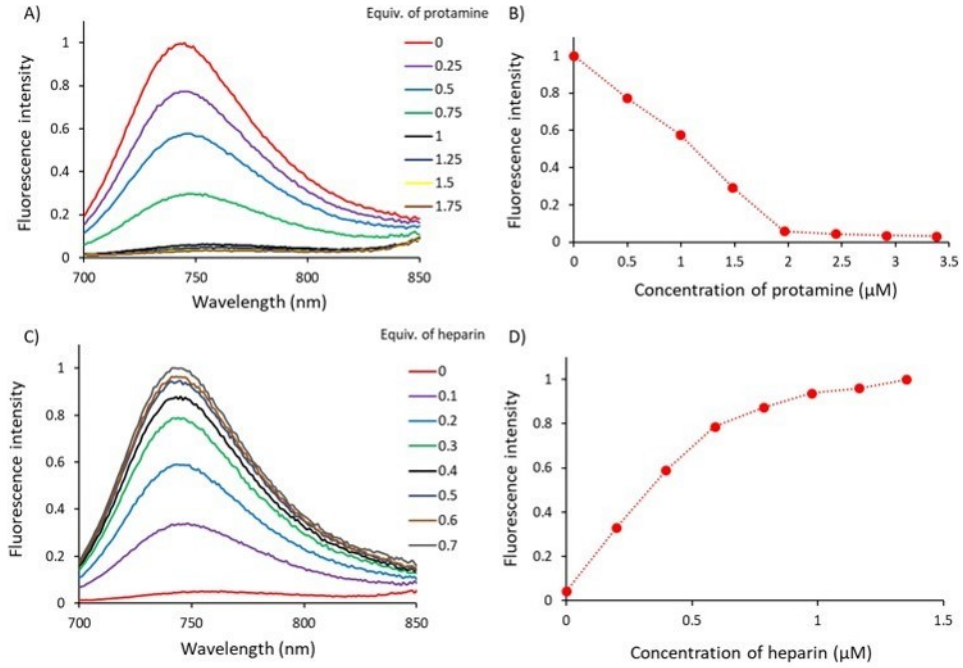

Figure 37 A) Fluorescence spectra of **DNA19_1T^{NNIR}** after addition of 0-1.75 equiv. of protamine. B) Fluorescence intensity plotted against concentration of protamine. C) Fluorescence spectra of complex of **DNA19_1T^{NNIR}** with protamine after addition of 0-0.7 equiv. of heparin. D) Fluorescence intensity plotted against concentration of heparin. Samples were excited at 690 nm in phosphate buffer at 25°C.

3.2.9 Real-time monitoring of *in vitro* DNA synthesis and replication

Encouraged by fluorogenic character of modified triphosphate **dT^{NNIR}TP**, we planned to use it for monitoring of DNA synthesis by PEX and also by PCR. At first, it was essential to find out if the free triphosphate also lights-up in presence of DNA, because that would create background fluorescence and it would be problematic to interpret the results. In this experiment, we prepared mixture of natural dsDNA DNA19_1T with nucleotide or alkyne in 1:1 ratio and we measured fluorescence. The results revealed that the intensity of **dT^{NNIR}TP** increased 2-fold and in the case of alkyne **43** the increase was 23-fold (Figure 38). We assume, that this minor (2-fold)

fluorescence increase of **dT^{NNIR}TP** is due to the low affinity to the DNA, which stems from repulsion between negatively charged DNA backbone and triphosphate moiety of **dT^{NNIR}TP**.

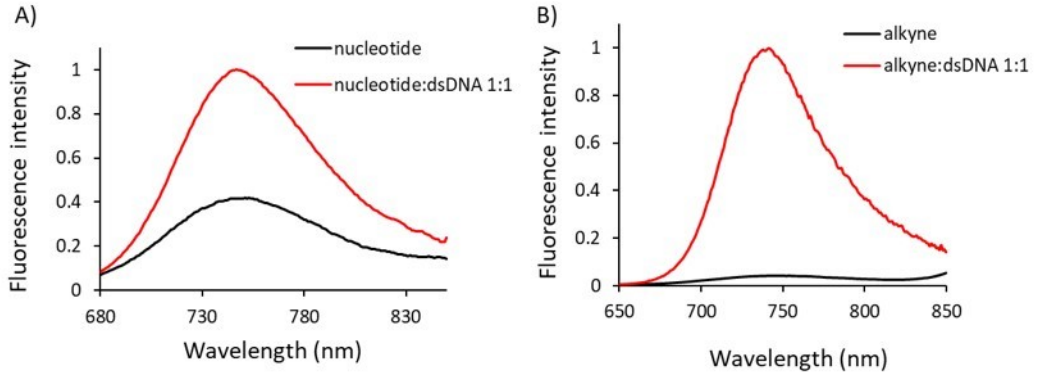

Figure 38 Fluorescence spectra of A) free nucleotide **dT^{NNIR}TP** and nucleotide in presence of natural DNA or B) free alkyne **43** and alkyne in presence of natural DNA.

Then we tested **dT^{NNIR}TP** for real-time monitoring of primer extension by single nucleotide. This experiment was performed in fluorimeter holder at 60°C, the reaction mixture contained template Temp8^{PEX}, primer Prim1^{PEX}, **dT^{NNIR}TP**, corresponding reaction buffer and KOD XL DNA polymerase. After addition of polymerase, the fluorescence spectra were recorded in time intervals. The results showed that fluorescence was increased with time when the polymerase was present and after 2 minutes the intensity was constant, indicating that the reaction was finished (Figure 39 B). Control experiments without enzyme and control experiment without template show no difference in fluorescence with time. This result clearly indicates that observed increase of fluorescence (12.5-fold) is due to the successful incorporation of modified nucleotide which results in light-up effect.

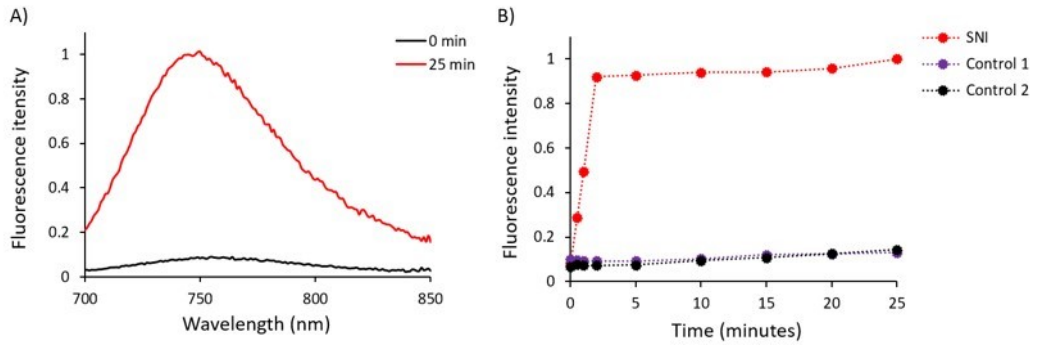

Figure 39 A) Fluorescence spectra of SNI reaction at 0 and 25 minutes, B) fluorescence intensity (at 745 nm) plotted against time. Red line represents experiment (SNI) with and purple line (Control 1) without KOD XL DNA polymerase, Control 2 (black line) contains reaction mixture without template. Samples were excited at 690 nm at 60°C.

Motivated by success of this SNI experiment, we decided to explore application of **dT^{NNIR}TP** in real-time PCR. Particularly, we opted for detection of SARS-CoV-2 virus,[169] the coronavirus responsible for COVID-19 pandemic. RdRP gene (encodes RNA-dependent RNA polymerase) was chosen as sequence of interest. First, RdRP DNA standard was prepared from the viral RNA. This RNA was reversely transcribed to DNA, then the RNA was hydrolyzed by RNase H and complementary DNA (cDNA) was obtained – this cDNA was provided by virology department of IOCB. Subsequently the cDNA was used as template in PCR and in presence of specific primers only desired RdRP region was amplified, product was purified by nucleospin columns and analyzed on gel. Preparation of DNA standard is shown in Figure 40 A. Agarose gel of purified PCR product is shown in Figure 40 B.

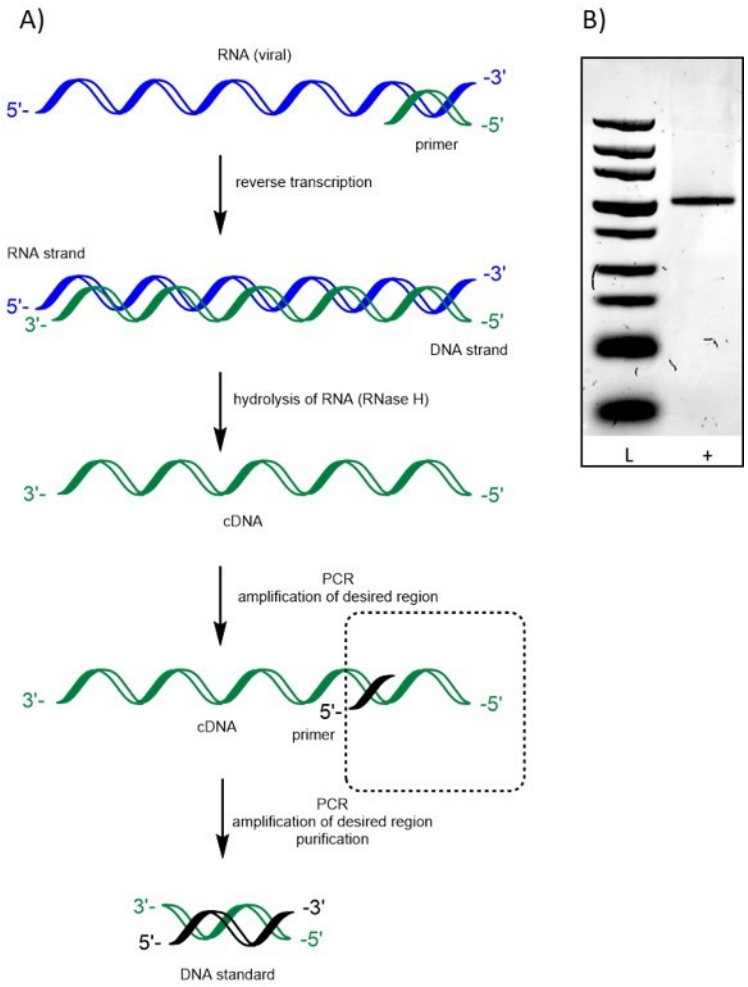

Figure 40 A) Preparation of RdRP DNA standard. B) Agarose gel electrophoresis analysis of purified PCR product (Temp3^{PCR}) after amplification of RdRP gene region of cDNA. L: DNA ladder. Purified product (+): all natural dNTPs are present.

DNA standard was then prepared in 10-fold serial dilutions (5.71 x 10^7 to 5.71 x 10 DNA copies) and was used as template for real-time PCR using modified nucleotide. The reaction mixture contained DNA standard (Temp3^{PCR}), reverse and forward primers (Prim5^{PCR} and Prim6^{PCR}), KOD XL DNA polymerase and corresponding buffer, natural dATP, dGTP, dCTP and dTTP: **dT^{NNIR}TP** 95:5. Figure 41 A, B shows observed amplification and standard curve. The efficiency of PCR was calculated to be 60.5% and was able to detect minimum of around 5710 DNA

copies. Then, melting curve analysis was performed and revealed a single peak for product (Figure 41 C, D). The PCR products were also analysed by agarose gel electrophoresis (Figure 41 E, F).

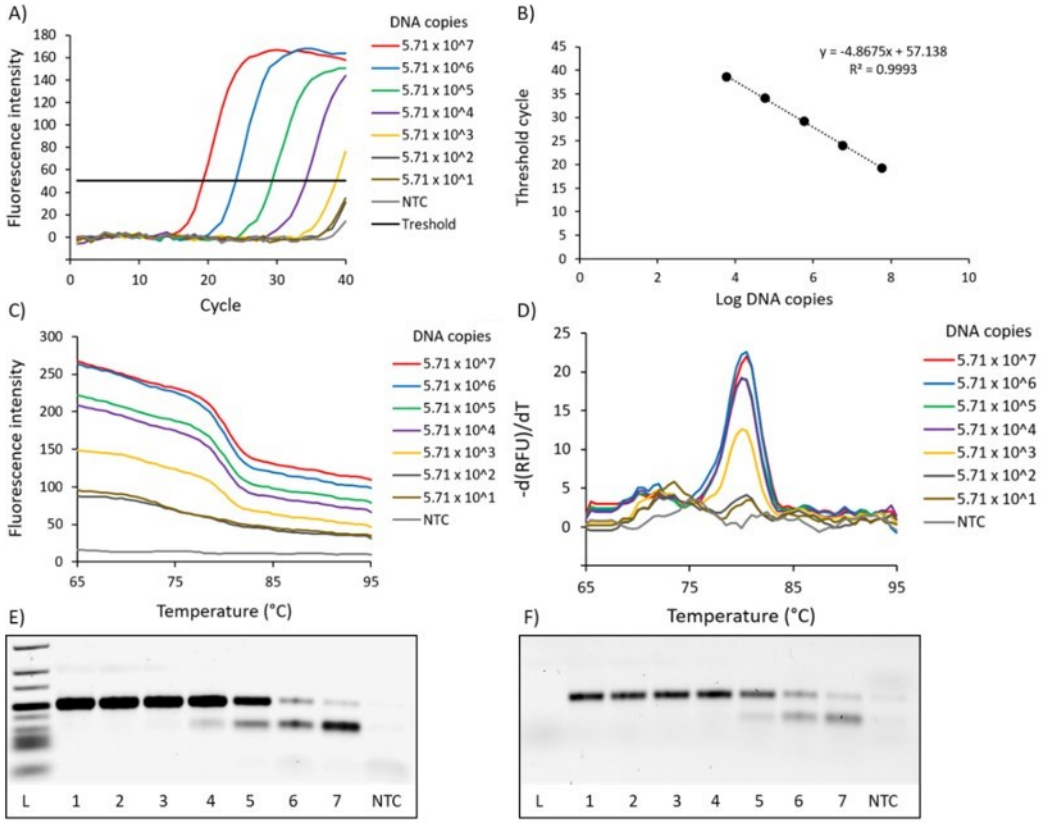

Figure 41 A) Amplification curve of rtPCR with **dT^{NNIR}TP** using 10-fold serial dilutions (5.71 x 10^7 to 5.71 x 10 DNA copies) of xyz template. B) Standard curve (5.71 x 10^7 to 5.71 x 10^3 DNA copies), C) melting curves, D) melting peaks. E), F) Agarose gel electrophoresis analysis after rtPCR amplification of Temp3^{PCR} (5.71 x 10^7 to 5.71 x 10 DNA copies) with KOD XL polymerase, Prim5^{PCR}, Prim6^{PCR}, dGTP, dCTP, dATP and a mixture of dTTP and **dT^{NNIR}TP** (95:5). L: DNA ladder. Lanes 1-7: Reaction with 5.71 x 10^7 to 5.71 x 10 DNA copies. NTC = no template control. E) Gel scanned using laser for GelRed, F) gel scanned using 635 nm laser.

Next, we attempted one-step reverse transcription (RT) real-time PCR using **dT^{NNIR}TP** and isolated viral RNA from a real sample. This experiment also showed

successful amplification and we detected fluorescence signal with Ct value 22.7 (Figure 42 A). Produt was also analysed by agarose gel (Figure 42 B, D). Melting curve analysis is shown in Figure 42 D, C. These results revealed that **dT^{NNIR}TP** could be also useful for visualization of DNA synthesis.

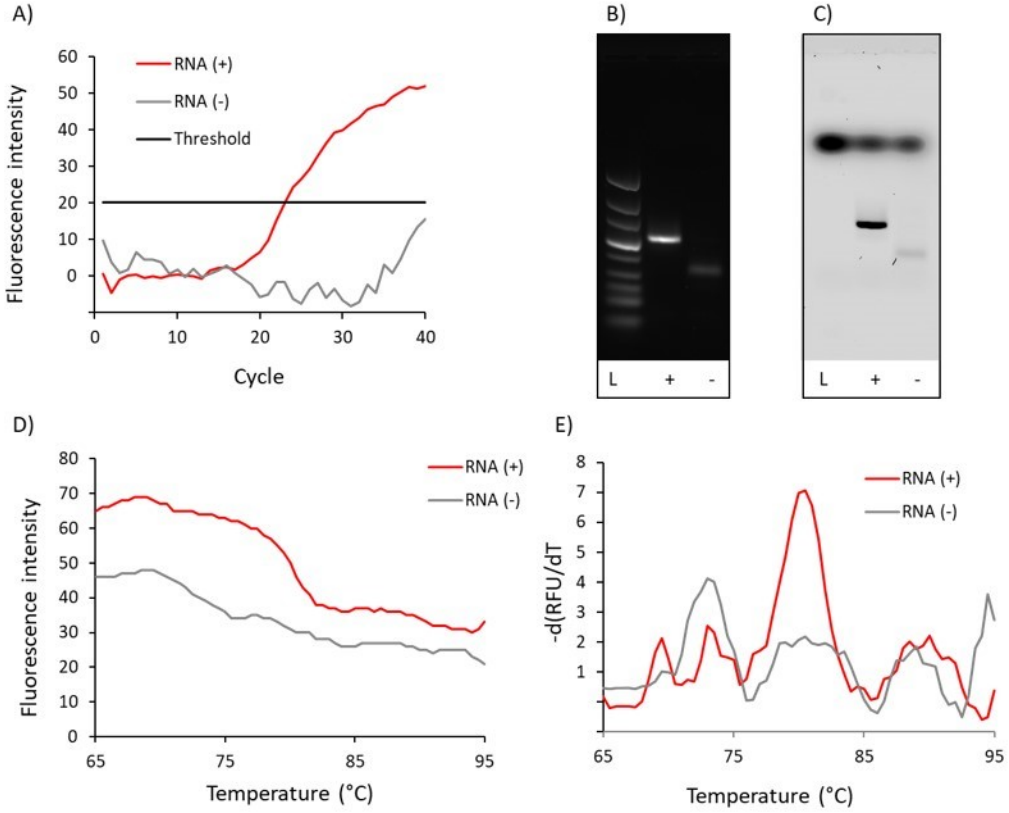

Figure 42 A) RT real-time PCR using **dT^{NNIR}TP** and viral RNA. B), C) Agarose gel electrophoresis analysis of products after reverse transcription rtPCR. L: DNA ladder. Reaction was performed in presence (+) and absence (-) of RNA. B) Gel scanned using laser for GelRed, C) gel scanned using 635 nm laser. D) Melting curves, E) melting peaks. Red lines represent experiments with and gray lines without RNA.

3.2.10 Transport of dT^{NNIR}TP into cells using SNTT

As a final task, we wanted to transport **dT^{NNIR}TP** into cells using synthetic nucleoside triphosphate transporter (experiments were performed by Dr. Tomáš Kraus). The experiment was performed using human bone osteosarcoma cells (U-2 OS), which were treated with a mixture of **dT^{NNIR}TP** and SNTT (1:1). Unfortunatelly, in this experiment we did not observe incorporation into genomic DNA, most probably due to the high cytotoxicity (shrunk nuclei visible in bright field) and low substrate activity of modified nucleotide (Figure 43).

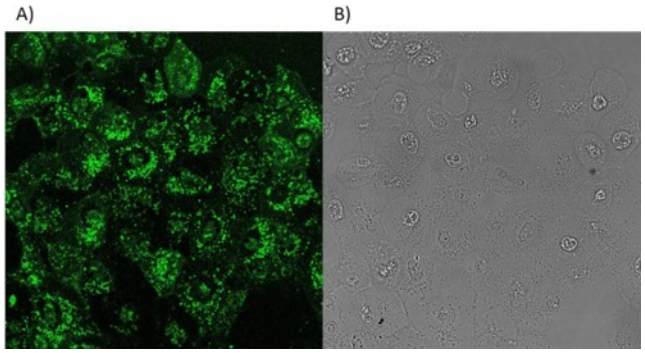

Figure 43 A) Fluorescence microscopy and B) bright field images.

3.3 Attachment of benzylidene-tetrahydroxanthylium fluorophore to 2'-deoxycytidine triphosphate via triethylene glycol linker. Synthesis, photophysical properties, enzymatic incorporation into DNA and applications

3.3.1 Introduction

As it was mentioned in chapter 3.2.10, the modified nucleotide **dT^{NNIR}TP** was not suitable for cell experiments probably due to the low substrate activity and toxicity. To address these issues, we decided to tether **NNIR** modification to the nucleotide via longer and hydrophilic triethylene glycol linker. We expected that the use of linker would increase recognition of the nucleotide by DNA polymerases and at the same time lower the propensity to bind hydrophobic organelles (possible source of toxicity).

We designed new azido-propargyloxy-triethylene glycol modified deoxycytidine triphosphate and using CuAAC we attached **NNIR** modification. The modified nucleotide was then tested for enzymatic incorporation into DNA. Light-up effect and cell-based experiments were also studied

3.3.2 Synthesis

Azido-propargyloxy-triethylene glycol conjugated dCTP was prepared by the Sonogashira cross-coupling reaction of 5-iodo-2'-deoxycytidine (**dC^{I}**) with the corresponding triethylene glycol alkyne **46**, followed by substitution with NaN_3 and phosphorylation. Alkyne **43** was then attached to the nucleotide using CuAAC (Scheme 19).

First, following the literature, tosyl-propargyloxy-triethylene glycol **46** was prepared by alkylation[170] of triethylene glycol **44** with propargyl bromide followed by tosylation[171].

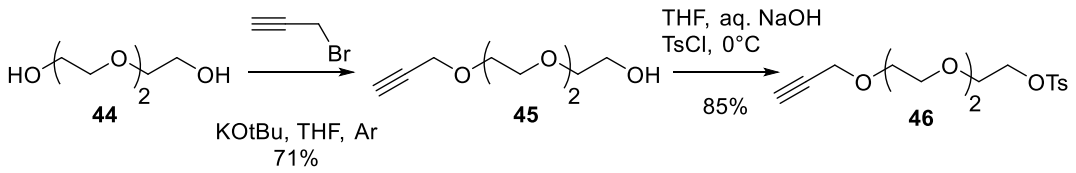

Scheme 18 Synthesis of tosyl-propargyloxy-triethylene glycol **46**.

Sonogashira cross-coupling of **dC^{I}** with alkyne **46** in the presence of $PdCl_2(PPh_3)_2$ and CuI in DMF and DIPEA afforded nucleoside **dC^{pegOTs}** in 89% yield. Substitution of tosylate in **dC^{pegOTs}** by sodium azide provided azido modified nucleoside **dC^{pegN3}** which was subsequently converted into triphosphate **dC^{pegN3}TP** with 22% yield. CuAAC of **dC^{pegN3}TP** with alkyne **43** afforded nucleotide **dC^{pegNNIR}TP** in 31% yield.

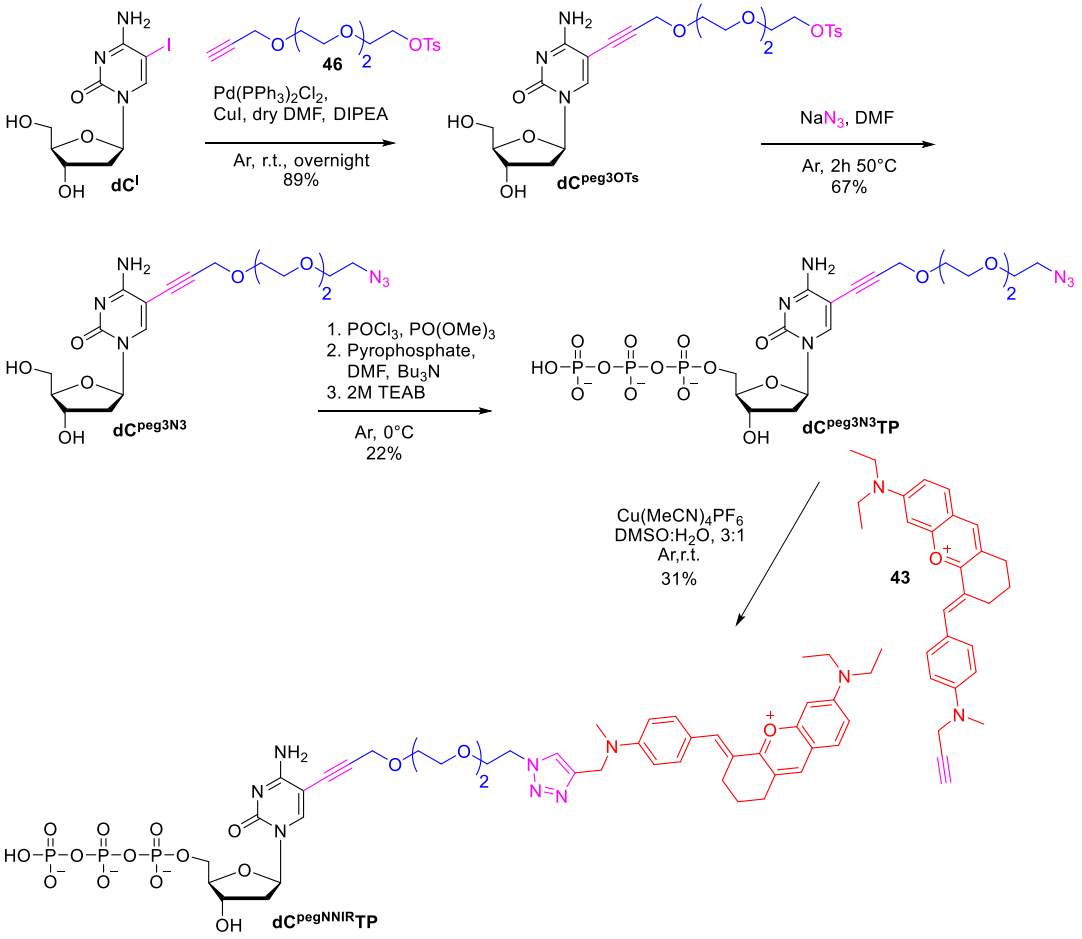

Scheme 19 Synthesis of azido-propargyloxy-triethylene glycol conjugated dCTP (**dC^{pegN3}TP**) and labelled nucleotide **dC^{pegNNIR}TP**.

3.3.3 Enzymatic synthesis of modified DNA, photophysical properties of DNA, cell experiments

Modified nucleotide **dC^{pegNNIR}TP** was tested as substrate for KOD XL DNA polymerase in primer extension (Scheme 44 A) and polymerase chain reaction experiments. PEX was tested using 19-mer template (Temp1^{PEX}) encoding for incorporation of one modification. PAGE analysis showed that the PEX product was formed and the mobility of modified DNA was faster than the natural DNA (Figure 44 B). Incorporation of **dC^{pegNNIR}TP** into DNA was slow and it was necessary

to perform reaction at 60°C for 60 min. Product was confirmed by MALDI-TOF analysis (Table 6). Absorption and fluorescence spectra of modified DNA were then compared with modified nucleotide. The modified DNA **DNA19_1C^{pegNIR}** exerted red-shifted absorption to 690 nm (35 nm shift) in regard to nucleotide **dC^{pegNNIR}TP** (Figure 45 A). The emission maximum remained the same (746 nm) and the intensity of fluorescence was 13-fold higher than in case of **dC^{pegNNIR}TP** (Figure 45 B).

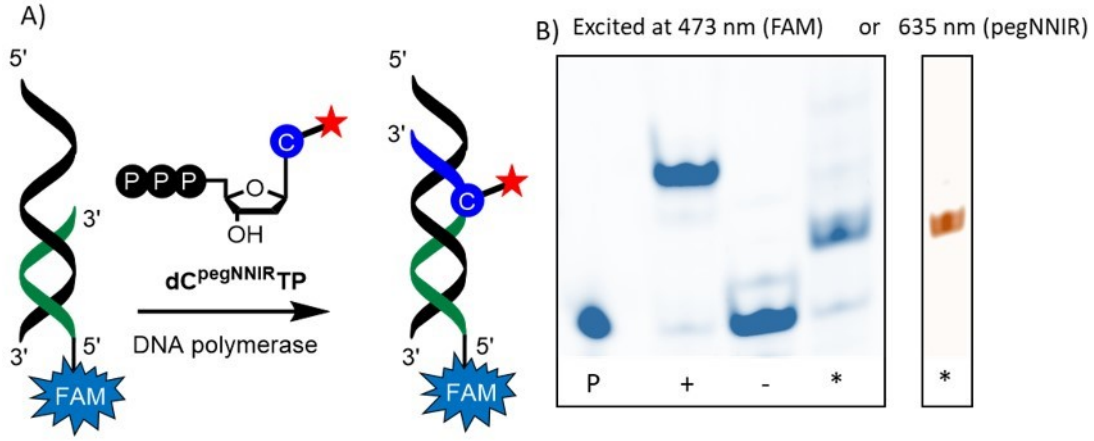

Figure 44 A) Scheme representing PEX with modified nucleotide for gel visualization. B) PAGE analysis of PEX using **dC^{pegNIR}TP**, KOD XL DNA polymerase. Primer (P), positive control (+; PEX with all natural dNTPs), negative control (-; PEX in absence of dCTP). PEX with **dC^{pegNIR}TP** (*).

Table 6 Oligonucleotide prepared in this study.

Oligonucleotide	Sequence (5′→3′). C*: modified nucleotide.	$M_{calculated}$ (Da)	M_{found} (Da)
ON19_1C^{pegNNIR}	5′-CATGGGCGGCATGGG**C***GGG-3′	6573.2	6574.6

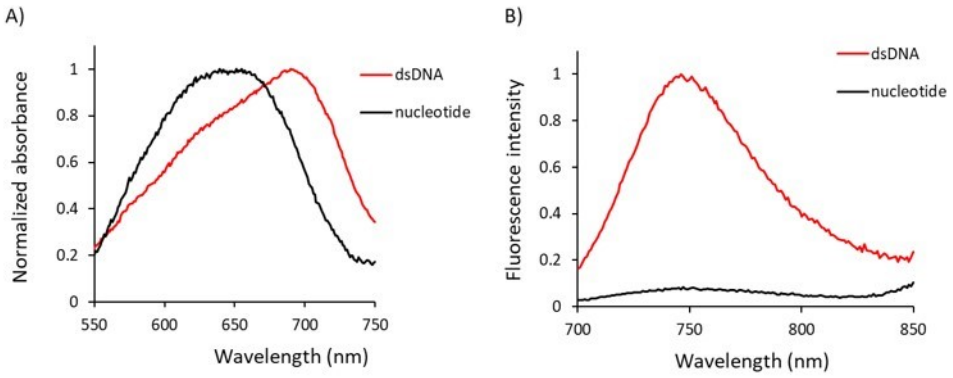

Figure 45 A) UV-vis absorption spectra of modified DNA (λ_{abs} = 690 nm) compared to **dC^{pegNNIR}TP** (λ_{abs} = 655 nm). B) Fluorescence spectra of modified dsDNA compared to **dC^{pegNNIR}TP** (λ_{ex} = 690 nm).

PCR was tested using different ratio of modified nucleotide **dC^{pegNNIR}TP** and natural dCTP (in presence of the natural dTTP, dATP and dGTP). Good amplification was observed when 5-40% of **dC^{pegNNIR}TP** was used (Figure 46). At 60% of **dC^{pegNNIR}TP** the PCR was inefficient and shorter product was observed. In comparison with **dT^{NNIR}TP** (PCR worked with max. 10%), the PCR with **dC^{pegNNIR}TP** was more efficient. Fluorescence light-up effect was also tested in real-time PCR using **dC^{pegNNIR}TP**. Figure 47 shows that indeed the nucleotide enhances its fluorescence during amplification and gradual increase of fluorescence was observed.

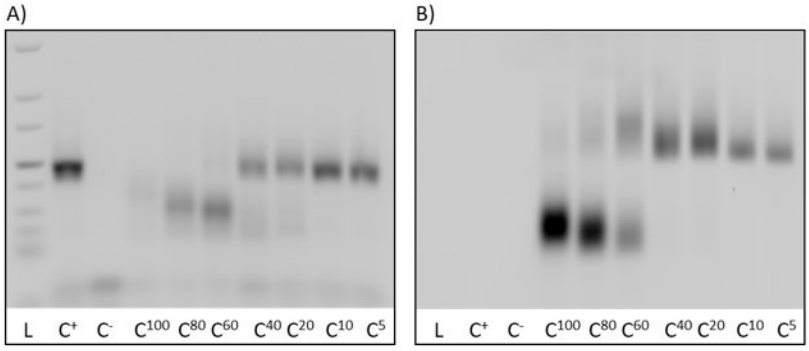

Figure 46 Agarose gel electrophoresis analysis of PCR amplification of 98bp template (Temp1^{PCR}) with KOD XL polymerase and **dC^{pegNIR}TP**. DNA ladder (L), positive control (C$^+$, PCR with all natural dNTPs), negative control (C$^-$, PCR in absence

of dCTP), PCR with mixture of modified nucleotide with natural dCTP (C^{100}-C^{5}, content of modified nucleotide decreases from 100% to 5%). A) Gel scanned using laser for GelRed, B) gel scanned using 635 nm laser.

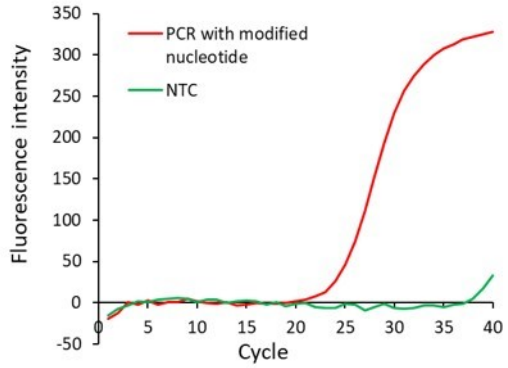

Figure 47 Amplification curve of real-time PCR with **dC^{pegNNIR}TP** using template Temp3^{PCR} with KOD XL polymerase, Prim5^{PCR}, Prim6^{PCR}, dGTP, dCTP, dATP and a mixture of dCTP and **dC^{pegNNIR}TP** (95:5). NTC = no template control.

3.3.4 Cell experiments

Transport of modified nucleotide into cells was performed by treatment of cells with a mixture of **dC^{pegNNIR}TP** and SNTT (1:1; experiments were performed by Dr. Tomáš Kraus). Incorporation into DNA was not detected and fluorescence signal was localized mostly outside of nucleus (Figure 48 A, B, C). Apparent toxicity was visible after 8 days (shrunk nuclei; Figure 48 D).

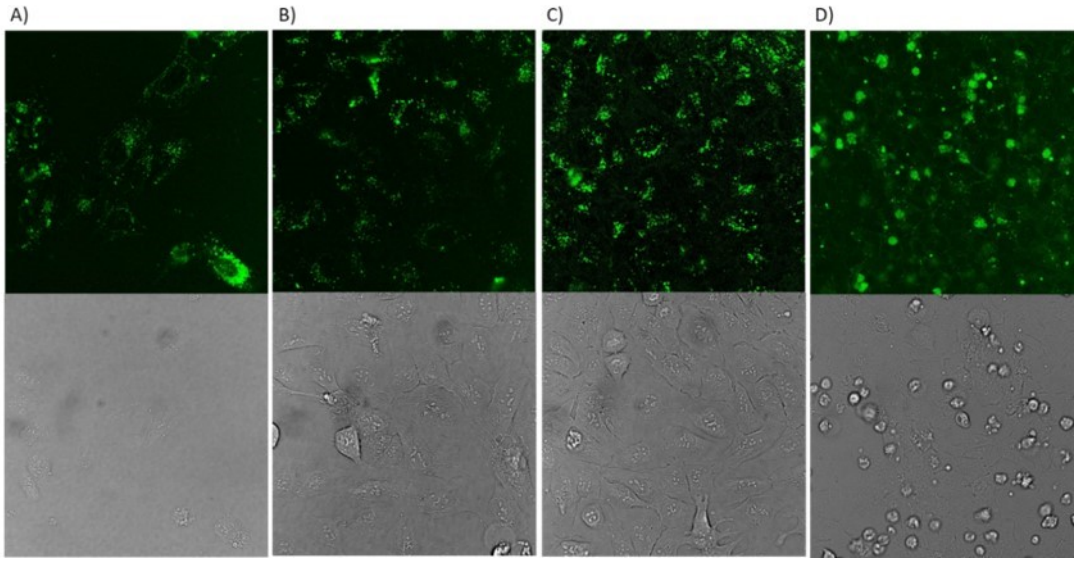

Figure 48 Fluorescence microscopy (top row), bright field (bottom row) images. Time after treatment: A) 2 hours, B) 24 hours, C) 48 hours, D) 8 days.

3.4 2'-Deoxycytidine and its triphosphate modified by thiazole orange fluorophore. Synthesis, photophysical properties, enzymatic incorporation into DNA and applications

3.4.1 Introduction

Our previous nucletides **dT^{NNIR}TP** and **dC^{pegNNIR}TP** showed increase of fluorescence upon incorporation to DNA and allowed visualization of DNA synthesis *in vitro* (chapter 3.2 and chapter 3.3 respectively). However, the nucleotides were not suitable for cell experiments and therefore we were not able to monitor DNA synthesis in live cells. In order to pursue this goal we opted to use different fluorescent dye with similar light-up properties.

Thiazole orange (TO; Figure 49 A) belongs to the group of asymmetrical cyanine dyes. TO consists of benzothiazole and quinoline aromatic rings conjugated via methine bridge. Free dye exhibits negligible fluorescence due to the intramolecular rotation around methine bond, however, blocking this motion by increased viscosity leads to dramatic increase of fluorescence intensity. Moreover, TO can stack between DNA base pairs or inside grooves of DNA which also leads to enhanced fluorescence and fluorescence lifetime.[129–131] It was also described that TO is well tolerated by cells and stains both cytoplasm and nucleus.[172]

Encouraged by the properties of TO, we synthesized dC and dCTP modified with TO tethered via triethylene glycol linker (Figure 49 B). Photophysical properties of new compounds were studied. Thiazole orange modified nucleotide was tested for enzymatic incorporation into DNA. Modified nucleotide was transported into live cells and its incorporation into genomic DNA was then studied by fluorescence microscopy.

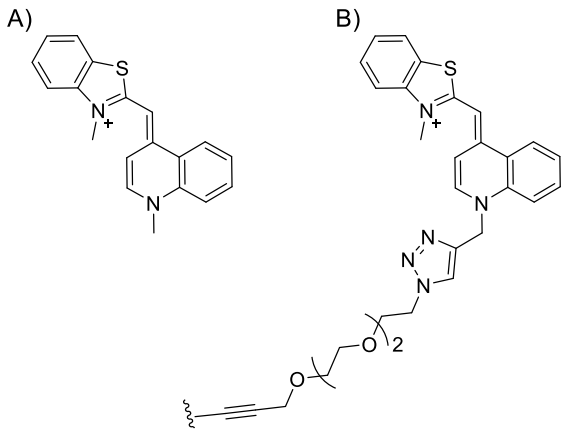

Figure 49 Structure of A) thiazole orange and B) our modification.

3.4.2 Synthesis

Thiazole orange modified nucleoside and nucleotide were prepared by CuAAC of azido-propargyloxy-triethylene glycol modified dC or dCTP with thiazole orange alkyne **51** (Scheme 21).

Alkyne **51** was prepared according to the literature.[173,174] Quinoline **47** was alkylated by propargyl bromide and benzothiazole **49** was methylated by iodomethane. Reaction of compound **48** and **50** in ethanol in presence of triethylamine led to formation of thiazole orange alkyne **51**.

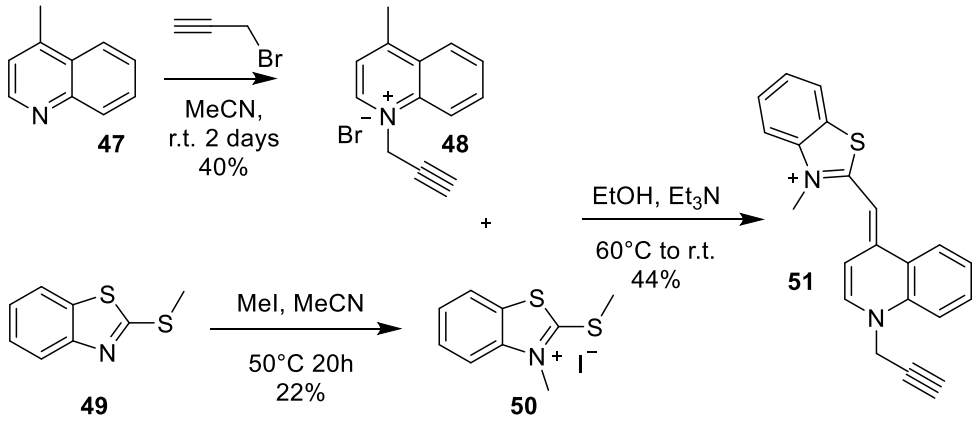

Scheme 20 Synthesis of thiazole orange alkyne **51**.

CuAAC of **dC^{pegN3}** or **dC^{pegN3}TP** with alkyne **51** afforded nucleoside **dC^{TO}** or nucleotide **dC^{TO}TP** in the yields of 43% and 15% respectively.

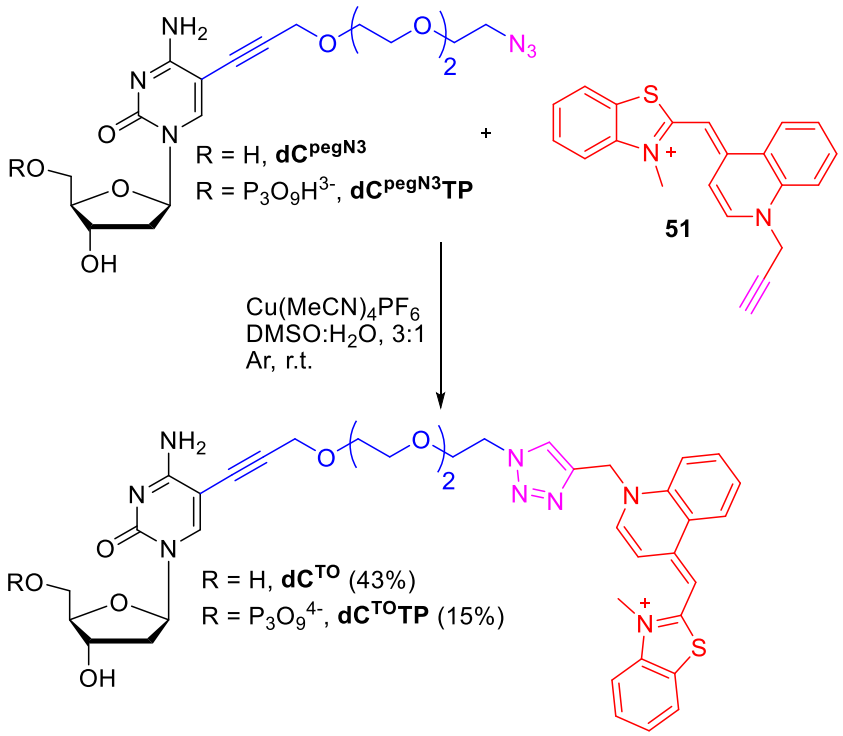

Scheme 21 Synthesis of thiazole orange modified nucleoside **dC^{TO}** and nucleotide **dC^{TO}TP**.

3.4.3 Photophysical properties

Absorption and emission spectra of modified nucleoside **dC^{TO}** were measured in various solvents in order to evaluate effect of the polarity and viscosity on photophysical properties of thiazole orange modified nucleoside (Table 7). The spectra revealed mild solvatochromic effect with absorption maxima at 506-513 nm. As expected, the modified nucleoside was non-fluorescent in low viscosity solvents (H_2O, MeOH, dioxane) and the fluorescence was observed only in glycerol (quantum yield of 4.6%). Sensitivity of **dC^{TO}** to the viscosity was also demonstrated by measuring solution of the nucleoside in glycerol at different temperatures

(Figure 51, Table 8). When the viscosity increases, the rotation of the fluorophore is inhibited and gradual increase of fluorescence quantum yield is observed (Figure 52).

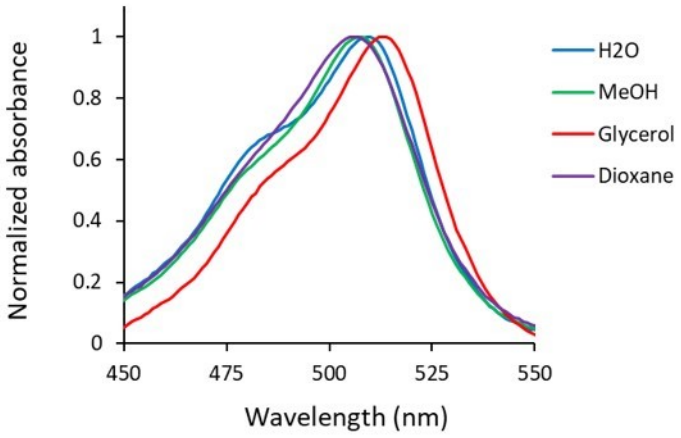

Figure 50 Normalized absorption spectra of **dC^{TO}** in different solvents.

Table 7 Photophysical properties of modified nucleoside and nucleotide.

Compound	Solvent	λ_{abs}[a] (nm)	ε[b] (M^{-1} cm^{-1})	λ_{em}[c] (nm)	Φ[d] (%)
dC^{TO}	H_2O	509	19109	n.d.	n.d.
	MeOH	507	24690	n.d.	n.d.
	Glycerol	513	20340	535	4.6
	Dioxane	506	23388	n.d.	n.d.

[a] Position of the absorption maximum. [b] Molar extinction coefficients. [c] Position of the emission maximum. [d] Fluorescence quantum yield measured using fluorescein in 0.1 M NaOH (Φ = 0.92 at 25°C) as standard, n.d. = not determined.

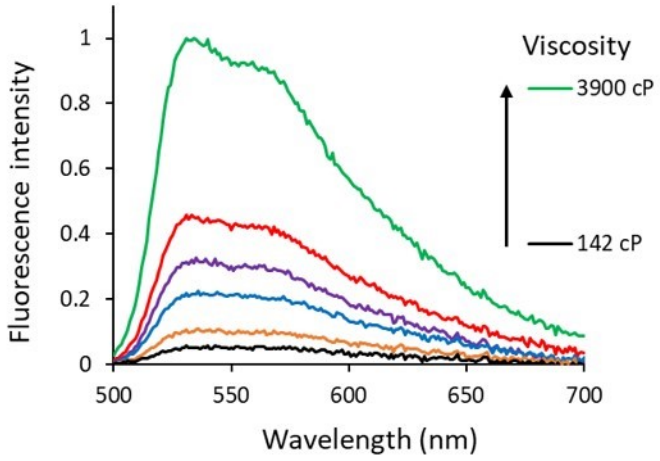

Figure 51 Fluorescence spectra of **dC^{TO}** in glycerol at different temperature (viscosity).

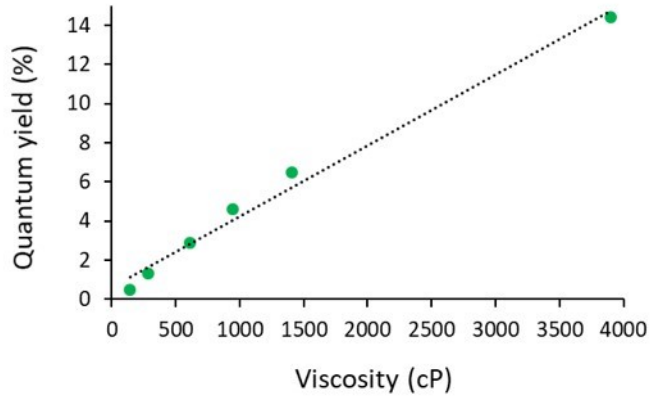

Figure 52 Fluorescence quantum yield of **dC^{TO}** in glycerol plotted against the viscosity.

Table 8 Fluorescence quantum yields of **dC^{TO}** in glycerol at different temperature (viscosity).

Temperature (°C)	Viscosity (cP)	Φ (%)
10	3900	14.4
20	1410	6.5
25	945	4.6
30	612	2.9
40	284	1.3
50	142	0.5

3.4.4 Enzymatic synthesis of modified DNA

In vitro incorporation of **dC^{TO}TP** was tested by primer extension (Figure 53 A) and polymerase chain reaction. PEX was performed with 19-mer template encoding for incorporation of single modification with adjacent AT pairs (Temp7^{PEX}-2P) or GC (Temp1^{PEX}-P). Products were analysed by PAGE, interestingly the mobility of modified DNA containing GC pairs (**ON19_GC_1C^{TO}**) was faster than the corresponding natural DNA or DNA containing AT pairs (**ON19_AT_1C^{TO}**, Figure 53 C, B). In case of DNA with adjacent AT pairs it was necessary to incubate the reaction mixture for 45 min at 60°C, at longer reaction time we observed formation of shorter product due to the exonuclease activity of polymerase. On the other hand, incorporation into DNA with adjacent GC pairs was performed at 60°C for 60 min and no shorter product was observed. Primer used was Cy5-labelled instead of FAM due to the interference of TO fluorescence with FAM. Modified single-stranded DNA was prepared by PEX with 5'-phosphorylated templates followed by λ exonuclease digestion of the phosphorylated strand. All the PEX products were confirmed by MALDI-TOF analysis (Table 9). PCR was studied using different proportions of modified nucleotide **dC^{TO}TP** and natural nucleotide dCTP (100-0%). PCR amplicon

was observed when maximum 10% of **dC^{TO}TP** was used in combination with 90% of dCTP (Figure 53 D). PCR was not very efficient, at 20% of **dC^{TO}TP** small amount of desired product and substantial amount of shorter product were observed, indicating inhibition of the PCR. Nevertheless, it was possible to monitor the amplification in real-time during the PCR due to the light-up effect of thiazole orange modification (Figure 54).

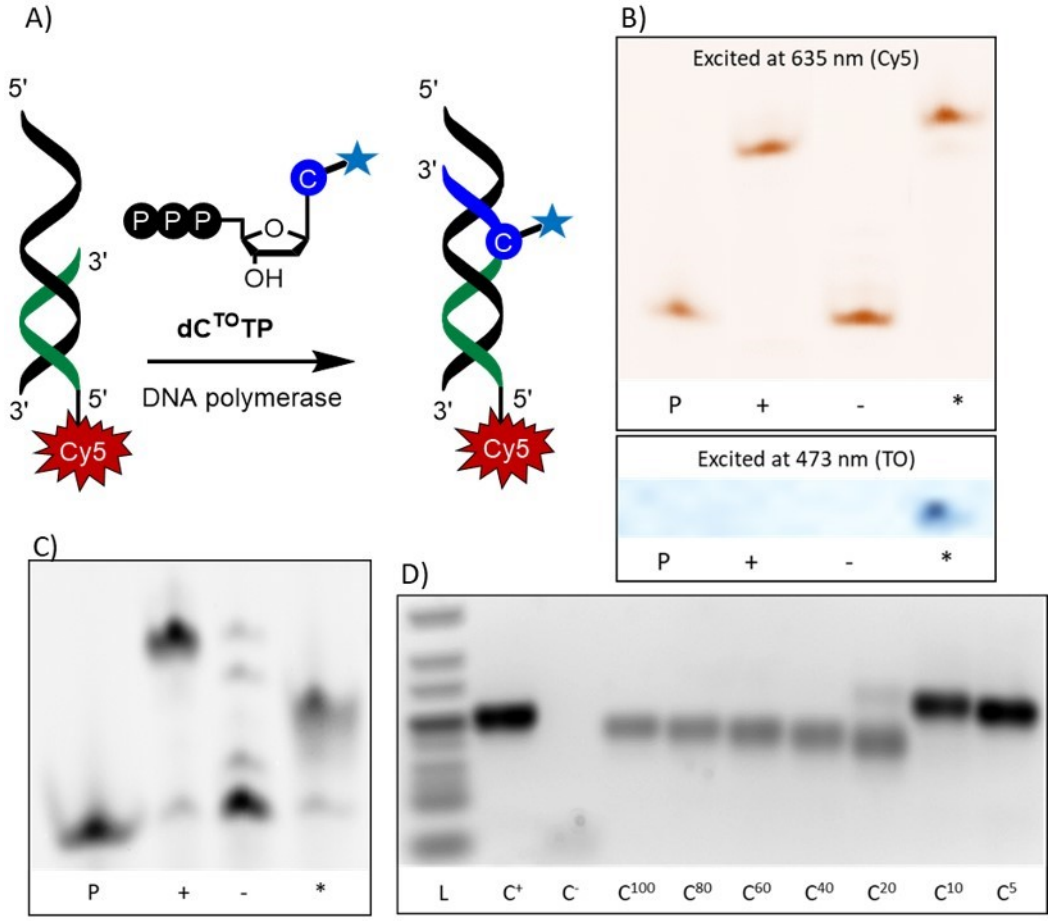

Figure 53 A) Scheme representing PEX with modified nucleotide for gel visualization. PAGE analysis of PEX using **dC^{TO}TP**, KOD XL DNA polymerase, B) Temp7^{PEX}-2P or C) Temp1^{PEX}-P, Primer (P), positive control (+; PEX with all natural dNTPs), negative control (-; PEX in absence of dCTP). PEX with dC^{TO}TP (*). D) Agarose gel electrophoresis analysis of PCR amplification of 98bp template with KOD XL

polymerase using **dC^{TO}TP**. DNA ladder (L), primer (P), positive control (C^+, PCR with all natural dNTPs), negative control (C^-, PCR in absence of dCTP), PCR with mixture of modified nucleotide with natural dCTP (C^{100}-C^5, content of modified nucleotide decreases from 100% to 5%).

Table 9 Table of oligonucleotides prepared in this study

Oligonucleotide	Sequence (5′→3′). C*: modified nucleotide.	$M_{calculated}$ (Da)	M_{found} (Da)
ON19_GC_1C^{TO}	5′-CATGGGCGGCATGGG**C***GGG-3′	6492.6	6493.7
ON19_AT_1C^{TO}	5′-CATGGGCGGCATAAA**C***AAA-3′	6396.6	6397.9

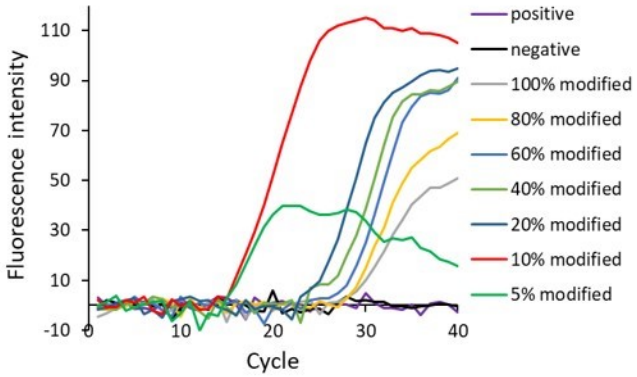

Figure 54 Real-time PCR using different proportions of modified nucleotide **dC^{TO}TP** and natural nucleotide dCTP (100-0%).

3.4.5 Properties of modified DNA

Photophysical properties of modified dsDNA and ssDNA were studied and the results are summarized in Table 10. Figure 55 shows absorption and fluorescence spectra of modified dsDNA. Modified dsDNA with adjacent GC pairs **DNA19_GC_1C^{TO}** showed quantum yield of 12% and the corresponding ssDNA **ON19_GC_1C^{TO}** showed higher quantum yield (18%). **DNA19_AT_1C^{TO}** containing

adjacent AT pairs showed quantum yield of 8% and ssDNA **ON19_AT_1C^{TO}** showed lower quantum yield (5%). Comparison of quantum yield is shown in Figure 56. As it was expected and desired, the nucleotide **dC^{TO}TP** is non-fluorescent in PBS buffer but begins to emit at 534 nm once it gets incorporated into DNA due to the interactions with DNA that most likely inhibit rotation of the fluorophore. Moreover, mean fluorescence lifetime of **dC^{TO}TP** is very short (0.1 ns) and increases to 1.1 ns (in case of **DNA19_GC_1C^{TO}**) or to 0.7 ns (in case of **DNA19_AT_1C^{TO}**) upon incorporation into DNA (lifetime measurements in this chapter were performed by Dr. Tomáš Kraus).

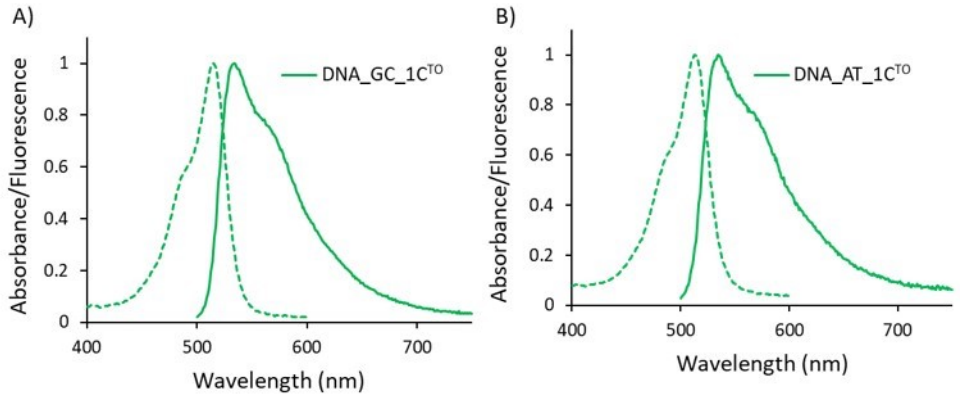

Figure 55 Absorption (dashed lines) and fluorescence (solid lines) spectra of A) **DNA19_GC_1C^{TO}** and B) **DNA19_AT_1C^{TO}**.

Table 10 Photophysical properties of modified ssDNA and dsDNA.

DNA	λ_{abs}[a] (nm)	λ_{em}[b] (nm)	Φ[c] (%)
DNA_GC_1C^{TO}	515	534	0.12
DNA_AT_1C^{TO}	513	534	0.08
ON_GC_1C^{TO}	517	534	0.18
ON_AT_1C^{TO}	516	534	0.05

[a] Position of the absorption maximum. [b] Position of the emission maximum. [c] Fluorescence quantum yield measured using fluorescein in 0.1 M NaOH (Φ = 0.92 at 25°C) as standard.

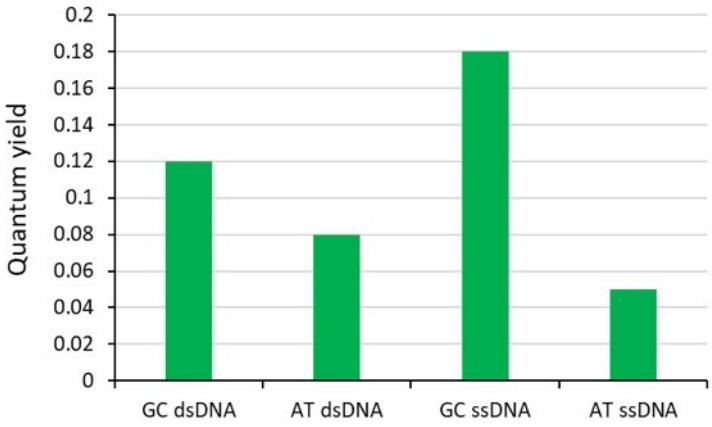

Figure 56 Fluorescence quantum yields of thiazole orange modified dsDNA and ssDNA.

Modified dsDNA products were further characterized by measuring UV melting temperatures (Figure 57). Melting curve analysis revealed that in case of **DNA19_GC_1C^{TO}** the melting temperature (81.5°C) did not differ from natural DNA. On the other hand, we observed increased melting temperature of **DNA19_AT_1C^{TO}** (73.5°C) in comparison with natural DNA (69.5°C). The variability in quantum yields, fluorescence lifetime and melting points suggests that thiazole orange could be useful for sensing various DNA structures of different composition.

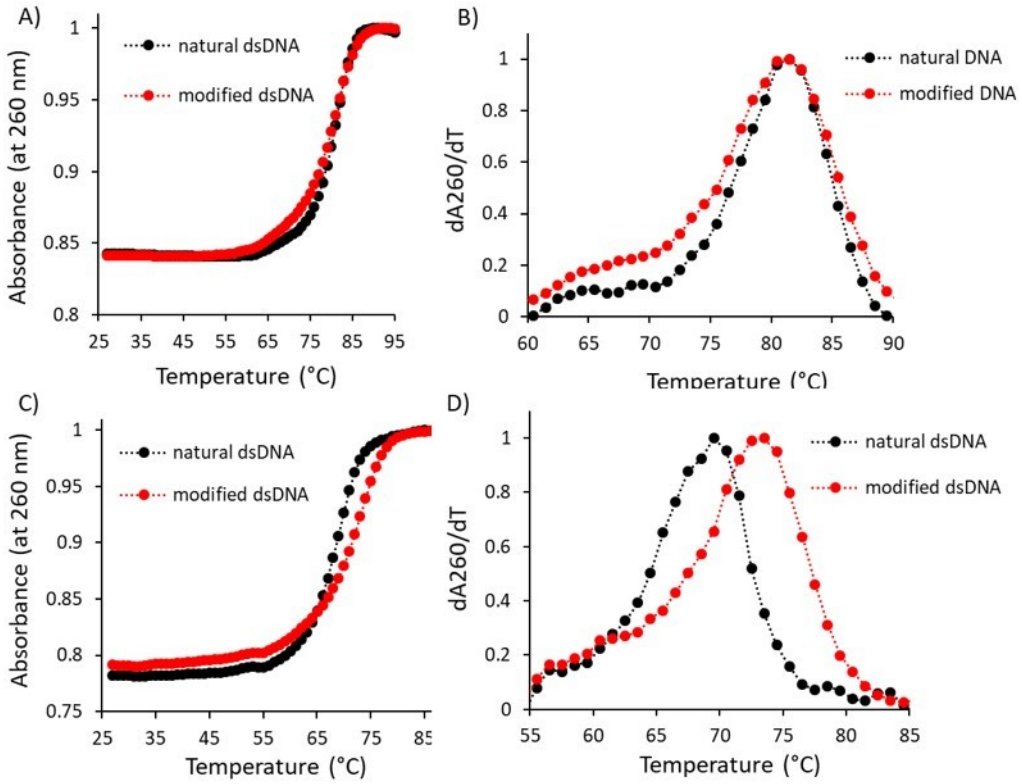

Figure 57 UV melting curves of A) **DNA19_GC_1C^{TO}** and C) **DNA19_AT_1C^{TO}** compared with corresponding natural DNA. Normalized derivatives B) **DNA19_GC_1C^{TO}** and D) **DNA19_AT_1C^{TO}** compared with corresponding natural DNA

3.4.6 Transport of dC^{TO}TP into cells using SNTT

U-2 OS cells were treated with a mixture of **dT^{TO}TP** and SNTT (1:1; experiments were performed by Dr. Tomáš Kraus). The cells were visualized 10 minutes after treatment of cells (Figure 58 A) and the fluorescence signal was detected both inside and outside of nucleus and it was difficult to differentiate between background signal of non-incorporated nucleotide or incorporated nucleotide. However, 2 hours after treatment of cells (Figure 58 B) we observed disappearance of the non-incorporated nucleotide, probably by the means of cellular efflux, and the

incorporation into DNA was apparent (indicated by visible nuclear foci). Desired light-up effect was not observed due to the excessive background signal of non-incorporated nucleotide, which most likely interacts with cellular nucleic acids and thus emit fluorescent signal. To address this issue, we employed fluorescence lifetime imaging (FLIM). Figure 58 C shows FLIM of cell 10 minutes after treatment and shows different mean fluorescence lifetimes corresponding to non-incorporated (3.3 ns) and incorporated nucleotide (1.7 ns). Figure 58 D (2 hours after treatment confirms that the shorter mean fluorescence lifetime (1.7 ns) corresponds to the incorporated nucleotide. At first sight it might seem that mean fluorescence lifetime decreases upon incorporation, however, free nucleotide **dC^{TO}TP** can interact with nucleic acids in cells in any preferred way and that could possibly lead to increased lifetime. On the other hand, once the nucleotide is incorporated, it is forced to be at certain position which might cause less favorable interaction with DNA. Consequently, the increase of lifetime is lower as compared to non-incorporated **dC^{TO}TP**.

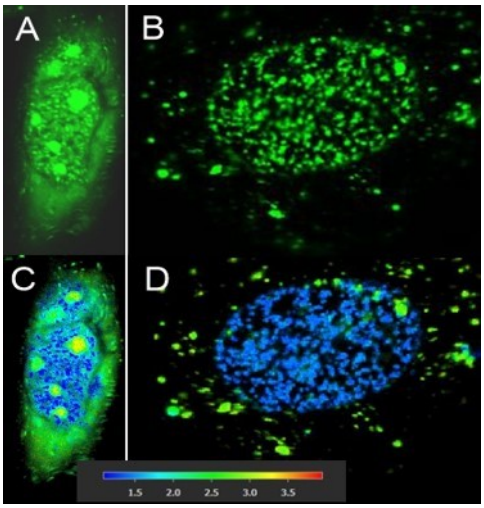

Figure 58 Comparison of intensity (A, B) vs. fluorescence-lifetime (C, D) imaging of live cells; 10 min (A, C) and 120 min (B, D) after treatment with a **dC^{TO}TP**/SNTT complex. DNA foci represented in blue. Bottom: fluorescence-lifetime scale in ns.

Figure 59 shows FLIM of cells treated with a mixture of **dT^{TO}TP** and SNTT (1:1) at different time intervals. In the beginning of the experiment, mostly green signal was detected (Figure 59 A). Eventually, new blue signal (indicating shorter lifetime) appeared and the green signal (longer lifetime) gradually disappeared (Figure 59 A-F). This result clearly shows that indeed we can use thiazole orange modified nucleotide for real-time imaging of DNA synthesis in live cells. Interestingly, we observed one cell that actually showed increase of intensity with time (Figure 59; cell highlighted with red circle). However, this phenomenon was probably caused by the cell being weakly permeable and at the same time in early S-phase and thus can not be neccessary acredited to light-up effect of **dT^{TO}TP**.

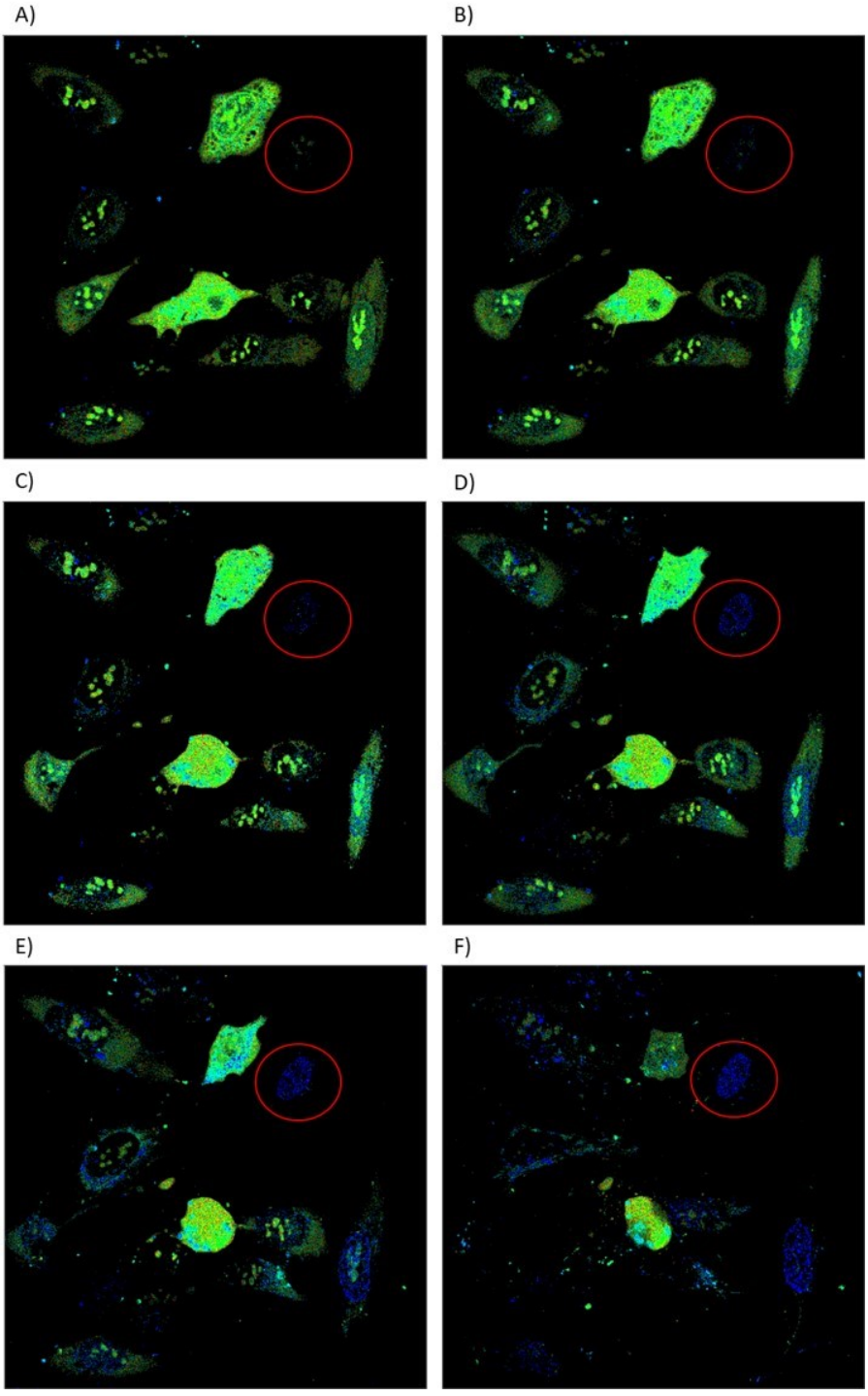

Figure 59 FLIM of live cells after treatment with a **dC^{TO}TP**/SNTT complex. Minutes after treatment: A) 18, B) 26, C) 34, D) 42, E) 54, F) 90.

Moreover, we also observed different lifetime in nucleus of live cell that is synthesising DNA and in the nucleus of dead cell (Figure 60). In case of dead cell, we can see signal outside of nucleus, which might be due to the degradation of nuclear DNA by endonucleases in apoptopic cell.[175]

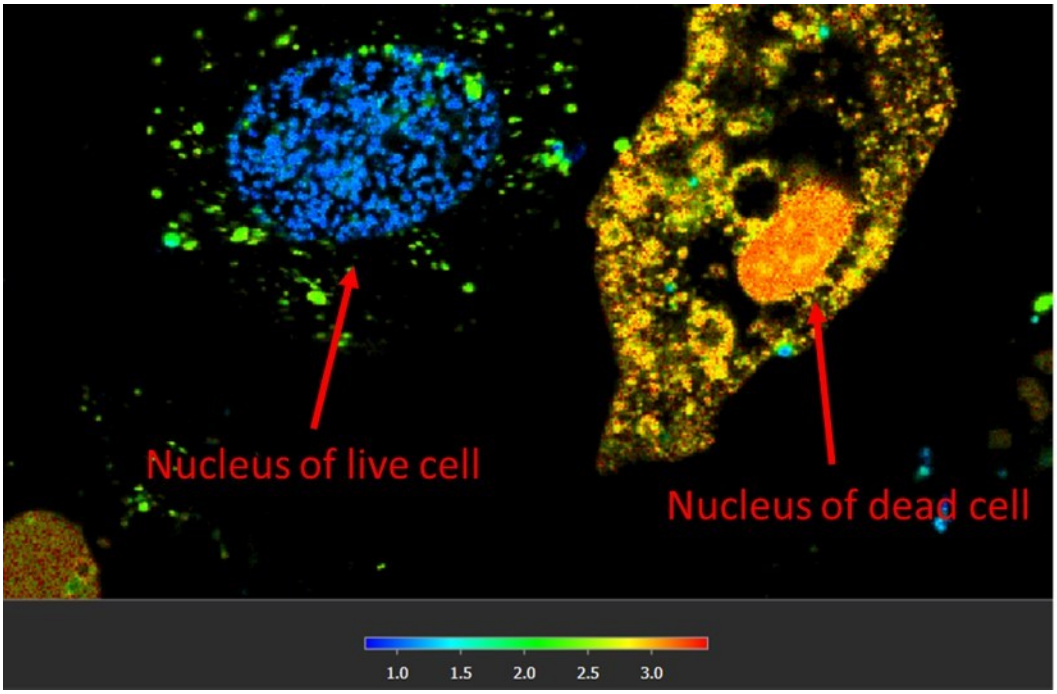

Figure 60 FLIM comparison of live vs dead cell nucleus.

To the best of our knowledge, nucleotide that changes fluorescence lifetime upon incorporation into genomic DNA in live cells has never been reported. Nucleotide **dC^{TO}TP** can be potentially used for investigation of DNA in healthy and cancer cells, or cells infected by virus. Moreover, it would be interesting to monitor processes such as reactivation of quiescent cells,[51] DNA repair[176,177] or pathogen entry and replication[178].

3.5 2'-Deoxycytidines and their triphosphates bearing dimethoxy-, diphenyl-BODIPY fluorophore. Synthesis, photophysical properties, enzymatic incorporation into DNA and applications

3.5.1 Introduction

BODIPY (4,4-difluoro-4-bora-3a,4a-diaza-s-indacene) dyes were first synthesized by Treibs and Kreuzer in 1968.[179] The spectroscopic properties of BODIPY dyes can be finely-tuned by introducing various modifications to BODIPY core, which led to array of BODIPY derivatives that are widely used as fluorescent labels.[180–187] Introduction of aryl substituents at the *meso* position of the BODIPY decreases the quantum yield of the fluorophore but makes it excellent viscosity sensor (as explained in chapter 1.5.).[188]

Previously, Hocek group reported labelling of DNA using dNTP bearing phenyl-BODIPY (BDP, Figure 61 A)[189] linked through flexible linker or bearing tetramethylated thiophene-BODIPY (TBDP, Figure 61 C)[132] conjugated with nucleobase. These rotational BODIPY labels are sensitive to viscosity and were used for monitoring DNA-protein interactions by change of fluorescence lifetime.[97,132] Moreover, dCTP bearing hexamethyl-BODIPY (mBDP, Figure 61 B),[98] which has hindered rotation, was used as strongly fluorescent nucleotide for staining of DNA even in live cells.[190] However, these modified dNTPs have some drawbacks for biological applications. For example, they emit in green region of spectrum and the environment sensitive dNTPs were bad substrates for eukaryotic polymerases in live cells.

Recently, a small library of new alkoxy-substituted NIR BODIPY dyes was developed.[133] Particularly inspired by dimethoxy-, diphenyl-BODIPY analogue (Figure 61 D), we designed new derivatives (Figure 61 E, F), the fluorophore was attached to dC and dCTP via short propargylether and long triethylene glycol linker using Sonogashira cross-coupling reaction. Modified nucleosides and nucleotides were then used for the study of photophysical properties and incorporation into DNA.

Modified DNA was used as fluorescence lifetime probe for DNA-protein interactions. Transport of modified nucleotides into cells and subsequent incorporation into genomic DNA was also studied.

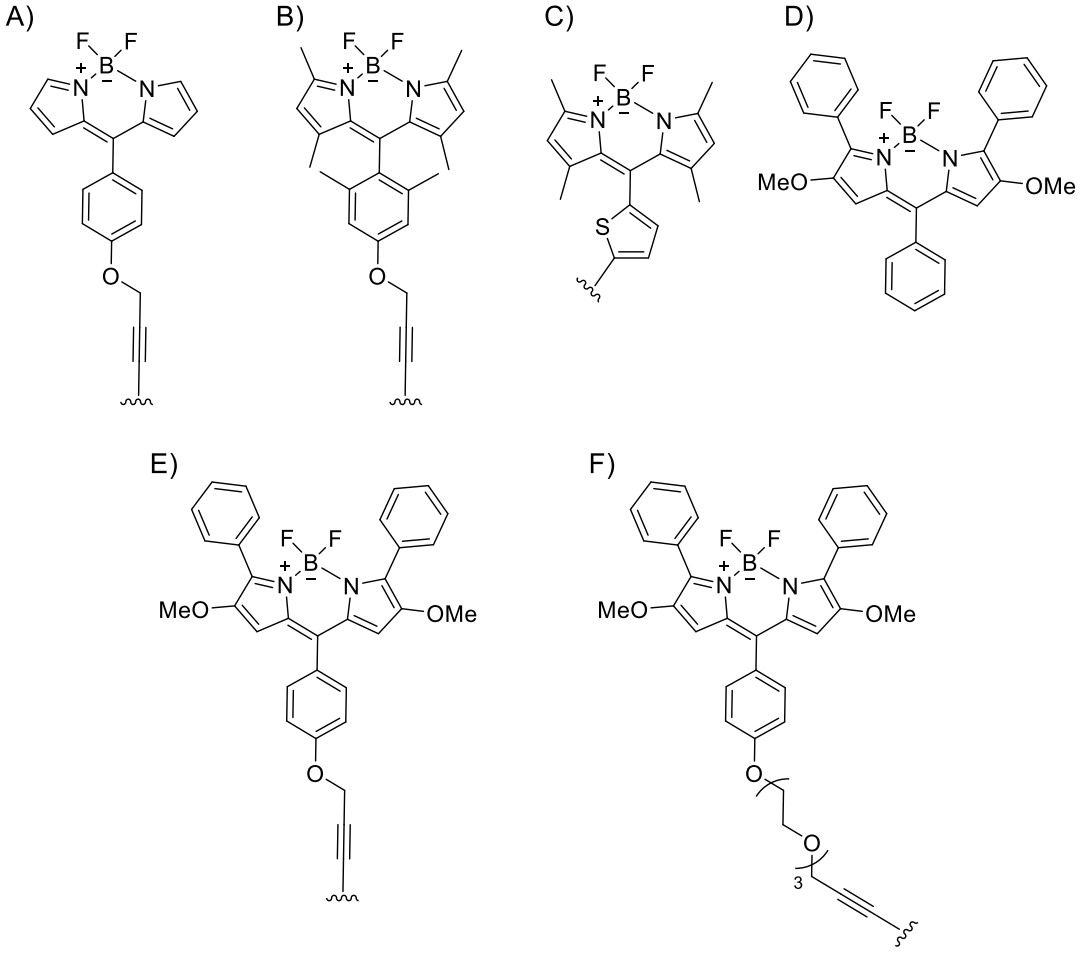

Figure 61 Structures of BODIPY dyes previously used for labelling of DNA - A) BDP, B) mBDP, C) TBDP. D) Structure of dimethoxy-, diphenyl-BODIPY analogue. E), F) Structures of new BODIPY derivatives for labelling of DNA.

3.5.2 Synthesis

Modified nucleosides and nucleotides were prepared by the Sonogashira cross-coupling reaction of 5-iodo-2'-deoxycytidine (**dC^{I}**) or the triphosphate (**dC^{I}TP**) with alkyne of the corresponding fluorophore (**61a** or **61b**, Scheme 23).

The synthesis of BODIPY fluorophore was done in analogy to the synthesis of related derivatives.[133] The required 3-methoxy-2-phenylpyrrole **57** for the synthesis of BODIPY was prepared according to the literature.[191] First, N-tosylimine **53** was prepared by the reaction of benzaldehyde **52** with *p*-toluenesulfonamide in presence of TFA. Then, methoxyallene **54** was lithiated in presence of BuLi and underwent reaction with N-tosylimine **53**, affording adduct **56** in 82% yield. The synthesis of the pyrrole **57** was finished by cyclization of allenylamine **56** in dry DMSO in presence of potassium *tert*-butoxide.

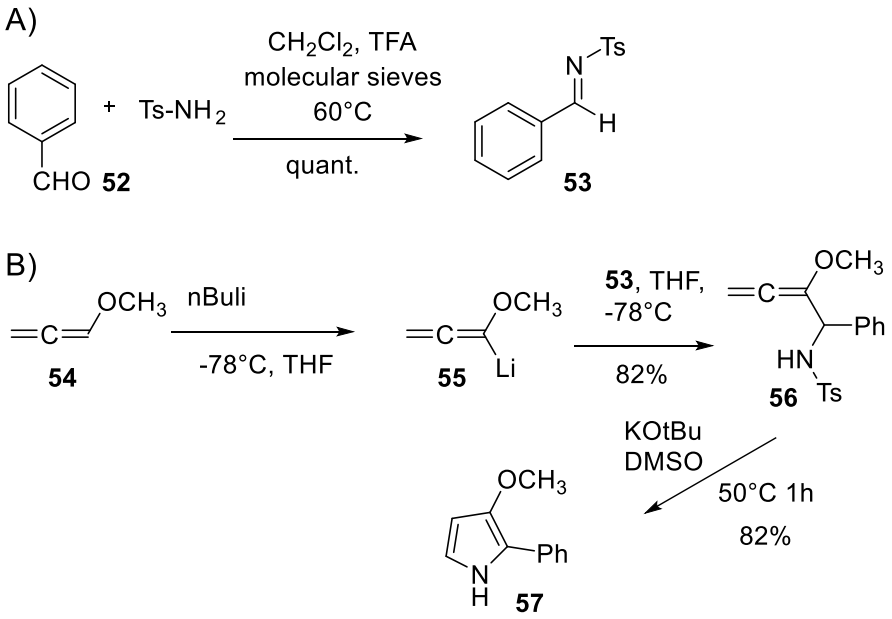

Scheme 22 Synthesis of methoxy pyrrole **57**.

Dipyrrin **59** was then prepared by one-pot two-step synthesis consisting of condensation reaction of benzaldehyde **58** with pyrrole **57** in presence of TFA and subsequent oxidation by chloranil. Solution of dipyrrin **59** in dry toluene was treated with triethylamine and then with boron trifluoride diethyl etherate, providing BODIPY **60** in 70% yield. Conversion of BODIPY **60** into alkyne **61a** or alkyne **61b** was achieved by alkylation of **60** using propargyl bromide or tosyl-propargyloxy-triethylene glycol **46** in acetonitrile in presence of K_2CO_3. Finally, the Sonogashira cross-coupling of **dC^{I}** or **dC^{I}TP** with alkyne **61a** or **61b** in the presence of $PdCl_2(PPh_3)_2$ and CuI in DMF and Et_3N provided nucleosides **62a**, **62b** and nucleotides **63a**, **63b** in yields of 84%, 77%, 28% and 28% respectively.

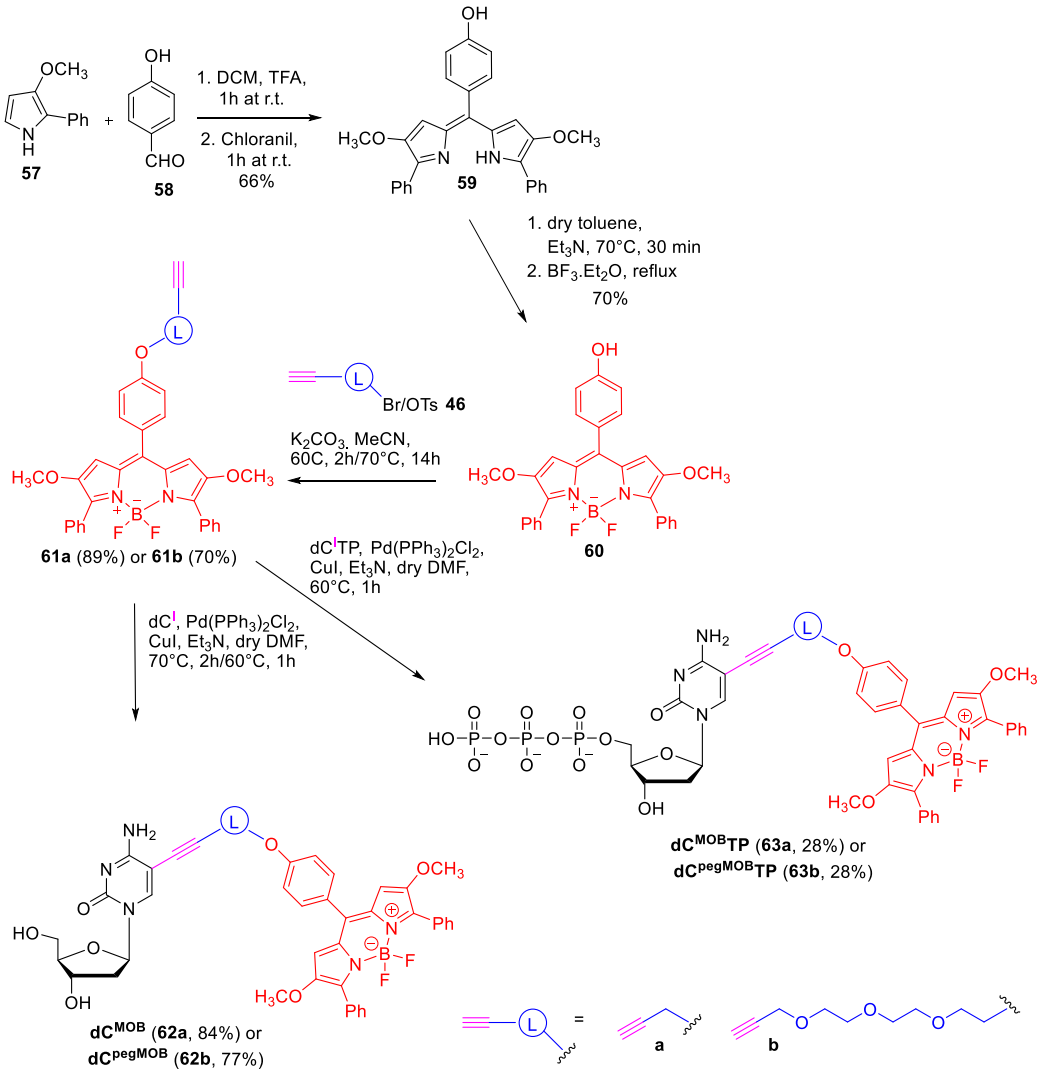

Scheme 23 Synthesis of **dC^{MOB}TP** and **dC^{pegMOB}TP**.

3.5.3 Photophysical properties

Table 11 summarizes basic photophysical properties of new compounds, Figure 62 shows corresponding absorption and fluorescence spectra. Absorption of nucleosides **dC^{MOB}** and **dC^{pegMOB}** in MeOH shows band with maximum at 625 nm and the corresponding nucleotides **dC^{MOB}TP** and **dC^{pegMOB}TP** show slightly blue-shifted absorption (616 nm and 617 nm respectively) in PBS buffer. **dC^{MOB}** and

dC^{MOB}TP show emission at 671-672 nm, **dC^{pegMOB}** and **dC^{pegMOB}TP** possessing triethylene glycol linkage show slightly red-shifted emission at 677-678 nm. Fluorescence quantum yields of nucleosides **dC^{MOB}** and **dC^{pegMOB}** in MeOH were 18% and 19%. The quantum yield of corresponding triphosphates **dC^{MOB}TP** and **dC^{pegMOB}TP** in PBS buffer was approximately 2 times lower (8% and 10% respectively), probably due to the formation of less fluorescent aggregates in aqueous buffer.

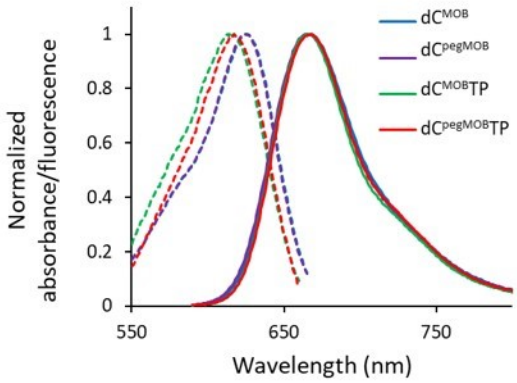

Figure 62 Normalized absorption (dashed lines) and fluorescence spectra (solid lines) of modified nucleosides and nucleotides.

Table 11 Photophysical properties of studied nucleosides and nucleotides.

Compound	Solvent	λ_{abs}[a] (nm)	ε[b] (M^{-1} cm^{-1})	λ_{em}[c] (nm)	$\Delta\lambda$[d] (nm)	Φ[e]
dC^{MOB}	MeOH	625	23425	672	47	0.18
dC^{pegMOB}	MeOH	625	21316	677	52	0.19
dC^{MOB}TP	PBS	616	19142	671	55	0.08
dC^{pegMOB}TP	PBS	617	22263	678	61	0.10

[a] Position of the absorption maximum. [b] Molar extinction coefficients. [c] Position of the emission maximum. [d] Stokes shift. [e] Fluorescence quantum yield measured using Cresyl violet perchlorate in MeOH (Φ = 0.54) as standard.

The fluorescence lifetime response of both nucleosides to viscosity was evaluated by measuring mean fluorescent lifetime in the mixtures of methanol/glycerol at different ratios at 25°C (Table 12). Mean τ of **dC^{MOB}** increased from 1.6 ns (at 0.6 cps) to 4.2 ns (at 793.0 cps) and from 1.7 ns (at 0.6 cps) to 4.6 ns (at 793.0 cps) for **dC^{pegMOB}**. Figure 63 shows mean τ plotted against viscosity, fluorescence lifetime decay curves are shown in Figure 64. The increase of fluorescence lifetime is due to the inhibited rotation between phenyl ring and boron dipyrromethene system at higher viscosity, and shows potential of these modifications for sensing local viscosity in vicinity of DNA. Comparison of new nucleosides with viscosity sensitive bodipy derivatives (structures shown in Figure 61) developed in Hocek lab is shown in Figure 65.

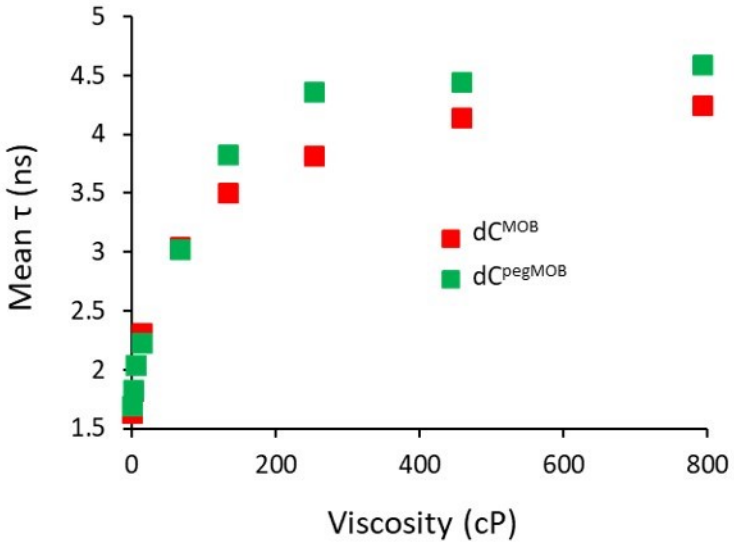

Figure 63 Mean fluorescence lifetime of nucleosides **dC^{MOB}** and **dC^{pegMOB}** at different viscosity.

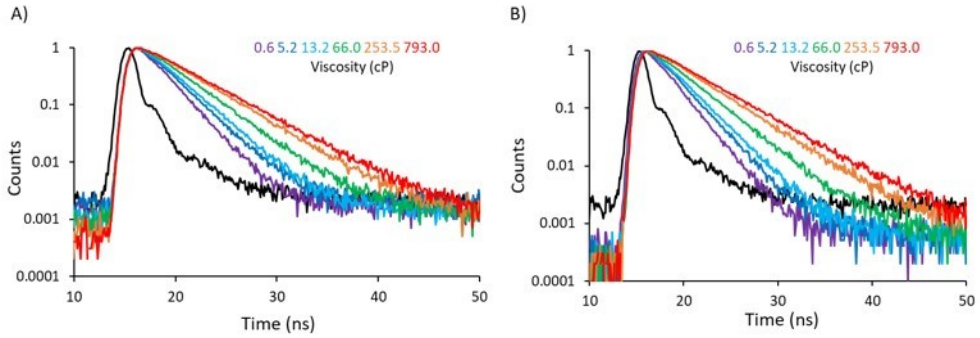

Figure 64 Fluorescence decays of nucleosides **dC^{MOB}** and **dC^{pegMOB}** at different viscosity. Black curves represent instrument response function.

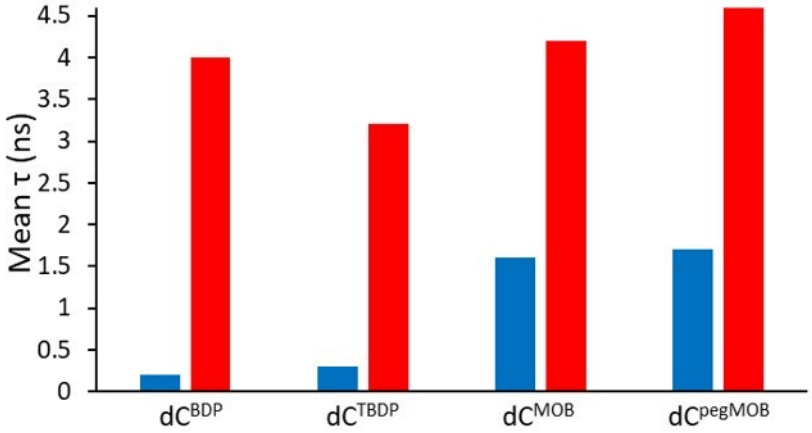

Figure 65 Comparison of fluorescence lifetime response of deoxycytidine bearing either BDP, TBDP, MOB or pegMOB at low viscosity (0.6-1.2 cP) or high viscosity (793-800 cP).

Table 12 Mean fluorescence lifetime of nucleosides **dC^{MOB}** and **dC^{pegMOB}** at different viscosity.

Nucleoside	Glycerol/Methanol %molar ratio	Mean τ (ns)	η (cP)
dC^{MOB}	90	1.64	0.6
	80	1.82	1.8
	70	2.04	5.2
	60	2.31	13.2
	50	3.01	66.0
	40	3.50	133.2
	30	3.81	253.5
	20	4.15	458.6
	10	4.24	793.0
dC^{pegMOB}	90	1.70	0.6
	80	1.83	1.8
	70	2.04	5.2
	60	2.23	13.2
	50	3.02	66.0
	40	3.83	133.2
	30	4.36	253.5
	20	4.45	458.6
	10	4.60	793.0

3.5.4 Enzymatic synthesis of modified DNA

The enzymatic incorporation of **dC^{pegMOB}** and **dC^{pegMOB}TP** was examined in primer extension (Figure 66 A) and polymerase chain reaction experiments. At first, we tested incorporation of single fluorescent modification into DNA by PEX with short 19-mer template (Temp1^{PEX}) encoding for incorporation of one modification using different enzymes. KOD XL and Vent (exo-) DNA polymerases were found to incorporate both modified nucleotides. PEX with BST large fragment DNA polymerase showed low amounts of the extended product. Products were analysed by PAGE (Figure 66) and MALDI-TOF spectromectry (Table 13). Primer extension using KOD XL DNA polymerase with 31-mer template encoding for incorporation of 4 modifications was also efficient and we observed full length products (Figure 68 A), products appeared as smears on gels probably as effect of multiple lipophilic modifications. However, we did not observe molecular mass of products **ON31_4C^{MOB}** or **ON31_4C^{pegMOB}** in MALDI-TOF spectra, probably due to the

possible degradation of modification during ionization. To explore the influence of linker on incorporation to DNA we performed kinetic experiments of single nucleotide extension of primer using Temp4^{PEX}, dCTP, **dC^{MOB}TP** and **dC^{pegMOB}TP**. The results show that the extension of primer with **dC^{pegMOB}TP** is somewhat faster (75% conversion after 5 min) than with **dC^{MOB}TP** (55% conversion after 5 min) and the extension with natural dCTP is the fastest (95% conversion after 5 min, Figure 67). Modified nucleotides were then compared in PCR amplification using KOD XL DNA polymerase and 98-mer template (Temp1^{PCR}). In case of **dC^{MOB}TP**, the PCR amplicon was obtained when a max. 40% of modified nucleotide was used in mixture with natural dCTP, at 40% of **dC^{MOB}TP** the inhibition of PCR was observed. In case of **dC^{pegMOB}TP** the amplification was somewhat less efficient and the amplicon was obtained when a max. 20% of modified nucleotide was used in mixture with natural dCTP and at 40% of **dC^{pegMOB}TP** we observed shorter products (Figure 68 B, C).

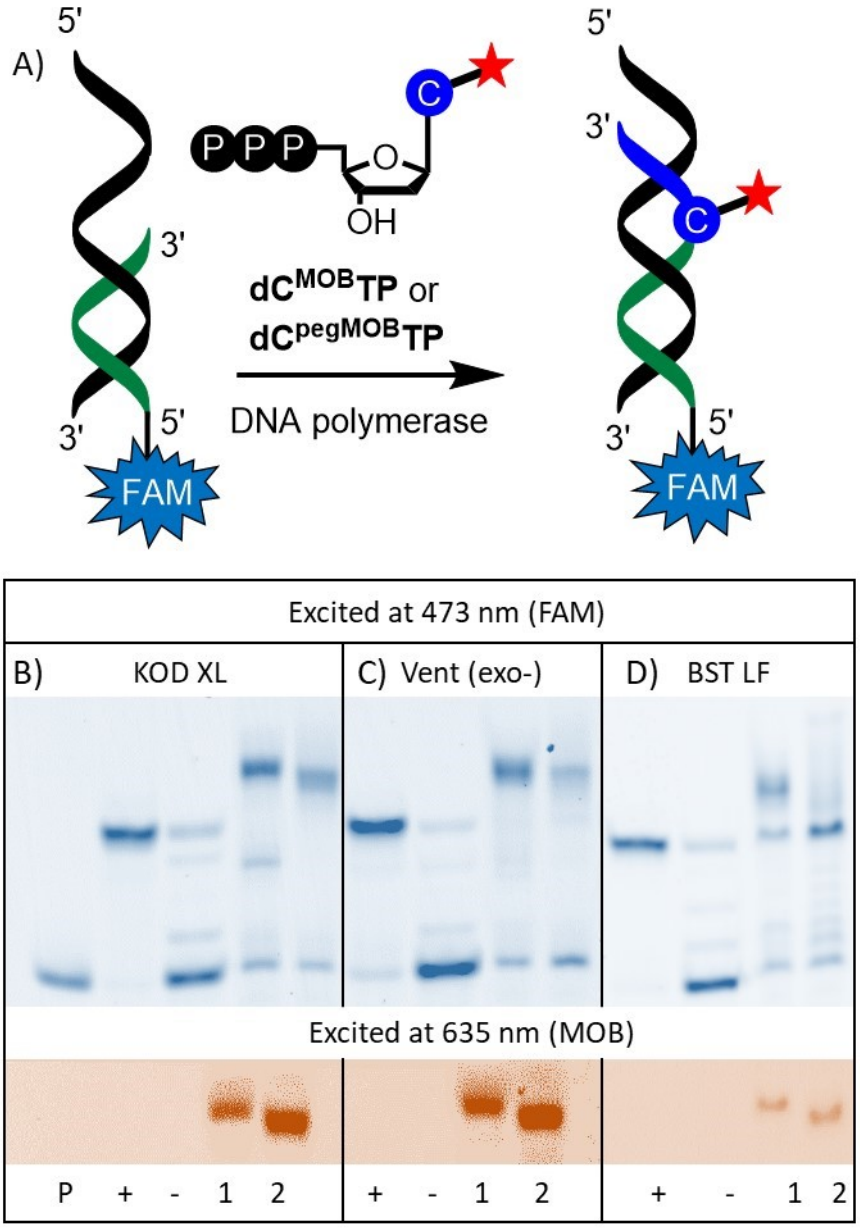

Figure 66 A) Scheme representing PEX with modified nucleotide for gel visualization. PAGE analysis of PEX using template Temp1, **dC^{MOB}TP** or **dC^{pegMOB}TP** and B) KOD XL polymerase, C) Vent (exo-) polymerase, D) BST LF polymerase. Primer (P), positive control (+, PEX with all natural dNTPs), negative control (-, PEX in absence of dCTP), PEX with **dC^{MOB}TP** (1), PEX with **dC^{pegMOB}TP** (2).

Table 13 Table of oligonucleotides prepared in this study.

Oligonucleotide	Sequence (5′→3′). C*: modified nucleotide.	$M_{calculated}$ (Da)	M_{found} (Da)
ON16_1C^{MOB}	5′-CATGGGCGGCATGGG**C***-3′	5496.5	5496.2
ON16_1C^{pegMOB}	5′-CATGGGCGGCATGGG**C***-3′	5628.9	5629.6
ON19_1C^{MOB}	5′-CATGGGCGGCATGGG**C***GGG-3′	6484.1	6484.9
ON19_1C^{pegMOB}	5′-CATGGGCGGCATGGG**C***GGG-3′	6616.5	6617.6

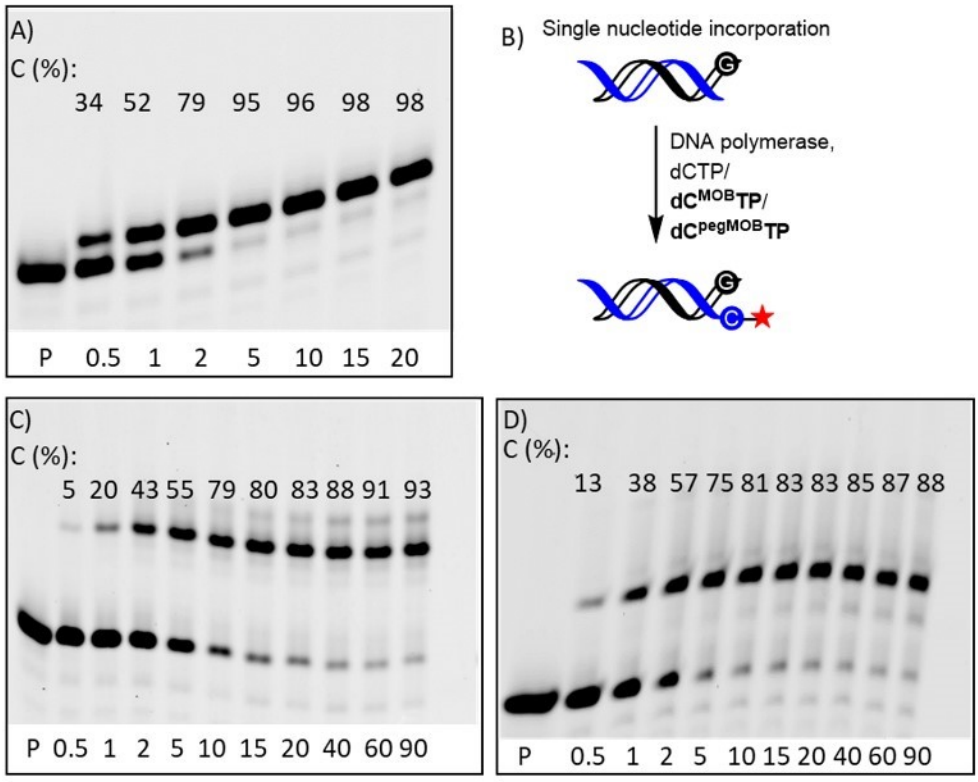

Figure 67 PAGE analysis of kinetics of single nucleotide incorporation. A) SNI using natural dCTP, B) scheme of SNI, C) SNI using **dC^{MOB}TP** and D) SNI using **dC^{pegMOB}TP**. C – conversion, primer (P), time is given in minutes (0.5-90).

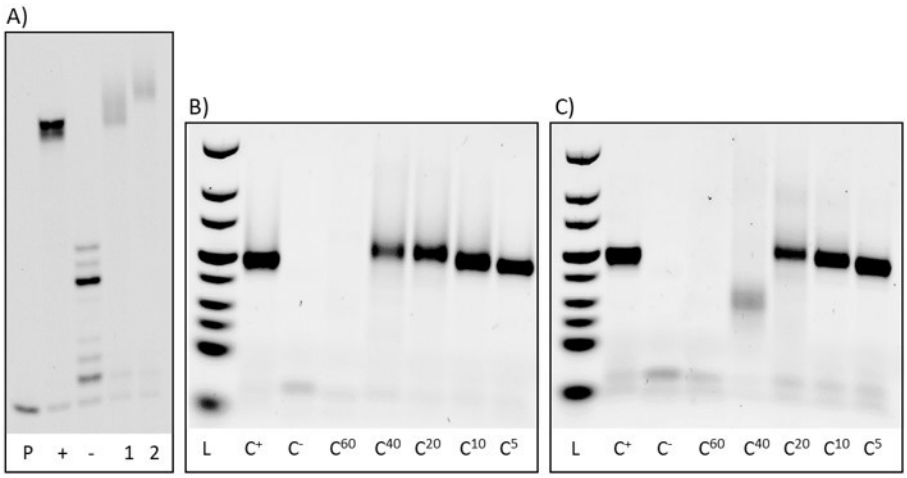

Figure 68 A) Page analysis of PEX using KOD XL polymerase, **dC^{MOB}TP** or **dC^{pegMOB}TP** and template Temp3. Primer (P), positive control (+, PEX with all natural dNTPs), negative control (-, PEX in absence of dCTP), PEX with **dC^{MOB}TP** (1), PEX with **dC^{pegMOB}TP** (2). Agarose gel electrophoresis analysis of PCR amplification of 98-mer template Temp4 with KOD XL polymerase using B) **dC^{MOB}TP** or C) using **dC^{pegMOB}TP**. DNA ladder (L), primer (P), positive control (C^+, PCR with all natural dNTPs), negative control (C^-, PCR in absence of dCTP), PCR with mixture of modified nucleotide with natural dCTP (C^{60}-C^5, content of modified nucleotide decreases from 60% to 5%).

The 19-mer PEX products containing single modification were also tested by measurement of UV-vis and fluorescence spectra. Absorption maximum of **DNA19_1C^{MOB}** (618 nm) was slightly higher than in case of nucleotide **dC^{MOB}TP** (616 nm), emission of modified DNA was lower (667 nm) than in case of modified nucleotide (671 nm). **DNA19_1C^{pegMOB}** shows absorption maximum at higher wavelength (622 nm) than the corresponding nucleotide **dC^{pegMOB}TP** (617 nm), modified DNA emits at lower wavelength (669 nm) than the modified nucleotide (678 nm; Figure 69). In both cases, the fluorescence is nicely visible by naked eye.

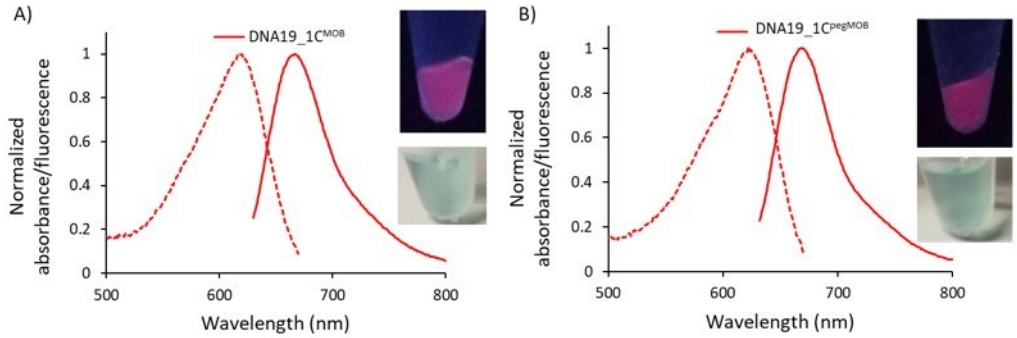

Figure 69 UV-vis absorption spectra (dashed lines) and fluorescence spectra (solid lines) of purified modified dsDNA obtained after PEX, A) **DNA19_C^{MOB}** (λ_{abs} = 618 nm, λ_{em} = 667 nm) and B) **DNA19_C^{pegMOB}** (λ_{abs} = 622 nm, λ_{em} = 669 nm). Inset – photography of modified DNA solution under irradiation with 365 nm UV lamp (top pictures) or no irradiation (bottom pictures).

3.5.5 Interaction of modified DNA with proteins

DNA19_1C^{MOB} and **DNA19_1C^{pegMOB}** were tested as fluorescence lifetime probes for *in vitro* studies of DNA-protein interactions. In this study recombinant H2A histone was chosen as protein of interest and non-DNA binding protein bovine serum albumin (BSA) was used as negative control. Corresponding modified dsDNA was titrated by histone or BSA and fluorescence decays were recorded (Table 14). Mean fluorescence lifetime of **DNA19_1C^{MOB}** increased from 3.2 ns to 5.3 ns in presence of histone (Figure 70 A), whereas in presence of BSA there was only minor effect on lifetime (from 3.2 ns to 3.62 ns; Figure 71 A). In case of **DNA19_1C^{pegMOB}** the lifetime increased from 3.5 ns to 5.6 ns (Figure 70 B), however the experiment with BSA showed stronger non-specific interaction (the lifetime increased from 3.5 ns to 4.4 ns) than with DNA bearing fluorophore via shorter linker (Figure 71 B). It is possible, that the fluorophore in **DNA19_1C^{pegMOB}** is more exposed due to the length of the linker and therefore it might interact even with proteins that have low affinity to DNA. Nevertheless, observed increase of fluorescence lifetime is probably due to the

restriction of BODIPY rotation upon binding of the protein to DNA and indicates potential of this label for sensing interactions.

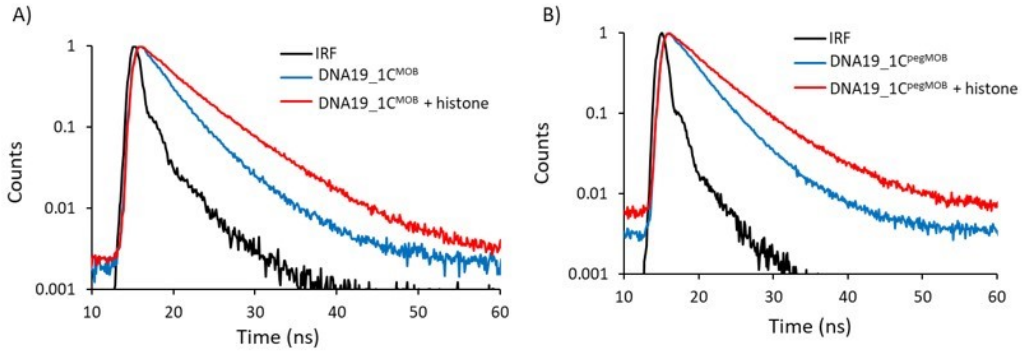

Figure 70 Fluorescence decays of A) **DNA19_1C^{MOB}** and B) **DNA19_1C^{pegMOB}** before and after binding to H2A histone.

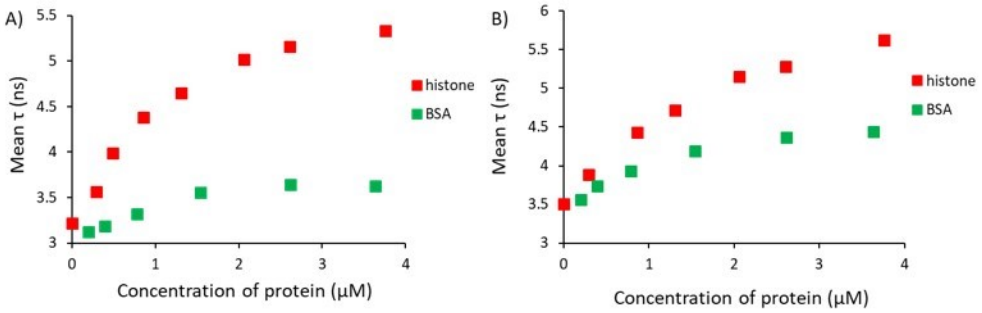

Figure 71 Changes of the mean fluorescence lifetime of A) **DNA19_1C^{MOB}** and B) **DNA19_1C^{pegMOB}** in the presence of H2A histone (red) or BSA (green).

Table 14 Mean fluorescence lifetime of **DNA19_1C^{MOB}** and **DNA19_1C^{pegMOB}** upon addition of H2A histone or BSA protein.

Concentration of H2A histone (μM)	**DNA19_1C^{MOB}** **Mean τ (ns)**	**DNA19_1C^{pegMOB}** **Mean τ (ns)**
0.00	3.22	3.50
0.30	3.56	3.88
0.86	4.38	4.43
1.31	4.65	4.72
2.06	5.02	5.15
2.61	5.16	5.28
3.76	5.33	5.63
Concentration BSA (μM)	**DNA19_1C^{MOB}** **Mean τ**	**DNA19_1C^{pegMOB}** **Mean τ**
0.78	3.32	3.93
1.54	3.56	4.19
2.62	3.64	4.37
3.64	3.62	4.44

3.5.6 Cell experiments

Transport of modified nucleotides into cells was performed by treatment of cells with **dC^{MOB}TP**/SNTT or **dC^{pegMOB}TP**/SNTT complex (experiments were performed by Dr. Tomáš Kraus). In case of **dC^{MOB}TP**, the incorporation into DNA was not detected even after 24 hours (Figure 72 A, B). On the other hand, incorporation of **dC^{pegMOB}TP** into genomic DNA was observed (Figure 72 C, D). However, unusually high power of the laser for the excitation of the fluorophore and long incubation of treated cells (24 hours) were required. Taking into account the relatively high brightness of the fluorophore, both observed phenomena indicate a low incorporation density of **dC^{pegMOB}TP** nucleotide in genomic DNA.

The reason behind low incoporation of **dC^{pegMOB}TP** could be lipophilicity of the fluorophore which might increase the propensity of the triphosphate to bind hydrophobic structures outside of nucleus, and therefore decrease the amount of the nucleotide available for DNA synthesis in nucleus.

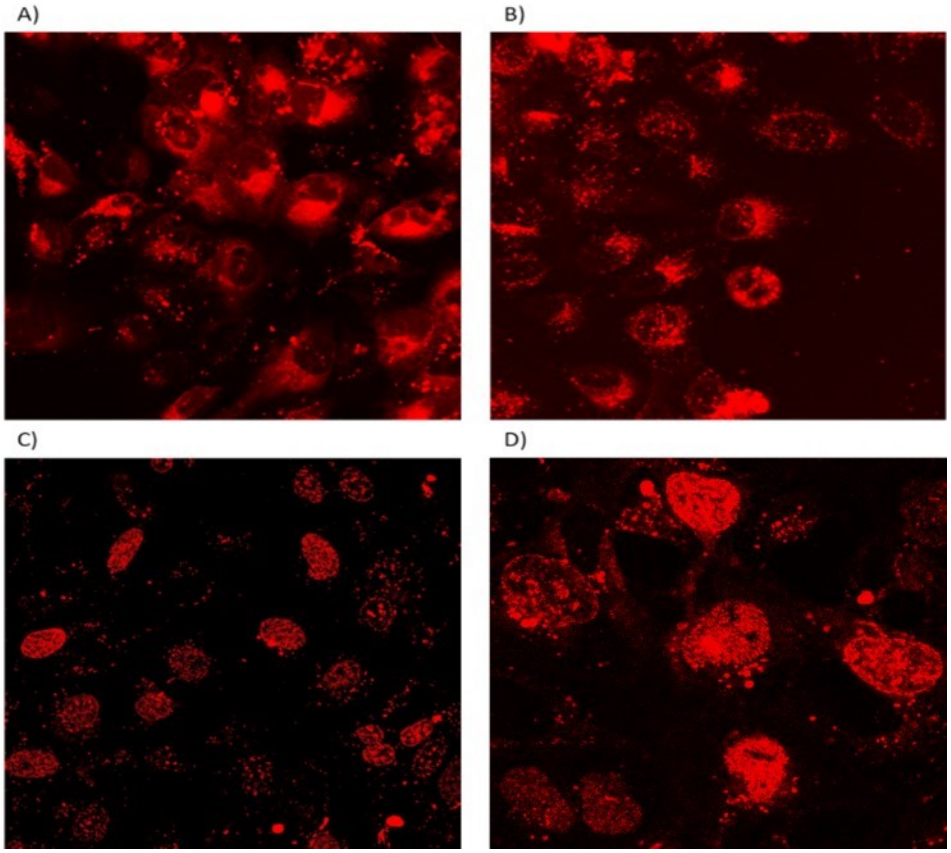

Figure 72 Fluorescence microscopy. Treatment of cells with **dC^{MOB}TP**/SNTT, A) 2 hours, B) 24 hours after treatment or with **dC^{pegMOB}TP**/SNTT, C) 24 hours after treatment, D) detail of few cells.

3.6 2'-Deoxycytidine triphosphate bearing silicon rhodamine fluorophore. Synthesis, phyotophysical properties, enzymatic incorporation into DNA and applications

3.6.1 Introduction

Silicon rhodamine derivatives, such as **SiR-carboxyl** (Figure 73 B), differ from classical rhodamines (for example 6-carboxytetramethylrhodamine – Figure 73 A) by replacement of the oxygen atom with silicon moiety of the pyronine skelet. This substitution of the oxygen with silicon results in a bathochromic shift of the excitation and emission wavelengths of the fluorophore. It is known, that rhodamines capable of forming spirolactones exist in a dynamic equilibrium between a non-fluorescent spirolacton and a fluorescent zwitterion form depending on the polarity of environment. Another feature of silicon in **SiR-carboxyl** is that it reduces the electron density of the xanthene, and thus increases its propensity to form non-fluorescent spirolactone in solvents of low dielectric constant. This effect of **SiR-carboxyl** dyes is very beneficial for cell-based imaging because it can lower background fluorescence signal of non-specific interactions of the fluorescent label with hydrophobic structures. On top of that, **SiR-carboxyl** shows high fluorescence brightness, photostability and is also compatible with stimulated emission depletion (STED) microscopy. **SiR-carboxyl** was previously used for cell super-resolution microscopy of cellular proteins and for imaging of cytoskeletal structures.[134–136]

Inspired by **SiR-carboxyl** and its properties, we synthesized new dCTP derivative bearing silicon rhodamine modification. Photophysical properties of new nucleotide were tested, as well as its enzymatic incorporation into DNA. Modified nucleotide was transported into live cells and its incorporation into genomic DNA was then studied by confocal and super-resolution microscopy.

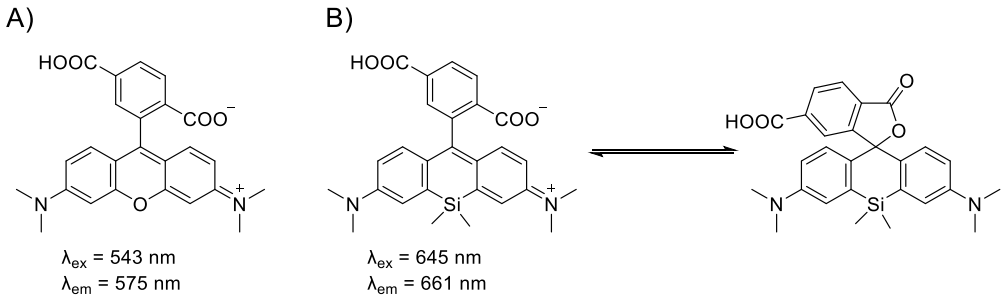

Figure 73 A) Structure of 6-carboxytetramethylrhodamine, B) structure of **SiR-carboxyl** and the formation of spirolactone.

3.6.2 Synthesis

Silicon rhodamine modified nucleoside triphosphate **dC^{SiR}TP** was prepared by strain-promoted azide-alkyne cycloaddition reaction of azido-propargyloxy-triethylene glycol modified 2'-deoxycytidine triphosphate **dC^{pegN3}TP** with bicyclononyne-linked silicon rhodamine fluorophore **SiR-BCN** (commercially available). The product was isolated in 50% yield after purification by reverse-phase HPLC.

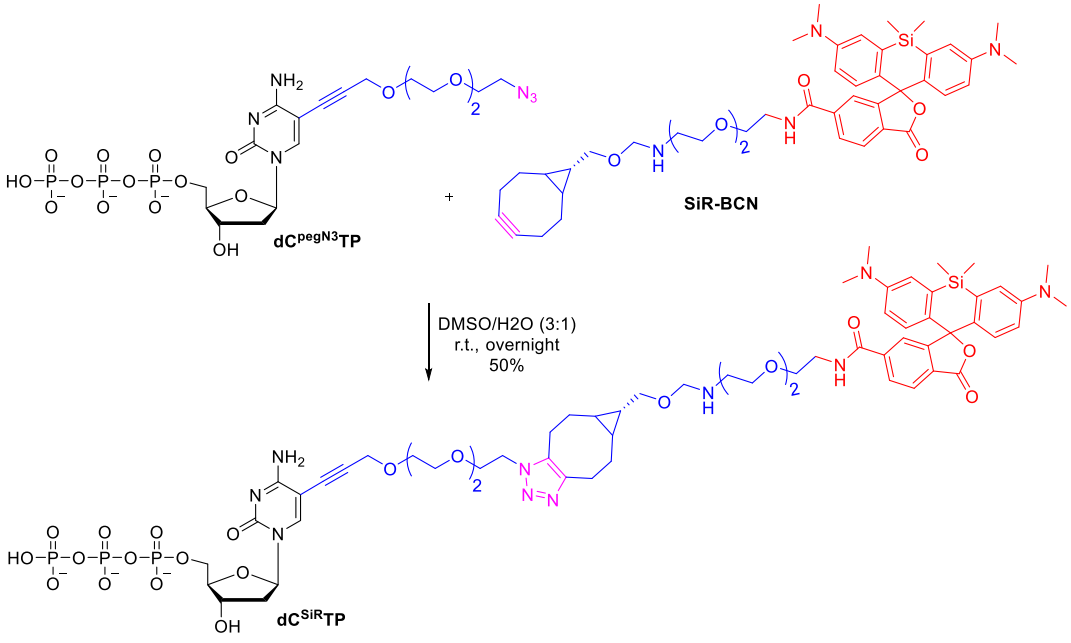

Scheme 24 Synthesis of silicon rhodamine modified nucleotide **dC^{SiR}TP**.

3.6.3 Photophysical properties

The modified nucleotide **dC^{SiR}TP** in PBS buffer shows absorption and emission maximum at 651 nm and 672 nm respectively (Figure 74). Extinction coefficient and quantum yield were calculated to be 124800 $M^{-1}cm^{-1}$ and 54% respectively. To study the influence of polarity on the spirolactone-zwitterion equilibrium, the absorption and fluorescence spectra of **dC^{SiR}TP** were measured in water/acetonitrile mixtures of different proportions (Figure 75). When the content of acetonitrile increased, we observed decrease of both absorbance (at 651 nm and 421 nm) and fluorescence intensity (at 672 nm). Also, the absorption at 309 nm decreased and the increase of absorption was observed at 286 nm, indicating formation of spirolactone. These results indicate that the fluorophore retained its fluorogenic character even after attachment to the nucleotide.

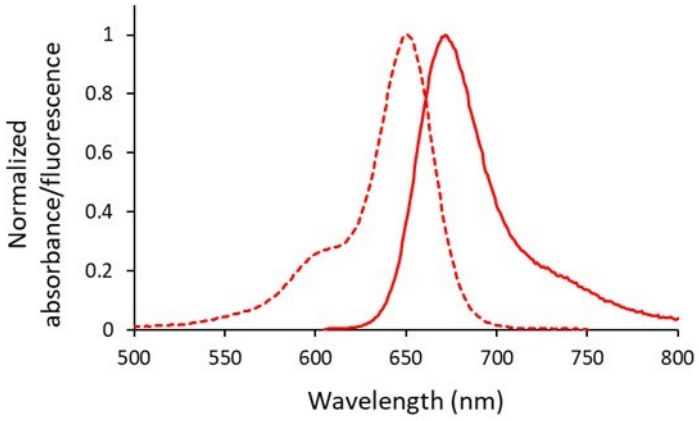

Figure 74 Absorption (dashed line) and fluorescence (solid line) spectra of **dC^{SiR}TP**.

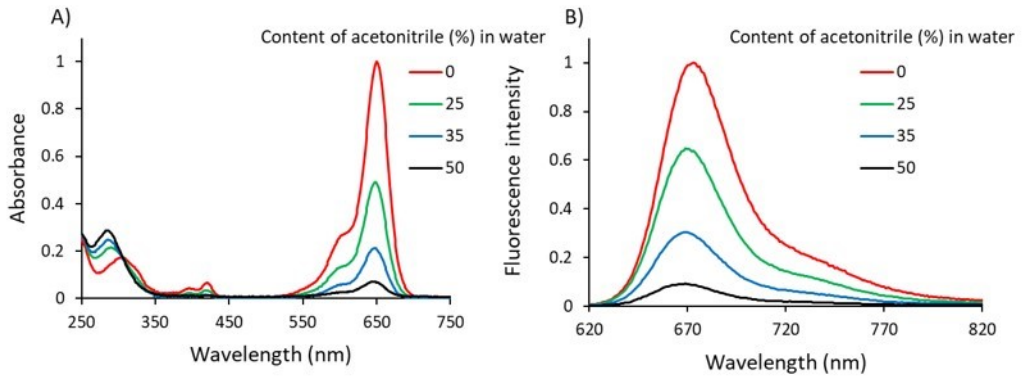

Figure 75 A) Absorption and B) fluorescence spectra of **dC^{SiR}TP** in acetonitrile/water mixtures of different proportions.

3.6.4 Enzymatic synthesis of modified DNA, photophysical properties of DNA

Silicon rhodamine modified dCTP was tested as substrate for KOD XL DNA polymerase in primer extension (Figure 76 A) and polymerase chain reaction experiments. PEX with 19-mer encoding for incorporation of one modification (Temp1^{PEX}) proceeded smoothly and the product was analyzed by PAGE (Figure 76 B) and by MALDI-TOF spectrometry (Table 15). The labelled DNA shows the same absorption and emission maximum as the corresponding nucleotide **dC^{SiR}TP** (651 nm and 672 nm respectively; Figure 77). The quantum yield of the modified DNA (48%) is slightly lower than the quantum yield of the triphosphate **dC^{SiR}TP** (54%). PCR was tested using mixtures of different proportions of **dC^{SiR}TP** and dCTP (100-0%). Agarose gel on Figure 76 C shows that the amplification was successful when maximum 60% of modified nucleotide was used, at 80% or 100% of **dC^{SiR}TP** the PCR was inhibited.

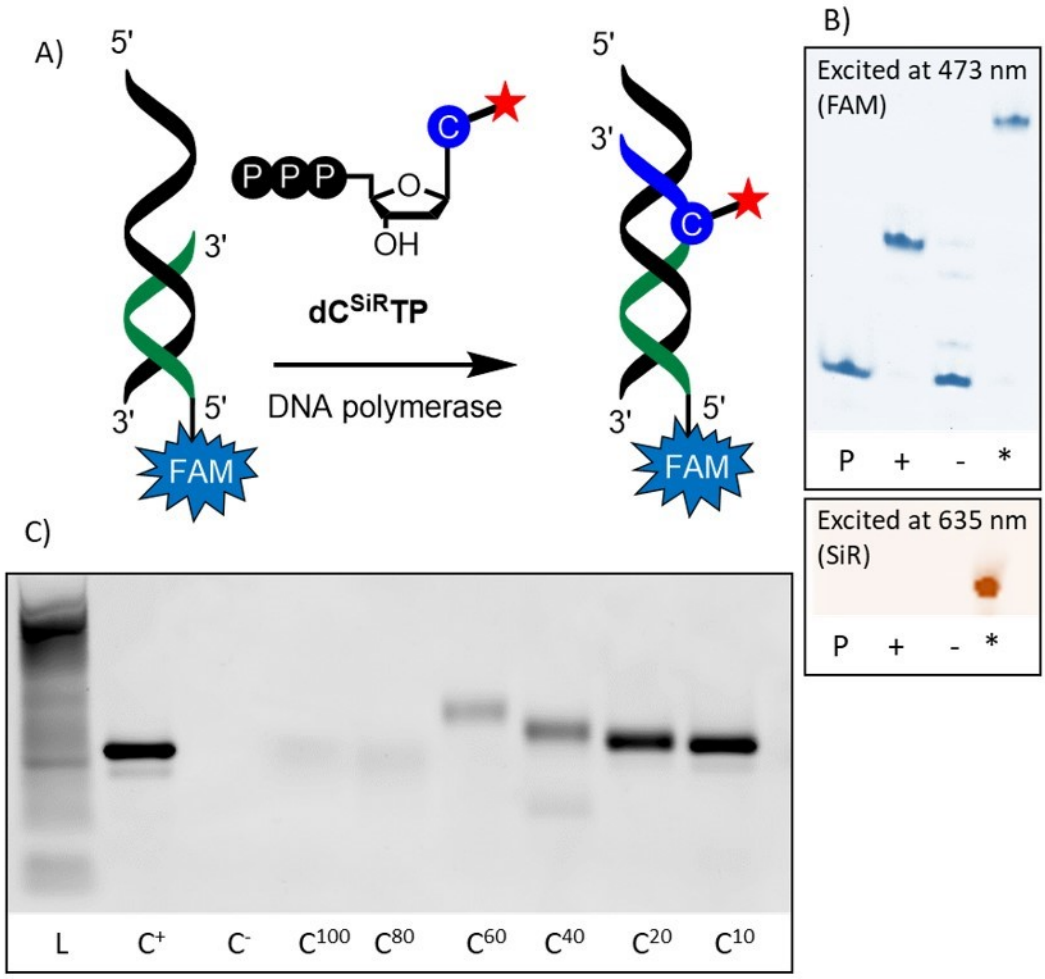

Figure 76 A) Scheme representing PEX with modified nucleotide for gel visualization. B) Page analysis of PEX using KOD XL polymerase, **dC^{SiR}TP** and template Temp1^{PEX}. Primer (P), positive control (+, PEX with all natural dNTPs), negative control (-, PEX in absence of dCTP), PEX with **dC^{SIR}TP** (*). C) Agarose gel electrophoresis analysis of PCR amplification of 98-mer template Temp1^{PCR} with KOD XL polymerase using **dC^{SiR}TP**. DNA ladder (L), primer (P), positive control (C^{+}, PCR with all natural dNTPs), negative control (C^{-}, PCR in absence of dCTP), PCR with mixture of modified nucleotide with natural dCTP (C^{100}-C^{10}, content of modified nucleotide decreases from 100% to 10%).

Table 15 Oligonucleotide prepared in this study.

Oligonucleotide	Sequence (5′→3′). C*: modified nucleotide.	$M_{calculated}$ (Da)	M_{found} (Da)
ON19_1C^{SiR}	5′-CATGGGCGGCATGGG**C***GGG-3′	6942.19	6940.9

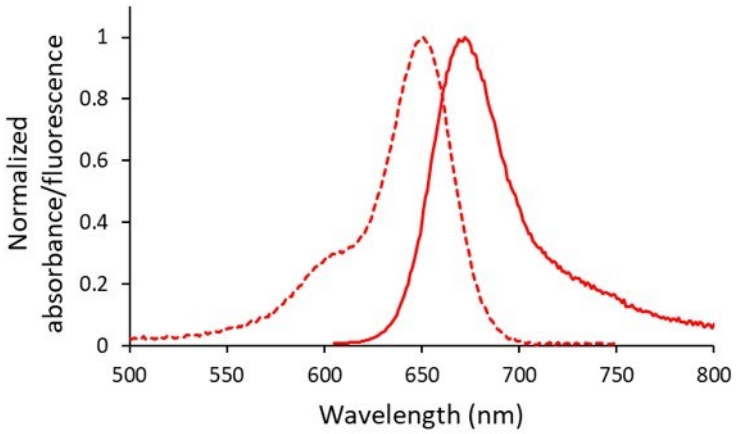

Figure 77 Normalized absorption and fluorescence spectra of **DNA19_1C^{SiR}**.

3.6.5 Cell experiments

Transport of modified nucleotide **dC^{SiR}TP** into cells was performed by treatment of cells with a mixture of nucleotide and SNTT (experiments were performed by Dr. Tomáš Kraus). Transport and incorporation of the nucleotide was monitored in time intervals. Figure 78 shows fluorescence microscopy images of the cells 5-55 minutes after treatment, revealing successful incorporation of silicon rhodamine modified nucleotide into DNA.

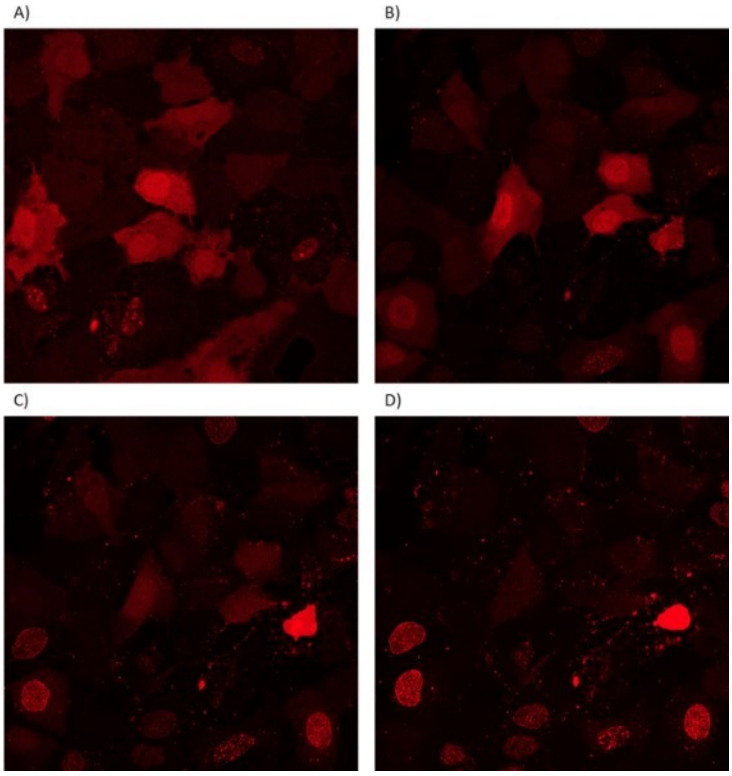

Figure 78 Fluorescence microscopy images of live cells after their treatment with a **dC^{SiR}TP**/SNTT complex. Minutes after treatment: A) 5, B) 20, C) 30, D) 55.

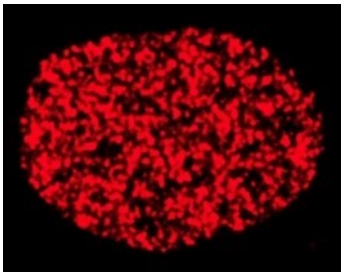

Figure 79 Detail of live cell 55 minutes after treatment with a **dC^{SiR}TP**/SNTT complex.

Additionally, the nucleotide was tested for super-resolution microscopy (using STED; experiments were performed at BIOCEV). Super-resolution microscopy revealed roughly 2.5-fold improvement in resolution in comparison with confocal

microscopy (Figure 80). To the best of our knowledge, it is the first nucleotide described for super-resolution imaging of genomic DNA in cells. Potential applications of **dC^{SiR}TP** include live-animal imaging,[56] monitoring dynamic processes such as asymmetric segregation of sister chromatids[192] or DNA repair[176,177].

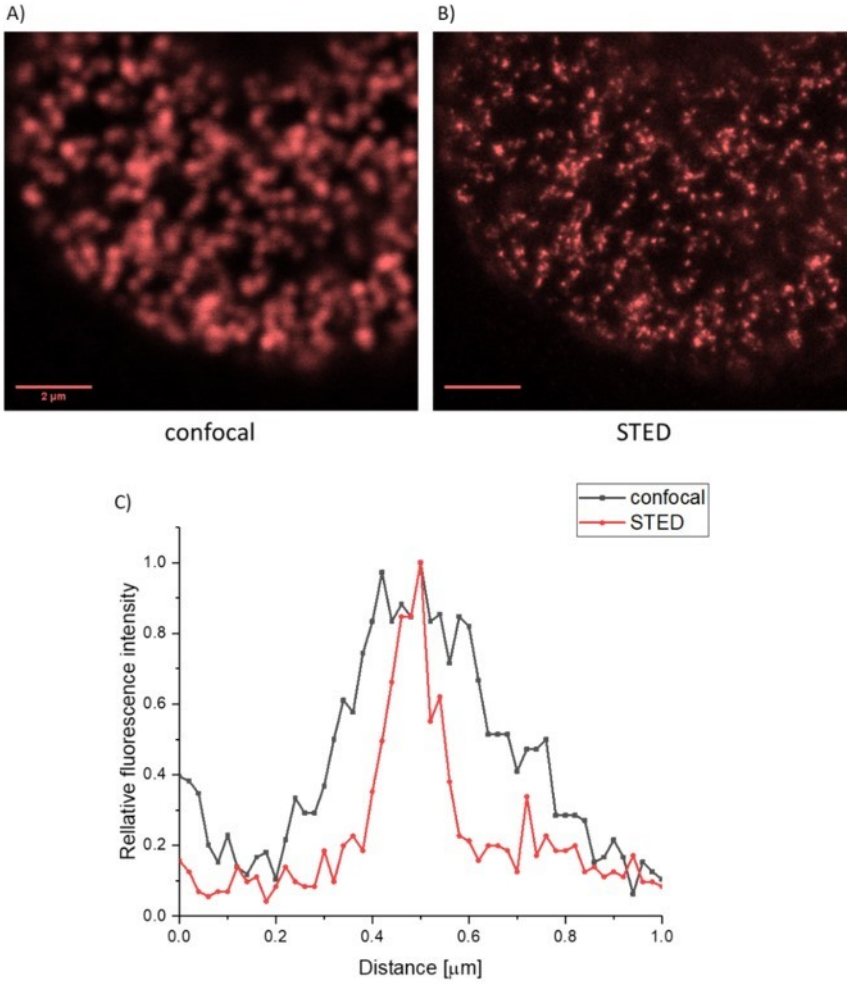

Figure 80 Detail of fixed cell 2 hours after treatment with a **dC^{SiR}TP**/SNTT complex. A) Confocal microscopy, B) super-resolution microscopy. C) STED vs confocal line intensity profiles.

4 CONCLUSION

This thesis describes synthesis of new fluorescently modified nucleoside triphosphates as tools for metabolic labelling and for the construction of DNA probes useful for bioanalytical applications.

New 2'-deoxycytidine nucleoside and nucleotide labelled with viscosity-sensitive dye based on CFP fluorophore were designed, prepared and characterized. The nucleoside **dC^{Trp}** is weakly fluorescent in low viscosity solvents, however, in viscous glycerol the fluorescence was enhanced approximately 10-fold. The nucleotide **dC^{Trp}TP** was a good substrate for KOD XL DNA polymerase in primer extension and polymerase chain reaction. The labelled oligonucleotide probe showed ca. 2-fold increase of fluorescence upon binding to single-strand binding protein. These results show that the new probe can be potentially useful for studying DNA-protein interactions.

New thymidine nucleoside and nucleotide labelled with benzylidene-tetrahydroxanthylium dye were designed, prepared and characterized. The nucleoside **dT^{NNIR}** changes fluorescence intensity depending on the polarity and viscosity of the environment. The nucleotide **dT^{NNIR}TP** was incorporation into DNA by PEX or PCR, which resulted in significant increase of fluorescence. Observed light-up effect is most probably due to a combination of the restricted bond motion of the fluorophore and less polar environment in the major groove of DNA. Unfortunately, the **dT^{NNIR}TP** was not suitable for in cellulo imaging due to its cytotoxicity. The labelled DNA probes were used for sensing interactions with small molecules and proteins by a change of fluorescence. The light-up effect after incorporation into DNA was applied in real-time PCR as a new approach to directly visualize the DNA synthesis. Bezylidene-tetrahydroxanthylium fluorophore was also attached to 2'-deoxycytidine triphosphate via triethylene glycol linker to address issues with cell experiments, however, the incorporation into DNA in live cells was not successful. Therefore, new nucleotides are useful for monitoring enzymatic reactions and sensing interactions with other

biomolecules, however, the use is limited to *in vitro* experiments.

New 2'-deoxycytidine triphosphate labelled with thiazole orange was designed, prepared and characterized. Incorporation of the **dC^{TO}TP** into DNA was tested in PEX and PCR. Thiazole orange binds nucleic acids and changes fluorescence intensity and lifetime depending on the environment. The **dC^{TO}TP** was delivered into live cells and found to be good substrate even for cellular polymerases. The new probe allowed real time-imaging of DNA synthesis in live cells using fluorescence lifetime imaging.

New 2'-deoxycytidine nucleosides and nucleotides bearing new near-infrared BODIPY dye tethered via propargylether or triethylene glycol linker were designed, prepared and characterized. The fluorophore-linked nucleosides **dC^{MOB}** and **dC^{pegMOB}** change fluorescence lifetime depending on viscosity. The nucleotides **dC^{MOB}TP** and **dC^{pegMOB}TP** were incorporated into DNA by PEX or PCR. The corresponding DNA probes were utilized for sensing interactions with histone by changing fluorescence lifetime. The probe containing BODIPY attached via longer triethylene glycol shows stronger non-specific interaction with non-DNA binding protein BSA than in case of the probe with propargylether linker. Therefore, only the DNA probe labelled by BODIPY via short linker has potential as lifetime probe for sensing DNA-protein interactions. On the other hand, the **dC^{pegMOB}TP** was substrate even for cellular polymerases and incorporation into genomic DNA was observed, albeit the use for the cell experiments is limited as high power of the laser for the excitation of the fluorophore and long incubation (24 hours) of treated cells were required.

New 2'-deoxycytidine triphosphate labelled with silicon rhodamine was designed, prepared and characterized. The modified nucleotide **dC^{SiR}TP** was tested as a substrate for KOD XL DNA polymerase in PEX and PCR. The **dC^{SiR}TP** was transported into the cells using synthetic nucleoside triphosphate transporter and incorporated to genomic DNA, allowing super-resolution imaging of DNA.

5 EXPERIMENTAL SECTION

5.1 General remarks for chemical synthesis

Solvents and reagents were purchased from commercial suppliers (Sigma-Aldrich, AlfaAesar). Thymidine (**35**) was purchased from SANTIAGO. Bicyclo[6.1.0]nonyne derivative of silicon rhodamine (**SiR-BCN**) was purchased from Spirochrome. The reactions were monitored by thin-layer chromatography (TLC) using Merck silica gel 60 F254 plates and visualized by UV (254 nm). Purification by column chromatography was performed using silica gel (40–63 μm). Separations of nucleotides were performed using HPLC (Waters modular HPLC system) on a column packed with 10 μm C18 reversed phase (Phenomenex, Luna C18). NMR spectra were measured on a Bruker AVANCE 400 (1H at 401.0 MHz, 13C at 100.8 MHz and 31P at 162.0 MHz), Bruker AVANCE 500 (1H at 500.0 MHz, 13C at 125.7 MHz and 31P at 202.3 MHz) and Bruker AVANCE 600 (1H at 600.1 MHz and 13C at 150.9 MHz) NMR spectrometers in corresponding deuteratured solvent at 25°C. Chemical shifts (in ppm, δ scale) were referenced to the residual solvent signal in ^{1}H spectra ($\delta((CHD_2)SO(CD_3)) = 2.5$ ppm, $\delta((CHD_2)OD) = 3.31$ ppm) or to the solvent signal in ^{13}C spectra ($\delta((CD_3)_2SO) = 39.7$ ppm, $\delta(CD_3OD) = 49.0$ ppm). Coupling constants (*J*) are given in Hz, chemical shifts in ppm (δ scale). Complete assignment of all NMR signals was achieved by using a combination of H,H-COSY, H,C-HSQC and H,C-HMBC experiments. Mass spectra and high resolution mass spectra were measured by ESI ionization technique and spectra were measured on a LTQ Orbitrap XL spectrometer (Thermo Fisher Scientific).

5.2 General remarks for biochemistry

Oligonucleotides used in presented work were purchased from Generi Biotech. Enzyme KOD XL DNA polymerase and the corresponding reaction buffer were obtained from Merck Millipore. Natural nucleoside triphosphates (dCTP, dATP, dGTP, dTTP), Bst DNA polymerase Large Fragment, Vent(exo-) DNA polymerase, corresponding reaction buffers and histone human recombinant protein (H2A) were

purchased from New England Biolabs. Streptavidin coated magnetic beads were obtained from Roche. Isolated RNA and corresponding cDNA were provided by virology department at IOCB Prague. All solutions for biochemistry experiments were prepared in Milli-Q water and in case of RNA experiments RNase free water was used. GelRed was obtained from Biotium. QIAquick nucleotide removal kit was purchased from QIAGEN. Stop solution contained 80% (v/v) formamide, 20 mM EDTA, 0.025% (w/v) bromophenol blue, 0.025% (w/v) xylene cyanol in water. Concentration of DNA solutions were calculated using A260 values measured on a Nanodrop 1000 Spectrophotometer (Thermo Scientific) and values obtained with OligoCalc.[193] Mass spectra of oligonucleotides were measured by MALDI-TOF mass spectrometry, on UltrafleXtreme MALDITOF/TOF mass spectrometer (Bruker Daltonics, Germany), with 1 kHz smartbeam II laser. All gels were analysed by fluorescence imaging using Typhoon FLA 9500 (GE Healthcare) or using transilluminator equipped with GBox iChemi-XRQ Bio imaging system (Syngene, Life Technologies). All oligonucleotide sequences used in enzymatic synthesis are shown in Table 16. Cell-based experiments were performed by Dr. Tomáš Kraus at IOCB Prague, super-resolution imaging was performed at BIOCEV.

Table 16 Table of oligonucleotide sequences used in enzymatic synthesis.

Oligonucleotide	Length	Sequence (5′→3′)
Prim1^{PEX}	15-mer	5′-CATGGGCGGCATGGG-3
Prim1^{PEX}-FAM [(a)]	15-mer	5′-FAM-CATGGGCGGCATGGG-3′
Prim1^{PEX}-Cy5 [(b)]	15-mer	5′-Cy5-CATGGGCGGCATGGG-3′
Temp1^{PEX}	19-mer	5′-CCCGCCCATGCCGCCCATG-3′
Temp1^{PEX}-bio [(c)]	19-mer	5′-bio-CCCACCCATGCCGCCCATG-3′
Temp1^{PEX}-P [(d)]	19-mer	5′-P-CCCACCCATGCCGCCCATG-3′
Temp2^{PEX}	31-mer	5′-CTAGCATGAGCTCAGTCCCATGCCGCCCATG-3′

Temp2^{PEX}-bio	31-mer	5′-bio-CTAGCATGAGCTCAGTCCCATGCCGCCCATG-3′
Temp2^{PEX}-TINA [(e)]	31-mer	5′-TINA-CTAGCATGAGCTCAGTCCCATGCCGCCCATG-3′
Prim2^{PEX}	15-mer	5′-TCAAGAGACATGCCT-3′
Prim2^{PEX}-FAM	15-mer	5′-FAM-TCAAGAGACATGCCT-3′
Temp3^{PEX}	30-mer	5′-ATAATAGACATGTCTAGGCATGTCTCTTGA-5′
Temp3^{PEX}-bio	30-mer	5′-bio-ATAATAGACATGTCTAGGCATGTCTCTTGA-5′
Temp4^{PEX}	16-mer	5′-GCCCATGCCGCCCATG-3′
Temp5^{PEX}	19-mer	5′-CCCACCCATGCCGCCCATG-3′
Temp5^{PEX}-bio	19-mer	5′-bio-CCCACCCATGCCGCCCATG-3′
Temp5^{PEX}-P	19-mer	5′-P-CCCACCCATGCCGCCCATG-3′
Temp6^{PEX}	31-mer	5′-CTAGCATGAGCTCAGACCCATGCCGCCCATG-3′
Temp6^{PEX}-bio	31-mer	5′-bio-CTAGCATGAGCTCAGACCCATGCCGCCCATG-3′
Prim3^{PEX}	15-mer	5′-CATGGGCGGCATAAA-3′
Prim3^{PEX}-Cy5	15-mer	5′-Cy5-CATGGGCGGCATAAA-3′
Temp7^{PEX}-2P [(f)]	15-mer	5′-P-TTTGTTTATGCCGCCCATG-P-3′
Temp8^{PEX}	16-mer	5′-ACCCATGCCGCCCATG-3′
Prim1^{PCR}	20-mer	5′-GACATCATGAGAGACATCGC-3′
Prim2^{PCR}	25-mer	5′-CAAGGACAAAATACCTGTATTCCTT-3′
Temp1^{PCR}	98-mer	5′-GACATCATGAGAGACATCGCCTCTGGGCTAATAGGACTACTTCTAATCTGTAAGAGCAGATCCCTGGACAGGCAAGGAATACAGGTATTTTGTCCTTG-3′
Prim3^{PCR}	24-mer	5′-CGTCTTCAAGAATTCTATTTGACA-3′
Prim4^{PCR}	18-mer	5′-GGAGAGCGTTCACCGACA-3′
Temp2^{PCR}	235-mer	CGTCTTCAAGAATTCTATTTGACAAAAATGGGCTCGTGTTGTACAATAAATGTGTCTAAGCTTGGGTCCCACCTGACCCCATGCCGAACTCAGAAGTGAAACGCCGTAGCGCCGATGGTAGTGTGGGGTCTCCCCATGCGAGAGTAGGGAACTGCCAGGCATCAAATAAAACGAAAGGCTCAGTCGAAAGACTGGGCCTTTCGTTTTATCT GTTGTTTGTCGGTGAACGCTCTCC
Prim5^{PCR}	22-mer	5′-GTGARATGGTCATGTGTGGCGG-3′
Prim6^{PCR}	26-mer	5′-CARATGTTAAASACACTATTAGCATA-3′

Temp3^{PCR}	100-mer	5′-GTGAAATGGTCATGTGTGGCGGTTCACTATATGTTAAACC AGGTGGAACCTCATCAGGAGATGCCACAACTGCTTATGCT AATAGTGTCTTTAACATTTG-3′

Underlined: segments of templates complementary to primers. R is G/A; S is G/C. [a] 6-carboxyfluorescein (6-FAM) used for oligonucleotide labelling at 5'-end, [b] Cyanine-5 (Cy5) used for oligonucleotide labelling at 5'-end, [c] template biotinylated at 5'-end, [d] template phosphorylated at 5'-end, [e] template labelled by *ortho*-TINA at 5'-end, [f] template phosphorylated at 5'- and 3'-end.

5.3 Determination of photophysical properties

5.3.1 Molar absorption coefficients

Absorption coefficients were measured using 1 mL quartz cuvettes. The absorption coefficients were calculated using the following equation

$$A = \varepsilon \times c \times l$$

where A is the absorbance of the sample, ε is absorption coefficient, c is the exact concentration of the sample and l is the length of the path that the light travels through the cuvette.

5.3.2 Fluorescence quantum yields

Relative determination of the fluorescence quantum yields (Φ) was performed using quinine sulfate in 0.5 M H_2SO_4 (Φ = 0.55 at 25°C) as reference for compounds **dC^{Trp}** and **dC^{Trp}TP**, indocyanine green in DMSO (Φ = 0.13 at 25°C) as reference for compounds **dT^{NNIR}**, **dT^{NNIR}TP** and **DNA19_1T^{NNIR}**, fluorescein in 0.1 M NaOH (Φ = 0.92 at 25°C) as reference for compounds **dC^{TO}**, **dC^{TO}TP** and corresponding dsDNA and ssDNA, Cresyl violet perchlorate in MeOH (Φ = 0.54) as reference for compounds **dC^{MOB}**, **dC^{pegMOB}**, **dC^{MOB}TP**, **dC^{pegMOB}TP**, **dC^{SiR}**, **dC^{SiR}TP** and

DNA19_1C^{SiR}. The absorbance of sample solutions was kept below 0.10 to avoid inner filter effects. The quantum yields were calculated using the following equation[194]

$$\Phi_{f,x} = \Phi_{f,st} \times \frac{F_x}{F_{st}} \times \frac{1 - 10^{-Abs_{st}}}{1 - 10^{-Abs_x}} \times \frac{n_x^2}{n_{st}^2}$$

where Φ_f is the quantum yield, F is the integrated fluorescence intensity, Abs is the absorbance of the solution at the excitation wavelength, n is the refractive index of the solvent, the subscripts x and st stand for the sample and standard respectively.

5.4 2'-Deoxycytidine and its triphosphate modified by tryptophan-based imidazolinone fluorophore. Synthesis, photophysical properties, enzymatic incorporation into DNA and applications

5.4.1 Chemical synthesis

(*Z*)-2-acetamido-3-(1*H*-indol-3-yl)-*N*-(prop-2-yn-1-yl)acrylamide (33)

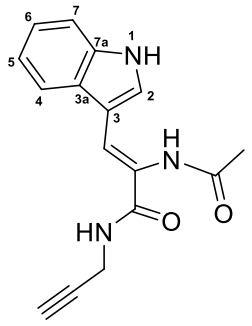

Propargylamine (86 mg, 1.56 mmol) was added to the solution of **32** (200 mg, 0.75 mmol) in DMF (15 mL) and the mixture was stirred at room temperature for 5h. Solvent was evaporated and crude product was purified by column chromatography with methanol in dichloromethane (0-5%). The desired product was obtained as yellowish solid (125.8 mg, 60%).

^{1}H NMR (500.0 MHz, DMSO-d_6): 2.07 (s, 3H, CH_3); 3.07 (t, 1H, ^{4}J = 2.5, HC≡C); 3.94 (dd, 2H, ^{3}J = 5.7, ^{4}J = 2.5, CH_2N); 7.12 (ddd, 1H, $J_{5,4}$ = 8.1, $J_{5,6}$ = 7.0, $J_{5,7}$ = 1.3, H-5); 7,17 (ddd, 1H, $J_{6,7}$ = 8.1, $J_{6,5}$ = 7.0, $J_{6,4}$ = 1.3, H-6); 7.44 (ddd, 1H, $J_{7,6}$ = 8.1, $J_{7,5}$ = 1.3, $J_{7,4}$ = 0.8, H-7); 7.55 (s, 1H, CH=); 7.70 (d, 1H, $J_{2,1}$ = 2.7, H-2); 7.72 (m, 1H, H-4); 8.27 (t, 1H, ^{3}J = 5.7, N**H**CH_2); 9.17 (bd, 1H, ^{4}J = 1.2, N**H**C=CH); 11.60 (bd, 1H, $J_{1,2}$ = 2.7, H-1).

^{13}C NMR (127.5 MHz, DMSO-d_6): 23.40 (CH_3); 28.67 (CH_2N); 72.63 (H**C**≡C); 81.99 (HC≡**C**); 109.27 (C-3); 112.09 (CH-7); 118.29 (CH-4); 120.18 (CH-5); 122.21 (CH-6); 122.63 (CH=); 124.40 (C=); 127.07 (CH-2); 127.31 (C-3a); 135.67 (C-5); 165.10 (NH**C**OC); 169.33 (NH**C**OCH_3).

HRMS-ESI for $C_{16}H_{15}O_2N_3Na$ $[M + Na]^+$: calculated 304.10565, found 304.10577.

(*Z*)-5-((1*H*-indol-3-yl)methylene)-2-methyl-3-(prop-2-yn-1-yl)-3,5-dihydro-4*H*-imidazol-4-one (34)

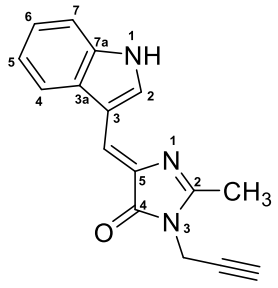

Z
major

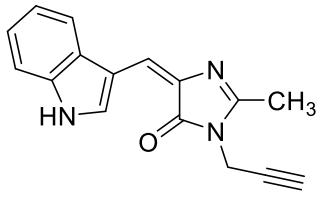

E
minor

Compound **33** (160 mg, 0.57 mmol) was dissolved in pyridine (2 mL) and the mixture was heated to reflux. After complete consumption of starting material, the mixture was concentrated and the product was obtained as orange solid (100 mg, 67%) after purification by column chromatography (hexane/ethyl acetate 2:1 as eluent). Mixture of *Z*/*E*-isomers 7:1.

^{1}H NMR (500.0 MHz, DMSO-d_6): 2.36 (s, 3H, CH_3-*E*); 2.43 (s, 3H, CH_3-*Z*); 3.36 (t, 2H, ^4J = 2.5, HC≡C-*E*,*Z*); 4.46 (d, 2H, ^4J = 2.5, CH_2N-*Z*); 4.50 (d, 2H, ^4J = 2.5, CH_2-*E*); 7.15 – 7.26 (m, 4H, H-5,6-indole-*E*,*Z*); 7.38 (s, 1H, indole-CH=imidazole-*Z*); 7.48 (m, 1H, H-7-indole-*Z*); 7.51 (m, 1H, H-7-indole-*E*); 7.70 (s, 1H, indole-CH=imidazole-*E*); 7.94 (m, 1H, H-4-indole-*E*); 8.23 (m, 1H, H-4-indole-*Z*); 8.41 (s, 1H, H-2-indole-*Z*); 9.29 (s, 1H, H-2-indole-*E*); 12.00 (bs, 1H, NH-1-indole-*Z*); 12.07 (bs, 1H, NH-1-indole-*E*).

^{13}C NMR (127.5 MHz, DMSO-d_6): 14.96 (CH_3-*E*); 15.50 (CH_3-*Z*); 29.06 (CH_2N-*Z*); 29.11 (CH_2N-E); 74.56 (H**C**≡C-*E*); 74.62 (H**C**≡C-*Z*); 78.91 (HC≡**C**-*Z*); 78.96 (HC≡**C**-*E*); 110.61 (C-3-indole-*E*); 111.28 (C-3-indole-*Z*); 112.42 (CH-7-indole-*Z*); 112.54 (CH-7-indole-*Z*); 118.32 (CH-4-indole-*E*); 119.97 (CH-4-indole-*Z*); 121.05 (CH-5-indole-*Z*); 121.08 (indole-CH=imidazole-*Z*); 121.17 (CH-5-indole-*E*); 122.83 (CH-6-

indole-*Z*); 122.88 (CH-6-indole-*E*); 126.85 (C-3a-indole-*Z*); 127.04 (indole-CH=imidazole-*E*); 128.05 (C-3a-indole-*E*); 132.51 (CH-2-indole-*E*); 133.09 (C-5-imidazole-*Z*); 133.51 (CH-2-indole-*Z*); 133.73 (C-5-imidazole-*E*); 136.21 (C-7a-indole-*E*); 136.62 (C-7a-indole-*Z*); 154.00 (C-2-imidazole-*E*); 157.74 (C-2-imidazole-*Z*); 166.08 (C-4-imidazole-*E*); 168.17 (C-4-imidazole-*Z*).

HRMS-ESI for $C_{16}H_{14}ON_3$ $[M + H]^+$: calculated 264.11314, found 264.11317. For $C_{16}H_{13}ON_3Na$ $[M + Na]^+$: calculated 286.09508, found 286.09512.

5-(3-((*Z*)-4-((1*H*-indol-3-yl)methylene)-2-methyl-5-oxo-4,5-dihydro-1*H*-imidazol-1-yl)prop-1-yn-1-yl)-2'-deoxycytidine (dC^{Trp})

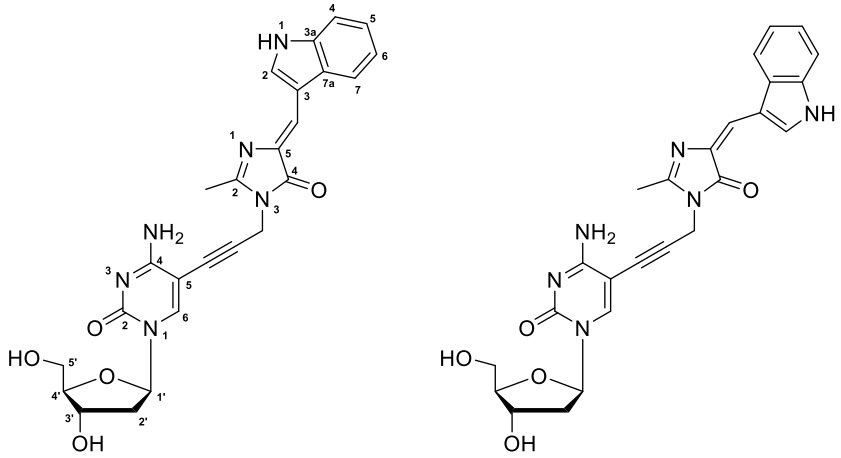

A flask containing 5-iodo-2'-deoxycytidine (42 mg, 0.12 mmol), alkyne **34** (40 mg, 0.15 mmol), $PdCl_2(PPh_3)_2$ (5 mg, 6% mol), CuI (1.5 mg, 6% mol) was purged and refilled with argon multiple times and the content was dissolved in dry DMF (2.5 mL). Triethylamine (300 µL, 2.15 mmol) was added and the mixture was stirred at 60°C for 2h. Then the reaction mixture was concentrated on rotavap and purified by column chromatography eluted with methanol in dichloromethane (0-20%) to give the modified nucleoside as orange solid (50 mg, 67%). Mixture of *Z/E*-isomers 5:1.

^{1}H NMR (500.0 MHz, DMSO-d_6): 1.99 (dt, 2H, J_{gem} = 13.0, $J_{2'b,1'} = J_{2'b,3'}$ = 6.5, H-2′b-*E,Z*); 2.13 (ddd, 2H, J_{gem} = 13.0, $J_{2'a,1'}$ = 6.0, $J_{2'a,3'}$ = 3.6, H-2′a-*E,Z*); 2.39 (s, 3H, CH_3-*E*); 2.47 (s, 3H, CH_3-*Z*); 3.50 – 3.64 (m, 4H, H-5′-*E,Z*); 3.75 – 3.79 (m, 2H, H-4′-*E,Z*); 4.16 – 4.22 (m, 2H, H-3′-*E,Z*); 4.69 (s, 2H, CH_2N-*Z*); 4.74 (d, 2H, CH_2-*E*); 6.09 (dd, 2H, $J_{1',2'}$ = 6.5, 6.0, H-1′-*E,Z*); 7.03 (bs, 2H, NH_a**H**$_b$-*E,Z*); 7.14 – 7.25 (m, 4H, H-5,6-indole-*E,Z*); 7.37 (s, 1H, indole-CH=imidazole-*Z*); 7.48 (m, 1H, H-7-indole-*Z*); 7.50 (m, 1H, H-7-indole-*E*); 7.69 (s, 1H, indole-CH=imidazole-*E*); 7.77 (bs, 2H, N**H**$_a$H$_b$-*E,Z*); 7.94 (bd, 1H, $J_{4,5}$ = 7.8, H-4-indole-*E*); 8.19 (s, H, H-6-cyt-*E*); 8.20 (s, H, H-6-cyt-*Z*); 8.23 (bd, 1H, $J_{4,5}$ = 7.8, H-4-indole-*Z*); 8.41 (d, 1H, $J_{2,1}$ = 2.8, H-2-indole-*Z*); 9.29 (d, 1H, $J_{2,1}$ = 2.9, H-2-indole-*E*); 12.03 (bd, 1H, d, 1H, $J_{1,2}$ = 2.8, NH-1-indole-*Z*); 12.08 (bd, 1H, d, 1H, $J_{1,2}$ = 2.9, NH-1-indole-*E*).

^{13}C NMR (127.5 MHz, DMSO-d_6): 15.29 (CH_3-*E*); 15.83 (CH_3-*Z*); 30.38 (CH_2N-*E,Z*); 40.92 (CH_2-2′-*E*); 40.95 (CH_2-2′-*Z*); 60.97 (CH_2-5′-E); 61.09 (CH_2-5′-Z); 70.06 (CH-3′-E); 70.15 (CH-3′-Z); 75.25 (C5-**C**≡C-*E*); 75.34 (C5-**C**≡C-*Z*); 85.44 (CH-1′-*E*); 85.56 (CH-1′-*Z*); 87.56 (CH-4′-*E*); 87.64 (CH-4′-*Z*); 88.98 (C-5-cyt-*E*); 89.03 (C-5-cyt-*Z*); 89.82 (C5-C≡**C**-*Z*); 89.90 (C5-C≡**C**-*E*); 110.63 (C-3-indole-*E*); 111.32 (C-3-indole-*Z*); 112.44 (CH-7-indole-*Z*); 112.56 (CH-7-indole-*E*); 118.33 (CH-4-indole-*E*); 119.97 (CH-4-indole-*Z*); 120.85 (indole-CH=imidazole-*Z*); 121.07 (CH-5-indole-*Z*); 121.16 (CH-5-indole-*E*); 122.83 (CH-6-indole-*Z*); 122.89 (CH-6-indole-*E*); 126.84 (indole-CH=imidazole-*E*); 126.86 (C-3a-indole-*Z*); 128.07 (C-3a-indole-*E*); 132.45 (CH-2-indole-*E*); 133.27 (C-5-imidazole-*Z*); 133.45 (CH-2-indole-*Z*); 133.91 (C-5-imidazole-*E*); 136.22 (C-7a-indole-*E*); 136.63 (C-7a-indole-*Z*); 145.11 (CH-6-cyt-*E,Z*); 153.61 (C-2-cyt-*E,Z*); 154.46 (C-2-imidazole-*E*); 158.19 (C-2-imidazole-*Z*); 164.47 (C-4-cyt-*E*); 164.54 (C-4-cyt-*Z*); 166.24 (C-4-imidazole-*E*); 168.39 (C-4-imidazole-*Z*).

HRMS-ESI for $C_{25}H_{25}O_5N_6$ $[M + H]^+$: calculated 489.18809, found 489.18812.

5-(3-((*Z*)-4-((1*H*-indol-3-yl)methylene)-2-methyl-5-oxo-4,5-dihydro-1*H*-imidazol-1-yl)prop-1-yn-1-yl)-2'-deoxycytidine-5'-*O*-triphosphate (dC^{Trp}TP)

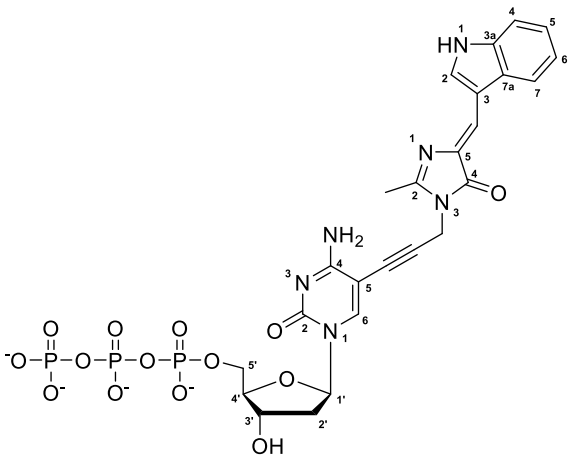

Flask containing 5-iodo-2'-deoxycytidine 5'-triphosphate (Et_3NH^+ form, 22 mg, 0.037 mmol), alkyne **34** (16 mg, 0.061 mmol), $PdCl_2(PPh_3)_2$ (2.6 mg, 10% mol), CuI (0.7 mg, 10% mol) was purged and refilled with argon multiple times and the content was dissolved in dry DMF (0.5 mL). Triethylamine (50 uL, 0.36 mmol) was added and the mixture was stirred at 55°C for 45 min. The solvent was evaporated in vacuum and product was purified by HPLC with the use of linear gradient methanol (5-100%) in 0.1 M TEAB buffer. Isolated product was co-evaporated with distilled water several times. Conversion of the product to sodium salt on an ion-exchange column (Dowex 50WX8 in Na^+ cycle) and freeze-drying from water afforded the final nucleotide as yellow solid (12 mg, 44%).

^{1}H NMR (500.0 MHz, D_2O, ref(dioxane) = 3.75 ppm): 2.24, 2.34 (2 × bm, 2 × 1H, H-2′); 2.38 (s, 3H, CH_3); 4.07 – 4.33 (m, 3H, H-4′,5′); 4.48 (bs, 2H, CH_2N); 4.57 (bm, 1H, H-3′); 6.05 (bm, 1H, H-1′); 7.18 – 7.28 (bm, 2H, H-5,6-indole); 7.30 (bs, 1H, indole-CH=imidazole); 7.43 (bm, 1H, H-7-indole); 7.81 (bm, 1H, H-4-indole); 8.07 (bs, H, H-6-cyt); 8.11 (bs, 1H, H-2-indole).

^{13}C NMR (127.5 MHz, D_2O, ref(dioxane) = 69.3 ppm): 17.11 (CH_3); 33.32 (CH_2N); 41.80 (CH_2-2′); 67.83 (b, CH_2-5′); 72.8 (CH-3′); 88.22 (CH-4′); 89.55 (CH-1′); 90.51

(C-5-cyt); 92.30 (C5-C≡**C**); 113.28 (C-3-indole); 115.03 (CH-7-indole); 121.29 (CH-4-indole); 124.40 (CH-5-indole); 126.04 (CH-6-indole); 126.85 (indole-CH=imidazole); 129.78 (C-3a-indole); 133.56 (C-5-imidazole); 136.05 (CH-2-indole); 138.68 (C-7a-indole); 147.72 (CH-6-cyt); 161.17 (C-2-imidazole); 172.51 (C-4-imidazole); (C5-**C**≡C-*E*, C-5-imidazole and C-2,4-cyt not detected).

^{31}P NMR (202.4 MHz, D_2O): -22.50 (br, P□); -10.59 (br, P□); -5.75 (br, P□).

HRMS-ESI for $(C_{25}H_{25}O_{14}N_6P_3)/2$ $[(M + 2H)]^{2-}$: calculated 363.03263, found 363.03214

5.4.2 Biochemistry

5.4.2.1 Primer extension experiments

Enzymatic synthesis of modified DNA bearing one or two modifications by primer extension (gel analysis)

The reaction mixture (20 µl) contained FAM labelled primer Prim1^{PEX}–FAM or Prim2^{PEX}–FAM (for sequence see Table 16; 3 µM, 1 µL), template Temp1^{PEX} or Temp3^{PEX} (for sequence see Table 16; 3 µM, 1.5 µL), KOD XL DNA polymerase (0.25 U/µL, 0.125 µL), natural dNTPs (dATP, dGTP and dTTP 4 mM each, 0.3 µL), either natural dCTP (4 mM, 0.3 µL) or modified dNTP (**dC^{Trp}TP**, 4 mM, 0.3 µL) in corresponding reaction buffer (10x, 2 µL) supplied by the manufacturer. The reaction mixture was incubated at 60°C for 30 min in thermal cycler. The reaction was stopped by the addition of PAGE stop solution (20 uL) and the reaction mixture was denatured at 95°C for 5 min and analyzed using 12.5% denaturing PAGE. Visualization was performed on Typhoon biological imager FLA 9500 (PAGE gels are shown in Figure 14 B, D).

Enzymatic incorporation of four modifications by primer extension (gel analysis)

The reaction mixture (20 µl) contained FAM labelled primer Prim1^{PEX}–FAM (for sequence see Table 16; 3 µM, 1 µL), template Temp2^{PEX} (for sequences see Table 16; 3 µM, 1.5 µL), KOD XL DNA polymerase (0.25 U/µL, 0.3 µL), natural dNTPs (dATP, dGTP, dTTP, 4 mM each, 0.7 µL), either natural dCTP (4 mM, 0.7 µL) or modified dNTP (**dC^{Trp}TP**, 4 mM, 0.7 µL) in corresponding reaction buffer (10x, 2 µL) supplied by the manufacturer. The reaction mixture was incubated at 60°C for 30 min in thermal cycler. The reaction was stopped by the addition of PAGE stop solution (20 µL) and the reaction mixture was denatured at 95°C for 5 min and analyzed using 12.5% denaturing PAGE. Visualization was performed on Typhoon biological imager FLA 9500 (PAGE gel is shown in Figure 14 C).

Preparation of modified oligonucleotides ON19_1C^{Trp}, ON31_4C^{Trp} and ON30_2C^{Trp} by primer extension and subsequent magnetic separation

The reaction mixture (50 µL) containing primer (for sequences see Table 16; Prim1^{PEX} or Prim2^{PEX}, 100 µM, 1.7 µL), biotinylated template (for sequences see Table 16; Temp1^{PEX}-bio, Temp2^{PEX}-bio or Temp3^{PEX}-bio, 100 µM, 1.7 µL), dNTPs (dATP, dGTP, dTTP, **dC^{Trp}TP**; 4 mM each, 1.6 µL, KOD XL DNA polymerase (2.5 U/µL, 0.5 µL), corresponding reaction buffer (10×, 3 µL) was incubated at 60°C for 30 min. Reactions were stopped by cooling at 4°C. Streptavidin magnetic beads (50 µl, Roche) were washed with binding buffer TEN 100 (3 × 300 µl, 10 mM Tris, 1 mM EDTA, 100 mM NaCl, pH 7.5). Then PEX solution (50 µL) and binding buffer (50 µl) were added to the magnetic beads. The mixture was incubated for 30 min at 15°C and 1400 rpm. Then the magnetic beads were separated and washed with washing buffer TEN 500 (3 × 200 µl, 10 mM Tris, 1 mM EDTA, 1 M NaCl, pH 7.5) and with milli-Q water (4 × 200 µl). Then 50 µl of milli-Q water was added and the sample was denatured for 2 min at 90°C and 900 rpm. The solution containing modified ssDNA was quickly transferred into clean Eppendorf and analysed by MALDI-TOF mass spectrometry.

5.4.2.2 Polymerase chain reaction experiments

Enzymatic incorporation of dC^{Trp}TP by polymerase chain reaction

The reaction mixture (20 µL) contained primer (for sequences see Table 16; Prim1^{PCR} and Prim2^{PCR} or Prim3^{PCR} and Prim4^{PCR}, 10 µM, 4 µL of each), template (Temp1^{PCR} or Temp2^{PCR}, 10 µM, 0.5 µL), dNTPs (dATP, dGTP, dTTP, **dC^{Trp}TP**; 0.4 mM, 1.5 µL of each), KOD XL DNA polymerase (2.5 U/µL, 1.1 µL) and corresponding reaction buffer (10×, 25 µL). After the initial denaturation for 3 min at 94°C, 30 (in case of template Temp1^{PCR}) or 40 (in case of template Temp2^{PCR}) PCR cycles were run under the following conditions: denaturation for 1 min at 94°C, annealing for 1 min at 51°C, extension for 2 min at 72°C. This PCR process was terminated with a final extension step for 5 min at 72°C. The reaction was stopped by cooling to 4°C. The reaction was stopped by cooling to 4°C. The PCR products were analyzed by agarose gel electrophoresis in 2% agarose gel stained with GelRed™ (Biotium, agarose gels are shown in Figure 16).

5.4.2.3 Interaction of modified DNA with protein

Binding study using SSB protein

SSB Protein from *E. coli* was purchased from Sigma-Aldrich. The measurements were performed in a 100 µL quartz cuvette at room temperature in 50 mM phosphate buffer pH 7.4 using three parallel samples for exact comparison (ssDNA mixed with SSB protein, ssDNA diluted with phosphate buffer, and ssDNA mixed with BSA protein and glycerol as control). To refine the data from the effect of glycerol present in the stock solution of SSB protein an appropriate amount of glycerol was added to negative control. The measurements were performed on a Fluoromax 4 spectrofluorimeter (HORIBA Scientific).

5.5 Thymidine and its triphosphate modified by benzylidene-tetrahydroxanthylium fluorophore. Synthesis, photophysical properties, enzymatic incorporation into DNA and applications

5.5.1 Chemical synthesis

6-(diethylamino)-4-(4-(methyl(prop-2-yn-1-yl)amino)benzylidene)-1,2,3,4-tetrahydroxanthylium (43)

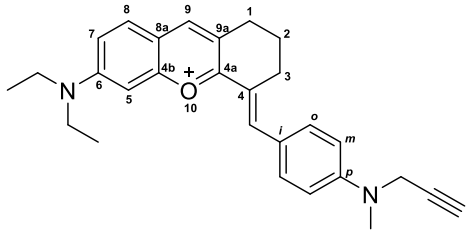

6-(diethylamino)-1,2,3,4-tetrahydroxanthylium (**39**, 887 mg, 3.46 mmol) and benzaldehyde **42** (1349 mg, 7.79 mmol) were dissolved in acetic acid (60 mL). The reaction mixture was stirred at 110°C for 2h. Then, the mixture was concentrated on rotavap and the crude product was purified by column chromatography using CH_2Cl_2 to CH_2Cl_2/methanol (20:1) as eluent. The alkyne **43** was isolated as a black solid in 50% yield (712 mg) after purification by column chromatography.

^{1}H NMR (500.0 MHz, DMSO-d_6): 1.24 (t, 6H, J_{vic} = 7.1, C**H$_3$**CH$_2$N); 1.83 – 1.89 (m, 2H, H-2); 2.84 (t, 2H, $J_{1,2}$ = 5.9, H-1); 2.92 – 2.97 (m, 2H, H-3); 3.05 (s, 3H, CH_3N); 3.23 (m, 1H, ^4J = 2.2, HC≡C); 3.67 (q, 4H, J_{vic} = 7.1, CH_3**CH$_2$**N); 4.30 (d, 2H, ^4J = 2.2, CH_2N); 6.94 – 6.98 (m, 2H, H-*m*-phenylene); 7.24 (d, 1H, $J_{5,7}$ = 2.5, H-5); 7.37 (dd, 1H, $J_{7,8}$ = 9.4, $J_{7,5}$ = 2.5, H-7); 7.62 – 7.67 (m, 2H, H-*o*-phenylene); 7.84 (d, 1H, $J_{8,7}$ = 9.4, H-8); 8.07 (s, 1H, CH=C4); 8.41 (s, 1H, H-9).

^{13}C NMR (125.7 MHz, DMSO-d_6): 12.76 (**C**H_3CH_2N); 21.21 (CH_2-2); 27.12 (CH_2-1); 27.24 (CH_2-3); 38.15 (CH_3N); 41.16 (CH_2N); 45.52 (CH_3**C**H_2N); 74.97 (H**C**≡C); 79.81 (HC≡**C**); 95.64 (CH-5); 113.34 (CH-*m*-phenylene); 117.47 (CH-7); 117.72 (C-8a); 123.18 (C-9a); 123.60 (C-4); 124.37 (C-*i*-phenylene); 131.76 (CH-8); 133.85 (CH-*o*-

phenylene); 138.64 (**C**H=C4); 147.54 (CH-9); 150.54 (C-*p*-phenylene); 155.28 (C-6); 158.37 (C-4b); 164.03 (C-4a).

HRMS (ESI^+): calculated for $C_{28}H_{31}ON_2$: 411.24309; found 411.24333.

6-(diethylamino)-4-((E)-4-(((1-((1-((2R,4S,5R)-4-hydroxy-5-(hydroxymethyl)tetrahydrofuran-2-yl)-2,4-dioxo-1,2,3,4-tetrahydropyrimidin-5-yl)methyl)-1H-1,2,3-triazol-4-yl)methyl)(methyl)amino)benzylidene)-1,2,3,4-tetrahydroxanthylium (dT^{NNIR})

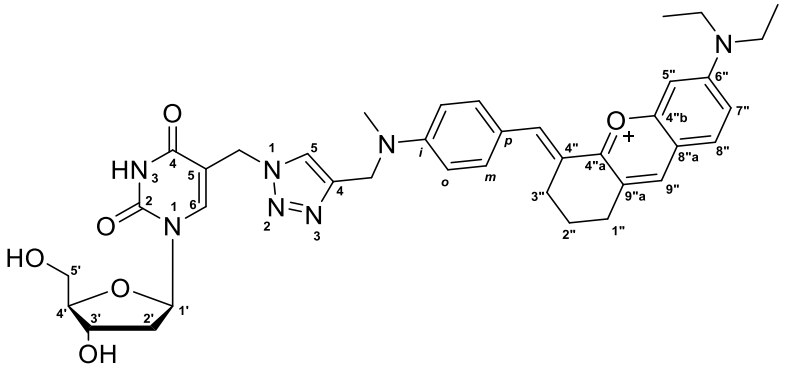

dT^{N3} (140 mg, 0.494 mmol), $CuSO_4.5H_2O$ (24.7 mg, 0.099 mmol), sodium ascorbate (39.23 mg, 0.198 mmol) and alkyne **43** (233.8 mg, 0.568 mmol) were placed in a round bottom flask and dissolved in mixture of H_2O/THF (1:3, 8 mL). The reaction mixture was stirred at room temperature until complete consumption of starting material (**dT^{N3}**) was observed according to TLC (CH_2Cl_2/methanol 10:1 as eluent). After evaporation the reaction mixture was purified by column chromatography using CH_2Cl_2 to CH_2Cl_2/methanol (10:1) as eluent. The nucleoside **dT^{NNIR}** was isolated in 55% yield (188.7 mg) as a black solid after column chromatography purification.

^{1}H NMR (500.0 MHz, DMSO-d_6): 1.24 (t, 6H, J_{vic} = 7.1, C**H**$_3$CH$_2$N); 1.82 – 1.89 (m, 2H, H-2″); 2.08 (ddd, 1H, J_{gem} = 13.3, $J_{2'b,1'}$ = 7.2, $J_{2'b,1'}$ = 6.0, H-2′b); H-2′); 2.13 (ddd, 1H, J_{gem} = 13.3, $J_{2'a,1'}$ = 6.2, $J_{2'a,1'}$ = 3.6, H-2′a); 2.83 (t, 2H, $J_{1'',2''}$ = 6.0, H-1″); 2.90 – 2.95 (m, 2H, H-3″); 3.13 (s, 3H, CH_3N); 3.53 (ddd, 1H, J_{gem} = 11.9, $J_{5'b,OH}$ = 5.3, $J_{5'b,4'}$

= 4.3, H-5′b); 3.58 (ddd, 1H, J_{gem} = 11.9, $J_{5'a,OH}$ = 5.3, $J_{5'a,4'}$ = 4.0, H-5′a); 3.66 (bq, 4H, J_{vic} = 7.1, $CH_3C\mathbf{H_2}N$); 3.78 (ddd, 1H, $J_{4',5'}$ = 4.3, 4.0, $J_{4',3'}$ = 3.7, H-4′); 4.22 (dddd, 1H, $J_{3',2'}$ = 6.0, 3.6, $J_{3',OH}$ = 4.3, $J_{3',2'}$ = 3.7, H-3′); 4.70 (s, 2H, CH_2NMe); 5.04 (t, 1H, $J_{OH,5'}$ = 5.3, OH-5′); 5.16 (s, 2H, CH_2N); 5.28 (d, 1H, $J_{OH,3'}$ = 4.3, OH-3′); 6.13 (d, 1H, $J_{1',2'}$ = 7.2, 6.2, H-1′); 6.95 – 7.00 (m, 2H, H-*o*-phenylene); 7.22 (d, 1H, $J_{5'',7''}$ = 2.3, H-5″); 7.34 (dd, 1H, $J_{7'',8''}$ = 9.4, $J_{7'',8''}$ = 2.3, H-7″); 7.59 – 7.63 (m, 2H, H-*m*-phenylene); 7.81 (d, 1H, $J_{8'',7''}$ = 9.4, H-8″); 8.00 (s, 1H, H-5-triazole); 8.06 (s, 1H, CH=); 8.12 (s, 1H, H-6); 8.36 (s, 1H, H-9″); 11.58 (s, 1H, NH).

^{13}C NMR (125.7 MHz, DMSO-d_6): 12.77 ($\mathbf{C}H_3CH_2N$); 21.19 (CH_2-2″); 27.17 (CH_2-1″); 27.31 (CH_2-3″); 38.46 (CH_3N); 39.94 (CH_2-2′); 45.45 ($CH_3\mathbf{C}H_2N$); 46.36 (CH_2N); 46.74 (CH_2NMe); 61.43 (CH_2-5′); 70.42 (CH-3′); 84.63 (CH-1′); 87.74 (CH-4′); 95.67 (CH-5″); 107.93 (C-5); 112.64 (CH-*o*-phenylene); 117.71 (CH-7″); 117.31 (C-8″a); 122.70 (C-4″); 123.13 (C-9″a); 123.30 (CH-5-triazole); 123.57 (C-*p*-phenylene); 131.62 (CH-8″); 134.28 (CH-*m*-phenylene); 139.35 (CH=); 141.20 (CH-6); 143.36 (C-4-triazole); 147.07 (CH-9″); 150.40 (C-2); 150.87 (C-*i*-phenylene); 155.04 (C-6″); 158.24 (C-4″b); 162.81 (C-4); 164.37 (C-4″a).

HRMS (ESI^+): calculated for $C_{38}H_{44}O_6N_7$: 694.3353; found 694.3341.

((2R,3S,5R)-5-(5-((4-(((4-(((E)-6-(diethylamino)-2,3-dihydroxanthylium-4(1H)-ylidene)methyl)phenyl)(methyl)amino)methyl)-1H-1,2,3-triazol-1-yl)methyl)-2,4-dioxo-3,4-dihydropyrimidin-1(2H)-yl)-3-hydroxytetrahydrofuran-2-yl)methyl triphosphate (dT^{NNIR}TP)

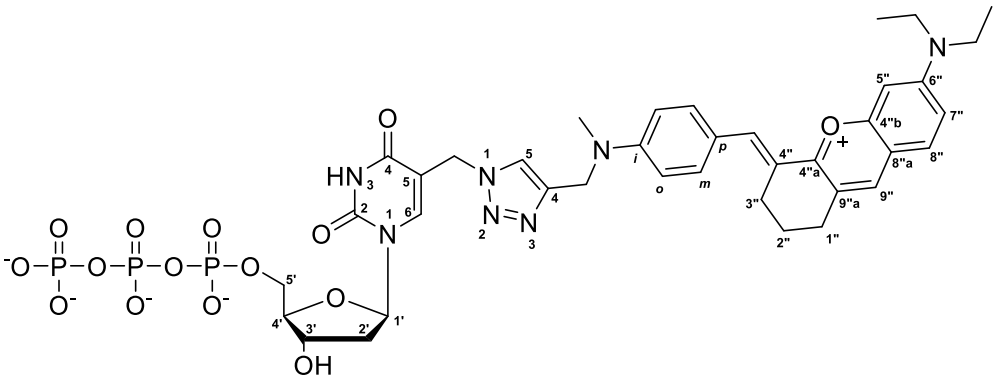

dT^{N3}TP (Et_3NH^+ salt; 9.45 mg, 11.4 μmol), $CuSO_4.5H_2O$ (1.1 mg, 6.9 μmol), sodium ascorbate (5 mg, 25.2 μmol) and alkyne **43** (13.8 mg, 33.5 μmol) were placed in a round bottom flask and dissolved in mixture of H_2O/THF (1:3, 1.6 mL). The reaction mixture was stirred at room temperature until complete consumption of starting material (**dT^{N3}TP**) was observed according to TLC (reverse phase; methanol/water 1:1 as eluent). After evaporation the reaction mixture was purified by HPLC with the use of linear gradient of methanol (5-100%) in water. The nucleotide **dT^{NNIR}TP** was isolated in 25% yield (3.65 mg) as a dark blue solid after HPLC purification. Nucleotide was susbsequently converted to sodium salt (Dowex 50WX8 in Na^+ cycle).

Substantial broadening of the peaks was observed in D_2O, probably due to the formation of aggregates or some particles. This problem was fixed using MeOD as solvent, which probably disrupted the particles.

^{1}H NMR (500.0 MHz, CD_3OD): 1.29 (bt, 27H, J_{vic} = 6.7 C**H$_3$**CH_2NH^+); 1.33 (t, 6H, J_{vic} = 7.1, C**H$_3$**CH_2N); 1.90 – 1.97 (bm, 2H, H-2″); 2.26 – 2.35 (bm, 2H, H-2′); 2.80 – 2.86 (bm, 2H, H-1″); 2.92 – 2.97 (m, 2H, H-3″); 3.14 – 3.21 (bm, 21H, CH_3N, CH_3C**H$_2$**NH^+); 3.69 (bq, 4H, J_{vic} = 7.1, CH_3C**H$_2$**N); 4.01 (bm, 1H, H-4′); 4.27 – 4.36 (bm, 2H, H-5′); 4.69 (bm, 1H, H-3′); 4.73 (s, 2H, CH_2NMe); 5.43 (s, 2H, CH_2N); 6.25

(t, 1H, $J_{1',2'}$ = 6.2, H-1′); 6.84 – 6.90 (m, 2H, H-*o*-phenylene); 7.11 (d, 1H, $J_{5'',7''}$ = 2.0, H-5″); 7.22 (bd, 1H, $J_{7'',8''}$ = 9.0, H-7″); 7.51 – 7.58 (m, 2H, H-*m*-phenylene); 7.60 (bd, 1H, $J_{8'',7''}$ = 9.0, H-8″); 7.99 (s, 2H, H-9″, CH=); 8.27 (H-5-triazole); 8.49 (s, 1H, H-6).

^{13}C NMR (125.7 MHz, CD_3OD): 9.08 (**C**$H_3CH_2NH^+$); 12.89 (**C**H_3CH_2N); 22.48 (CH_2-2″); 28.65, 28.73 (CH_2-1″,3″); 39.20 (CH_3N); 41.20 (CH_2-2′); 46.83 (CH_3**C**H_2N); 47.32 (CH_3**C**H_2NH^+); 47.80 (CH_2N); 48.03 (CH_2NMe); 66.30 (d, $J_{C,P}$ = 3.8, CH_2-5′); 71.53 (CH-3′); 86.66 (CH-1′); 87.59 (d, $J_{C,P}$ = 8.5, CH-4′); 96.68 (CH-5″); 109.77 (C-5); 113.76 (CH-*o*-phenylene); 117.65 (CH-7″); 118.53 (C-8″a); 123.56 (C-4″); 124.53 (C-9″a); 124.96 (CH-5-triazole); 125.32 (C-*p*-phenylene); 132.50 (CH-8″); 135.69 (CH-*m*-phenylene); 141.72 (CH=); 143.19 (CH-6); 145.10 (C-4-triazole); 147.63 (CH-9″); 152.06 (C-2); 152.50 (C-*i*-phenylene); 156.56 (C-6″); 159.83 (C-4″b); 164.71 (C-4); 166.53 (C-4″a).

^{31}P{^{1}H} NMR (202.4 MHz, CD_3OD): -21.61 (bt, J = 20.9, P$_\beta$); -9.73 (d, J = 20.9, P$_\gamma$); -8.62 (d, J = 20.9, P$_\alpha$).

HRMS (ESI^-): calculated for $(C_{38}H_{44}O_{15}N_7P_3)/2$: 465.60596; found 465.60571.

5.5.2 Biochemistry

5.5.2.1 Primer extension experiments

Enzymatic synthesis of modified DNA bearing one NNIR modification by primer extension (gel analysis)

The reaction mixture (20 µl) contained FAM labelled primer Prim1^{PEX}-FAM (for sequence see Table 16; 3 µM, 1 µL), template Temp5^{PEX} (for sequence see Table 16; 3 µM, 1.5 µL), KOD XL DNA polymerase (0.25 U/µL, 0.25 µL), natural dGTP (4 mM, 0.6 µL), either natural dTTP (4 mM, 0.3 µL) or **dT^{NNIR}TP** (4 mM, 0.3 µL) in corresponding reaction buffer (10x, 2 µL) supplied by the manufacturer. The reaction mixture was incubated for 60 min at 60°C in thermal cycler. The reaction was stopped by the addition of PAGE stop solution (20 uL) and the reaction mixture was denatured at 95°C for 5 min and analyzed using 12.5% denaturing PAGE. The gel was visualized by a fluorescent scanner (PAGE gel is shown in Figure 20 B).

Enzymatic synthesis of modified DNA bearing one azido modification by primer extension (gel analysis)

The reaction mixture (20 µl) contained FAM labelled primer Prim1^{PEX}-FAM (for sequence see Table S3; 3 µM, 1 µL), template Temp5^{PEX} (for sequence see Table S3; 3 µM, 1.5 µL), KOD XL DNA polymerase (0.25 U/µL, 0.125 µL), natural dGTP (4 mM, 0.3 µL), either natural dTTP (4 mM, 0.3 µL) or **dT^{N3}TP** (4 mM, 0.3 µL) in corresponding reaction buffer (10x, 2 µL) supplied by the manufacturer. The reaction mixture was incubated for 30 min at 60°C in a thermal cycler. The reaction was stopped by the addition of PAGE stop solution (20 uL) and the reaction mixture was denatured for 5 min at 95°C and analyzed using 12.5% denaturing PAGE. The gel was visualized by a fluorescent scanner (PAGE gels are shown in Figure 22 A).

Enzymatic synthesis of modified DNA bearing four NNIR modification by primer extension (gel analysis)

The reaction mixture (20 µl) contained FAM labelled primer Prim1^{PEX}-FAM (for sequence see Table 16; 3 µM, 1 µL), template Temp2^{PEX} (for sequence see Table 16; 3 µM, 1.5 µL), KOD XL DNA polymerase (0.25 U/µL, 0.3 µL), natural dNTPs (dATP, dGTP, dCTP, 4 mM each, 0.7 µL), either natural dTTP (4 mM, 0.7 µL) or **dT^{NNIR}TP** (4 mM, 0.7 µL) in corresponding reaction buffer (10x, 2 µL) supplied by the manufacturer. The reaction mixture was incubated for 60 min at 60°C in a thermal cycler. The reaction was stopped by the addition of PAGE stop solution (20 µL) and the reaction mixture was denatured for 5 min at 95°C and analyzed using 12.5% denaturing PAGE. The gel was visualized by a fluorescent scanner (PAGE gel is shown in Figure 20 C).

Enzymatic synthesis of modified DNA bearing one azido modification by primer extension (gel analysis)

The reaction mixture (20 µl) contained FAM labelled primer Prim1^{PEX}-FAM (for sequence see Table 16; 3 µM, 1 µL), template Temp2^{PEX} (for sequence see Table 16; 3 µM, 1.5 µL) KOD XL DNA polymerase (0.25 U/µL, 0.3 µL), natural dNTPs (dATP, dGTP, dCTP, 4 mM each, 0.7 µL), either natural dTTP (4 mM, 0.7 µL) or **dT^{N3}TP** (4 mM, 0.7 µL) in corresponding reaction buffer (10x, 2 µL) supplied by the manufacturer. The reaction mixture was incubated for 30 min at 60°C in a thermal cycler. The reaction was stopped by the addition of PAGE stop solution (20 µL) and the reaction mixture was denatured for 5 min at 95°C and analyzed using 12.5% denaturing PAGE. The gel was visualized by a fluorescent scanner (PAGE gel is shown in Figure 22 B).

Single nucleotide incorporation of $dT^{NNIR}TP$ and subsequent primer extension (SNI-PEX; gel analysis)

The reaction mixture (20 µl) contained FAM labelled primer $Prim1^{PEX}$-FAM (for sequence see Table 16; 3 µM, 1 µL), template $Temp6^{PEX}$ (for sequence see Table 16; 3 µM, 1.5 µL), KOD XL DNA polymerase (0.25 U/µL, 0.125 µL), either natural dTTP (0.04 mM, 0.5 µL) or **$dT^{NNIR}TP$** (0.04 mM, 0.5 µL) in corresponding reaction buffer (10x, 2 µL) supplied by the manufacturer. The reaction mixture was incubated for 10 min at 60°C in a thermal cycler. For the subsequent extension, a mixture of all natural dNTPs (8 mM, 0.5 µL) was added and the reaction mixture was incubated for further 20 min at 60°C. The reaction was stopped by the addition of PAGE stop solution (20 µL) and the reaction mixture was denatured for 5 min at 95°C and analyzed using 12.5% denaturing PAGE. The gel was visualized by a fluorescent scanner (For scheme of reaction see Figure 21 A, PAGE gel is shown in Figure 21 B, C).

Preparation of modified oligonucleotide ON19_1T^{N3} by primer extension and subsequent magnetic separation

The reaction mixture (200 µL) contained primer (for sequence see Table 16; $Prim1^{PEX}$,100 µM, 10 µL), template (for sequence see Table 16; $Temp5^{PEX}$-bio, 100 µM, 10 µL), dGTP (4 mM, 5 µL), **$dT^{N3}TP$** (4 mM, 5 uL), KOD XL DNA polymerase (2.5 U/µL, 1.14 µL) in corresponding reaction buffer (10x, 25 µL) supplied by the manufacturer. The reaction mixture was incubated for 30 min at 60°C in a thermal cycler. The reaction was stopped by cooling at 4°C. Streptavidin magnetic beads (100 µl, Roche) were washed with binding buffer TEN 100 (3 × 600 µl, 10 mM Tris, 1 mM EDTA, 100 mM NaCl, pH 7.5). Then PEX solution (200 µL) and binding buffer (200 µl) were added to the magnetic beads. The mixture was incubated for 30 min at 15°C and 1400 rpm. Then the magnetic beads were separated and washed with washing buffer TEN 500 (3 × 400 µl, 10 mM Tris, 1 mM EDTA, 1 M NaCl, pH 7.5) and with milli-Q water (4 × 400 µl). Then 100 µl of milli-Q water was added and

the sample was denatured for 2 min at 70°C and 900 rpm. The solution containing modified ssDNA was quickly transferred into clean Eppendorf and analysed by MALDI-TOF mass spectrometry. Product was used for click reactions.

Preparation of modified oligonucleotide ON31_4T^{N3} by primer extension and subsequent magnetic separation

The reaction mixture (200 µL) contained primer (for sequence see Table 16; Prim1^{PEX}, 100 µM, 10 µL), template (for sequence see Table 16; Temp2^{PEX}-bio, 100 µM, 10 µL), dNTPs (dATP, dGTP, dCTP, 4 mM each, 5 µL), **dT^{N3}TP** (4 mM, 5 uL), KOD XL DNA polymerase (2.5 U/µL, 1.14 µL) in corresponding reaction buffer (10×, 25 µL) supplied by the manufacturer. The reaction mixture was incubated for 30 min at 60°C in a thermal cycler. The reaction was stopped by cooling at 4°C. Streptavidin magnetic beads (100 µl, Roche) were washed with binding buffer TEN 100 (3 × 600 µl, 10 mM Tris, 1 mM EDTA, 100 mM NaCl, pH 7.5). Then PEX solution (200 µL) and binding buffer (200 µl) were added to the magnetic beads. The mixture was incubated for 30 min at 15°C and 1400 rpm. Then the magnetic beads were separated and washed with washing buffer TEN 500 (3 × 400 µl, 10 mM Tris, 1 mM EDTA, 1 M NaCl, pH 7.5) and with milli-Q water (4 × 400 µl). Then 100 µl of milli-Q water was added and the sample was denatured for 2 min at 70°C and 900 rpm. The solution containing modified ssDNA was quickly transferred into clean Eppendorf and analysed by MALDI-TOF mass spectrometry. Product was used for click reactions.

Preparation of modified oligonucleotides ON16_1T^{NNIR} and ON31_1T^{NNIR} by SNI or SNI-PEX and subsequent magnetic separation

The reaction mixture (100 µl) contained primer Prim1^{PEX} (for sequence see Table 16; 100 µM, 1 µL), template Temp6^{PEX}-bio (for sequence see Table 16; 100 µM, 1.2 µL), KOD XL DNA polymerase (0.25 U/µL, 0.5 µL), **dT^{NNIR}TP** (0.04 mM, 20 µL) in

corresponding reaction buffer (10x, 10 µL) supplied by the manufacturer. The reaction mixture was incubated for 10 min at 60°C in a thermal cycler. For the subsequent extension, a mixture of all natural dNTPs (24 mM, 2 µL) and additional KOD XL DNA polymerase (0.25 U/µL, 0.2 µL) were added and the reaction mixture was incubated for further 60 min at 60°C. Reactions were stopped by cooling at 4°C. Streptavidin magnetic beads (100 µl, Roche) were washed with binding buffer TEN 100 (3 × 450 µl, 10 mM Tris, 1 mM EDTA, 100 mM NaCl, pH 7.5). Then PEX solution and binding buffer (100 µl) were added to the magnetic beads. The mixture was incubated for 30 min at 15°C and 1400 rpm. Then the magnetic beads were separated and washed with washing buffer TEN 500 (3 × 350 µl, 10 mM Tris, 1 mM EDTA, 1 M NaCl, pH 7.5) and with milli-Q water (4 × 350 µl). Then 100 µl of milli-Q water was added and the sample was denatured for 2 min at 70°C and 900 rpm. The solution containing modified ssDNA was quickly transferred into clean Eppendorf and analysed by MALDI-TOF mass spectrometry.

Preparation of modified dsDNA bearing one NNIR modification by primer extension (DNA19_1T^{NNIR}; semi-preparative scale)

The reaction mixture (125 µL) containing primer (for sequence see Table 16; Prim1^{PEX}, 100 µM, 5 µL), template (for sequence see Table 16; Temp5^{PEX}, 100 µM, 5 µL), dGTP (4 mM, 2.5 µL), **dT^{NNIR}TP** (4 mM, 2.5 uL), KOD XL DNA polymerase (2.5 U/µL, 0.6 µL) in corresponding reaction buffer (10×, 12.5 µL) supplied by the manufacturer. The reaction mixture was incubated for 60 min at 60°C in a thermal cycler. The reaction was stopped by cooling at 4°C. The modified dsDNA was purified using spin columns (QIAquick® Nucleotide Removal Kit, QIAGEN) and eluted by milli-Q water. Prepared dsDNA was used for fluorescence measurements. To prepare dsDNA for lambda exonuclease digestion, the PEX and purification was performed as described above using phosphorylated template (for sequence see Table 16; Temp5^{PEX}-P).

Preparation of modified ssDNA bearing one NNIR modification using lambda exonuclease digestion (ON19_1T^{NNIR})

The reaction mixture (100 µL) containing modified dsDNA (prepared using Temp5^{PEX}-P as described above; 0.2 nmol), lambda exonuclease buffer 10x (4 uL) and lambda exonuclease enzyme (10 U/µL, 3 µL) was incubated for 60 min 37°C in a thermal cycler. The reaction was stopped by cooling at 4°C. The modified ssDNA was purified using spin columns (QIAquick® Nucleotide Removal Kit, QIAGEN) and eluted by milli-Q water. Product was analysed by MALDI-TOF mass spectrometry. Prepared ssDNA was used for fluorescence measurements.

5.5.2.2 Polymerase chain reaction experiments

Enzymatic incorporation of dT^{NNIR}TP by polymerase chain reaction

The reaction mixture (20 µL) contained primer (for sequences see Table 16; Prim1^{PCR} and Prim2^{PCR}, 10 µM, 4 µL of each), template (Temp1^{PCR}, 10 µM, 0.5 µL), natural dNTPs (dATP, dGTP, dCTP, 0.4 mM each, 1.5 µL) and either dTTP (0.4 mM, 1.5 uL), **dT^{N3}TP** (0.4 mM, 1.5 µL), **dT^{NNIR}TP** (0.4 mM, 1.5 µL) or mixture of **dT^{NNIR}TP** with natural dTTP (0-95%), KOD XL DNA polymerase (2.5 U/µL, 1 µL) and corresponding reaction buffer (10×, 2 µL) supplied by the manufacturer. After the initial denaturation for 3 min at 94°C, 30 PCR cycles were run under the following conditions: denaturation for 1 min at 94°C, annealing for 1 min at 51°C, extension for 2 min at 72°C. The PCR process was terminated with a final extension step for 5 min at 72°C. The reaction was stopped by cooling to 4°C. The PCR products were analyzed by agarose gel electrophoresis in 2% agarose gel stained with GelRed™ (Biotium, agarose gel is shown in Figure 24 A). The PCR products (Figure 24 A, lane 6 and 7) were purified using spin columns (QIAquick® Nucleotide Removal Kit, QIAGEN) and the fluorescence spectra were measured (Figure 25).

Preparation of template Temp3^{PCR} by PCR

The reaction mixture (20 µL) contained primer (for sequences see Table 16; Prim5^{PCR} and Prim6^{PCR}, 10 µM, 0.8 µL of each), cDNA (provided by virology department at the IOCB Prague, 1 µL), all natural dNTPs (0.4 mM, 1.5 µL), KOD XL DNA polymerase (2.5 U/µL, 0.5 µL) and corresponding reaction buffer (10x, 2 µL). After the initial denaturation for 3 min at 94°C, 40 PCR cycles were run under the following conditions: denaturation for 20 sec at 94°C, annealing/extension for 10 sec at 64°C. The reaction was stopped by cooling to 4°C. PCR was performed 4 times and products were purified by nucleospin® Gel and PCR Clean-up columns (MACHEREY-NAGEL). Products were subsequently loaded on 2% agarose gel (Figure 40 B) and then calculated concentration using Nanodrop and OligoCalc.

Real-time PCR using dT^{NNIR}TP

The reaction mixture (20 µL) contained primer (for sequences see Table 16; Prim5^{PCR} and Prim6^{PCR}, 10 µM, 0.8 µL of each), template (Temp3^{PCR}, 10-fold serial dilutions, 100 pM – 100 aM, 1 µL), natural dNTPs (dATP, dGTP, dCTP, 0.4 mM, 1.5 µL), mixture of dTTP:**dT^{NNIR}TP** 95:5 (dTTP, 0.4 mM, 1.43 µL, **dT^{NNIR}TP**, 0.04 mM, 0.75 µL), KOD XL DNA polymerase (2.5 U/µL, 0.5 µL) and corresponding reaction buffer (10x, 2 µL). After the initial denaturation for 3 min at 94°C, 40 PCR cycles were run under the following conditions: denaturation for 20 sec at 94°C, annealing/extension for 10 sec at 64°C. Samples were excited at 672-684 nm and emission was detected 705-730 nm (as Quasar 705, dye predefined in machine). Then, melting curve analysis was performed under the following conditions: 10 sec at 94°C, 5 sec at 65°C, then followed by a slow increase from 65°C to 95°C with a speed of 0.5°C per second. The reaction was stopped by cooling to 4°C. Standard curve (established from results obtained using 5.71 x 10^7 to 5.71 x 10^3 DNA copies) was determined to be y = -4.8678x + 57.138 (Figure 41 B). The efficiency was calculated to be 60.5% and the correlation coefficient (R^2) was 0.9993. Melting curve analysis

revealed a single peak for product (Figure Figure 41 C, D). The PCR products were analyzed by agarose gel electrophoresis in 2% agarose gel stained with GelRed™ (agarose gels are shown in Figure 41 E, F).

Reverse transcription real-time PCR using dT^{NNIR}TP

The reaction mixture (20 µL) contained primer (for sequences see Table 16; Prim5^{PCR} and Prim6^{PCR}, 10 µM, 0.8 µL of each), RNA (provided by virology department at the IOCB Prague, 4 µL), natural dNTPs (dATP, dGTP, dCTP, 0.4 mM, 1.5 µL), mixture of dTTP:**dT^{NNIR}TP** 95:5 (dTTP, 0.4 mM, 1.43 µL, **dT^{NNIR}TP**, 0.04 mM, 0.75 µL), KOD XL DNA polymerase (2.5 U/µL, 0.5 µL) and corresponding reaction buffer (10x, 2 µL), SuperScript III Reverse Transcriptase (200 U/µL, 0.5 µL), DTT (0.1 M, 2 uL), RNase Inhibitor (1 uL). First, reverse transcription was run for 30 min at 50°C followed by denaturation for 3 min at 94°C and then 40 PCR cycles were run under the following conditions: denaturation for 20 sec at 94°C, annealing/extension for 10 sec at 64°C. Samples were excited at 672-684 nm and emission was detected 705-730 nm (as Quasar 705 dye predefined in machine). Then, melting curve analysis was performed under the following conditions: 10 sec at 94°C, 5 sec at 65°C, then followed by a slow increase from 65°C to 95°C with a speed of 0.5°C per second. The reaction was stopped by cooling to 4°C. Melting curve analysis revealed a single peak (at 80.5°C) for product (Figure 42 E). The PCR products were analyzed by agarose gel electrophoresis in 2% agarose gel stained with GelRed™ (agarose gels are shown in Figure 42 B, C).

5.5.2.3 Copper-catalysed azide-alkyne cycloaddition reaction on ssDNA

CuAAC reaction of ON19_1T^{N3} or ON31_4T^{N3} with alkyne 43

To ssDNA (**ON19_1T^{N3}** or **ON31_4T^{N3}**; 2 nmol) in 30 µL H_2O were added 3 µL of DMSO/tBuOH 3:1 mixture, DMSO/tBuOH 3:1 solution of alkyne **43** (50 mM, 2 µL) and a freshly prepared solution of TBTA (50 mM) and CuBr (25 mM) 5:1 (5 µL) in DMSO/tBuOH 3:1. The reaction mixture was incubated at 37°C and 800 rpm overnight. Then the reaction mixtures were freeze-dried, re-suspended in 50 µL water and purified by QIAquick Nucleotide Removal kit (QIAGEN). Control experiments were performed using non-modified ssDNA following the same procedure. Samples of single-stranded DNA for MALDI-TOF MS analysis were prepared following the same procedure. To analyze the product of click reaction using PAGE, the reaction was perfomed as described above using ssDNA (0.5 nmol in 30 µL H_2O) after PEX with FAM labelled primer and DMSO/tBuOH 3:1 solution of alkyne **43** (50 mM, 1 µL). The click reaction products were purified with QIAquick® Nucleotide Removal kit (QIAGEN). The products were analysed using 20% PAGE gel and visualized by a fluorescent scanner (PAGE gel is shown in Figure 23 B, C).

5.5.3 Absorption, fluorescence measurements and applications

UV melting temperatures of DNA19_1T and DNA19_1T^{NNIR}

All solutions of DNA (1 nmol) were prepared in 25 mM phosphate buffered saline (1 mL). Melting curve analysis was performed by a slow increase of temperature from 10°C to 90°C with a speed of 1°C per minute. Then samples were cooled to 10°C with a speed of 1°C per minute. The process of denaturation and annealing was repeated three times. Figure 30 shows UV melting curves.

Hybridization and digestion studies

A series of 3 solutions (final volume of each solution was 100 µL) were prepared by mixing **ON19_1T^{NNIR}** (104.8 pmol), lambda exonuclease buffer (10x, 1.5 µL) and either just diluting with milli-Q water (solution 1) or adding phosphorylated complementary strand (for sequence see Table 16; Temp5^{PEX}-P, 100 µM, 1.15 µL, solution 2) or adding phosphorylated complementary strand (Temp5^{PEX}-P, 100 µM, 1.15 µL) and lambda exonuclease enzyme (10 U/µL, 1.2 µL, solution 3). All solutions were heated to 95°C for 3 min and then left to cool down at room temperature. All solutions were then incubated for 60 min at 37°C in a thermal cycler. After cooling down to room temperature each sample was equilibrated for 2 min in fluorimeter holder (100 µL quartz cuvette, 25°C) before recording the fluorescence spectrum (λ_{ex} = 690 nm).

5.5.3.1 Interaction of modified DNA with small molecules and biomolecules

Interaction of DNA binding dyes with DNA19_1T^{NNIR}

Titrations were performed in 100 µL quartz cuvette at 25°C. Solution of modified dsDNA (100 µL, 50 pmol) in phosphate buffer (4.5 mM, pH 7.4) was titrated by either thiazole orange, DAPI or methyl green. After every addition (0-20 equiv.) the solution was mixed carefully with a pipette and equilibrated for 1-2 min before recording the fluorescence spectrum (λ_{ex} = 690 nm).

Interaction of spermine with DNA19_1T^{NNIR}

Titrations were performed in 100 µL quartz cuvette at 25°C. Solution of modified dsDNA (100 µL, 2 µM) in phosphate buffer (4.5 mM, pH 7.4) was titrated by solution of spermine (0.4 mM, in the same buffer). After every addition (0-256 equiv.) the solution was mixed carefully with a pipette and equilibrated for 1-2 min before

recording the fluorescence spectrum (λ_{ex} = 690 nm).

Interaction of histone with DNA19_1T^{NNIR}

Titrations were performed in 100 µL quartz cuvette at 25°C. Solution of dsDNA (100 µL, 2 µM) in phosphate buffer (4.5 mM, pH 7.4) was titrated by H2A histone and by BSA (Bovine serum albumin) as control experiment. After every addition (0-4 equiv.) the solution was mixed carefully with a pipette and equilibrated for 1-2 min before recording the fluorescence spectrum (λ_{ex} = 690 nm).

Interaction of protamine with DNA19_1T^{NNIR}

Titrations were performed in 100 µL quartz cuvette at 25°C. Solution of dsDNA (100 µL, 2 µM) in phosphate buffer (4.5 mM, pH 7.4) was titrated by solution of protamine (protamine sulfate; 0.1 mM, in the same buffer). After every addition (0-1.75 equiv.) the solution was mixed carefully with a pipette and equilibrated for 1-2 min before recording the fluorescence spectrum (λ_{ex} = 690 nm).

5.5.3.2 Displacement assays

Displacement assay using 98-mer dsDNA

Titrations were performed in 100 µL quartz cuvette at 25°C. Solution of dsDNA (**DNA19_1T^{NNIR}**) and histone H2A (in the ratio 1:2) was prepared in phosphate buffer (4.5 mM, pH 7.4). Solution of dsDNA-histone complex was titrated by 98-mer dsDNA. After every addition (0-1.75 equiv.) the solution was mixed carefully with a pipette and equilibrated for 1-2 min before recording the fluorescence spectrum (λ_{ex} = 690 nm).

Displacement assay using heparin

Titrations were performed in 100 μL quartz cuvette at 25°C. Solution of dsDNA (**DNA19_1T^{NNIR}**) and protamine 1:1.75 (in the ratio 1:1.75) was prepared in phosphate buffer (4.5 mM, pH 7.4). Solution of dsDNA-protamine complex was titrated by solution of heparin (40 μM, in the same buffer). After every addition (0-0.7 equiv.) the solution was mixed carefully with a pipette and equilibrated for 1-2 min before recording the fluorescence spectrum (λ_{ex} = 690 nm).

5.5.3.3 Monitoring of enzymatic reactions

Kinetics of lambda exonuclease digestion

Digestion was performed in 100 μL quartz cuvette at 37°C in fluorimeter holder. The initial solution (100 μL) contained **DNA19_1T^{NNIR}-P** (0.2 nmol) and buffer for lambda exonuclease (4 μL). The mixture was equilibrated in fluorimeter holder for 3 min at 37°C and then fluorescence spectrum was recorded. Then lambda exonuclease (3 μL) was added and fluorescence spectra were recorded in time intervals (0-75 min).

Digestion of histone with Proteinase K

Solution of dsDNA (**DNA19_1T^{NNIR}**) and histone H2A (in the ratio 1:2) was prepared in phosphate buffer (4.5 mM, pH 7.4). Equilibrated for 2 min at 25°C and measured fluorescence. Then Proteinase K (40 μM, 0.3 μL) was added and fluorescence spectra (λ_{ex} = 690 nm) were recorded in 10 sec intervals reaching peak at 20 min.

Real-time monitoring of single nucleotide incorporation (SNI)

SNI was performed in 100 μL quartz cuvette at 60°C in fluorimeter holder. The initial solution (100 μl) contained primer Prim1^{PEX} (for sequence see Table 16; 100 μM, 1 μL), template Temp8^{PEX} (for sequence see Table 16; 100 μM, 1.2 μL), **dT^{NNIR}TP**

(0.04 mM, 20 µL), corresponding reaction buffer (10x, 10 µL) supplied by the manufacturer and KOD XL polymerase (2.5 U/µL, 0.5 µL). After addition of polymerase the cuvette was placed in fluorimeter holder (preheated to 60°C) and fluorescence spectra were recorded in time intervals (0-25 min). Control experiments contained reaction mixture without enzyme (control 1) or without template (control 2). All samples were excited at 690 nm.

5.6 Attachment of benzylidene-tetrahydroxanthylium fluorophore to 2'-deoxycytidine triphosphate via triethylene glycol linker. Synthesis, photophysical properties, enzymatic incorporation into DNA and applications

5.6.1 Chemical synthesis

Tosyl-propargyloxy-triethylene glycol modified deoxycytidine (dC^{pegOTs})

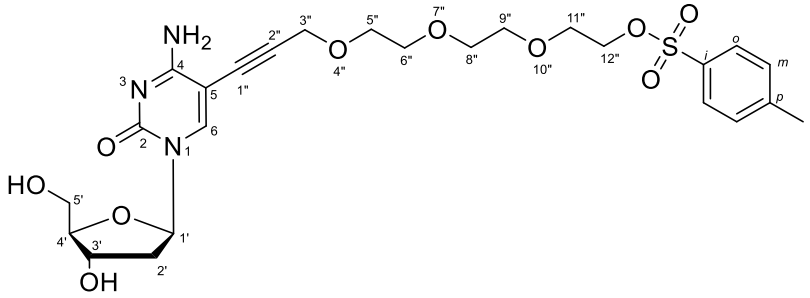

A reaction flask containing 5-iodo-2'-deoxycytidine (202 mg, 0.57 mmol), alkyne **46** (391.3 g, 1.15 mmol, 2 equiv.), $PdCl_2(PPh_3)_2$ (25.2 mg, 0.036 mmol, 6.3% mol), CuI (9.7 mg, 0.051 mmol, 9% mol) was evacuated and refilled with argon 3 times and the content was dissolved in dry DMF (5.5 mL). Then *N*,*N*-diisopropylethylamine (0.5 ml, 2.29 mmol, 4 equiv.) was added dropwise and the reaction mixture was stirred at room temperature overnight. The reaction mixture was concentrated on rotavap and purified by silica column chromatography eluted with methanol in dichloromethane (0-10%). Product was isolated as orange sticky oil (288.8 mg, 89%).

^{1}H NMR (500.0 MHz, CD_3OD): 2.14 (dt, 1H, J_{gem} = 13.6, $J_{2'b,1'} = J_{2'b,3'}$ = 6.3, H-2′b); 2.39 (ddd, 1H, J_{gem} = 13.6, $J_{2'a,1'}$ = 6.3, $J_{2'a,3'}$ = 4.0, H-2′a); 2.45 (s, 3H, CH_3-Tos); 3.54 – 3.60 (m, 4H, H-8″,9″); 3.63 – 3.68 (m, 4H, H-6″.11″); 3.69 – 3.72 (m, 2H, H-5″); 3.73 (dd, 1H, J_{gem} = 12.1, $J_{5'b,4'}$ = 3.7, H-5′b); 3.82 (dd, 1H, J_{gem} = 12.1, $J_{5'a,4'}$ = 3.1, H-5′a); 3.94 (ddd, 1H, $J_{4',3'}$ = 4.0, $J_{4',5'}$ = 3.7, 3.1, H-4′); 4.13 – 4.16 (m, 2H, H-12″); 4.36 (dt, 1H, $J_{3',2'}$ = 6.3, 4.0, $J_{3',4'}$ = 4.0, H-3′); 4.42 (s, 2H, H-3″); 6.20 (t, 1H, $J_{1',2'}$ = 6.3, H-1′); 7.41 – 7.46 (m, 2H, H-*m*-Tos); 7.76 – 7.82 (m, 2H, H-*o*-Tos); 8.37 (s, 1H, H-6).

^{13}C NMR (125.7 MHz, CD_3OD): 21.59 (CH_3-Tos); 42.44 (CH_2-2′); 59.79 (CH_2-3″);

62.43 (CH_2-5′); 69.75 (CH_2-11″); 70.28 (CH_2-5″); 70.94 (CH_2-12″); 71.48, 71.52, 71.53 (CH_2-6″,8″,9″); 71.67 (CH-3′); 78.13 (C-1″); 88.00 (CH-1′); 89.08 (CH-4′); 92.03 (C-5); 92.46 (C-2″); 129.07 (CH-*o*-Tos); 131.06 (CH-*m*-Tos); 134.44 (C-*i*-Tos); 146.34 (CH-6); 146.49 (C-*p*-Tos); 156.70 (C-2); 166.38 (C-4).

HRMS (ESI^+): calculated for $C_{25}H_{34}O_{10}N_3S$: 568.1959; found 568.1963.

Azido-propargyloxy-triethylene glycol modified deoxycytidine (dC^{pegN3})

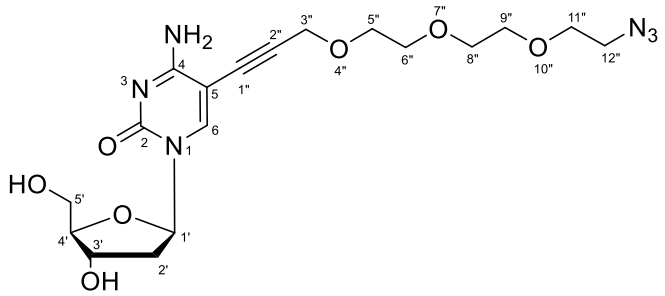

dC^{PegOTs} (399 g, 0.703 mmol) was dissolved in dry DMF (3.8 mL) under argon atmosphere, then NaN_3 (104 mg, 1.6 mmol, 2.3 equiv.) was added. The reaction mixture was stirred for 2 hours at 50°C under argon atmosphere. After 2 hours solvent was evaporated and crude reaction mixture was purified by silica column chromatography eluted with methanol in dichloromethane (0-8%). Product was isolated as pale yellow sticky oil (207 mg, 67%).

OH and NH_2 are partially exchanged with D => therefore we see more than 1 set of signals in NMR.

^{1}H NMR (500.0 MHz, DMSO-d_6): 1.99 (ddd, 1H, J_{gem} = 13.2, $J_{2'b,1'}$ = 7.0, $J_{2'b,3'}$ = 6.1, H-2′b); 2.15 (ddd, 1H, J_{gem} = 13.2, $J_{2'a,1'}$ = 6.0, $J_{2'a,3'}$ = 3.6, H-2′a); 3.37 – 3.40 (m, 2H, CH_2N_3); 3.51 – 3.64 (m, 12H, H-5′, CH_2O); 3.79 (q, 1H, $J_{4',3'} = J_{4',5'}$ = 3.5, H-4′); 4.20 (m, 1H, H-3′); 4.36 (s, 2H, $CH_2C{\equiv}C$-); 5.08 (t, 1H, $J_{OH,5'}$ = 5.1, OH-5′); 5.21 (d, 1H, $J_{OH,3'}$ = 4.3 OH-3′); 6.10 (dd, 1H, $J_{1',2'}$ = 7.0, 6.0, H-1′); 6.90, 7.74 (2 × bs, 2 × 1H, NH_2); 8.20 (s, 1H, H-6).

^{13}C NMR (125.7 MHz, DMSO-d_6): 41.01 (CH_2-2′); 50.17 (CH_2N_3); 58.64 (**C**H_2C≡C); 61.15 (CH_2-5′); 68.84, 69.44, 69.82, 69.87, 69.98 (CH_2O); 70.26 (CH-3′); 77.96 (**C**≡CCH_2); 85.58 (CH-1′); 87.66 (CH-4′); 89.26 (C-5); 91.64 (C≡**C**CH_2); 145.09 (CH-6); 153.62 (C-2); 164.52 (C-4).

HRMS (ESI$^+$): calculated for $C_{18}H_{26}O_7N_6Na$: 461.1755; found 461.1758.

Azido-propargyloxy-triethylene glycol modified deoxycytidine-5′-*O*-triphosphate (dC^{pegN3}TP)

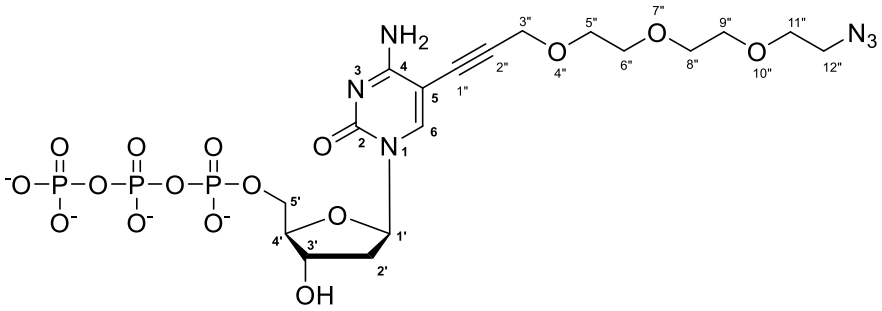

dC^{PegN3} (42 mg, 0.096 mmol) was dried overnight at room temperature and then 1h at 70°C under vacuum. After cooling down to room temperature dry trimethyl phosphate (300 µL) was added, the solution was cooled down to 0°C and then $POCl_3$ (10.9 µL, 1.2 equiv.) was added dropwise. After 2 hours of stirring at 0–4°C (water/ice bath) all starting nucleoside was consumed according to the TLC (CH_2Cl_2:MeOH 10:1). Then ice-cold solution of bis-tributylammonium pyrophosphate (308 mg, 0.542 mmol) and tributylamine (70 µL, 0.297 mmol) in dry DMF (0.9 mL) was added. After stirring for 1 hour at 0–4°C the reaction was quenched by addition of 2 M solution of TEAB (1 mL). The reaction mixture was concentrated on rotavap and the residue was co-evaporated with HPLC-grade water. The product was purified by HPLC with the use of gradient methanol (0-100%) in 0.1 M TEAB buffer. Isolated product was co-evaporated with HPLC-grade water several times. Freeze-drying from water afforded the final nucleotide as sticky oil (23 mg, 22%).

^{1}H NMR (500.0 MHz, D_2O, ref(*t*BuOH) = 1.24 ppm): 1.27 (t, 36H, J_{vic} = 7.3, C**H**$_3$CH_2N); 2.32 (dt, 1H, J_{gem} = 14.0, $J_{2'b,1'} = J_{2'b,3'}$ = 6.6, H-2′b); 2.43 (ddd, 1H, J_{gem} = 14.0, $J_{2'a,1'}$ = 6.6, $J_{2'a,3'}$ = 4.4, H-2′a); 3.19 (q, 24H, J_{vic} = 7.3, CH_3C**H**$_2$N); 3.47 – 3.50 (m, 2H, H-12″); 3.69 – 3.76, 3.81 – 3.83 (2 × m, 10H, H-5″,6″,8″,9″,11″); 4.17 – 4.28 (m, 3H, H-4′,5′); 4.48 (s, 2H, H-3″); 4.58 (ddd, 1H, $J_{3',2'}$ = 6.6, 4.4, $J_{3',4'}$ = 3.8, H-3′); 6.25 (t, 1H, $J_{1',2'}$ = 6.6, H-1′); 8.19 (s, 1H, H-6).

^{13}C NMR (125.7 MHz, D_2O, ref(*t*BuOH) = 32.43 ppm): 11.05 (**C**H_3CH_2N); 41.97 (CH_2-2′); 49.43 (CH_3**C**H_2N); 53.00 (CH_2-12″); 61.42 (CH_2-3″); 67.78 (d, $J_{C,P}$ = 5.4, CH_2-5′); 71.66, 72.04, 72.31, 72.36 (CH_2-5″,6″,8″,9″,11″); 72.75 (CH-3′); 79.85 (C-1″); 88.43 (d, $J_{C,P}$ = 8.8, CH-4′); 88.98 (CH-1′); 94.36 (C-2″); 94.75 (C-5); 148.08 (CH-6); 158.86 (C-2); 167.92 (C-4).

^{31}P NMR (202.4 MHz, D_2O): -22.0 (t, *J* = 20.0, P$_\beta$); -10.64 (d, *J* = 20.0, P$_\gamma$); -6.02 (bd, *J* = 20.0, P$_\alpha$). P$_\beta$);

HRMS (ESI$^-$): calculated for $C_{18}H_{28}O_{16}N_6P_3$: 677.0780; found 677.0778.

((2R,3S,5R)-5-(4-amino-5-(3-(2-(2-(4-(((4-(((E)-6-(diethylamino)-2,3-dihydroxanthylium-4(1H)-ylidene)methyl)phenyl)(methyl)amino)methyl)-1H-1,2,3-triazol-1-yl)ethoxy)ethoxy)prop-1-yn-1-yl)-2-oxopyrimidin-1(2H)-yl)-3-hydroxytetrahydrofuran-2-yl)methylhydrogen triphosphate (dC^{pegNNIR}TP)

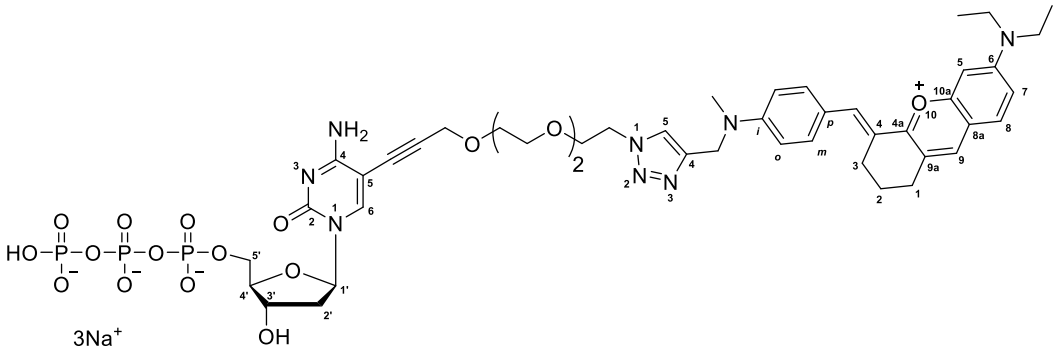

Alkyne **43** (8 mg, 0.0194 mmol) in schlenk flask was evacuated and purged with argon 3 times, then 100 μL of degassed DMSO was added under flow of argon and the mixture was stirred. Then solution of **dC^{PegN3}TP** (10.4 mg, 0.0096 mmol) in HPLC-grade water (50 μL) was added and stirred for 2 minutes. Freshly prepared solution of $Cu(CH_3CN)_4PF_6$ (5.4 mg, 0.0145 mmol) in degassed DMSO (50 μL) was added and the reaction mixture continued to stir at room temperature under argon. After 1 hour the reaction mixture was diluted with HPLC-grade water (0.8 mL), centrifuged and transferred to new eppendorf in order to remove insoluble particles. Then the residue was filtered through dowex (Dowex 50WX8 in Na^+ cycle). Final freeze-drying from water afforded the final nucleotide **dC^{pegNNIR}TP** as dark blue solid (3.4 mg, 31%).

^{1}H NMR (500.0 MHz, D_2O, ref(*t*BuOH) = 1.24 ppm): 1.33 (bt, 6H, J_{vic} = 6.5, C**H$_3$**CH$_2$N); 1.84 – 2.01 (m, 3H, H-2′b, H-2-xanth); 2.23 (m, 1H, H-2′a); 2.66 – 2.82 (bm, 4H, H-1,3-xanth); 3.02 (s, 3H, CH_3N); 3.19 – 3.41, 3.45 – 3.52 (2 × m, 8H, OCH_2CH_2O); 3.58 – 3.68 (m, 4H, CH_3C**H$_2$**N); 3.85 – 3.92 (m, 2H, OC**H$_2$**CH$_2$N); 3.95 (m, 1H, H-4′); 4.02 (bm, 1H, H-5′b); 4.10 (d, 1H, J_{gem} = 15.9, CH_a**H$_b$**C≡C); 4.11 (m, 1H, H-5′a); 4.15 (d, 1H, J_{gem} = 15.9, C**H$_a$**H$_b$C≡C); 4.43 (m, 1H, H-4′); 4.51 – 4.61 (m,

4H, C**H₂**NCH$_3$, OCH$_2$C**H₂**N); 5.65 (t, 1H, $J_{1',2'}$ = 6.3, H-1′); 6.52 – 6.64 (m, 3H, H-5-xanth, H-*o*-phenylene); 7.12 (d, 1H, $J_{7,8}$ = 9.0, H-7-xanth); 7.28 – 7.34 (m, 2H, H-*m*-phenylene); 7.37 (bs, 1H, CH=); 7.45 (d, 1H, $J_{8,7}$ = 9.0, H-8-xanth); 7.67 (s, 1H, H-6); 7.79 (bs, 1H, H-9-xanth); 7.94 (s, 1H, H-5-triazole).

^{13}C NMR (125.7 MHz, D$_2$O, ref(*t*BuOH) = 30.29 ppm): 12.78 (**C**H$_3$CH$_2$N); 21.44 (CH$_2$-2-xanth); 27.78, 27.85 (CH$_2$-1,3-xanth); 38.80 (CH$_3$N); 40.13 (CH$_2$-2′); 46.60 (CH$_3$**C**H$_2$N); 47.16 (**C**H$_2$NCH$_3$); 50.90 (N**C**H$_2$CH$_2$O); 59.06 (**C**H$_2$C≡C); 65.40 (d, $J_{C,P}$ = 4.4, CH$_2$-5′); 69.37 (N**C**H$_2$CH$_2$O, OCH$_2$CH$_2$O); 69.91, 70.01 (OCH$_2$CH$_2$O); 70.40 (CH-3′); 70.60 (OCH$_2$CH$_2$O); 77.44 (CH$_2$C≡**C**); 86.33 (d, $J_{C,P}$ = 8.0, CH-4′); 87.02 (CH-1′); 91.75 (C-5, CH$_2$**C**≡C); 95.39 (CH-5-xanth); 112.80 (CH-*o*-phenylene); 117.42 (CH-7-xanth); 117.80 (C-8a-xanth); 123.11, 123.56 (C-4,9a-xanth); 124.50 (C-*p*-phenylene); 125.02 (CH-5-triazole); 131.69 (CH-8-xanth); 134.86 (CH-m-phenylene); 139.23 (CH=); 144.65 (CH-6); 144.88 (C-4-triazole); 164.55 (CH-9-xanth); 150.58 (C-*i*-phenylene); 155.74 (C-2, C-6-xanth); 158.34 (C-10a-xanth); 164.25 (C-4a-xanth); 164.87 (C-4).

^{31}P{^{1}H} NMR (202.4 MHz, D$_2$O): -21.49, -10.69, -5.61 (3 x bm).

HRMS (ESI$^-$): calculated for $C_{46}H_{58}O_{17}N_8P_3$: 1087.3138; found 1087.3129.

5.6.2 Biochemistry

5.6.2.1 Primer extension experiments

Preparation of modified DNA bearing one pegNNIR modification by primer extension (DNA19_1C^{pegNNIR}; semi-preparative scale, gel analysis)

The reaction mixture (125 µL) containing primer (for sequence see Table 16; Prim1^{PEX}, 100 µM, 5 µL), template (for sequence see Table 16; Temp1^{PEX}, 100 µM, 5 µL), dGTP (4 mM, 2.5 µL), either dCTP (4 mM, 2.5 µL), or **dC^{pegNIR}TP** (4 mM, 2.5 µL), KOD XL DNA polymerase (2.5 U/µL, 0.6 µL) in corresponding reaction buffer (10×, 12.5 µL) supplied by the manufacturer. The reaction mixture was incubated for 60 min

at 60°C in a thermal cycler. The reaction was stopped by cooling at 4°C. The modified dsDNA was purified using spin columns (QIAquick® Nucleotide Removal Kit, QIAGEN) and eluted by milli-Q water. Prepared DNA was used for fluorescence measurements. To prepare DNA for PAGE analysis (gel is shown in Figure 44 B), the PEX and purification was performed as described above using FAM-labelled primer (for sequence see Table 16; $Temp1^{PEX}$-FAM).

5.6.2.2 Polymerase chain reaction experiments

Enzymatic incorporation of $dC^{pegNNIR}TP$ by polymerase chain reaction

The reaction mixture (20 µL) contained primer (for sequences see Table 16; $Prim1^{PCR}$ and $Prim2^{PCR}$, 10 µM, 4 µL of each), template ($Temp1^{PCR}$, 1 µM, 0.5 µL), natural dNTPs (dATP, dGTP, dTTP, 0.4 mM each, 1.5 µL) and either dCTP (0.4 mM, 1.5 µL), **$dC^{pegNNIR}TP$** (0.4 mM, 1.5 µL) or mixture of **$dC^{pegNNIR}TP$** with natural dCTP (0-95%), KOD XL DNA polymerase (2.5 U/µL, 1 µL) and corresponding reaction buffer (10×, 2 µL) supplied by the manufacturer. After the initial denaturation for 3 min at 94°C, 30 PCR cycles were run under the following conditions: denaturation for 1 min at 94°C, annealing for 1 min at 55°C, extension for 1 min at 72°C. The PCR process was terminated with a final extension step for 5 min at 72°C. The reaction was stopped by cooling to 4°C. The PCR products were analyzed by agarose gel electrophoresis in 2% agarose gel stained with GelRed™ (Biotium, agarose gels are shown in Figure 46).

Real-time PCR using $dC^{pegNNIR}TP$

The reaction mixture (20 µL) contained primer (for sequences see Table 16; $Prim5^{PCR}$ and $Prim6^{PCR}$, 10 µM, 0.8 µL of each), $Temp3^{PCR}$ (cDNA provided by virology department at the IOCB Prague, unknown concentration, 1 µL), natural dNTPs (dATP, dGTP, dTTP, 0.4 mM, 1.5 µL), mixture of dCTP:**$dC^{pegNNIR}TP$** 95:5 (dTTP, 0.4 mM, 1.43 µL; **$dC^{pegNNIR}TP$**, 0.04 mM, 0.75 µL), KOD XL DNA polymerase (2.5 U/µL,

0.5 µL) and corresponding reaction buffer (10x, 2 µL). After the initial denaturation for 3 min at 94°C, 40 PCR cycles were run under the following conditions: denaturation for 20 sec at 94°C, annealing/extension for 10 sec at 64°C. Samples were excited at 672-684 nm and emission was detected 705-730 nm (as Quasar 705, dye predefined in machine).

5.7 2'-Deoxycytidine and its triphosphate modified by thiazole orange fluorophore. Synthesis, photophysical properties, enzymatic incorporation into DNA and applications

5.7.1 Chemical synthesis

Thiazole orange modified deoxycytidine (dC^{TO})

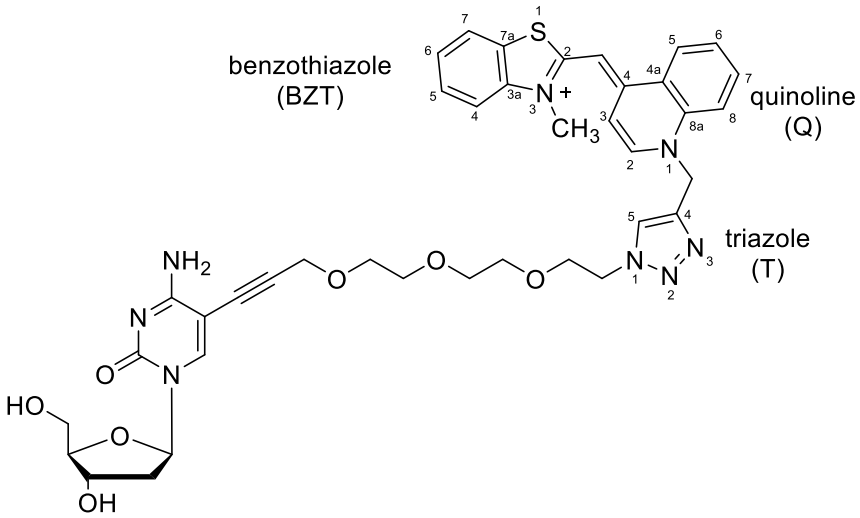

Alkyne **51** (42.6 mg, 0.0936 mmol), **dC^{PegN3}** (34.2 mg, 0.078 mmol) and $Cu(CH_3CN)_4PF_6$ (43.6 mg, 0.117 mmol) were weighted into reaction flask, evacuated and purged with argon 3 times. Then the content of the reaction flask was dissolved with 1.5 mL of DMSO:H_2O (3:1) solution and the reaction was stirred at room temperature under argon atmosphere for 75 min. The reaction mixture was then freeze-dried from water and subsequently purified by silica column chromatography eluted with methanol in dichloromethane (0-10%). Product was isolated as orange solid (26 mg, 43%).

^{1}H NMR (500 MHz, DMSO-d_6): 1.97 (ddd, 1H, J_{gem} = 13.1, $J_{2'b,1'}$ = 7.1, $J_{2'b,3'}$ = 6.1, H-2′b); 2.14 (ddd, 1H, J_{gem} = 13.2, $J_{2'a,1'}$ = 6.0, $J_{2'a,3'}$ = 3.6, H-2′a); 3.41 – 3.44, 3.45 – 3.49 (2 × m, 6H, OCH_2CH_2O); 3.51 – 3.56 (m, 3H, H-5′b, OCH_2CH_2O); 3.60 (bddd, 1H, J_{gem} = 11.8, $J_{5'a,OH}$ = 5.0, $J_{5'a,4'}$ = 3.6, H-5′a); 3.76 – 3.80 (m, 3H, H-4′, O**H_2**CH_2N); 4.04 (s, 3H, CH_3N); 4.19 (m, 1H, H-3′); 4.33 (s, 2H, OCH_2-C≡C); 4.45 – 4.55 (m, 2H,

NC**H₂**CH_2O); 5.08 (bt, 1H, $J_{OH,5'}$ = 5.0, OH-5′); 5.21 (bd, 1H, $J_{OH,3'}$ = 3.5, OH-3′); 5.90 (s, 2H, CH_2N); 6.09 (dd, 1H, $J_{1',2'}$ = 7.1, 6.0, H-1′); 6.90 (bs, 1H, NH_a**H**$_b$); 6.94 (s, 1H, CH=C4-Q); 7.42 (d, 1H, $J_{3,2}$ = 7.3, H-3-Q); 7.43 (ddd, 1H, $J_{6,7}$ = 8.0, $J_{6,5}$ = 7.3, $J_{6,4}$ = 0.9, H-6-BZT); 7.63 (ddd, 1H, $J_{5,8}$ = 8.5, $J_{5,6}$ = 7.3, $J_{5,7}$ = 1.2, H-5-BZT); 7.71 (ddd, 1H, $J_{6,5}$ = 8.3, $J_{6,7}$ = 7.0, $J_{6,8}$ = 1.1, H-6-Q); 7.74 (bs, 1H, N**H**$_a$H$_b$); 7.81 (ddd, 1H, $J_{4,5}$ = 7.9, $J_{4,6}$ = 0.9, $J_{4,7}$ = 0.6, H-4-BZT); 7.93 (ddd, 1H, $J_{7,8}$ = 8.7, $J_{7,6}$ = 7.0, $J_{7,5}$ = 1.3, H-7-Q); 8.07 (dd, 1H, $J_{7,6}$ = 8.0, $J_{7,5}$ = 1.2, H-7-BZT); 8.18 (s, 1H, H-6); 8.20 (dd, 1H, $J_{8,7}$ = 8.7, $J_{8,6}$ = 1.1, H-8-Q); 8.28 (s, 1H, H-5-T); 8.76 (dd, 1H, $J_{5,6}$ = 8.9, $J_{5,7}$ = 1.3, H-5-Q); 8.77 (d, 1H, $J_{2,3}$ = 7.3, H-2-Q).

^{13}C NMR (125.7 MHz, DMSO): 34.15 (CH_3N); 41.02 (CH_2-2′); 49.18 (CH_2N); 49.80 (N**C**H_2CH_2O); 58.65 (C≡C-**C**H_2O); 61.15 (CH_2-5′); 68.78, 68.83, 69.71, 69.73, 69.78 (O**C**H_2CH_2N, O**C**H_2**C**H_2O); 70.24 (CH-3′); 78.00 (**C**≡C-CH_2O); 85.62 (CH-1′); 87.67 (CH-4′); 88.81 (**C**H=C4-Q); 89.20 (C-5); 91.65 (C≡**C**-CH_2O); 108.02 (CH-3-Q); 113.43 (CH-4-BZT); 118.52 (CH-8-Q); 123.13 (CH-7-BZT); 124.25 (C-4a-Q); 124.35 (C-7a-BZT); 124.72 (CH-5-T); 124.93 (CH-6-BZT); 125.92 (CH-5-Q); 126.95 (CH-6-Q); 128.46 (CH-5-BZT); 133.28 (CH-7-Q); 137.25 (C-8a-Q); 140.67 (C-3a-BZT); 141.14 (C-4-T); 144.74 (CH-2-Q); 145.06 (CH-6); 148.86 (C-4-Q); 153.55 (C-2); 160.83 (C-2-BZT); 164.46 (C-4).

HRMS (ESI^+): calculated for $C_{39}H_{43}O_7N_8S$: 767.2970; found 767.2968.

Thiazole orange modified deoxycytidine-5′-*O*-triphosphate (dC^{TO}TP)

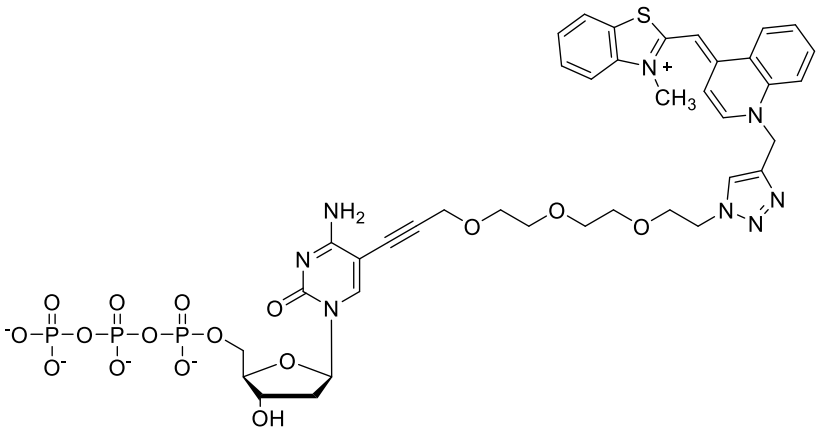

Alkyne **51** (12.1 mg, 0.0266 mmol) in schlenk flask was evacuated and purged with argon 3 times, then 254 μL of degassed DMSO was added under flow of argon and the mixture was stirred. Then solution of **dC^{Peg3N3}TP** (14.9 mg, 0.0137 mmol) in water (127 μL) was added and stirred for 2 minutes. Freshly prepared solution of $Cu(CH_3CN)_4PF_6$ (7.67 mg, 0.0206 mmol) in degassed DMSO (127 μL) was added and the reaction mixture continued to stir at room temperature under argon. After 2.5 hours the reaction mixture was freeze-dried from water. Then the lyophilized reaction mixture was dissolved in 40 mL H_2O and washed with 40 mL dichloromethane and 40 mL ethyl acetate respectively. Water phase (red solution) was lyophilized, then redissolved with 5 mL H_2O and filtered using ultra filtration (Millipore, Ultrafiltration Discs, 1 kDa), and washed with additional 60 mL H_2O. Retentate was dissolved with water, lyophilized, filtered through dowex (Dowex 50WX8 in Na^+ cycle). Final freeze-drying from water afforded the final nucleotide **dC^{TO}TP** as orange solid (2.26 mg, 15%).

Due to the nature of the compound, it was difficult to assign the peaks due to the substantial broadening of the peaks. The compound contains both positive and negative charge and therefore it might self-aggregate or form some kind of particles that interfere with the measurement. Use of MeOD, mixtures of MeOD with D_2O or using triethylammonium salt of the triphosphate, did not solve this issue.

^{1}H NMR (500.0 MHz, D_2O, ref(*t*BuOH ext) = 1.24 ppm): 1.77 (bm, 1H); 2.02 (bm, 1H); 3.03 (bm, 5H); 3.25 (bm, 3H); 3.43-3.57 (bm, 8H); 3.79 (bm, 6H); 3.83 (bm, 3H); 4.00 (bm, 1H); 5.36-5.49 (bm, 3H); 6.90-7.11 (bm, 4H); 7.49 (bm, 3H); 7.64 (bm, 2H); 8.20 (bm, 3H).

^{13}C NMR (125.7 MHz, D_2O, ref(*t*BuOH) = 30.29 ppm): 33.23; 39.24; 48.71; 50.31; 58.20; 85.28; 87.98; 107.80; 112.13; 117.22; 122.07; 123.52; 123.90; 124.57; 126.96; 127.98; 133.04; 136.15; 139.10; 142.98; 147.24; 159.95.

^{31}P{^{1}H} NMR (202.4 MHz, D_2O): -21.82, -10.64, -6.81 (3 × bm).

HRMS (ESI$^-$): calculated for $C_{39}H_{44}O_{16}N_8P_3S$: 1005.1814; found 1005.1807.

5.7.2 Biochemistry

5.7.2.1 Primer extension experiments

Enzymatic synthesis of modified DNA (adjacent GC pairs) bearing one thiazole orange modification by primer extension (gel analysis)

The reaction mixture (20 µl) contained Cy5 labelled primer Prim1^{PEX}–Cy5 (for sequence see Table 16; 3 µM, 1 µL), template Temp1^{PEX} (for sequence see Table 16; 3 µM, 1.5 µL) KOD XL DNA polymerase (0.25 U/µL, 0.3 µL), dGTP (4 mM, 0.6 µL), either dCTP (4 mM, 0.3 µL) or modified dNTP (**dC^{TO}TP**, 4 mM, 0.3 µL) in corresponding reaction buffer (10x, 2 µL) supplied by the manufacturer. The reaction mixture was incubated at 60°C for 60 min in thermal cycler. The reaction was stopped by the addition of PAGE stop solution (20 µL) and the reaction mixture was denatured at 95°C for 5 min and analyzed using 12.5% denaturing PAGE. Visualization was performed on Typhoon biological imager FLA 9500 (PAGE gel is shown in Figure 53 C).

Preparation of modified dsDNA (adjacent GC pairs) bearing one thiazole orange modification by primer extension (DNA19_GC_1C^{TO}; semi-preparative scale)

The reaction mixture (100 µL) containing primer (for sequence see Table 16; Prim1^{PEX}, 100 µM, 5 µL), template (for sequence see Table 16; Temp1^{PEX}, 100 µM, 5 µL), dGTP (4 mM, 1 µL), **dC^{TO}TP** (4 mM, 1 uL), KOD XL DNA polymerase (2.5 U/µL, 0.6 µL) in corresponding reaction buffer (10×, 10 µL) supplied by the manufacturer. The reaction mixture was incubated for 60 min at 60°C in a thermal cycler. The reaction was stopped by cooling at 4°C. The modified dsDNA was purified using spin columns (QIAquick® Nucleotide Removal Kit, QIAGEN) and eluted by milli-Q water. Prepared dsDNA was used for fluorescence measurements.

Preparation of modified ssDNA (adjacent GC pairs) bearing one thiazole orange modification using lambda exonuclease digestion (ON19_GC_1C^{TO})

The reaction mixture (75.6 µL) containing modified dsDNA (prepared using Temp1^{PEX}-P as described above; 0.48 nmol), lambda exonuclease buffer 10x (5 uL) and lambda exonuclease enzyme (10 U/µL, 2 µL) was incubated for 90 min at 37°C in a thermal cycler. The reaction was stopped by cooling at 4°C. The modified ssDNA was purified using spin columns (QIAquick® Nucleotide Removal Kit, QIAGEN) and eluted by milli-Q water. Prepared ssDNA was used for fluorescence measurements.

Preparation of modified dsDNA (adjacent AT pairs) bearing one thiazole orange modification by primer extension (DNA19_AT_1C^{TO}; semi-preparative scale, gel analysis)

The reaction mixture (100 µL) containing primer (for sequence see Table 16; Prim1^{PEX}, 100 µM, 5 µL), template (for sequence see Table 16; Temp7^{PEX}-2P, 100 µM, 5 µL), dATP (4 mM, 1 µL), either dCTP (4 mM, 1 uL) or **dC^{TO}TP** (4 mM, 1 uL), KOD XL DNA polymerase (2.5 U/µL, 0.6 µL) in corresponding reaction buffer (10×, 10 µL)

supplied by the manufacturer. The reaction mixture was incubated for 45 min at 60°C in a thermal cycler. The reaction was stopped by cooling at 4°C. The modified dsDNA was purified using spin columns (QIAquick® Nucleotide Removal Kit, QIAGEN) and eluted by milli-Q water. Prepared dsDNA was used for fluorescence measurements. To prepare DNA for PAGE analysis, the PEX and purification was performed as described above using Cy5 labelled primer (for sequence see Table 16; $Prim1^{PEX}$-Cy5). PAGE gel is shown in Figure 53 B.

Preparation of modified ssDNA (adjacent AT pairs) bearing one thiazole orange modification using lambda exonuclease digestion (ON19_AT_1C^{TO})

The reaction mixture (50 µL) containing modified dsDNA (prepared using $Temp7^{PEX}$-2P as described above; 0.1 nmol), lambda exonuclease buffer 10x (5 uL) and lambda exonuclease enzyme (10 U/µL, 2 µL) was incubated for 90 min at 37°C in a thermal cycler. The reaction was stopped by cooling at 4°C. The modified ssDNA was purified using spin columns (QIAquick® Nucleotide Removal Kit, QIAGEN) and eluted by milli-Q water. Prepared ssDNA was used for fluorescence measurements.

5.7.2.2 Polymerase chain reaction experiments

Enzymatic incorporation of dC^{TO}TP by polymerase chain reaction

The reaction mixture (20 µL) contained primer (for sequences see Table 16; $Prim1^{PCR}$ and $Prim2^{PCR}$, 10 µM, 1 µL of each), template ($Temp1^{PCR}$, 1 nM, 0.5 µL), natural dNTPs (dATP, dGTP, dTTP, 0.4 mM each, 1.5 µL) and either dCTP (0.4 mM, 1.5 uL), **dC^{TO}TP** (0.4 mM, 1.5 uL) or mixture of **dC^{TO}TP** with natural dCTP (0-95%), KOD XL DNA polymerase (2.5 U/µL, 0.5 µL) and corresponding reaction buffer (10×, 2 µL) supplied by the manufacturer. After the initial denaturation for 3 min at 94°C, 30 PCR cycles were run under the following conditions: denaturation for 20 sec. at 94°C, annealing for 30 sec. at 58°C, extension for 30 sec. at 72°C. The reaction was

stopped by cooling to 4°C. The PCR products were analyzed by agarose gel electrophoresis in 2% agarose gel stained with GelRed™ (Biotium, agarose gel is shown in Figure 53 D). Samples were excited after each cycle at 672-684 nm and emission was detected 705-730 nm (as Quasar 705, dye predefined in machine). Figure 54 shows fluorescence signals observed during PCR.

5.7.3 Absorption measurements

UV melting temperatures of DNA19_GC_1C, DNA19_GC_1C^{TO}, DNA19_AT_1C, DNA19_AT_1C^{TO}

All solutions of DNA were prepared in PBS buffer (1 mL). Melting curve analysis was performed by a slow increase of temperature from 10°C to 90°C with a speed of 1°C per minute. Then samples were cooled to 10°C with a speed of 1°C per minute. The process of denaturation and annealing was repeated three times. Figure 57 shows UV melting curves and normalized derivatives.

5.8 2'-Deoxycytidines and their triphosphates bearing dimethoxy-, diphenyl-BODIPY fluorophore. Synthesis, photophysical properties, enzymatic incorporation into DNA and applications

5.8.1 Chemical synthesis

(Z)-4-((4-methoxy-5-phenyl-1H-pyrrol-2-yl)(4-methoxy-5-phenyl-2H-pyrrol-2-ylidene)methyl)phenol (59)

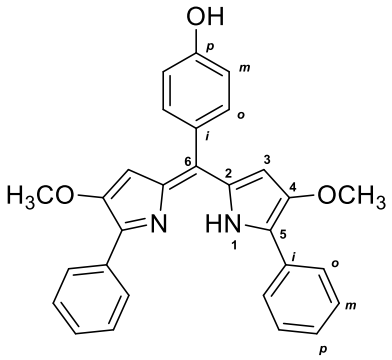

To a solution of 3-methoxypyrrole **57** (200 mg, 1.154 mmol) in DCM (6 mL) was added mixture of 4-hydroxybenzaldehyde (70 mg, 0.577 mmol, dissolved in 6 mL DCM) and TFA (2 drops). After stirring at room temperature for 1 hour, p-chloranil (156 mg, 0.635 mmol) was added and stirred at r.t. After 1 h the reaction mixture was filtered and concentrated on rotavap. Purification of the crude product by column chromatography eluted with ethyl acetate in dichloromethane (0-10%) provided product **59** (171 mg, 66%) as purple solid.

^{1}H NMR (500.0 MHz, DMSO-d_6): 3.79 (s, 6H, CH_3O); 6.04 (s, 2H, H-3); 6.90 – 6.95 (m, 2H, H-*m*-C_6H_4OH); 7.35 – 7.42 (m, 4H, H-*o*-C_6H_4OH, H-*p*-Ph); 7.51 – 7.56 (m, 4H, H-*m*-Ph); 7.98 – 8.02 (m, 4H, H-*o*-Ph); 9.91 (bs, 1H, OH); 13.33 (bs, 1H, NH).

^{13}C NMR (125.7 MHz, DMSO-d_6): 58.40 (CH_3O); 105.92 (CH-3); 115.23 (CH-*m*-C_6H_4OH); 126.16 (CH-*o*-Ph); 127.35 (C-*i*-C_6H_4OH); 128.47 (CH-*p*-Ph); 129.24 (CH-*m*-Ph); 132.14 (C-*i*-Ph); 132.35 (CH-*o*-C_6H_4OH); 135.83 (C-6); 137.51 (C-2); 140.19 (C-5); 153.55 (C-4); 158.55 (C-*p*-C_6H_4OH).

HRMS (ESI$^+$): calculated for $C_{29}H_{25}O_3N_2$: 449.1860; found 449.1857.

4-(5,5-difluoro-2,8-dimethoxy-3,7-diphenyl-5H-4l4,5l4-dipyrrolo[1,2-c:2',1'-f][1,3,2]diazaborinin-10-yl)phenol (60)

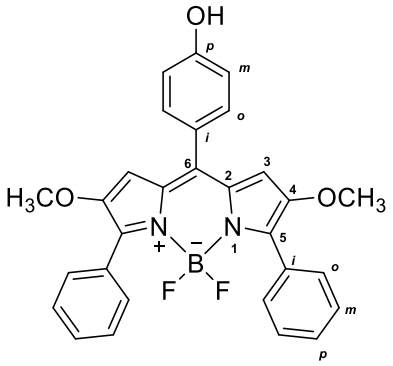

Solution of dipyrrin **59** (1061 mg, 2.366 mmol) in toluene (76) was heated to 70°C and then triethylamine (4.9 mL, 35.226 mmol) was added dropwise. After stirring at 70°C for 30 min $BF_3.Et_2O$ (8.75 mL, 70,909 mmol) was added dropwise and the mixture was heated to 110°C (reflux). After 1 hour all the starting material was consumed and the reaction mixture was cooled down to room temperature. Then the reaction was quenched with cold 1M aqueous solution of NaOH (10 mL/mmol), organic phase was separated and aqueous phase was acidified by 1 M HCl to pH 5-6 and then extracted with ethyl acetate. The combined organic phases were dried with anh. Na_2SO_4, filtered and concentrated on rotavap. Purification of the crude product by column chromatography eluted with ethyl acetate in dichloromethane (0-10%) provided product **60** (826 mg, 70%) as black solid.

^{1}H NMR (500.0 MHz, DMSO-d_6): 3.72 (s, 6H, CH_3O); 6.43 (s, 2H, H-3); 6.99 – 7.02 (m, 2H, H-*m*-C_6H_4OH); 7.36 – 7.43 (m, 6H, H-*m,p*-Ph); 7.52 – 7.56 (m, 2H, H-*o*-C_6H_4OH); 7.58 – 7.62 (m, 4H, H-*o*-Ph); 10.20 (bs, 1H, OH).

^{13}C NMR (125.7 MHz, DMSO-d_6): 58.35 (CH_3O); 108.20 (CH-3); 115.81 (CH-*m*-C_6H_4OH); 124.70 (C-*i*-C_6H_4OH); 127.95 (CH-*m*-Ph); 129.19 (CH-*p*-Ph); 129.91 (C-*i*-

Ph); 130.20 (t, $J_{C,F}$ = 2.8, CH-*o*-Ph); 131.10 (C-2); 132.69 (CH-*o*-C_6H_4OH); 141.06 (C-6); 144.52 (C-5); 153.02 (b, C-4); 159.95 (C-*p*-C_6H_4OH).

^{19}F NMR (470.4 MHz, DMSO-d_6): -131.02 (4lines, $J_{F,B}$ = 31.6).

^{11}B NMR (160.4 MHz, DMSO-d_6): 037 (t, $J_{B,F}$ = 31.6).

HRMS (ESI^+): calculated for $C_{32}H_{25}O_3N_2BF_2Na$: 557.1830; found 557.1819.

5,5-difluoro-2,8-dimethoxy-3,7-diphenyl-10-(4-(prop-2-yn-1-yloxy)phenyl)-5H-4l4,5l4-dipyrrolo[1,2-c:2',1'-f][1,3,2]diazaborinine (61a)

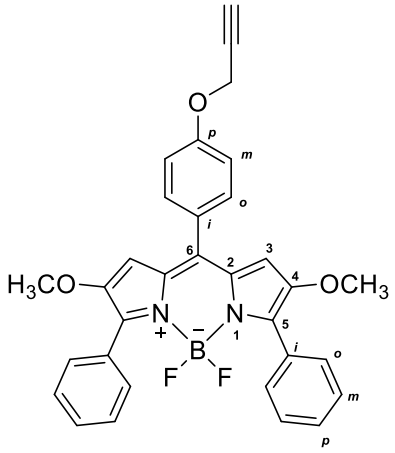

Propargyl bromide (80% w/w solution in toluene, 2.253 mmol, 0.25 mL) was added to pressure tube containing bodipy **60** (616 mg, 1.241 mmol), K_2CO_3 (523.7 mg, 3.961 mmol) and acetonitrile (25 mL, HPLC-grade). The reaction mixture was stirred at 60°C for 2 h. After cooling down to room temperature the reaction mixture was filtered, concentrated on rotavap, redissolved with ethyl acetate and washed with water. Organic phase was dried over anhydrous Na_2SO_4, filtered and concentrated on rotavap to give product **61a** (590 mg, 89%) as black solid.

^1H NMR (500.0 MHz, DMSO-d_6): 3.71 (t, 1H, ^4J = 2.4, HC≡C); 3.72 (s, 6H, CH_3O); 4.96 (d, 2H, ^4J = 2.4, CH_2O); 6.39 (s, 2H, H-3); 7.21 – 7.25 (m, 2H, H-*m*-C_6H_4O); 7.37 – 7.44 (m, 6H, H-*m,p*-Ph); 7.59 – 7.62 (m, 4H, H-*o*-Ph); 7.65 – 7.69 (m, 2H, H-*o*-

C_6H_4O).

^{13}C NMR (125.7 MHz, DMSO-d_6): 55.87 (CH_2O); 58.38 (CH_3O); 79.01 (H**C**≡C); 79.28 (HC≡**C**); 108.03 (CH-3); 115.12 (CH-*m*-C_6H_4O); 126.93 (C-*i*-C_6H_4O); 127.98 (CH-*m*-Ph); 129.29 (CH-*p*-Ph); 129.82 (C-*i*-Ph); 130.20 (CH-*o*-Ph); 131.20 (C-2); 132.39 (CH-*o*-C_6H_4O); 140.22 (C-6); 145.01 (C-5); 153.14 (C-4); 159.15 (C-*p*-C_6H_4O).

^{19}F NMR (470.4 MHz, DMSO-d_6): -127.29 (4lines, $J_{F,B}$ = 31.6).

^{11}B NMR (160.4 MHz, DMSO-d_6): 0.58 (t, $J_{B,F}$ = 31.6).

HRMS (ESI^+): calculated for $C_{32}H_{25}O_3N_2BF_2Na$: 557.1830; found 557.1819.

5,5-difluoro-2,8-dimethoxy-3,7-diphenyl-10-(4-(2-(2-(2-(prop-2-yn-1-yloxy)ethoxy)ethoxy)ethoxy)phenyl)-5H-4l4,5l4-dipyrrolo[1,2-c:2',1'-f][1,3,2]diazaborinine (61b)

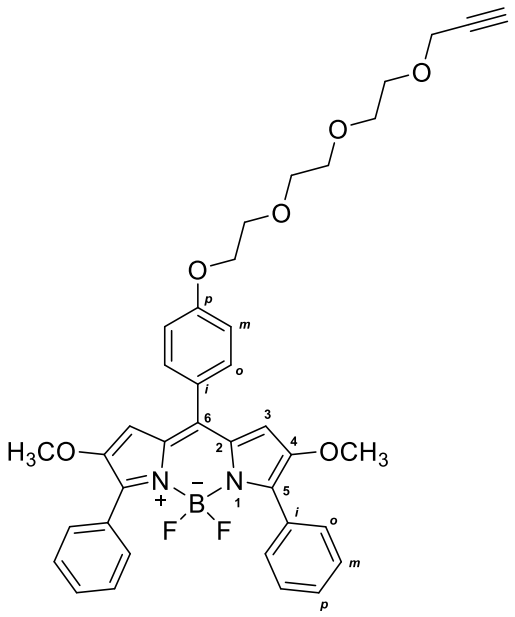

Bodipy **60** (104 mg, 0.209 mmol) and K_2CO_3 (99 mg, 0.716 mmol) were stirred in acetonitrile (5.4 mL, HPLC-grade) for 5 min at room temperature. Then tosylate **46** (99

mg, 0.291 mmol) was added and the reaction mixture was heated to 70°C and stirred for 14 hours. After cooling down to room temperature the reaction mixture concentrated on rotavap, redissolved with ethyl acetate and washed with water and saturated solution of NaCl. Organic phase was dried over anhydrous Na_2SO_4, filtered and concentrated on rotavap. Purification of the crude product by column chromatography eluted with increasing gradient of cyclohexane/ethyl acetate (4:1 to 1:1) provided product **61b** (97.7 mg, 70%) as sticky black solid.

^{1}H NMR (500.0 MHz, DMSO-d_6): 3.44 (t, 1H, ^4J = 2.4, HC≡C); 3.55 – 3.60, 3.61 – 3.65 (2 × m, 8H, OCH_2CH_2O); 3.72 (s, 6H, CH_3O); 3.80 – 3.84 (m, 2H, phenylene-$OCH_2C\mathbf{H_2}O$); 4.15 (d, 2H, ^4J = 2.4, $C\mathbf{H_2}C{\equiv}CH$); 4.22 – 4.26 (m, 2H, phenylene-$OC\mathbf{H_2}CH_2O$); 6.40 (s, 2H, H-3); 7.17 – 7.22 (m, 2H, H-*m*-phenylene); 7.36 – 7.44 (m, 6H, H-*m,p*-Ph); 7.58 – 7.66 (m, 6H, H-*o*-phenylene, H-*o*-Ph).

^{13}C NMR (125.7 MHz, DMSO-d_6): 57.69 ($O\mathbf{C}H_2C{\equiv}CH$); 58.35 ($CH_3O$); 67.62 (phenylene-$O\mathbf{C}H_2CH_2O$); 68.71 ($OCH_2CH_2O$); 69.05 (phenylene-$OCH_2\mathbf{C}H_2O$); 69.74, 70.01, 70.11 ($OCH_2CH_2O$); 77.34 ($H\mathbf{C}{\equiv}C$); 80.54 ($HC{\equiv}\mathbf{C}$); 108.73 (CH-3); 114.84 (CH-*m*-phenylene); 126.28 (C-*i*-phenylene); 127.93 (CH-*m*-Ph); 129.23 (CH-*p*-Ph); 129.82 (C-*i*-Ph); 130.16 (t, $J_{C,F}$ = 3.1, CH-*o*-Ph); 131.18 (C-2); 132.38 (CH-*o*-phenylene); 140.42 (C-6); 144.88 (C-5); 153.11 (C-4); 160.40 (C-*p*-phenylene).

^{19}F NMR (470.4 MHz, DMSO-d_6): -131.05 (4lines, $J_{F,B}$ = 31.6).

^{11}B NMR (160.4 MHz, DMSO-d_6): 0.37 (t, $J_{B,F}$ = 31.6).

HRMS (ESI^+): calculated for $C_{38}H_{37}O_6N_2BF_2Na$: 689.26049; found 689.26083.

Dimethoxy-BODIPY modified deoxycytidine (dC^{MOB}, 62a)

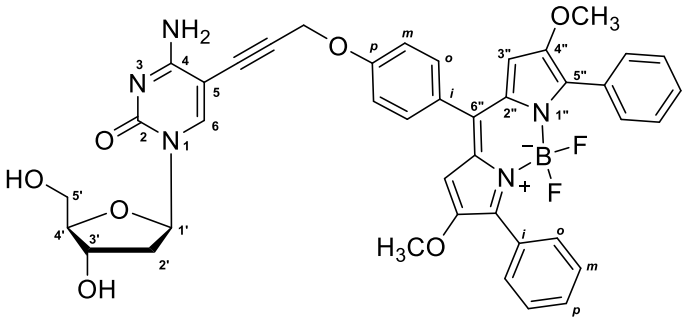

A flask containing 5-iodo-2'-deoxycytidine (50 mg, 0.142 mmol), alkyne **61a** (90 mg, 0.168 mmol), $PdCl_2(PPh_3)_2$ (6 mg, 6% mol), CuI (1.8 mg, 6.6% mol) was purged and refilled with argon multiple times and the content was dissolved in dry DMF (3 mL). Triethylamine (0.3 mL, 2.15 mmol) was added and the mixture was stirred at 70°C for 2 hours. Then the reaction mixture was concentrated on rotavap and purified by column chromatography eluted with methanol in dichloromethane (0-20 %) to give the nucleoside **62a** as black solid (90 mg, 84%).

^{1}H NMR (500.0 MHz, DMSO-d_6): 1.99 (ddd, 1H J_{gem} = 13.2, $J_{2'b,1'}$ = 7.0, $J_{2'b,3'}$ = 6.0, H-2′b); 2.16 (ddd, 1H J_{gem} = 13.2, $J_{2'a,1'}$ = 6.0, $J_{2'a,3'}$ = 3.7, H-2′a); 3.55, 3.62 (2 × ddd, 2 × 1H, J_{gem} = 11.9, $J_{5',OH}$ = 5.1, $J_{5',4'}$ = 3.5, H-5′); 3.71 (s, 6H, CH_3O); 3.80 (q, 1H, $J_{4',3'}$ = $J_{4',5'}$ = 3.5, H-4′); 4.20 (m, 1H, H-3′); 5.13 – 5.17 (m, 3H, CH_2O, OH-5′); 5.27 (d, 1H, $J_{OH,3'}$ = 4.3, OH-3′); 6.09 (dd, 1H, $J_{1',2'}$ = 7.0, 6.0, H-1′); 6.39 (s, 2H, H-3″); 7.09 (bs, 1H, $NH_a\mathbf{H_b}$); 7.30 – 7.34 (m, 2H, H-*m*-phenylene); 7.36 – 7.44 (m, 6H, H-*m,p*-Ph); 7.58 – 7.62 (m, 4H, H-*o*-Ph); 7.65 – 7.69 (m, 2H, H-*o*-phenylene); 7.83 (bs, 1H, $N\mathbf{H_a}H_b$); 8.29 (s, 1H, H-6).

^{13}C NMR (125.7 MHz, DMSO-d_6): 41.19 (CH_2-2′); 57.00 (CH_2O); 58.47 (CH_3O); 61.17 (CH_2-5′); 70.26 (CH-3′); 79.65 ($CH_2C{\equiv}\mathbf{C}$); 85.81 (CH-1′); 87.77 (CH-4′); 89.00 (C-5); 90.50 ($CH_2\mathbf{C}{\equiv}C$); 108.11 (CH-3″); 115.32 (CH-*m*-phenylene); 126.92 (C-*i*-phenylene); 128.08 (CH-*m*-Ph); 129.41 (CH-*p*-Ph); 129.89 (C-*i*-Ph); 130.28 (t, $J_{C,F}$ = 2.8, CH-*o*-Ph); 131.27 (C-2″); 132.52 (CH-*o*-phenylene); 140.34 (C-6″); 145.08 (C-5″); 145.75 (CH-6); 153.24 (b, C-4″); 153.70 (C-2); 159.43 (C-*p*-phenylene); 164.71

(C-4).

^{19}F NMR (470.4 MHz, DMSO-d_6): -126.93 ("q", $J_{F,B}$ = 31.5).

^{11}B NMR (160.4 MHz, DMSO-d_6): 0.57 (t, $J_{B,F}$ = 31.5).

HRMS (ESI$^+$): calculated for $C_{41}H_{36}O_7N_5BF_2Na$: 782.25681; found 782.25751.

Triethylene glycol dimethoxy-BODIPY modified deoxycytidine (dC^{pegMOB}, 62b)

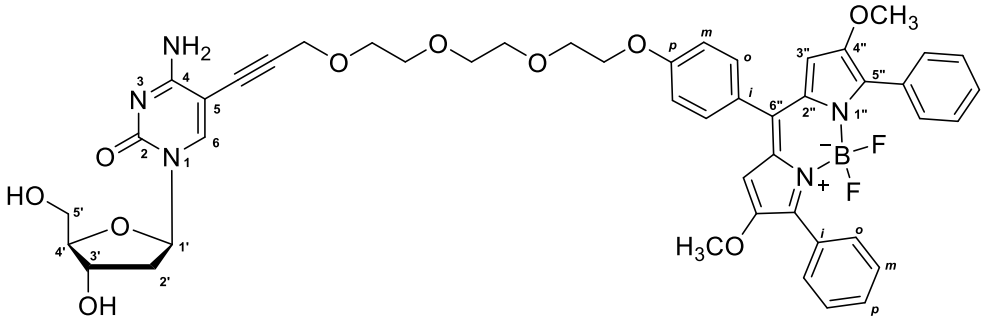

A flask containing 5-iodo-2'-deoxycytidine (18.1 mg, 0.051 mmol), alkyne **61b** (47.5 mg, 0.071 mmol), $PdCl_2(PPh_3)_2$ (2 mg, 5.5% mol), CuI (1.05 mg, 10.8% mol) was purged and refilled with argon multiple times and the content was dissolved in dry DMF (1.25 mL). Triethylamine (0.1 mL, 0.716 mmol) was added and the mixture was stirred at 60°C for 1 hour. Then the reaction mixture was concentrated on rotavap and purified by column chromatography eluted with methanol in dichloromethane (0-10 %) to give the nucleoside **62b** as black solid (35 mg, 77%).

^{1}H NMR (500.0 MHz, DMSO-d_6): 1.99 (ddd, 1H J_{gem} = 13.2, $J_{2'b,1'}$ = 7.0, $J_{2'b,3'}$ = 6.0, H-2′b); 2.14 (ddd, 1H J_{gem} = 13.2, $J_{2'a,1'}$ = 6.0, $J_{2'a,3'}$ = 3.7, H-2′a); 3.52 – 3.65 (m, 10H, H-5′, OCH_2CH_2O); 3.72 (s, 6H, CH_3O); 3.79 (q, 1H, $J_{4',3'}$ = $J_{4',5'}$ = 3.5, H-4′); 3.80 – 3.83 (m, 2H, phenylene-$OCH_2C\mathbf{H_2}O$); 4.20 (m, 1H, H-3′); 4.22 – 4.25 (m, 2H, phenylene-$OCH_2C\mathbf{H_2}O$); 4.38 (s, 2H, $OCH_2C{\equiv}C$); 5.09 (t, 1H, $J_{OH,5'}$ = 5.0, OH-5′); 5.21 (d, 1H, $J_{OH,3'}$ = 4.3, OH-3′); 6.10 (dd, 1H, $J_{1',2'}$ = 7.0, 6.0, H-1′); 6.39 (s, 2H, H-3″); 6.91 (bs, 1H, $NH_a\mathbf{H_b}$); 7.15 – 7.21 (m, 2H, H-*m*-phenylene); 7.36 – 7.45 (m, 6H,

H-*m,p*-Ph); 7.57 – 7.66 (m, 6H, H-*o*-Ph, H-*o*-phenylene); 7.76 (bs, 1H, N**H**$_a$H$_b$); 8.22 (s, 1H, H-6).

^{13}C NMR (125.7 MHz, DMSO-d_6): 41.02 (CH_2-2′); 58.35 (CH_3O); 58.64 (CH_2O); 61.14 (CH_2-5′); 67.60 (phenylene-O**C**H_2CH_2O); 68.84 (OCH_2CH_2O); 69.05 (phenylene-OCH_2**C**H_2O); 69.82, 70.02, 70.10 (OCH_2CH_2O); 70.25 (CH-3′); 78.14 ($CH_2C{\equiv}$**C**); 85.66 (CH-1′); 87.66 (CH-4′); 89.64 (C-5); 91.70 (CH_2**C**≡C); 108.03 (CH-3″); 114.82 (CH-*m*-phenylene); 126.28 (C-*i*-phenylene); 127.93 (CH-*m*-Ph); 129.23 (CH-*p*-Ph); 129.82 (C-*i*-Ph); 130.16 (t, $J_{C,F}$ = 2.9, CH-*o*-Ph); 131.18 (C-2″); 132.38 (CH-*o*-phenylene); 140.41 (C-6″); 144.88 (C-5″); 145.05 (CH-6); 153.09 (b, C-4″); 153.53 (C-2); 160.38 (C-*p*-phenylene); 164.56 (C-4).

^{19}F NMR (470.4 MHz, DMSO-d_6): -131.03 (“q“, $J_{F,B}$ = 31.5).

^{11}B NMR (160.4 MHz, DMSO-d_6): 0.59 (t, $J_{B,F}$ = 31.5).

HRMS (ESI$^-$): calculated for $C_{47}H_{47}O_{10}N_5BF_2$: 890.33895; found 890.33825.

Dimethoxy-BODIPY modified deoxycytidine-5′-*O*-triphosphate (dC^{MOB}TP, 63a)

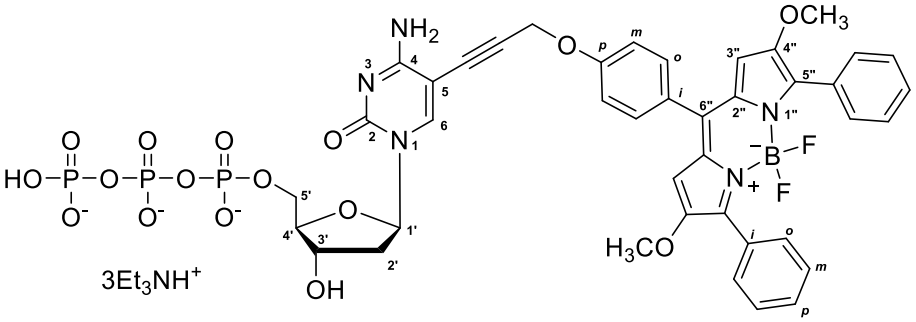

A flask containing 5-iodo-2'-deoxycytidine 5'-triphosphate (Et_3NH^+ form, 19.5 mg, 0.022 mmol), alkyne **61a** (25 mg, 0.046 mmol), $PdCl_2(PPh_3)_2$ (1.5 mg, 9.7% mol), CuI (0.8 mg, 19% mol) was purged and refilled with argon multiple times and the content was dissolved in dry DMF (0.5 mL). Triethylamine (46 µL, 0.33 mmol) was added and the mixture was stirred at 60°C for 1 hour. The reaction mixture was diluted with water

and lyophilized. Then the crude product was purified by HPLC with the use of linear gradient of methanol (5–100%) in 0.1 M TEAB buffer followed by additional purification with the use of linear gradient of methanol (50–100%) in 0.1 M TEAB buffer. Isolated product was co-evaporated with HPLC-grade water several times and freeze-drying from water afforded the final nucleotide **63a** as dark blue solid (9.3 mg, 28%).

^{1}H NMR (500.0 MHz, D_2O+CD_3OD (1:1)): 1.28 (t, 27H, J_{vic} = 7.3, C**H$_3$**CH_2N); 2.21 (ddd, 1H J_{gem} = 13.8, $J_{2'b,1'}$ = 7.0, $J_{2'b,3'}$ = 6.4, H-2′b); 2.37 (ddd, 1H J_{gem} = 13.8, $J_{2'a,1'}$ = 6.2, $J_{2'a,3'}$ = 3.9, H-2′a); 3.17 (q, 18H, J_{vic} = 7.3, CH_3C**H$_2$**N); 3.61 (s, 6H, CH_3O); 4.14 (qd, 1H, $J_{4',3'}$ = $J_{4',5'}$ = 3.9, $J_{H,P}$ = 1.5, H-4′); 4.18 (ddd, 1H, J_{gem} = 11.0, $J_{H,P}$ = 5.3, $J_{5'b,4'}$ = 3.9, H-5′b); 4.25 (ddd, 1H, J_{gem} = 11.0, $J_{H,P}$ = 6.9, $J_{5'a,4'}$ = 3.9, H-5′a); 4.58 (dt, 1H, $J_{3',2'}$ = 6.4, 3.9, $J_{3',4'}$ = 3.9, H-3′); 5.08, 5.12 (2 × d, 2 × 1H, J_{gem} = 16.7, CH_2O); 6.16 (dd, 1H, $J_{1',2'}$ = 7.0, 6.2, H-1′); 6.25 (s, 2H, H-3″); 7.17 – 7.21 (m, 2H, H-*m*-phenylene); 7.33 – 7.40 (m, 6H, H-*m,p*-Ph); 7.44 – 7.47 (m, 2H, H-*o*-phenylene); 7.54 – 7.58 (m, 4H, H-*o*-Ph); 8.16 (s, 1H, H-6).

^{13}C NMR (125.7 MHz, D_2O+CD_3OD (1:1)): 9.19 (**C**H_3CH_2N); 40.63 (CH_2-2′); 57.68 (CH_2O); 58.83 (CH_3O); 66.25 (d, $J_{C,P}$ = 5.4, CH_2-5′); 71.44 (CH-3′); 78.96 (CH_2C≡**C**); 86.97 (d, $J_{C,P}$ = 8.8, CH-4′); 87.55 (CH-1′); 91.58 (CH_2**C**≡C); 92.24 (C-5); 108.73 (CH-3″); 116.02 (CH-*m*-phenylene); 128.36 (C-*i*-phenylene); 128.79 (CH-*m*-Ph); 130.34 (CH-*p*-Ph); 130.68 (C-*i*-Ph); 131.00 (t, $J_{C,F}$ = 2.8, CH-*o*-Ph); 132.53 (C-2″); 133.21 (CH-*o*-phenylene); 141.35 (C-6″); 146.51 (CH-6); 146.61 (C-5″); 154.13 (b, C-4″); 156.55 (C-2); 160.14 (C-*p*-phenylene); 165.93 (C-4).

^{31}P NMR (202.4 MHz, D_2O+CD_3OD (1:1)): -22.33 (t, J = 20.5, P□); -10.55 (d, J = 20.6, P□); -9.26 (bd, J = 20.6, P□).

^{19}F NMR (470.4 MHz, D_2O+CD_3OD (1:1)): -129.24 (“q“, $J_{F,B}$ = 31.0).

^{11}B NMR (160.4 MHz, D_2O+CD_3OD (1:1)): 0.63 (t, $J_{B,F}$ = 31.0).

HRMS (ESI^-): calculated for $C_{41}H_{38}O_{16}N_5BF_2P_3$: 998.15930; found 998.15878.

Triethylene glycol dimethoxy-BODIPY modified deoxycytidine-5′-*O*-triphosphate (dC^{pegMOB}TP, 63b)

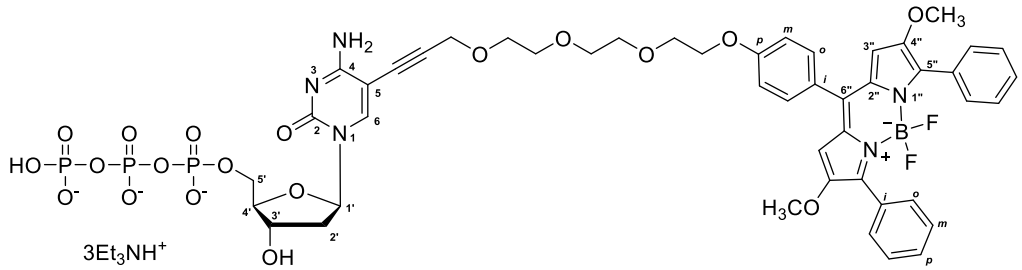

A flask containing 5-iodo-2'-deoxycytidine 5'-triphosphate (Et_3NH^+ form, 20 mg, 0.023 mmol), alkyne **61b** (25 mg, 0.038 mmol), $PdCl_2(PPh_3)_2$ (1.5 mg, 9.2% mol), CuI (1.4 mg, 32% mol) was purged and refilled with argon multiple times and the content was dissolved in dry DMF (0.8 mL). Triethylamine (65 µL, 0.466 mmol) was added and the mixture was stirred at 60°C for 1 hour. The reaction mixture was diluted with water and lyophilized. Then the crude product was purified by HPLC with the use of linear gradient of methanol (5–100%) in 0.1 M TEAB buffer followed by additional purification with the use of linear gradient of methanol (50–100%) in 0.1 M TEAB buffer. Isolated product was co-evaporated with HPLC-grade water several times and freeze-drying from water afforded the final nucleotide **63b** as dark blue solid (13.68 mg, 28%).

^{1}H NMR (600.1 MHz, CD_3OD): 1.21 – 1.38 (bm, 27H, C**H**$_3$CH$_2$N); 2.16 (bm, 1H, H-2′b); 2.36 (bm, 1H, H-2′a); 3.08 – 3.25 (bm, 18H, CH$_3$C**H**$_2$N); 3.64 – 3.80 (m, 16H, H-5′, OCH$_2$CH$_2$O, CH$_3$O); 3.86 – 3.95 (bm, 2H, phenylene-OCH$_2$C**H**$_2$O); 4.09 (bm, 1H, H-4′); 4.20 – 4.28 (bm, 2H, phenylene-OCH$_2$C**H**$_2$O); 4.47 (bs, 2H, OCH$_2$C≡C); 4.56 (bm, 1H, H-3′); 6.21 (bm, 1H, H-1′); 6.32 (bs, 2H, H-3″); 7.12 – 7.18 (m, 2H, H-*m*-phenylene); 7.32 – 7.49 (m, 6H, H-*m,p*-Ph); 7.54 – 7.58 (m, 2H, H-*o*-phenylene); 7.76 – 7.72 (m, 4H, H-*o*-Ph); 8.16 (bs, 1H, H-6).

^{13}C NMR (150.9 MHz, CD_3OD): 9.09 (**C**H$_3$CH$_2$N); 41.42 (CH$_2$-2′); 47.34 (**C**H$_3$CH$_2$N); 58.67 (CH$_3$O); 59.87 (CH$_2$O); 66.36 (b, CH$_2$-5′); 68.97 (phenylene-O**C**H$_2$CH$_2$O); 70.42 (OCH$_2$CH$_2$O); 70.77 (phenylene-OCH$_2$**C**H$_2$O); 71.56, 71.59

(OCH_2CH_2O); 71.73 (CH-3′); 71.76 (OCH_2CH_2O); 87.76 (CH-1′,4′); 108.41 (CH-3″); 115.74 (CH-*m*-phenylene); 128.30 (C-*i*-phenylene); 128.57 (CH-*m*-Ph); 129.94 (CH-*p*-Ph, C-*i*-Ph); 131.44 – 131.54 (m, CH-*o*-Ph); 132.94 (C-2″); 133.34 (CH-*o*-phenylene); 141.59 (C-6″); 145.78 (CH-6); 146.90 (C-5″); 154.69 (b, C-4″); 162.05 (C-*p*-phenylene); (CH_2**C**≡**C**, C-2,4,5 not detected).

$^{31}P\{^1H\}$ NMR (202.4 MHz, CD_3OD): -22.41, -9.93, -9.06 (3 × bs).

^{11}B NMR (160.4 MHz, CD_3OD): 0.51 (t, $J_{B,F}$ = 31.1).

HRMS (ESI^-): calculated for $C_{47}H_{50}O_{19}N_5BF_2P_3$: 1130.23794; found 1130.23820.

5.8.2 Biochemistry

5.8.2.1 Primer extension experiments

Enzymatic synthesis of modified DNA (19-mer) bearing one MOB of pegMOB modification by primer extension (DNA19_1C^{MOB} and DNA19_1C^{pegMOB}; gel analysis)

The reaction mixture (20 µl) contained FAM labelled primer Prim1^{PEX}-FAM (for sequence see Table 16; 3 µM, 1 µL), template Temp1^{PEX} (for sequence see Table 16; 3 µM, 1.5 µL), either KOD XL DNA polymerase (0.25 U/µL, 0.3 µL), Vent (exo-) (10x dil 0.3 uL) or BST LF (10 x dil 0.6 uL), natural dGTP (4 mM, 0.6 µL), either natural dCTP (4 mM, 0.3 µL) or **dC^{MOB}TP** or **dC^{pegMOB}TP** (4 mM, 0.3 µL) in corresponding reaction buffer (10x, 2 µL) supplied by the manufacturer. The reaction mixture was incubated for 30 min at 60°C in thermal cycler. The reaction was stopped by the addition of PAGE stop solution (20 uL) and the reaction mixture was denatured at 95°C for 5 min and analyzed using 12.5% denaturing PAGE. The gel was visualized by a fluorescent scanner (PAGE gels are shown in Figure 66).

Enzymatic synthesis of modified DNA bearing four MOB of pegMOB modification by primer extension (DNA31_4C^{MOB} and DNA31_4C^{pegMOB}; semi-preparative scale, gel analysis)

The reaction mixture (142.1 µl) contained FAM labelled primer Prim1^{PEX}-FAM (for sequence see Table 16; 3 µM, 7 µL), template Temp2^{PEX}-TINA (for sequence see Table 16; 3 µM, 10.5 µL), KOD XL DNA polymerase (0.25 U/µL, 2.1 µL), natural dNTPs (dATP, dGTP, dTTP, 4 mM each, 4.9 µL), either natural dCTP (4 mM, 7 µL) or **dC^{MOB}TP** or **dC^{pegMOB}TP** (4 mM, 7 µL) in corresponding reaction buffer (10x, 14 µL) supplied by the manufacturer. The reaction mixture was incubated for 60 min at 60°C in a thermal cycler. The reaction was stopped by cooling at 4°C. The modified dsDNA was purified using spin columns (QIAquick® Nucleotide Removal Kit, QIAGEN) and eluted by milli-Q water. The purified reaction mixture was mixed 1:1 with PAGE stop solution and then the mixture was denatured for 5 min at 95°C and analyzed using 12.5% denaturing PAGE. The gel was visualized by a fluorescent scanner (PAGE gel is shown in Figure 68 A).

Preparation of modified dsDNA (16-mer) bearing one MOB or pegMOB modification by primer extension (DNA16_1C^{MOB} and DNA16_1C^{pegMOB}; semi-preparative scale)

The reaction mixture (125 µL) containing primer Prim1^{PEX}-FAM (for sequence see Table 16; 100 µM, 5 µL), template Temp4^{PEX} (for sequence see Table 16; 100 µM, 5 µL), **dC^{MOB}TP** or **dC^{pegMOB}TP** (4 mM, 1 uL), KOD XL DNA polymerase (2.5 U/µL, 0.6 µL) in corresponding reaction buffer (10×, 12.5 µL) supplied by the manufacturer. The reaction mixture was incubated for 30 min at 60°C in a thermal cycler. The reaction was stopped by cooling at 4°C. The modified dsDNA was purified using spin columns (QIAquick® Nucleotide Removal Kit, QIAGEN) and eluted by milli-Q water.

Preparation of modified dsDNA (19-mer) bearing one MOB or pegMOB modification by primer extension (DNA19_1C^{MOB} and DNA19_1C^{pegMOB}; semi-preparative scale)

The reaction mixture (100 µL) containing primer Prim1^{PEX} (for sequence see Table 16; 100 µM, 5 µL), template Temp1^{PEX} (for sequence see Table 16; 100 µM, 5 µL), dGTP (4 mM, 1.25 µL), **dC^{MOB}TP** or **dC^{pegMOB}TP** (4 mM, 1 uL), KOD XL DNA polymerase (2.5 U/µL, 0.6 µL) in corresponding reaction buffer (10×, 12.5 µL) supplied by the manufacturer. The reaction mixture was incubated for 30 min at 60°C in a thermal cycler. The reaction was stopped by cooling at 4°C. The modified dsDNA was purified using spin columns (QIAquick® Nucleotide Removal Kit, QIAGEN) and eluted by milli-Q water. Prepared dsDNA was used for fluorescence measurements.

Kinetic study of incorporation of dC^{MOB}TP or dC^{pegMOB}TP

The reaction mixtures (10 µL) contained primer Prim1^{PEX}-FAM (for sequence see Table 16; 100 µM, 0.1 µL), template Temp4^{PEX} (for sequence see Table 16; 100 µM, 0.12 µL), dCTP, **dC^{MOB}TP** or **dC^{pegMOB}TP** (0.04 mM, 2 uL), KOD XL DNA polymerase (2.5 U/µL, 0.05 µL) in corresponding reaction buffer (10×, 1 µL) supplied by the manufacturer. The reaction mixture s were incubated for at 60°C for indicated time intervals (0.5, 1, 2, 5, 10, 15, 20, 40, 60 and 90 min) in a thermal cycler. The reactions were stopped by the addition of PAGE stop solution (10 uL) and the reaction mixtures were denatured at 95°C for 5 min and analyzed using 12.5% denaturing PAGE. The gel was visualized by a fluorescent scanner (PAGE gels are shown in Figure 67).

5.8.2.2 Polymerase chain reaction experiments

Enzymatic incorporation of dC^{MOB}TP or dC^{pegMOB}TP by polymerase chain reaction

The reaction mixture (20 µL) contained primer Prim1^{PCR} and Prim2^{PCR} (for sequences

see Table 16; 10 μM, 3 μL of each), template Temp1^{PCR} (10 nM, 0.5 μL), natural dNTPs (dATP, dGTP, dTTP, 0.4 mM each, 1.5 μL) and either dCTP (0.4 mM, 1.5 uL) or mixture of **dC^{MOB}TP** or **dC^{pegMOB}TP** with natural dCTP (0-95%), KOD XL DNA polymerase (2.5 U/μL, 0.5 μL) and corresponding reaction buffer (10×, 2 μL) supplied by the manufacturer. After the initial denaturation for 3 min at 94°C, 30 PCR cycles were run under the following conditions: denaturation for 1 min at 94°C, annealing for 1 min at 55°C, extension for 1 min at 72°C. The PCR process was terminated with a final extension step for 5 min at 72°C. The reaction was stopped by cooling to 4°C. The PCR products were analyzed by agarose gel electrophoresis in 2% agarose gel stained with GelRed™ (Biotium, agarose gels are shown in Figure 68 B, C).

5.8.3 Fluorescence lifetime measurements

Fluorescence lifetime

Time-correlated single photon counting (TCSPC) was performed using FluoroMax-4 spectrofluorometer (NL-C2 Pulsed diode Control, DH-HT High throughput TCSPC controller, DataStation software). The samples were thermostated at 25°C. TCSPC was performed using pulsed diode laser (model: N-455, HORIBA Jobin Yvon IBH Ltd, U. K; peak wavelength 452 nm, pulse duration 25 nm, repetition rate 1 MHz), detector HV: 900 volts. Fluorescence decays were fitted to biexponential functions using iterative reconvolution procedure in DAS6 software. Mean fluorescence lifetime was calculated using formula:

$$\frac{\int_0^\infty D(t)tdt}{\int_0^\infty D(t)dt} - \frac{\int_0^\infty IRF(t)tdt}{\int_0^\infty IRF(t)dt}$$

D(t) is the measured fluorescent decay, IRF(t) is instrument response function, and t is time after electronic excitation.

Measurement of the mean fluorescence lifetime at different viscosity

Nucleosides **dC^{MOB}** and **dC^{pegMOB}** were dissolved in different mixtures of glycerol/methanol (final concentration of each nucleosides was 1.84 μM). The samples were thermostated at 25°C and fluorescence lifetime decays were measured. The viscosities of the mixtures were estimated using equation[195]

$$\ln\eta_{mix} = w_{MeOH} \times \ln\eta_{MeOH} + w_{glycerol} \times \ln\eta_{glycerol}$$

where η stands for viscosity, *w* stands for weight fraction.

Interaction of DNA19_1C^{MOB} and DNA19_1C^{pegMOB} with histone or BSA

Titrations were performed in 100 μL quartz cuvette at 25°C. Solution of dsDNA (100 μL, 0.4 μM) in phosphate buffer (25 mM, pH 7.4) was titrated by H2A histone and by BSA (Bovine serum albumin) as control experiment. After every addition of the protein the solution was mixed carefully with a pipette and equilibrated for 1-2 min before measuring the fluorescence lifetime decays.

5.9 2'-Deoxycytidine triphosphate bearing silicon rhodamine fluorophore. Synthesis, phyotophysical properties, enzymatic incorporation into DNA and applications

5.9.1 Chemical synthesis

Silicon rhodamine modified deoxycytidine-5′-*O*-triphosphate (dC^{SiR}TP)

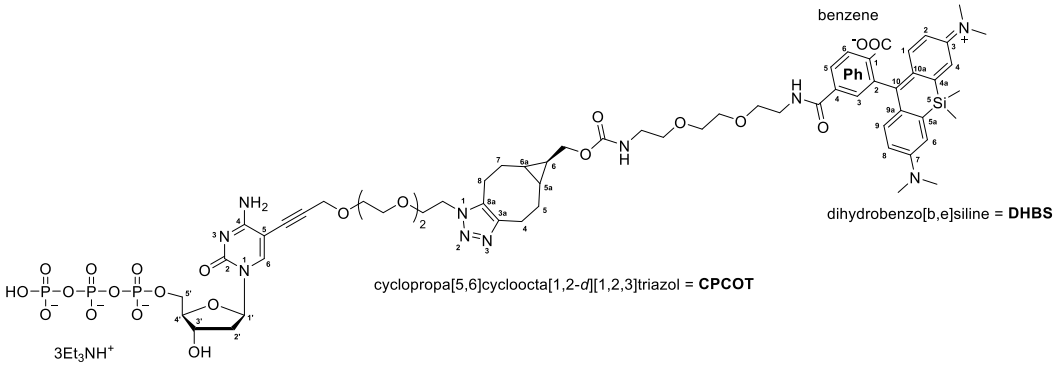

Solution of **SiR-BCN** (2.5 mg, 3.23 µmol, in 420 µL DMSO) was added to solution of **dC^{pegN3}TP** (3.5 mg, 3.23 µmol, in 140 µL HPLC grade H_2O) and the reaction mixture was stirred overnight at room temperature. Then, the DMSO was removed by lyophilization and the reaction mixture was purified by reverse-phase HPLC (eluent: H_2O/0.1 M triethylammonium acetate/acetonitrile 37/20/43). Collected fractions were lyophilized, excess of buffer was removed by repetitive freeze-drying from water. The product was obtained as pale yellow solid (2.84 mg, 50%).

^{1}H NMR (500.0 MHz, D_2O, ref(*t*BuOH) = 1.24 ppm): 0.46, 0.58 (2 × s, 2 × 3H, CH_3Si); 0.66 – 0.78 (bm, 2H, H-5a,6a-CPCOT); 0.86 (bm, 1H, H-6-CPCOT); 1.10 – 1.24 (bm, 2H, H-5b,7b-CPCOT); 1.27 (t, 27H, J_{vic} = 7.3, C**H$_3$**CH$_2$N); 1.91, 2.02 (2 × bm, 2 × 1H, H-5a,7a-CPCOT); 2.18, 2.38 (2 × bm, 2 × 1H, H-2′); 2.54 – 2.66 (bm, 1H, H-4b,8b-CPCOT); 2.69 – 2.83 (bm, 1H, H-4a,8a-CPCOT); 2.95 – 3.15 (bm, 2H, NC**H$_2$**CH$_2$O); 3.15 – 3.30 (bm, 30H, $(CH_3)_2$N, CH_3C**H$_2$**N); 3.40 – 3.56, 3.56 – 3.71, 3.71 – 3.77, 3.77 – 3.85, 3.92 (5 × bm, 22H, OC**H$_2$**C**H$_2$**O, NC**H$_2$**C**H$_2$**O, triazoleNCH$_2$C**H$_2$**O, CH$_2$O); 4.09 – 4.23 (bm, 3H, H-4′,5′); 4.30 – 4.41 (bm, 4H, C**H$_2$**C≡C, triazoleNC**H$_2$**CH$_2$O); 4.55 (bm, 1H, H-3′); 6.12 (bm, 1H, H-1′); 6.49, 6.60 (2 × bm, 2 × 1H, H-2,8-DHBS);

6.90 – 7.04 (bm, 2H, H-1,9-DHBS); 7.20 – 7.29 (bm, 2H, H-4,6-DHBS); 7.69 (bm, 1H, H-3-Ph); 7.95 – 8.03 (H-5,6-Ph); 8.05 (bm, 1H, H-6).

^{13}C NMR (125.7 MHz, D_2O, ref(*t*BuOH) = 30.29 ppm): -2.79, -0.31, -0.28 (CH_3Si); 8.92 (**C**H_3CH_2N); 17.65, 17.69 (CH-6-CPCOT); 19.28, 19.36, 19.78, 19.81 (CH-5a,6a-CPCOT); 21.79, 22.23 (CH_2-5,7-CPCOT); 23.04, 25.87 (CH_2-4,8-CPCOT); 40.14 (CH_2-2′); 40.50 (N**C**H_2CH_2O); 40.70, 40.75, 40.79 (($CH_3)_2N$); 40.84 (N**C**H_2CH_2O); 47.36 (CH_3**C**H_2N); 48.46 (triazoleN**C**H_2CH_2O); 59.19 (**C**$H_2C{\equiv}C$); 63.80 (CH_2O); 65.90 (CH_2-5′); 69.45, 69.65, 69.79, 70.07, 70.22, 70.78 (O**C**H_2**C**H_2O, triazoleNCH_2**C**H_2O, NCH_2**C**H_2O); 71.21 (CH-3′); 77.61 ($CH_2C{\equiv}$**C**); 86.27 (d, $J_{C,P}$ = 7.3, CH-4′); 87.10 (CH-1′); 92.40 (C-5, CH_2**C**≡C); 114.28, 114.42, 114.49 (CH-2,8-DHBS); 121.02, 121.07, 121.16 (CH-4,6-DHBS); 128.12 (CH-5-Ph or CH-6-Ph); 128.58 (C-9a,10a-DHBS); 129.28 (CH-3-Ph); 129.78 (CH-5-Ph or CH-6-Ph); 135.64 (C-4-Ph); 140.21, 140.25, 140.53 (CH-1,9-DHBS); 140.63 (C-1-Ph); 145.69 (CH-6); 147.64, 147.67, 147.79 (C-4a,5a-DHBS); 153.85, 153.95 (C-3,7-DHBS); 155.95 (C-2); 158.69 (OCONH); 165.20 (C-4); 169.88 (CONH-4-Ph); 173.66 (COO-1-Ph); C-2-Ph, C-10-DHBS and C-3a,8a-CPCOT not detected.

$^{31}P\{^1H\}$ NMR (202.4 MHz, D_2O): -22.52, -10.90, -10.18 (3 × bm).

HRMS (ESI^-): calculated for $C_{62}H_{82}O_{23}N_{10}P_3Si$: 1455.4542; found 1455.4529.

5.9.2 Biochemistry

5.9.2.1 Primer extension experiments

Enzymatic synthesis of modified DNA bearing one silicon rhodamine modification by primer extension (gel analysis)

The reaction mixture (20 µl) contained FAM labelled primer Prim1^{PEX}-FAM (for sequence see Table 16; 3 µM, 1 µL), template Temp1^{PEX} (for sequence see Table 16; 3 µM, 1.5 µL), KOD XL DNA polymerase (0.25 U/µL, 0.3 µL), natural dGTP (4 mM, 0.6 µL), either natural dCTP (4 mM, 0.3 µL) or **dC^{SiR}TP** (4 mM, 0.3 µL) in

corresponding reaction buffer (10x, 2 µL) supplied by the manufacturer. The reaction mixture was incubated for 30 min at 60°C in thermal cycler. The reaction was stopped by the addition of PAGE stop solution (20 uL) and the reaction mixture was denatured at 95°C for 5 min and analyzed using 12.5% denaturing PAGE. The gel was visualized by a fluorescent scanner (PAGE gel is shown in Figure 76 A).

Preparation of modified dsDNA bearing one silicon rhodamine modification by primer extension (semi-preparative scale)

The reaction mixture (50 µL) containing primer (for sequence see Table 16; $Prim1^{PEX}$, 100 µM, 2.5 µL), template (for sequence see Table 16; $Temp1^{PEX}$, 100 µM, 2.5 µL), dGTP (4 mM, 1 µL), **$dC^{SiR}TP$** (4 mM, 2.5 uL), KOD XL DNA polymerase (2.5 U/µL, 1.5 µL) in corresponding reaction buffer (10×, 5 µL) supplied by the manufacturer. The reaction mixture was incubated for 75 min at 60°C in a thermal cycler. The reaction was stopped by cooling at 4°C. The modified dsDNA was purified using spin columns (QIAquick® Nucleotide Removal Kit, QIAGEN) and eluted by milli-Q water. Prepared dsDNA was used for measurement of photophysical properties.

5.9.2.2 Polymerase chain reaction experiments

Enzymatic incorporation of dC^{SiR}TP by polymerase chain reaction

The reaction mixture (20 µL) contained primer (for sequences see Table 16; Prim1^{PCR} and Prim2^{PCR}, 10 µM, 1 µL of each), template (Temp1^{PCR}, 1 nM, 0.5 µL), natural dNTPs (dATP, dGTP, dTTP, 0.4 mM each, 1.5 µL) and either dCTP (0.4 mM, 1.5 uL), **dC^{SiR}TP** (0.4 mM, 1.5 uL) or mixture of **dC^{SiR}TP** with natural dCTP (0-95% of dCTP), KOD XL DNA polymerase (2.5 U/µL, 0.5 µL) and corresponding reaction buffer (10×, 2 µL) supplied by the manufacturer. After the initial denaturation for 3 min at 94°C, 40 PCR cycles were run under the following conditions: denaturation for 20 sec. at 94°C, annealing for 30 sec. at 58°C, extension for 30 sec. at 72°C. The reaction was stopped by cooling to 4°C. The PCR products were analyzed by agarose gel electrophoresis in 2% agarose gel stained with GelRed™ (Biotium, agarose gels are shown in Figure 76 B).

6 List of publications of the author

Publications related to the thesis

(1) Kuba, M.; Pohl, R.; Hocek, M.: "Synthesis of 2'-deoxycytidine and its triphosphate bearing tryptophan-based imidazolinone fluorophore for environment sensitive fluorescent labelling of DNA" *Tetrahedron* **2018**, *74*, 6621-6629.

(2) Kuba, M.; Kraus, T.; Pohl. R.; Hocek, M.: "Nucleotide bearing benzylidene-tetrahydroxanthylium near-IR fluorophore for sensing DNA replication, secondary structures and interactions" *Chem. Eur. J.* **2020**, *26*, 11950-11954.

Other publications of the author

(3) Matyašovský, J.; Tack, L.; Palágyi, A.; Kuba, M.; Pohl, R.; Kraus, T.; Güixens-Gallardo, P.; Hocek, M.: "Nucleotides bearing aminophenyl- or aminonaphthyl-3-methoxychromone solvatochromic fluorophores for the enzymatic construction of DNA probes for the detection of protein–DNA binding" *Org. Biomol. Chem.* **2021**, *19*, 9966-9974.

7 Literature

(1) Dahm, R. Discovering DNA: Friedrich Miescher and the Early Years of Nucleic Acid Research. *Hum. Genet.* **2008**, *122* (6), 565–581. https://doi.org/10.1007/s00439-007-0433-0.

(2) Dahm, R. Friedrich Miescher and the Discovery of DNA. *Dev. Biol.* **2005**, *278* (2), 274–288. https://doi.org/10.1016/j.ydbio.2004.11.028.

(3) Watson, J. D.; Crick, F. H. C. Molecular Structure of Nucleic Acids: A Structure for Deoxyribose Nucleic Acid. *Nature* **1953**, *171* (4356), 737–738. https://doi.org/10.1038/171737a0.

(4) Elson, D.; Chargaff, E. On the Desoxyribonucleic Acid Content of Sea Urchin Gametes. *Experientia* **1952**, *8* (4), 143–145. https://doi.org/10.1007/BF02170221.

(5) Chargaff, E.; Lipshitz, R.; Green, C. COMPOSITION OF THE DESOXYPENTOSE NUCLEIC ACIDS OF FOUR GENERA OF SEA-URCHIN. *J. Biol. Chem.* **1952**, *195* (1), 155–160. https://doi.org/10.1016/S0021-9258(19)50884-5.

(6) Belmont, P.; Constant, J.-F.; Demeunynck, M. Nucleic Acid Conformation Diversity: From Structure to Function and Regulation. *Chem. Soc. Rev.* **2001**, *30* (1), 70–81. https://doi.org/10.1039/A904630E.

(7) Matta, C. F.; Castillo, N.; Boyd, R. J. Extended Weak Bonding Interactions in DNA: Pi-Stacking (Base-Base), Base-Backbone, and Backbone-Backbone Interactions. *J. Phys. Chem. B* **2006**, *110* (1), 563–578. https://doi.org/10.1021/jp054986g.

(8) Huang, C. C.; Couch, G. S.; Petersen, E. F.; Ferrin, T. E. Huang C. C., Couch G. S., Petersen E. F., Ferrin T. E., Proc. Pacific Symp. On Biocomputing, 1996, 1, 724. *Proc. Pacific Symp. On Biocomputing* **1996**, *1*, 724.

(9) Leslie, A. G. W.; Arnott, S.; Chandrasekaran, R.; Ratliff, R. L. Polymorphism of DNA Double Helices. *J. Mol. Biol.* **1980**, *143* (1), 49–72. https://doi.org/10.1016/0022-2836(80)90124-2.

(10) Wang, J. C. Helical Repeat of DNA in Solution. *Proc. Natl. Acad. Sci.* **1979**, *76* (1), 200–203. https://doi.org/10.1073/pnas.76.1.200.

(11) Rosalind, F. Rosalind F., Acta Crystallographica, 1953, 6, 673-677. *Acta Crystallographica* **1953**, *6*, 673–677.

(12) Rosa, M. de; Sanctis, D. de; Rosario, A. L.; Archer, M.; Rich, A.; Athanasiadis, A.; Carrondo, M. A. Crystal Structure of a Junction between Two Z-DNA Helices. *Proc. Natl. Acad. Sci.* **2010**, *107* (20), 9088–9092. https://doi.org/10.1073/pnas.1003182107.

(13) Syvänen, A. C. Accessing Genetic Variation: Genotyping Single Nucleotide Polymorphisms. *Nat. Rev. Genet.* **2001**, *2* (12), 930–942. https://doi.org/10.1038/35103535.

(14) Michelson, A. M.; Todd, A. R. Nucleotides Part XXXII. Synthesis of a Dithymidine Dinucleotide Containing a 3′: 5′-Internucleotidic Linkage. *J. Chem. Soc. Resumed* **1955**, No. 0, 2632–2638. https://doi.org/10.1039/JR9550002632.

(15) Hall, R. H.; Todd, A.; Webb, R. F. 644. Nucleotides. Part XLI. Mixed Anhydrides as Intermediates in the Synthesis of Dinucleoside Phosphates. *J. Chem. Soc. Resumed* **1957**, No. 0, 3291–3296. https://doi.org/10.1039/JR9570003291.

(16) Letsinger, R. L.; Finnan, J. L.; Heavner, G. A.; Lunsford, W. B. Nucleotide Chemistry. XX. Phosphite Coupling Procedure for Generating Internucleotide Links. *J. Am. Chem. Soc.* **1975**, *97* (11), 3278–3279. https://doi.org/10.1021/ja00844a090.

(17) Gilham, P. T.; Khorana, H. G. Studies on Polynucleotides. I. A New and General Method for the Chemical Synthesis of the C5″-C3″ Internucleotidic Linkage. Syntheses of Deoxyribo-Dinucleotides1. *J. Am. Chem. Soc.* **1958**, *80* (23), 6212–6222. https://doi.org/10.1021/ja01556a016.

(18) Letsinger, R. L.; Ogilvie, K. K. Nucleotide Chemistry. XIII. Synthesis of Oligothymidylates via Phosphotriester Intermediates. *J. Am. Chem. Soc.* **1969**, *91* (12), 3350–3355. https://doi.org/10.1021/ja01040a042.

(19) Reese, C. B. The Chemical Synthesis of Oligo- and Poly-Nucleotides by the Phosphotriester Approach. *Tetrahedron* **1978**, *34* (21), 3143–3179. https://doi.org/10.1016/0040-4020(78)87013-6.

(20) Beaucage, S. L.; Caruthers, M. H. Deoxynucleoside Phosphoramidites—A New Class of Key Intermediates for Deoxypolynucleotide Synthesis. *Tetrahedron Lett.* **1981**, *22* (20), 1859–1862. https://doi.org/10.1016/S0040-4039(01)90461-7.

(21) Kleppe, K.; Ohtsuka, E.; Kleppe, R.; Molineux, I.; Khorana, H. G. Studies on Polynucleotides. XCVI. Repair Replications of Short Synthetic DNA's as Catalyzed by DNA Polymerases. *J. Mol. Biol.* **1971**, *56* (2), 341–361. https://doi.org/10.1016/0022-2836(71)90469-4.

(22) Bartlett, J. M. S.; Stirling, D. A Short History of the Polymerase Chain Reaction. *Methods Mol. Biol. Clifton NJ* **2003**, *226*, 3–6. https://doi.org/10.1385/1-59259-384-4:3.

(23) Wong, M. L.; Medrano, J. F. Real-Time PCR for MRNA Quantitation. *BioTechniques* **2005**, *39* (1), 75–85. https://doi.org/10.2144/05391RV01.

(24) Higuchi, R.; Fockler, C.; Dollinger, G.; Watson, R. Kinetic PCR Analysis: Real-Time Monitoring of DNA Amplification Reactions. *Bio/Technology* **1993**, *11* (9), 1026–1030. https://doi.org/10.1038/nbt0993-1026.

(25) Ishiguro, T.; Saitoh, J.; Yawata, H.; Yamagishi, H.; Iwasaki, S.; Mitoma, Y. Homogeneous Quantitative Assay of Hepatitis C Virus RNA by Polymerase Chain Reaction in the Presence of a Fluorescent Intercalater. *Anal. Biochem.* **1995**, *229* (2), 207–213. https://doi.org/10.1006/abio.1995.1404.

(26) Tseng, S. Y.; Macool, D.; Elliott, V.; Tice, G.; Jackson, R.; Barbour, M.;

Amorese, D. Tseng S. Y., Macool D., Elliott V., Tice G., Jackson R., Barbour M., Amorese D., Anal. Biochem., 1997, 245, 207-212. *Anal. Biochem.* **1997**, *245*, 207–212.

(27) Ponchel, F.; Toomes, C.; Bransfield, K.; Leong, F. T.; Douglas, S. H.; Field, S. L.; Bell, S. M.; Combaret, V.; Puisieux, A.; Mighell, A. J.; Robinson, P. A.; Inglehearn, C. F.; Isaacs, J. D.; Markham, A. F. Real-Time PCR Based on SYBR-Green I Fluorescence: An Alternative to the TaqMan Assay for a Relative Quantification of Gene Rearrangements, Gene Amplifications and Micro Gene Deletions. *BMC Biotechnol.* **2003**, *3* (1), 18. https://doi.org/10.1186/1472-6750-3-18.

(28) Mackay, I. M.; Arden, K. E.; Nitsche, A. Real-Time PCR in Virology. *Nucleic Acids Res.* **2002**, *30* (6), 1292–1305. https://doi.org/10.1093/nar/30.6.1292.

(29) Holland, P. M.; Abramson, R. D.; Watson, R.; Gelfand, D. H. Detection of Specific Polymerase Chain Reaction Product by Utilizing the 5'----3' Exonuclease Activity of Thermus Aquaticus DNA Polymerase. *Proc. Natl. Acad. Sci. U. S. A.* **1991**, *88* (16), 7276–7280. https://doi.org/10.1073/pnas.88.16.7276.

(30) Livak, K. J.; Marmaro, J.; Todd, J. A. Towards Fully Automated Genome-Wide Polymorphism Screening. *Nat. Genet.* **1995**, *9* (4), 341–342. https://doi.org/10.1038/ng0495-341.

(31) Bustin, S. A. Absolute Quantification of MRNA Using Real-Time Reverse Transcription Polymerase Chain Reaction Assays. *J. Mol. Endocrinol.* **2000**, *25* (2), 169–193. https://doi.org/10.1677/jme.0.0250169.

(32) Yang, D. K.; Kim, B. H.; Kweon, C. H.; Kwon, J. H.; Lim, S. I.; Han, H. R. Biophysical Characterization of Japanese Encephalitis Virus (KV1899) Isolated from Pigs in Korea. *J. Vet. Sci.* **2004**, *5* (2), 125–130. https://doi.org/10.4142/jvs.2004.5.2.125.

(33) Wang, C. C.-Y.; Seo, T. S.; Li, Z.; Ruparel, H.; Ju, J. Site-Specific Fluorescent Labeling of DNA Using Staudinger Ligation. *Bioconjug. Chem.* **2003**, *14* (3), 697–701. https://doi.org/10.1021/bc0256392.

(34) Panattoni, A.; Pohl, R.; Hocek, M. Flexible Alkyne-Linked Thymidine Phosphoramidites and Triphosphates for Chemical or Polymerase Synthesis and Fast Postsynthetic DNA Functionalization through Copper-Catalyzed Alkyne–Azide 1,3-Dipolar Cycloaddition. *Org. Lett.* **2018**, *20* (13), 3962–3965. https://doi.org/10.1021/acs.orglett.8b01533.

(35) Ren, X.; El-Sagheer, A. H.; Brown, T. Azide and Trans-Cyclooctene DUTPs: Incorporation into DNA Probes and Fluorescent Click-Labelling. *Analyst* **2015**, *140* (8), 2671–2678. https://doi.org/10.1039/C5AN00158G.

(36) Motorin, Y.; Seidu-Larry, S.; Helm, M. Motorin Y., Seidu-Larry S., Helm M., in DNA Methyltransferases – Role and Function, Springer International Publishing, 2016, 945, 19-33. *in DNA methyltransferases - Role and Function, Springer International Publishing* **2016**, *945*, 19–33.

(37) Seela, F.; Roling, A. Seela F., Roling A., Nucleic Acids Research, 1991, 20,

55-61. *Nucleic Acids Research* **1991**, *20*, 55–61.
(38) Yoshikawa, M.; Kato, T.; Takenishi, T. A Novel Method for Phosphorylation of Nucleosides to 5'-Nucleotides. *Tetrahedron Lett.* **1967**, *50*, 5065–5068. https://doi.org/10.1016/s0040-4039(01)89915-9.
(39) Sonogashira, K. Development of Pd/Cu-Catalyzed Cross-Coupling of Terminal Acetylenes with Sp2-Carbon Halides. *J. Organomet. Chem. - J ORGANOMET CHEM* **2002**, *653*, 46–49. https://doi.org/10.1016/S0022-328X(02)01158-0.
(40) Chinchilla, R.; Nájera, C. The Sonogashira Reaction: A Booming Methodology in Synthetic Organic Chemistry. *Chem. Rev.* **2007**, *107* (3), 874–922. https://doi.org/10.1021/cr050992x.
(41) Riedl, J.; Pohl, R.; Ernsting, N. P.; Orság, P.; Fojta, M.; Hocek, M. Labelling of Nucleosides and Oligonucleotides by Solvatochromic 4-Aminophthalimide Fluorophore for Studying DNA–Protein Interactions. *Chem. Sci.* **2012**, *3* (9), 2797–2806. https://doi.org/10.1039/C2SC20404E.
(42) Dziuba, D.; Pospíšil, P.; Matyašovský, J.; Brynda, J.; Nachtigallová, D.; Rulíšek, L.; Pohl, R.; Hof, M.; Hocek, M. Solvatochromic Fluorene-Linked Nucleoside and DNA as Color-Changing Fluorescent Probes for Sensing Interactions. *Chem. Sci.* **2016**, *7* (9), 5775–5785. https://doi.org/10.1039/C6SC02548J.
(43) Kumara, G. S. R.; Pandith, A.; Seo, Y. J. Highly Fluorescent Morpholine Naphthalimide Deoxyuridine Nucleotide for the Detection of MiRNA 24-3P through Rolling Circle Amplification. *Analyst* **2020**, *145* (14), 4777–4781. https://doi.org/10.1039/D0AN00723D.
(44) Tornøe, C. W.; Christensen, C.; Meldal, M. Peptidotriazoles on Solid Phase: [1,2,3]-Triazoles by Regiospecific Copper(I)-Catalyzed 1,3-Dipolar Cycloadditions of Terminal Alkynes to Azides. *J. Org. Chem.* **2002**, *67* (9), 3057–3064. https://doi.org/10.1021/jo011148j.
(45) Rostovtsev, V. V.; Green, L. G.; Fokin, V. V.; Sharpless, K. B. A Stepwise Huisgen Cycloaddition Process: Copper(I)-Catalyzed Regioselective "Ligation" of Azides and Terminal Alkynes. *Angew. Chem. Int. Ed.* **2002**, *41* (14), 2596–2599. https://doi.org/10.1002/1521-3773(20020715)41:14<2596::AID-ANIE2596>3.0.CO;2-4.
(46) Worrell, B. T.; Malik, J. A.; Fokin, V. V. Direct Evidence of a Dinuclear Copper Intermediate in Cu(I)-Catalyzed Azide-Alkyne Cycloadditions. *Science* **2013**, *340* (6131), 457–460. https://doi.org/10.1126/science.1229506.
(47) Jin, L.; Tolentino, D. R.; Melaimi, M.; Bertrand, G. Isolation of Bis(Copper) Key Intermediates in Cu-Catalyzed Azide-Alkyne "Click Reaction." *Sci. Adv.* **2015**, *1* (5), e1500304. https://doi.org/10.1126/sciadv.1500304.
(48) Gramlich, P. M. E.; Wirges, C. T.; Manetto, A.; Carell, T. Postsynthetic DNA Modification through the Copper-Catalyzed Azide-Alkyne Cycloaddition Reaction. *Angew. Chem. Int. Ed Engl.* **2008**, *47* (44), 8350–8358. https://doi.org/10.1002/anie.200802077.

(49) El-Sagheer, A. H.; Brown, T. Click Chemistry with DNA. *Chem. Soc. Rev.* **2010**, *39* (4), 1388–1405. https://doi.org/10.1039/B901971P.
(50) Salic, A.; Mitchison, T. J. A Chemical Method for Fast and Sensitive Detection of DNA Synthesis in Vivo. *Proc. Natl. Acad. Sci.* **2008**, *105* (7), 2415–2420. https://doi.org/10.1073/pnas.0712168105.
(51) Neef, A. B.; Luedtke, N. W. Dynamic Metabolic Labeling of DNA in Vivo with Arabinosyl Nucleosides. *Proc. Natl. Acad. Sci.* **2011**, *108* (51), 20404–20409. https://doi.org/10.1073/pnas.1101126108.
(52) Neef, A. B.; Samain, F.; Luedtke, N. W. Metabolic Labeling of DNA by Purine Analogues in Vivo. *ChemBioChem* **2012**, *13* (12), 1750–1753. https://doi.org/10.1002/cbic.201200253.
(53) Neef, A. B.; Pernot, L.; Schreier, V. N.; Scapozza, L.; Luedtke, N. W. A Bioorthogonal Chemical Reporter of Viral Infection. *Angew. Chem. Int. Ed Engl.* **2015**, *54* (27), 7911–7914. https://doi.org/10.1002/anie.201500250.
(54) Tera, M.; Glasauer, S. M. K.; Luedtke, N. W. In Vivo Incorporation of Azide Groups into DNA by Using Membrane-Permeable Nucleotide Triesters. *Chembiochem Eur. J. Chem. Biol.* **2018**, *19* (18), 1939–1943. https://doi.org/10.1002/cbic.201800351.
(55) Haque, M. M.; Sun, H.; Liu, S.; Wang, Y.; Peng, X. Photo-Switchable DNA Interstrand Cross-Link Formation by a Coumarin-Modified Nucleotide. *Angew. Chem. Int. Ed Engl.* **2014**, *53* (27), 7001–7005. https://doi.org/10.1002/anie.201310609.
(56) Schreier, V. N.; Loehr, M. O.; Deng, T.; Lattmann, E.; Hajnal, A.; Neuhauss, S. C. F.; Luedtke, N. W. Fluorescent DATP for DNA Synthesis In Vivo. *ACS Chem. Biol.* **2020**, *15* (11), 2996–3003. https://doi.org/10.1021/acschembio.0c00654.
(57) Agard, N. J.; Prescher, J. A.; Bertozzi, C. R. A Strain-Promoted [3 + 2] Azide−Alkyne Cycloaddition for Covalent Modification of Biomolecules in Living Systems. *J. Am. Chem. Soc.* **2004**, *126* (46), 15046–15047. https://doi.org/10.1021/ja044996f.
(58) Ren, X.; El-Sagheer, A. H.; Brown, T. Efficient Enzymatic Synthesis and Dual-Colour Fluorescent Labelling of DNA Probes Using Long Chain Azido-DUTP and BCN Dyes. *Nucleic Acids Res.* **2016**, *44* (8), e79–e79. https://doi.org/10.1093/nar/gkw028.
(59) Abendroth, F.; Seitz, O. Double-Clicking Peptides onto Phosphorothioate Oligonucleotides: Combining Two Proapoptotic Agents in One Molecule. *Angew. Chem. Int. Ed.* **2014**, *53* (39), 10504–10509. https://doi.org/10.1002/anie.201406674.
(60) Eördögh, Á.; Steinmeyer, J.; Peewasan, K.; Schepers, U.; Wagenknecht, H.-A.; Kele, P. Polarity Sensitive Bioorthogonally Applicable Far-Red Emitting Labels for Postsynthetic Nucleic Acid Labeling by Copper-Catalyzed and Copper-Free Cycloaddition. *Bioconjug. Chem.* **2016**, *27* (2), 457–464. https://doi.org/10.1021/acs.bioconjchem.5b00557.

(61) Neef, A. B.; Luedtke, N. W. An Azide-Modified Nucleoside for Metabolic Labeling of DNA. *ChemBioChem* **2014**, *15* (6), 789–793. https://doi.org/10.1002/cbic.201400037.
(62) Nikić, I.; Kang, J. H.; Girona, G. E.; Aramburu, I. V.; Lemke, E. A. Labeling Proteins on Live Mammalian Cells Using Click Chemistry. *Nat. Protoc.* **2015**, *10* (5), 780–791. https://doi.org/10.1038/nprot.2015.045.
(63) Beatty, K. E.; Fisk, J. D.; Smart, B. P.; Lu, Y. Y.; Szychowski, J.; Hangauer, M. J.; Baskin, J. M.; Bertozzi, C. R.; Tirrell, D. A. Live-Cell Imaging of Cellular Proteins by a Strain-Promoted Azide–Alkyne Cycloaddition. *Chembiochem Eur. J. Chem. Biol.* **2010**, *11* (15), 2092–2095. https://doi.org/10.1002/cbic.201000419.
(64) Zayas, J.; Annoual, M.; Das, J. K.; Felty, Q.; Gonzalez, W. G.; Miksovska, J.; Sharifai, N.; Chiba, A.; Wnuk, S. F. Strain Promoted Click Chemistry of 2- or 8-Azidopurine and 5-Azidopyrimidine Nucleosides and 8-Azidoadenosine Triphosphate with Cyclooctynes. Application to Living Cell Fluorescent Imaging. *Bioconjug. Chem.* **2015**, *26* (8), 1519–1532. https://doi.org/10.1021/acs.bioconjchem.5b00300.
(65) Sahoo, H. Fluorescent Labeling Techniques in Biomolecules: A Flashback. *RSC Adv.* **2012**, *2* (18), 7017–7029. https://doi.org/10.1039/C2RA20389H.
(66) Varki, A. Radioactive Tracer Techniques in the Sequencing of Glycoprotein Oligosaccharides. *FASEB J.* **1991**, *5* (2), 226–235. https://doi.org/10.1096/fasebj.5.2.2004668.
(67) Ong, S.-E.; Mann, M. A Practical Recipe for Stable Isotope Labeling by Amino Acids in Cell Culture (SILAC). *Nat. Protoc.* **2006**, *1* (6), 2650–2660. https://doi.org/10.1038/nprot.2006.427.
(68) van Staveren, D. R.; Metzler-Nolte, N. Bioorganometallic Chemistry of Ferrocene. *Chem. Rev.* **2004**, *104* (12), 5931–5986. https://doi.org/10.1021/cr0101510.
(69) Li, H.; Rothberg, L. Colorimetric Detection of DNA Sequences Based on Electrostatic Interactions with Unmodified Gold Nanoparticles. *Proc. Natl. Acad. Sci.* **2004**, *101* (39), 14036–14039. https://doi.org/10.1073/pnas.0406115101.
(70) Haugland, R. P. R. P. Haugland, Handbook of Fluorescent Probes and Research Products; Molecular Probes: Eugene, OR, 2002. *Handbook of Fluorescent Probes and Research Products* **2002**.
(71) Song, L.; Hennink, E. J.; Young, I. T.; Tanke, H. J. Photobleaching Kinetics of Fluorescein in Quantitative Fluorescence Microscopy. *Biophys. J.* **1995**, *68* (6), 2588–2600.
(72) Geisow, M. J. Fluorescein Conjugates as Indicators of Subcellular PH. A Critical Evaluation. *Exp. Cell Res.* **1984**, *150* (1), 29–35. https://doi.org/10.1016/0014-4827(84)90698-0.
(73) Gonçalves, M. S. T. Fluorescent Labeling of Biomolecules with Organic Probes. *Chem. Rev.* **2009**, *109* (1), 190–212.

https://doi.org/10.1021/cr0783840.
(74) Shindy, H. A. Fundamentals in the Chemistry of Cyanine Dyes: A Review. *Dyes Pigments* **2017**, *145*, 505–513. https://doi.org/10.1016/j.dyepig.2017.06.029.
(75) McCorquodale, E. M.; Colyer, C. L. Indocyanine Green as a Noncovalent, Pseudofluorogenic Label for Protein Determination by Capillary Electrophoresis. *Electrophoresis* **2001**, *22* (12), 2403–2408. https://doi.org/10.1002/1522-2683(200107)22:12<2403::AID-ELPS2403>3.0.CO;2-B.
(76) Zhang, G.; Zheng, S.; Liu, H.; Chen, P. R. Illuminating Biological Processes through Site-Specific Protein Labeling. *Chem. Soc. Rev.* **2015**, *44* (11), 3405–3417. https://doi.org/10.1039/C4CS00393D.
(77) Demchenko, A. P.; Mély, Y.; Duportail, G.; Klymchenko, A. S. Monitoring Biophysical Properties of Lipid Membranes by Environment-Sensitive Fluorescent Probes. *Biophys. J.* **2009**, *96* (9), 3461–3470. https://doi.org/10.1016/j.bpj.2009.02.012.
(78) Haidekker, M. A.; Theodorakis, E. A. Molecular Rotors—Fluorescent Biosensors for Viscosity and Flow. *Org. Biomol. Chem.* **2007**, *5* (11), 1669–1678. https://doi.org/10.1039/B618415D.
(79) Kuimova, M. K. Mapping Viscosity in Cells Using Molecular Rotors. *Phys. Chem. Chem. Phys.* **2012**, *14* (37), 12671–12686. https://doi.org/10.1039/C2CP41674C.
(80) Goh, W. L.; Lee, M. Y.; Joseph, T. L.; Quah, S. T.; Brown, C. J.; Verma, C.; Brenner, S.; Ghadessy, F. J.; Teo, Y. N. Molecular Rotors As Conditionally Fluorescent Labels for Rapid Detection of Biomolecular Interactions. *J. Am. Chem. Soc.* **2014**, *136* (17), 6159–6162. https://doi.org/10.1021/ja413031h.
(81) Hawe, A.; Filipe, V.; Jiskoot, W. Fluorescent Molecular Rotors as Dyes to Characterize Polysorbate-Containing IgG Formulations. *Pharm. Res.* **2010**, *27* (2), 314–326. https://doi.org/10.1007/s11095-009-0020-2.
(82) Sarder, P.; Maji, D.; Achilefu, S. Molecular Probes for Fluorescence Lifetime Imaging. *Bioconjug. Chem.* **2015**, *26* (6), 963–974. https://doi.org/10.1021/acs.bioconjchem.5b00167.
(83) Amaro, M.; Šachl, R.; Jurkiewicz, P.; Coutinho, A.; Prieto, M.; Hof, M. Time-Resolved Fluorescence in Lipid Bilayers: Selected Applications and Advantages over Steady State. *Biophys. J.* **2014**, *107* (12), 2751–2760. https://doi.org/10.1016/j.bpj.2014.10.058.
(84) Gryczynski, Z.; Gryczynski, I.; Lakowicz, J. R. Fluorescence-Sensing Methods. *Methods Enzymol.* **2003**, *360*, 44–75. https://doi.org/10.1016/s0076-6879(03)60106-0.
(85) Hosny, N. A.; Mohamedi, G.; Rademeyer, P.; Owen, J.; Wu, Y.; Tang, M.-X.; Eckersley, R. J.; Stride, E.; Kuimova, M. K. Mapping Microbubble Viscosity Using Fluorescence Lifetime Imaging of Molecular Rotors. *Proc. Natl. Acad. Sci. U. S. A.* **2013**, *110* (23), 9225–9230.

https://doi.org/10.1073/pnas.1301479110.
(86) Kuimova, M. K.; Yahioglu, G.; Levitt, J. A.; Suhling, K. Molecular Rotor Measures Viscosity of Live Cells via Fluorescence Lifetime Imaging. *J. Am. Chem. Soc.* **2008**, *130* (21), 6672–6673. https://doi.org/10.1021/ja800570d.
(87) Olšinová, M.; Jurkiewicz, P.; Pozník, M.; Šachl, R.; Prausová, T.; Hof, M.; Kozmík, V.; Teplý, F.; Svoboda, J.; Cebecauer, M. Di- and Tri-Oxalkyl Derivatives of a Boron Dipyrromethene (BODIPY) Rotor Dye in Lipid Bilayers. *Phys. Chem. Chem. Phys.* **2014**, *16* (22), 10688–10697. https://doi.org/10.1039/C4CP00888J.
(88) Klymchenko, A. S. Solvatochromic and Fluorogenic Dyes as Environment-Sensitive Probes: Design and Biological Applications. *Acc. Chem. Res.* **2017**, *50* (2), 366–375. https://doi.org/10.1021/acs.accounts.6b00517.
(89) Kucherak, O. A.; Didier, P.; Mély, Y.; Klymchenko, A. S. Fluorene Analogues of Prodan with Superior Fluorescence Brightness and Solvatochromism. *J. Phys. Chem. Lett.* **2010**, *1* (3), 616–620. https://doi.org/10.1021/jz9003685.
(90) Greenspan, P.; Mayer, E. P.; Fowler, S. D. Nile Red: A Selective Fluorescent Stain for Intracellular Lipid Droplets. *J. Cell Biol.* **1985**, *100* (3), 965–973. https://doi.org/10.1083/jcb.100.3.965.
(91) Halim, R.; Webley, P. A. Nile Red Staining for Oil Determination in Microalgal Cells: A New Insight through Statistical Modelling. *Int. J. Chem. Eng.* **2015**, *2015*, e695061. https://doi.org/10.1155/2015/695061.
(92) Collot, M.; Bou, S.; Fam, T. K.; Richert, L.; Mély, Y.; Danglot, L.; Klymchenko, A. S. Probing Polarity and Heterogeneity of Lipid Droplets in Live Cells Using a Push–Pull Fluorophore. *Anal. Chem.* **2019**, *91* (3), 1928–1935. https://doi.org/10.1021/acs.analchem.8b04218.
(93) Ryu, J. H.; Seo, Y. J.; Hwang, G. T.; Lee, J. Y.; Kim, B. H. Triad Base Pairs Containing Fluorene Unit for Quencher-Free SNP Typing. *Tetrahedron* **2007**, *63* (17), 3538–3547. https://doi.org/10.1016/j.tet.2006.10.091.
(94) Okamoto, A.; Tainaka, K.; Nishiza, K.; Saito, I. Monitoring DNA Structures by Dual Fluorescence of Pyrene Derivatives. *J. Am. Chem. Soc.* **2005**, *127* (38), 13128–13129. https://doi.org/10.1021/ja053609e.
(95) Tanpure, A. A.; Srivatsan, S. G. Conformation-Sensitive Nucleoside Analogues as Topology-Specific Fluorescence Turn-on Probes for DNA and RNA G-Quadruplexes. *Nucleic Acids Res.* **2015**, *43* (22), e149–e149. https://doi.org/10.1093/nar/gkv743.
(96) Dziuba, D.; Pohl, R.; Hocek, M. Polymerase Synthesis of DNA Labelled with Benzylidene Cyanoacetamide-Based Fluorescent Molecular Rotors: Fluorescent Light-up Probes for DNA-Binding Proteins. *Chem. Commun.* **2015**, *51* (23), 4880–4882. https://doi.org/10.1039/C5CC00530B.
(97) Dziuba, D.; Jurkiewicz, P.; Cebecauer, M.; Hof, M.; Hocek, M. A Rotational BODIPY Nucleotide: An Environment-Sensitive Fluorescence-Lifetime Probe for DNA Interactions and Applications in Live-Cell Microscopy. *Angew. Chem. Int. Ed.* **2016**, *55* (1), 174–178. https://doi.org/10.1002/anie.201507922.

(98) Güixens-Gallardo, P.; Hocek, M. Acetophenyl-Thienyl-Aniline-Linked Nucleotide for Construction of Solvatochromic Fluorescence Light-Up DNA Probes Sensing Protein-DNA Interactions. *Chem. – Eur. J.* **2021**, *27* (24), 7090–7093. https://doi.org/10.1002/chem.202100575.

(99) Brinkmann, V.; Reichard, U.; Goosmann, C.; Fauler, B.; Uhlemann, Y.; Weiss, D. S.; Weinrauch, Y.; Zychlinsky, A. Neutrophil Extracellular Traps Kill Bacteria. *Science* **2004**, *303* (5663), 1532–1535. https://doi.org/10.1126/science.1092385.

(100) Reorganization of Inter-Chromosomal Interactions in the 2q37-Deletion Syndrome. *EMBO J.* **2018**, *37* (15), e96257. https://doi.org/10.15252/embj.201696257.

(101) Triemer, T.; Messikommer, A.; Glasauer, S. M. K.; Alzeer, J.; Paulisch, M. H.; Luedtke, N. W. Superresolution Imaging of Individual Replication Forks Reveals Unexpected Prodrug Resistance Mechanism. *Proc. Natl. Acad. Sci.* **2018**, *115* (7), E1366–E1373. https://doi.org/10.1073/pnas.1714790115.

(102) Durand, R. E.; Olive, P. L. Cytotoxicity, Mutagenicity and DNA Damage by Hoechst 33342. *J. Histochem. Cytochem.* **1982**, *30* (2), 111–116. https://doi.org/10.1177/30.2.7061816.

(103) Smith, P. J.; Wiltshire, M.; Davies, S.; Patterson, L. H.; Hoy, T. A Novel Cell Permeant and Far Red-Fluorescing DNA Probe, DRAQ5, for Blood Cell Discrimination by Flow Cytometry. *J. Immunol. Methods* **1999**, *229* (1), 131–139. https://doi.org/10.1016/S0022-1759(99)00116-7.

(104) Weiss, L. E.; Naor, T.; Shechtman, Y. Observing DNA in Live Cells. *Biochem. Soc. Trans.* **2018**, *46* (3), 729–740. https://doi.org/10.1042/BST20170301.

(105) Rieder, U.; Luedtke, N. W. Alkene–Tetrazine Ligation for Imaging Cellular DNA. *Angew. Chem. Int. Ed.* **2014**, *53* (35), 9168–9172. https://doi.org/10.1002/anie.201403580.

(106) Tera, M.; Luedtke, N. W. Three-Component Bioorthogonal Reactions on Cellular DNA and RNA. *Bioconjug. Chem.* **2019**, *30* (12), 2991–2997. https://doi.org/10.1021/acs.bioconjchem.9b00630.

(107) Deville-Bonne, D.; El Amri, C.; Meyer, P.; Chen, Y.; Agrofoglio, L. A.; Janin, J. Human and Viral Nucleoside/Nucleotide Kinases Involved in Antiviral Drug Activation: Structural and Catalytic Properties. *Antiviral Res.* **2010**, *86* (1), 101–120. https://doi.org/10.1016/j.antiviral.2010.02.001.

(108) Jantsch, V.; Tang, L.; Pasierbek, P.; Penkner, A.; Nayak, S.; Baudrimont, A.; Schedl, T.; Gartner, A.; Loidl, J. Caenorhabditis Elegans Prom-1 Is Required for Meiotic Prophase Progression and Homologous Chromosome Pairing. *Mol. Biol. Cell* **2007**, *18* (12), 4911–4920. https://doi.org/10.1091/mbc.e07-03-0243.

(109) Zink, D. Live-cell microscopy of single nuclear chromosomes and genome compartments: evaluation of labeling procedure and imaging conditions. *Cytometry* **2001**, *45* (3), 214–224. https://doi.org/10.1002/1097-0320(20011101)45:3<214::AID-CYTO1165>3.0.CO;2-B.

(110) Jaramillo-Lambert, A.; Ellefson, M.; Villeneuve, A. M.; Engebrecht, J. Differential Timing of S Phases, X Chromosome Replication, and Meiotic Prophase in the C. Elegans Germ Line. *Dev. Biol.* **2007**, *308* (1), 206–221. https://doi.org/10.1016/j.ydbio.2007.05.019.

(111) Manders, E. M. M.; Kimura, H.; Cook, P. R. Direct Imaging of DNA in Living Cells Reveals the Dynamics of Chromosome Formation. *J. Cell Biol.* **1999**, *144* (5), 813–822. https://doi.org/10.1083/jcb.144.5.813.

(112) Zink, D.; Cremer, T.; Saffrich, R.; Fischer, R.; Trendelenburg, M. F.; Ansorge, W.; Stelzer, E. H. Structure and Dynamics of Human Interphase Chromosome Territories in Vivo. *Hum. Genet.* **1998**, *102* (2), 241–251. https://doi.org/10.1007/s004390050686.

(113) Zawada, Z.; Tatar, A.; Mocilac, P.; Buděšínský, M.; Kraus, T. Transport of Nucleoside Triphosphates into Cells by Artificial Molecular Transporters. *Angew. Chem. Int. Ed.* **2018**, *57* (31), 9891–9895. https://doi.org/10.1002/anie.201801306.

(114) Güixens-Gallardo, P.; Zawada, Z.; Matyašovský, J.; Dziuba, D.; Pohl, R.; Kraus, T.; Hocek, M. Brightly Fluorescent 2′-Deoxyribonucleoside Triphosphates Bearing Methylated Bodipy Fluorophore for in Cellulo Incorporation to DNA, Imaging, and Flow Cytometry. *Bioconjug. Chem.* **2018**, *29* (11), 3906–3912. https://doi.org/10.1021/acs.bioconjchem.8b00721.

(115) Dziuba, D.; Postupalenko, V. Y.; Spadafora, M.; Klymchenko, A. S.; Guérineau, V.; Mély, Y.; Benhida, R.; Burger, A. A Universal Nucleoside with Strong Two-Band Switchable Fluorescence and Sensitivity to the Environment for Investigating DNA Interactions. *J. Am. Chem. Soc.* **2012**, *134* (24), 10209–10213. https://doi.org/10.1021/ja3030388.

(116) Hallé, F.; Fin, A.; Rovira, A. R.; Tor, Y. Emissive Synthetic Cofactors: Enzymatic Interconversions of TzA Analogues of ATP, NAD+, NADH, NADP+, and NADPH. *Angew. Chem. Int. Ed Engl.* **2018**, *57* (4), 1087–1090. https://doi.org/10.1002/anie.201711935.

(117) Greco, N. J.; Tor, Y. Simple Fluorescent Pyrimidine Analogues Detect the Presence of DNA Abasic Sites. *J. Am. Chem. Soc.* **2005**, *127* (31), 10784–10785. https://doi.org/10.1021/ja052000a.

(118) Samaan, G. N.; Wyllie, M. K.; Cizmic, J. M.; Needham, L.-M.; Nobis, D.; Ngo, K.; Andersen, S.; Magennis, S. W.; Lee, S. F.; Purse, B. W. Single-Molecule Fluorescence Detection of a Tricyclic Nucleoside Analogue. *Chem. Sci.* **2021**, *12* (7), 2623–2628. https://doi.org/10.1039/D0SC03903A.

(119) Kužmová, E.; Zawada, Z.; Navrátil, M.; Günterová, J.; Kraus, T. Flow Cytometric Determination of Cell Cycle Progression via Direct Labeling of Replicated DNA. *Anal. Biochem.* **2021**, *614*, 114002. https://doi.org/10.1016/j.ab.2020.114002.

(120) Chudakov, D. M.; Matz, M. V.; Lukyanov, S.; Lukyanov, K. A. Fluorescent Proteins and Their Applications in Imaging Living Cells and Tissues. *Physiol. Rev.* **2010**, *90* (3), 1103–1163. https://doi.org/10.1152/physrev.00038.2009.

(121) Goedhart, J.; von Stetten, D.; Noirclerc-Savoye, M.; Lelimousin, M.; Joosen, L.; Hink, M. A.; van Weeren, L.; Gadella, T. W. J.; Royant, A. Structure-Guided Evolution of Cyan Fluorescent Proteins towards a Quantum Yield of 93%. *Nat. Commun.* **2012**, *3* (1), 751. https://doi.org/10.1038/ncomms1738.

(122) Gotthard, G.; von Stetten, D.; Clavel, D.; Noirclerc-Savoye, M.; Royant, A. Chromophore Isomer Stabilization Is Critical to the Efficient Fluorescence of Cyan Fluorescent Proteins. *Biochemistry* **2017**, *56* (49), 6418–6422. https://doi.org/10.1021/acs.biochem.7b01088.

(123) Sarkisyan, K. S.; Yampolsky, I. V.; Solntsev, K. M.; Lukyanov, S. A.; Lukyanov, K. A.; Mishin, A. S. Tryptophan-Based Chromophore in Fluorescent Proteins Can Be Anionic. *Sci. Rep.* **2012**, *2* (1), 608. https://doi.org/10.1038/srep00608.

(124) Karasawa, S.; Araki, T.; Nagai, T.; Mizuno, H.; Miyawaki, A. Cyan-Emitting and Orange-Emitting Fluorescent Proteins as a Donor/Acceptor Pair for Fluorescence Resonance Energy Transfer. *Biochem. J.* **2004**, *381* (Pt 1), 307–312. https://doi.org/10.1042/BJ20040321.

(125) Kremers, G.-J.; Goedhart, J.; van Munster, E. B.; Gadella, T. W. J. Cyan and Yellow Super Fluorescent Proteins with Improved Brightness, Protein Folding, and FRET Förster Radius,. *Biochemistry* **2006**, *45* (21), 6570–6580. https://doi.org/10.1021/bi0516273.

(126) Yuan, L.; Lin, W.; Zheng, K.; He, L.; Huang, W. Far-Red to near Infrared Analyte-Responsive Fluorescent Probes Based on Organic Fluorophore Platforms for Fluorescence Imaging. *Chem. Soc. Rev.* **2012**, *42* (2), 622–661. https://doi.org/10.1039/C2CS35313J.

(127) Guo, Z.; Park, S.; Yoon, J.; Shin, I. Recent Progress in the Development of Near-Infrared Fluorescent Probes for Bioimaging Applications. *Chem. Soc. Rev.* **2013**, *43* (1), 16–29. https://doi.org/10.1039/C3CS60271K.

(128) Zhou, L.; Wang, Q.; Tan, Y.; Lang, M. J.; Sun, H.; Liu, X. Rational Development of Near-Infrared Fluorophores with Large Stokes Shifts, Bright One-Photon, and Two-Photon Emissions for Bioimaging and Biosensing Applications. *Chem. - Eur. J.* **2017**, *23* (36), 8736–8740. https://doi.org/10.1002/chem.201701365.

(129) Lee, L. G.; Chen, C.-H.; Chiu, L. A. Thiazole Orange: A New Dye for Reticulocyte Analysis. *Cytometry* **1986**, *7* (6), 508–517. https://doi.org/10.1002/cyto.990070603.

(130) Suss, O.; Motiei, L.; Margulies, D. Broad Applications of Thiazole Orange in Fluorescent Sensing of Biomolecules and Ions. *Molecules* **2021**, *26* (9), 2828. https://doi.org/10.3390/molecules26092828.

(131) Athanasiadis, A. Athanasiadis Kniha. In *https://doi.org/10.25560/67946*; Imperial College London, 2016.

(132) Güixens-Gallardo, P.; Humpolickova, J.; Miclea, S. P.; Pohl, R.; Kraus, T.; Jurkiewicz, P.; Hof, M.; Hocek, M. Thiophene-Linked Tetramethylbodipy-Labeled Nucleotide for Viscosity-Sensitive Oligonucleotide Probes of

Hybridization and Protein–DNA Interactions. *Org. Biomol. Chem.* **2020**, *18* (5), 912–919. https://doi.org/10.1039/C9OB02634G.

(133) Schoder, S.; Kord Daoroun Kalai, S.; Reissig, H.-U. Novel Alkoxy-Substituted Dipyrrins and Near-IR BODIPY Dyes-Preparation and Photophysical Properties. *Chem. - Eur. J.* **2017**, *23* (51), 12527–12533. https://doi.org/10.1002/chem.201701108.

(134) Wang, T.; Zhao, Q.-J.; Hu, H.-G.; Yu, S.-C.; Liu, X.; Liu, L.; Wu, Q.-Y. Spirolactonized Si-Rhodamine: A Novel NIR Fluorophore Utilized as a Platform to Construct Si-Rhodamine-Based Probes. *Chem. Commun.* **2012**, *48* (70), 8781–8783. https://doi.org/10.1039/C2CC34159J.

(135) Lukinavičius, G.; Umezawa, K.; Olivier, N.; Honigmann, A.; Yang, G.; Plass, T.; Mueller, V.; Reymond, L.; Corrêa Jr, I. R.; Luo, Z.-G.; Schultz, C.; Lemke, E. A.; Heppenstall, P.; Eggeling, C.; Manley, S.; Johnsson, K. A Near-Infrared Fluorophore for Live-Cell Super-Resolution Microscopy of Cellular Proteins. *Nat. Chem.* **2013**, *5* (2), 132–139. https://doi.org/10.1038/nchem.1546.

(136) Lukinavičius, G.; Reymond, L.; D'Este, E.; Masharina, A.; Göttfert, F.; Ta, H.; Güther, A.; Fournier, M.; Rizzo, S.; Waldmann, H.; Blaukopf, C.; Sommer, C.; Gerlich, D. W.; Arndt, H.-D.; Hell, S. W.; Johnsson, K. Fluorogenic Probes for Live-Cell Imaging of the Cytoskeleton. *Nat. Methods* **2014**, *11* (7), 731–733. https://doi.org/10.1038/nmeth.2972.

(137) Bozhanova, N. G.; Baranov, M. S.; Sarkisyan, K. S.; Gritcenko, R.; Mineev, K. S.; Golodukhina, S. V.; Baleeva, N. S.; Lukyanov, K. A.; Mishin, A. S. Yellow and Orange Fluorescent Proteins with Tryptophan-Based Chromophores. *ACS Chem. Biol.* **2017**, *12* (7), 1867–1873. https://doi.org/10.1021/acschembio.7b00337.

(138) Chalfie, M.; Tu, Y.; Euskirchen, G.; Ward, W. W.; Prasher, D. C. Green Fluorescent Protein as a Marker for Gene Expression. *Science* **1994**, *263* (5148), 802–805. https://doi.org/10.1126/science.8303295.

(139) Ormö, M.; Cubitt, A. B.; Kallio, K.; Gross, L. A.; Tsien, R. Y.; Remington, S. J. Crystal Structure of the Aequorea Victoria Green Fluorescent Protein. *Science* **1996**, *273* (5280), 1392–1395. https://doi.org/10.1126/science.273.5280.1392.

(140) Niwa, H.; Inouye, S.; Hirano, T.; Matsuno, T.; Kojima, S.; Kubota, M.; Ohashi, M.; Tsuji, F. I. Chemical Nature of the Light Emitter of the Aequorea Green Fluorescent Protein. *Proc. Natl. Acad. Sci.* **1996**, *93* (24), 13617–13622. https://doi.org/10.1073/pnas.93.24.13617.

(141) Brejc, K.; Sixma, T. K.; Kitts, P. A.; Kain, S. R.; Tsien, R. Y.; Ormö, M.; Remington, S. J. Structural Basis for Dual Excitation and Photoisomerization of the Aequorea Victoria Green Fluorescent Protein. *Proc. Natl. Acad. Sci. U. S. A.* **1997**, *94* (6), 2306–2311. https://doi.org/10.1073/pnas.94.6.2306.

(142) Paige, J. S.; Wu, K. Y.; Jaffrey, S. R. RNA Mimics of Green Fluorescent Protein. *Science* **2011**, *333* (6042), 642–646. https://doi.org/10.1126/science.1207339.

(143) Riedl, J.; Ménová, P.; Pohl, R.; Orság, P.; Fojta, M.; Hocek, M. GFP-like Fluorophores as DNA Labels for Studying DNA–Protein Interactions. *J. Org. Chem.* **2012**, *77* (18), 8287–8293. https://doi.org/10.1021/jo301684b.
(144) Follenius-Wund, A.; Bourotte, M.; Schmitt, M.; Iyice, F.; Lami, H.; Bourguignon, J.-J.; Haiech, J.; Pigault, C. Fluorescent Derivatives of the GFP Chromophore Give a New Insight into the GFP Fluorescence Process. *Biophys. J.* **2003**, *85* (3), 1839–1850. https://doi.org/10.1016/S0006-3495(03)74612-8.
(145) Lee, C. Y.; Chen, Y. C.; Lin, H. C.; Jhong, Y.; Chang, C. W.; Tsai, C. H.; Kao, C. L.; Chien, T. C. Facile Synthesis of 4-Arylidene-5-Imidazolinones as Synthetic Analogs of Fluorescent Protein Chromophore. *Tetrahedron* **2012**, *68* (29), 5898–5907. https://doi.org/10.1016/j.tet.2012.04.102.
(146) Zhang, C.; Xu, D.; Wang, J.; Kang, C. Efficient Synthesis and Biological Activity of Novel Indole Derivatives as VEGFR-2 Tyrosine Kinase Inhibitors. *Russ. J. Gen. Chem.* **2017**, *87* (12), 3006–3016. https://doi.org/10.1134/S1070363217120465.
(147) Kojima, S.; Ohkawa, H.; Hirano, T.; Maki, S.; Niwa, H.; Ohashi, M.; Inouye, S.; Tsuji, F. I. Fluorescent Properties of Model Chromophores of Tyrosine-66 Substituted Mutants of Aequorea Green Fluorescent Protein (GEP). *Tetrahedron Lett.* **1998**, *39* (29), 5239–5242. https://doi.org/10.1016/S0040-4039(98)01031-4.
(148) Cahová, H.; Havran, L.; Brázdilová, P.; Pivoňková, H.; Pohl, R.; Fojta, M.; Hocek, M. Aminophenyl- and Nitrophenyl-Labeled Nucleoside Triphosphates: Synthesis, Enzymatic Incorporation, and Electrochemical Detection. *Angew. Chem. Int. Ed.* **2008**, *47* (11), 2059–2062. https://doi.org/10.1002/anie.200705088.
(149) Brázdilová, P.; Vrábel, M.; Pohl, R.; Pivoňková, H.; Havran, L.; Hocek, M.; Fojta, M. Ferrocenylethynyl Derivatives of Nucleoside Triphosphates: Synthesis, Incorporation, Electrochemistry, and Bioanalytical Applications. *Chem. – Eur. J.* **2007**, *13* (34), 9527–9533. https://doi.org/10.1002/chem.200701249.
(150) Shereda, R. D.; Kozlov, A. G.; Lohman, T. M.; Cox, M. M.; Keck, J. L. SSB as an Organizer/Mobilizer of Genome Maintenance Complexes. *Crit. Rev. Biochem. Mol. Biol.* **2008**, *43* (5), 289–318. https://doi.org/10.1080/10409230802341296.
(151) Bujalowski, W.; Lohman, T. M. Negative Co-Operativity in Escherichia Coli Single Strand Binding Protein-Oligonucleotide Interactions. I. Evidence and a Quantitative Model. *J. Mol. Biol.* **1989**, *207* (1), 249–268. https://doi.org/10.1016/0022-2836(89)90454-3.
(152) Escobedo, J. O.; Rusin, O.; Lim, S.; Strongin, R. M. NIR Dyes for Bioimaging Applications. *Curr. Opin. Chem. Biol.* **2010**, *14* (1), 64. https://doi.org/10.1016/j.cbpa.2009.10.022.
(153) Nguyen, N.-H.; Bogliotti, N.; Chennoufi, R.; Henry, E.; Tauc, P.; Salas, E.; Roman, L. J.; Slama-Schwok, A.; Deprez, E.; Xie, J. Convergent Synthesis and

Properties of Photoactivable NADPH Mimics Targeting Nitric Oxide Synthases. *Org. Biomol. Chem.* **2016**, *14* (40), 9519–9532. https://doi.org/10.1039/C6OB01533F.
(154) Drug Action at the Molecular Level; Roberts, G. C. K., Ed.; Palgrave Macmillan UK, 1977; pp 167–189.
(155) Mechanism of Action of Antieukaryotic and Antiviral Compounds; Hahn, F. E., Ed.; Springer-Verlag Berlin Heidelberg, 1979; Vol. 5, p 173.
(156) Kumar, C. V.; Turner, R. S.; Asuncion, E. H. Groove Binding of a Styrylcyanine Dye to the DNA Double Helix: The Salt Effect. *J. Photochem. Photobiol. Chem.* **1993**, *74* (2–3), 231–238. https://doi.org/10.1016/1010-6030(93)80121-O.
(157) Porschke, D. Specificity and Dynamics of Protein-Nucleic Acid Interactions. In *DNA—Ligand Interactions: From Drugs to Proteins*; Guschlbauer, W., Saenger, W., Eds.; NATO ASI Series; Springer US: Boston, MA, 1987; pp 85–104. https://doi.org/10.1007/978-1-4684-5383-6_5.
(158) *Crystallographic and Modeling Methods in Molecular Design*; Bugg, C. E., Ealick, S. E., Eds.; Springer-Verlag: New York, 1990. https://doi.org/10.1007/978-1-4612-3374-9.
(159) Wicks, S. L.; Hargrove, A. E. Fluorescent Indicator Displacement Assays to Identify and Characterize Small Molecule Interactions with RNA. *Methods San Diego Calif* **2019**, *167*, 3–14. https://doi.org/10.1016/j.ymeth.2019.04.018.
(160) Boger, D. L.; Tse, W. C. Thiazole Orange as the Fluorescent Intercalator in a High Resolution Fid Assay for Determining DNA Binding Affinity and Sequence Selectivity of Small Molecules. *Bioorg. Med. Chem.* **2001**, *9* (9), 2511–2518. https://doi.org/10.1016/s0968-0896(01)00243-7.
(161) Kapuscinski, J. DAPI: A DNA-Specific Fluorescent Probe. *Biotech. Histochem. Off. Publ. Biol. Stain Comm.* **1995**, *70* (5), 220–233. https://doi.org/10.3109/10520299509108199.
(162) Kim, S. K.; Nordén, B. Methyl Green. A DNA Major-Groove Binding Drug. *FEBS Lett.* **1993**, *315* (1), 61–64. https://doi.org/10.1016/0014-5793(93)81133-k.
(163) Maeda, Y.; Nunomura, K.; Ohtsubo, E. Differential Scanning Calorimetric Study of the Effect of Intercalators and Other Kinds of DNA-Binding Drugs on the Stepwise Melting of Plasmid DNA. *J. Mol. Biol.* **1990**, *215* (2), 321–329. https://doi.org/10.1016/S0022-2836(05)80350-X.
(164) Bjorndal, M. T.; Fygenson, D. K. DNA Melting in the Presence of Fluorescent Intercalating Oxazole Yellow Dyes Measured with a Gel-Based Assay. *Biopolymers* **2002**, *65* (1), 40–44. https://doi.org/10.1002/bip.10220.
(165) Little, J. W. An Exonuclease Induced by Bacteriophage Lambda. II. Nature of the Enzymatic Reaction. *J. Biol. Chem.* **1967**, *242* (4), 679–686.
(166) Kabir, A.; Suresh Kumar, G. Binding of the Biogenic Polyamines to Deoxyribonucleic Acids of Varying Base Composition: Base Specificity and the Associated Energetics of the Interaction. *PLoS ONE* **2013**, *8* (7), e70510.

https://doi.org/10.1371/journal.pone.0070510.
(167) Gupta, S.; Tiwari, N.; Munde, M. A Comprehensive Biophysical Analysis of the Effect of DNA Binding Drugs on Protamine-Induced DNA Condensation. *Sci. Rep.* **2019**, *9* (1), 5891. https://doi.org/10.1038/s41598-019-41975-8.
(168) Pang, S.; Liu, S.; Su, X. A Fluorescence Assay for the Trace Detection of Protamine and Heparin. *RSC Adv.* **2014**, *4* (49), 25857–25862. https://doi.org/10.1039/C4RA02936D.
(169) Corman, V. M.; Landt, O.; Kaiser, M.; Molenkamp, R.; Meijer, A.; Chu, D. K.; Bleicker, T.; Brünink, S.; Schneider, J.; Schmidt, M. L.; Mulders, D. G.; Haagmans, B. L.; Veer, B. van der; Brink, S. van den; Wijsman, L.; Goderski, G.; Romette, J.-L.; Ellis, J.; Zambon, M.; Peiris, M.; Goossens, H.; Reusken, C.; Koopmans, M. P.; Drosten, C. Detection of 2019 Novel Coronavirus (2019-NCoV) by Real-Time RT-PCR. *Eurosurveillance* **2020**, *25* (3), 2000045. https://doi.org/10.2807/1560-7917.ES.2020.25.3.2000045.
(170) Percec, V.; Leowanawat, P.; Sun, H.-J.; Kulikov, O.; Nusbaum, C. D.; Tran, T. M.; Bertin, A.; Wilson, D. A.; Peterca, M.; Zhang, S.; Kamat, N. P.; Vargo, K.; Moock, D.; Johnston, E. D.; Hammer, D. A.; Pochan, D. J.; Chen, Y.; Chabre, Y. M.; Shiao, T. C.; Bergeron-Brlek, M.; André, S.; Roy, R.; Gabius, H.-J.; Heiney, P. A. Modular Synthesis of Amphiphilic Janus Glycodendrimers and Their Self-Assembly into Glycodendrimersomes and Other Complex Architectures with Bioactivity to Biomedically Relevant Lectins. *J. Am. Chem. Soc.* **2013**, *135* (24), 9055–9077. https://doi.org/10.1021/ja403323y.
(171) Lu, Y.; Song, S.; Hou, C.; Pang, S.; Li, X.; Wu, X.; Shao, C.; Pei, Y.; Pei, Z. Facile Fabrication of Branched-Chain Carbohydrate Chips for Studying Carbohydrate-Protein Interactions by QCM Biosensor. *Chin. Chem. Lett.* **2018**, *29* (1), 65–68. https://doi.org/10.1016/j.cclet.2017.08.003.
(172) Rastede, E. E.; Tanha, M.; Yaron, D.; Watkins, S. C.; Waggoner, A. S.; Armitage, B. A. Spectral Fine Tuning of Cyanine Dyes: Electron Donor–Acceptor Substituted Analogues of Thiazole Orange. *Photochem. Photobiol. Sci.* **2015**, *14* (9), 1703–1712. https://doi.org/10.1039/C5PP00117J.
(173) Klimkowski, P.; Ornellas, S. D.; Singleton, D.; El-Sagheer, A. H.; Brown, T. Design of Thiazole Orange Oligonucleotide Probes for Detection of DNA and RNA by Fluorescence and Duplex Melting. *Org. Biomol. Chem.* **2019**, *17* (24), 5943–5950. https://doi.org/10.1039/C9OB00885C.
(174) Gahtory, D.; Murtola, M.; Smulders, M. M. J.; Wennekes, T.; Zuilhof, H.; Strömberg, R.; Albada, B. Facile Functionalization of Peptide Nucleic Acids (PNAs) for Antisense and Single Nucleotide Polymorphism Detection. *Org. Biomol. Chem.* **2017**, *15* (32), 6710–6714. https://doi.org/10.1039/C7OB01592E.
(175) Sakahira, H.; Enari, M.; Nagata, S. Cleavage of CAD Inhibitor in CAD Activation and DNA Degradation during Apoptosis. *Nature* **1998**, *391* (6662), 96–99. https://doi.org/10.1038/34214.
(176) Nickson, C. M.; Parsons, J. L. Monitoring Regulation of DNA Repair Activities

of Cultured Cells In-Gel Using the Comet Assay. *Front. Genet.* **2014**, *5*. https://doi.org/10.3389/fgene.2014.00232.

(177) Apelt, K.; Lans, H.; Schärer, O. D.; Luijsterburg, M. S. Nucleotide Excision Repair Leaves a Mark on Chromatin: DNA Damage Detection in Nucleosomes. *Cell. Mol. Life Sci.* **2021**, *78* (24), 7925–7942. https://doi.org/10.1007/s00018-021-03984-7.

(178) Wang, I.-H.; Suomalainen, M.; Andriasyan, V.; Kilcher, S.; Mercer, J.; Neef, A.; Luedtke, N. W.; Greber, U. F. Tracking Viral Genomes in Host Cells at Single-Molecule Resolution. *Cell Host Microbe* **2013**, *14* (4), 468–480. https://doi.org/10.1016/j.chom.2013.09.004.

(179) Treibs, A.; Kreuzer, F.-H. Difluorboryl-Komplexe von Di- und Tripyrrylmethenen. *Justus Liebigs Ann. Chem.* **1968**, *718* (1), 208–223. https://doi.org/10.1002/jlac.19687180119.

(180) Wagner, R. W.; Lindsey, J. S. Boron-dipyrromethene dyes for incorporation in synthetic multi-pigment light-harvesting arrays. *Pure Appl. Chem.* **1996**, *68* (7), 1373–1380. https://doi.org/10.1351/pac199668071373.

(181) Tan, K.; Jaquinod, L.; Paolesse, R.; Nardis, S.; Di Natale, C.; Di Carlo, A.; Prodi, L.; Montalti, M.; Zaccheroni, N.; Smith, K. M. Synthesis and Characterization of β-Fused Porphyrin-BODIPY® Dyads. *Tetrahedron* **2004**, *60* (5), 1099–1106. https://doi.org/10.1016/j.tet.2003.11.072.

(182) Karolin, J.; Johansson, L. B.-A.; Strandberg, L.; Ny, T. Fluorescence and Absorption Spectroscopic Properties of Dipyrrometheneboron Difluoride (BODIPY) Derivatives in Liquids, Lipid Membranes, and Proteins. *J. Am. Chem. Soc.* **1994**, *116* (17), 7801–7806. https://doi.org/10.1021/ja00096a042.

(183) Yee, M.; Fas, S. C.; Stohlmeyer, M. M.; Wandless, T. J.; Cimprich, K. A. A Cell-Permeable, Activity-Based Probe for Protein and Lipid Kinases*. *J. Biol. Chem.* **2005**, *280* (32), 29053–29059. https://doi.org/10.1074/jbc.M504730200.

(184) Kodr, D.; Stanková, J.; Rumlová, M.; Džubák, P.; Řehulka, J.; Zimmermann, T.; Křížová, I.; Gurská, S.; Hajdúch, M.; Dražar, P. B.; Jurášek, M. Betulinic Acid Decorated with Polar Groups and Blue Emitting BODIPY Dye: Synthesis, Cytotoxicity, Cell-Cycle Analysis and Anti-HIV Profiling. *Biomedicines* **2021**, *9* (9), 1104. https://doi.org/10.3390/biomedicines9091104.

(185) Cheng, M. H. Y.; Savoie, H.; Bryden, F.; Boyle, R. W. A Convenient Method for Multicolour Labelling of Proteins with BODIPY Fluorophores via Tyrosine Residues. *Photochem. Photobiol. Sci.* **2017**, *16* (8), 1260–1267. https://doi.org/10.1039/C7PP00091J.

(186) Deore, P. S.; Soldatov, D. V.; Manderville, R. A. A 5′-BODIPY End-Label for Monitoring DNA Duplex-Quadruplex Exchange. *Sci. Rep.* **2018**, *8* (1), 16874. https://doi.org/10.1038/s41598-018-35352-0.

(187) Bernecic, N. C.; Zhang, M.; Gadella, B. M.; Brouwers, J. F. H. M.; Jansen, J. W. A.; Arkesteijn, G. J. A.; de Graaf, S. P.; Leahy, T. BODIPY-Cholesterol Can Be Reliably Used to Monitor Cholesterol Efflux from Capacitating

Mammalian Spermatozoa. *Sci. Rep.* **2019**, *9* (1), 9804. https://doi.org/10.1038/s41598-019-45831-7.

(188) Bañuelos, J.; Arroyo-Córdoba, I. J.; Valois-Escamilla, I.; Alvarez-Hernández, A.; Peña-Cabrera, E.; Hu, R.; Tang, B. Z.; Esnal, I.; Martínez, V.; Arbeloa, I. L. Modulation of the Photophysical Properties of BODIPY Dyes by Substitution at Their Meso Position. *RSC Adv.* **2011**, *1* (4), 677–684. https://doi.org/10.1039/C1RA00020A.

(189) Dziuba, D.; Pohl, R.; Hocek, M. Bodipy-Labeled Nucleoside Triphosphates for Polymerase Synthesis of Fluorescent DNA. *Bioconjug. Chem.* **2014**, *25* (11), 1984–1995. https://doi.org/10.1021/bc5003554.

(190) Güixens-Gallardo, P.; Zawada, Z.; Matyašovský, J.; Dziuba, D.; Pohl, R.; Kraus, T.; Hocek, M. Brightly Fluorescent 2′-Deoxyribonucleoside Triphosphates Bearing Methylated Bodipy Fluorophore for in Cellulo Incorporation to DNA, Imaging, and Flow Cytometry. *Bioconjug. Chem.* **2018**, *29* (11), 3906–3912. https://doi.org/10.1021/acs.bioconjchem.8b00721.

(191) Amombo, G. M. O.; Flögel, O.; Kalai, S. K. D.; Schoder, S.; Warzok, U.; Reissig, H.-U. Efficient Syntheses of 2,5-Dihydropyrroles, Pyrrolidin-3-Ones, and Electron-Rich Pyrroles from N-Tosylimines and Lithiated Alkoxyallenes. *Eur. J. Org. Chem.* **2017**, *2017* (14), 1965–1972. https://doi.org/10.1002/ejoc.201700073.

(192) Liu, W.; Jeganathan, G.; Amiri, S.; Morgan, K. M.; Ryan, B. M.; Pine, S. R. Asymmetric Segregation of Template DNA Strands in Basal-like Human Breast Cancer Cell Lines. *Mol. Cancer* **2013**, *12* (1), 139. https://doi.org/10.1186/1476-4598-12-139.

(193) Kibbe, W. A. OligoCalc: An Online Oligonucleotide Properties Calculator. *Nucleic Acids Res.* **2007**, *35* (Web Server issue), W43-46. https://doi.org/10.1093/nar/gkm234.

(194) Würth, C.; Grabolle, M.; Pauli, J.; Spieles, M.; Resch-Genger, U. Relative and Absolute Determination of Fluorescence Quantum Yields of Transparent Samples. *Nat. Protoc.* **2013**, *8* (8), 1535–1550. https://doi.org/10.1038/nprot.2013.087.

(195) Sinkeldam, R. W.; Wheat, A. J.; Boyaci, H.; Tor, Y. Emissive Nucleosides as Molecular Rotors. *ChemPhysChem* **2011**, *12* (3), 567–570. https://doi.org/10.1002/cphc.201001002.